



## Central and Eastern Europe Climate Change Impact and Vulnerability Assessment

Specific targeted research project

1.1.6.3.I.3.2: Climate change impacts in central-eastern Europe

### **D4.4: Corresponding analyses on the CECILIA high-resolution simulations**

Due date of deliverable: 31<sup>st</sup> May 2009

Actual submission date: 31<sup>th</sup> October 2009

Start date of project: 1st June 2006

Duration: 43 months

**Lead contractor for this deliverable: NMA**

Project co-funded by the European Commission within the Sixth Framework Programme (2002-2006)		
Dissemination Level		
<b>PU</b>	Public	X
<b>PP</b>	Restricted to other programme participants (including the Commission Services)	
<b>RE</b>	Restricted to a group specified by the consortium (including the Commission Services)	
<b>CO</b>	Confidential, only for members of the consortium (including the Commission Services)	



## **CECILIA Deliverable 4.4: Corresponding analyses on the CECILIA high-resolution simulations:**

*Lead partner for deliverable:* NMA

*Contributing partners:* CHMI, IAP, CUNI, ELU, OMSZ, NMA, NIMH, ETH, DMI

Final revision December 31st, 2009

The present report contains sub-reports from the individual institutions

[CHMI](#), [IAP](#), [CUNI](#), [ELU](#), [OMSZ](#), [NMA](#), [NIMH](#), [ETH](#), [DMI](#)) contributing to deliverable D4.4

The deliverable focused on the analysis of the extreme core indices for different domains simulated with both RegCM and Aladin Climate regional models.

### **D4.4.a Analysis for Czech Republic**

#### **D4.4. a1 (led by CHMI and IAP)**

##### **D4.4 a1.1 Effect of bias correction for computed extremes based on simulations of ALADIN-Climate/CZ for the area of the Czech and Slovak republics**

Petr Štěpánek (CHMI), Pavel Zahradníček (CHMI), Petr Skalák (CHMI), Aleš Farda (CHMI),

Jan Kyselý (IAP)

Outputs of regional climate models are biased to some extent, resulting either from biases in driving GCM or from given RCM itself (smoothed orography, parametrization etc.). Such biased outputs can lead then to biased results for computed extreme indices. The influence of correction of scenario data upon extreme indices calculation was investigated based on corrected and uncorrected RCM ALADIN-Climate/CZ outputs (driven by GCM ARPEGE with the IPCC A1B emission scenario for two time slices: 2021-2050 and 2071-2100 resp.). RCM description can be found e.g. in Farda et al. (2007) or Farda (2008).

The model data were corrected according to validation results carried out for the period 1961-1990. For this task a new gridded dataset of station observation was created. All input station observations were quality controlled and homogenized in daily scale (Štěpánek et al., 2009) and then recalculated to the ALADIN-Climate/CZ grid of 10 km horizontal resolution. Daily station measurements in a vicinity of each grid point were first reduced on the grid point's (model's) altitude by a local linear regression and then weighted averaged to a grid point location according to their distance form the grid point. The inverse distance (1/d) factor was used as a weight for air temperature, while 1/d<sup>3</sup> factor was taken for precipitation.

Gridded dataset of station observations was then compared with the past climate (1961-1990) GCM driven ALADIN-Climate/CZ simulations in each grid point. According to relationship between these two datasets (validation details are given e.g. in Skalák et al., 2008), outputs of A1B scenario integrations of

the future climate were corrected applying an approach of Déqué (2007) that is based on a variable correction using individual percentiles. After the correction, the model outputs are fully compatible with the station (measured) data. The gridding and all data processing including the presented analysis were done by ProClimDB database software (free download from <http://www.climahom.eu/>) for processing of climatological datasets (Štěpánek, 2008).

For further analysis, only grid points with the highest (29 grid points) and lowest altitudes (21 grid points) were selected (see Fig. 1) in the area of the Czech and Slovak republics. In the Slovak Republic, mountainous regions Vysoké and Nízke Tatry (grid points altitudes vary between 1013 – 1633 m a.s.l.) can be distinguish, in the Czech Republic smaller areas in Krkonoše, Šumava and Jeseníky (altitudes 885 – 1124 m a.s.). As for lower parts the points were selected around Labe, Morava, Dunaj and Tisa rivers (altitudes of the grid points range between 91 and 177 m a.s.l.).

Further results are given both for corrected and uncorrected results. In case of reference period 1961-1990 we applied outputs of the RCM ALADIN-Climate/CZ driven by ARPEGE (control run, marked as uncorrected outputs) and station data recalculated into grid points of the RCM (marked as corrected data in the following text).

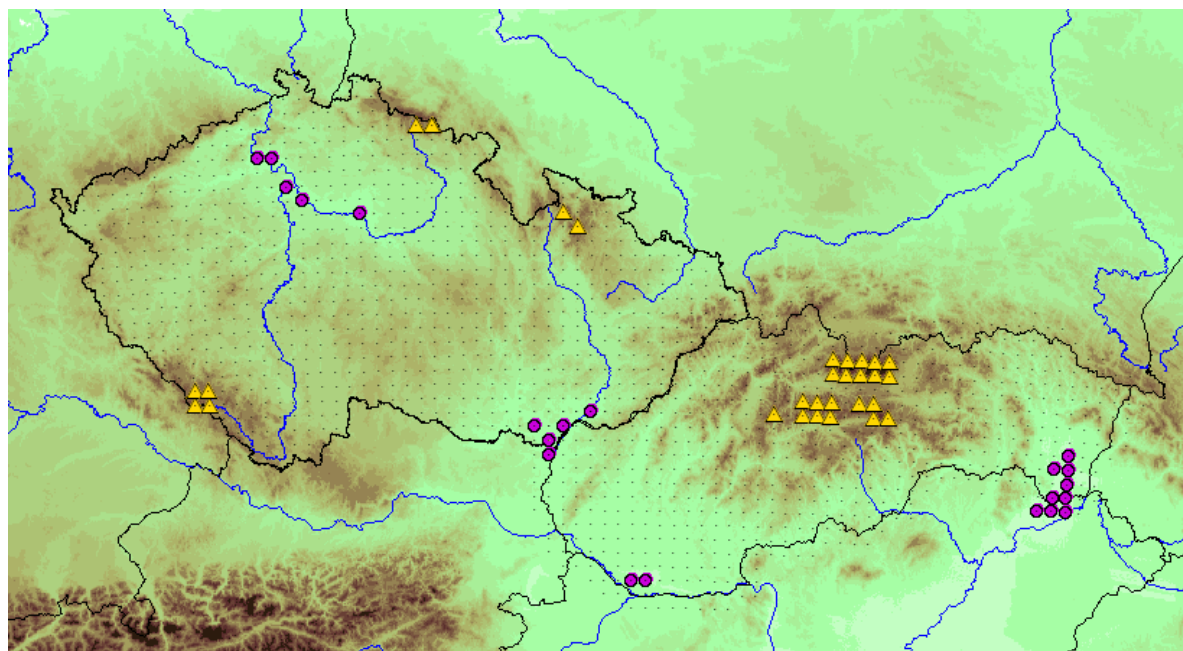


Fig. 1. Studied area and selected grid points for the analysis. Yellow triangles mark mountainous regions, purple circles mark lowland regions.

## 1) Air temperature (index 003)

Table 1. Corrected and uncorrected air temperature [°C] for Czech and Slovak lowlands and mountains regions in the periods 1961-1990, 2021-2050 and 2071-2100

Region	Model	Period	YEAR	DJF	MAM	JJA	SON
Lowlands	uncorr	1961-1990	8,9	-0,7	7,9	20,1	8,7
Lowlands	corr	1961-1990	9,1	-0,7	9,7	18,7	9,4
Mountains	uncorr	1961-1990	3,0	-4,8	1,4	12,4	2,7
Mountains	corr	1961-1990	4,0	-4,6	3,3	12,2	4,7
Lowlands	uncorr	2021-2050	10,5	0,5	9,3	21,9	10,4
Lowlands	corr	2021-2050	10,8	1,1	10,9	20,7	10,6
Mountains	uncorr	2021-2050	4,5	-3,4	2,6	14,4	4,3
Mountains	corr	2021-2050	5,7	-2,7	4,3	14,8	5,8
Lowlands	uncorr	2071-2100	12,2	1,6	11,0	24,1	12,2
Lowlands	corr	2071-2100	12,3	2,9	12,0	22,3	12,0
Mountains	uncorr	2071-2100	6,0	-2,5	4,0	16,4	5,8
Mountains	corr	2071-2100	7,9	-0,5	6,4	17,4	7,7

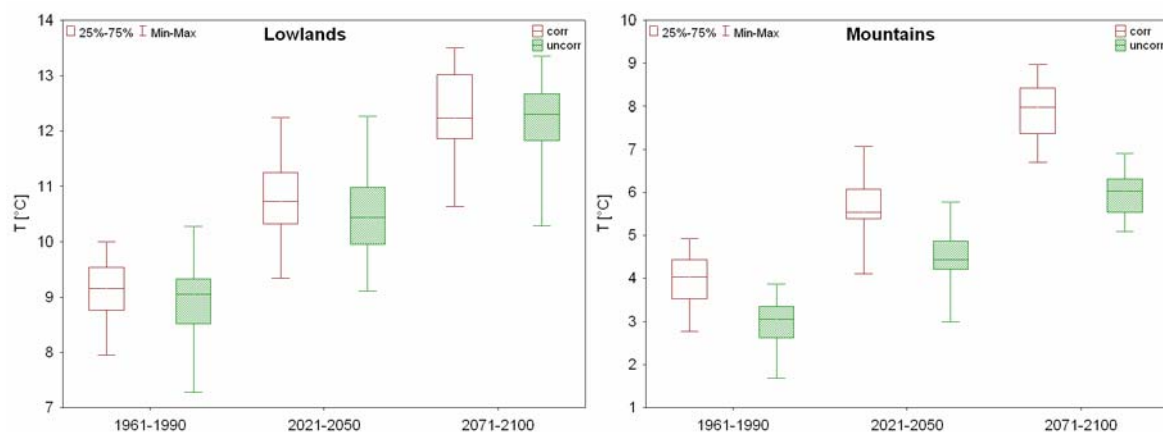


Fig. 2. Corrected and uncorrected air temperature [°C] for Czech and Slovak lowland (left) and mountainous regions (right) in the periods 1961-1990, 2021-2050 and 2071-2100

Differences between corrected and uncorrected outputs are found mainly for mountains regions. The biggest difference occurs in the period 2071-2100. The corrected annual temperature is about 1.9°C higher than uncorrected one. The results for lowlands are similar for both model outputs.

According to RCM outputs for the period 2021-2050 annual temperatures in lowlands will be about 1.6-1.7°C higher both for uncorrected and corrected model outputs. For mountains regions the results are similar (1.5-1.7°C). The prediction for the second time slice is +3.2 - 3.3°C for lowlands, for mountains regions we get bigger differences. The corrected outputs lead to temperatures higher by about 3.9°C, while uncorrected ones give warming of 3.0°C only.

Linear trend for the whole period 1961-2100 is statistically significant for annual values and all seasons. Annual trend is 0.29°C per 10 years for lowlands for both outputs. Differences between corrected and uncorrected model outputs are higher for individual seasons. Higher trends are found for spring, summer and autumn in the uncorrected model outputs while for winter the trend is lower. In the mountains regions and corrected temperatures linear trend is higher especially for year, winter and summer while for spring and autumn the results are lower and comparable with uncorrected outputs. Fluctuations of air temperature with marked linear trends are shown in Fig. 3 (lowlands) and Fig. 4 (mountains).

Table 2. Linear trends of the corrected and uncorrected air temperature [°C] for Czech and Slovak lowland and mountainous regions in the periods 1961-1990, 2021-2050 and 2071-2100

Region	Model	Period	YEAR	DJF	MAM	JJA	SON
Lowlands	uncorr	1961-2100	0,029	0,022	0,027	0,035	0,031
Lowlands	corr	1961-2100	0,029	0,033	0,020	0,032	0,023
Mountains	uncorr	1961-2100	0,027	0,023	0,023	0,036	0,027
Mountains	corr	1961-2100	0,035	0,039	0,028	0,046	0,026

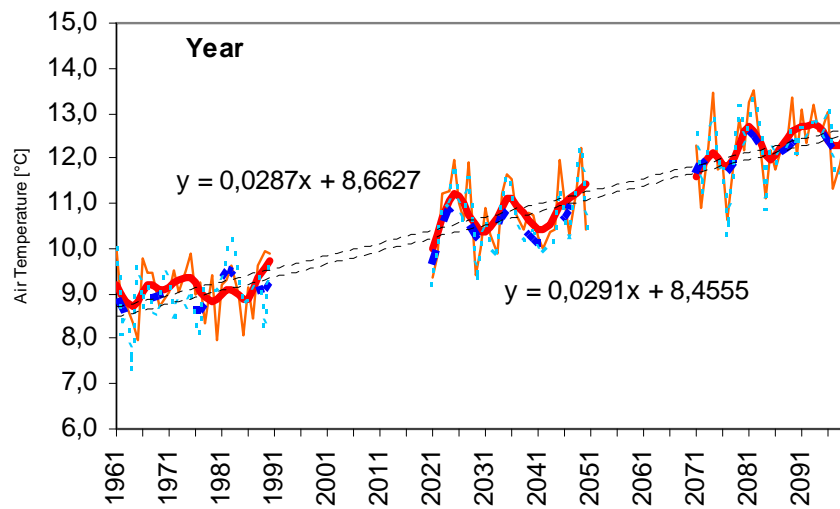


Fig. 3. Fluctuations of corrected and uncorrected air temperature [°C] for Czech and Slovak lowland regions in the period 1961-2100 (solid line – corrected model outputs; dashed line uncorrected outputs)

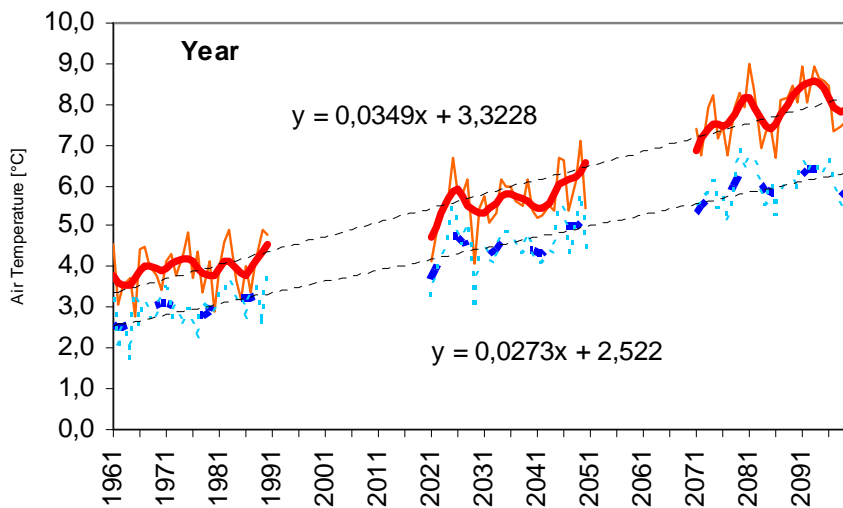


Fig. 4. Fluctuations of corrected and uncorrected air temperature [°C] for Czech and Slovak mountainous regions in the periods 1961-2100 (solid line – corrected model outputs; dashed line uncorrected outputs)

## 2) Maximum temperature (index 001)

Table 3. Corrected and uncorrected maximum temperature [°C] for Czech and Slovak lowland and mountainous regions in the periods 1961-1990, 2021-2050 and 2071-2100

Region	Model	Period	YEAR	DJF	MAM	JJA	SON
Lowlands	uncorr	1961-1990	13,0	2,4	12,6	24,6	12,9
Lowlands	corr	1961-1990	14,2	2,5	15,4	25,0	14,6
Mountains	uncorr	1961-1990	6,6	-2,1	5,2	16,7	6,5
Mountains	corr	1961-1990	8,5	-0,7	8,1	17,3	9,4
Lowlands	uncorr	2021-2050	14,5	3,9	13,8	26,4	14,6
Lowlands	corr	2021-2050	15,9	4,4	16,5	27,0	16,0
Mountains	uncorr	2021-2050	8,1	-0,6	6,5	18,2	7,9
Mountains	corr	2021-2050	10,3	1,4	9,2	19,8	10,6
Lowlands	uncorr	2071-2100	16,3	4,9	15,3	28,9	16,6
Lowlands	corr	2071-2100	17,8	5,7	18,4	29,3	17,8
Mountains	uncorr	2071-2100	9,7	0,4	7,8	20,4	9,8
Mountains	corr	2071-2100	12,1	2,5	10,9	22,1	12,4

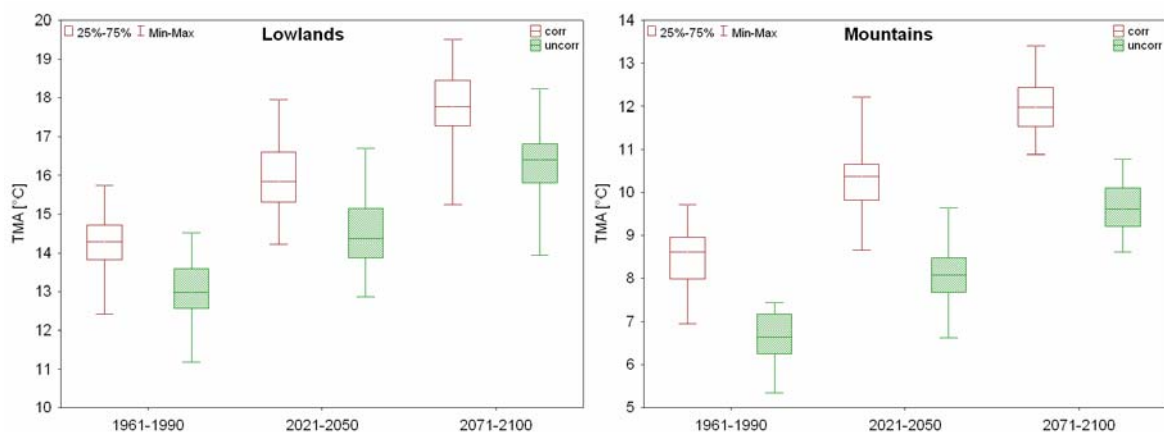


Fig. 5. Corrected and uncorrected maximum temperature [°C] for Czech and Slovak lowland (left) and mountainous regions (right) in the periods 1961-1990, 2021-2050 and 2071-2100

Differences between corrected and uncorrected outputs for maximum temperature are higher than for mean temperature. For lowlands differences span between 1.2°C and 1.5°C depending on the period (see Tab. 3). Differences for mountains region are again higher than for mean temperature (about 1.9-2.4°C; see Fig. 5).

In the period 2021-2050 we can expect according to RCM outputs annual maximum temperature higher by about 1.5-1.8°C, both for lowland and mountainous regions. Uncorrected model outputs in the second time slice predicts maximum temperature for lowlands higher by about 3.3°C and for mountains by about 3.1°C. Corrected model outputs give increase in maximum temperature by about +3.6°C for both regions.

Linear trends for the period 1961-2100 are statistically significant for year and all seasons. Trend values are higher for corrected outputs (compared to uncorrected ones) with exception of autumn. Highest trends are expected for summer (0.38-0.43°C per 10 years, corrected model outputs), followed by year and winter.

Table 4. Linear trends of the corrected and uncorrected maximum temperature [°C] for Czech and Slovak lowland and mountainous regions in the periods 1961-1990, 2021-2050 and 2071-2100

Region	Model	Period	YEAR	DJF	MAM	JJA	SON
Lowlands	uncorr	1961-2100	0,030	0,024	0,023	0,037	0,032
Lowlands	corr	1961-2100	0,032	0,031	0,027	0,038	0,027
Mountains	uncorr	1961-2100	0,027	0,024	0,023	0,033	0,029
Mountains	corr	1961-2100	0,032	0,030	0,025	0,043	0,026

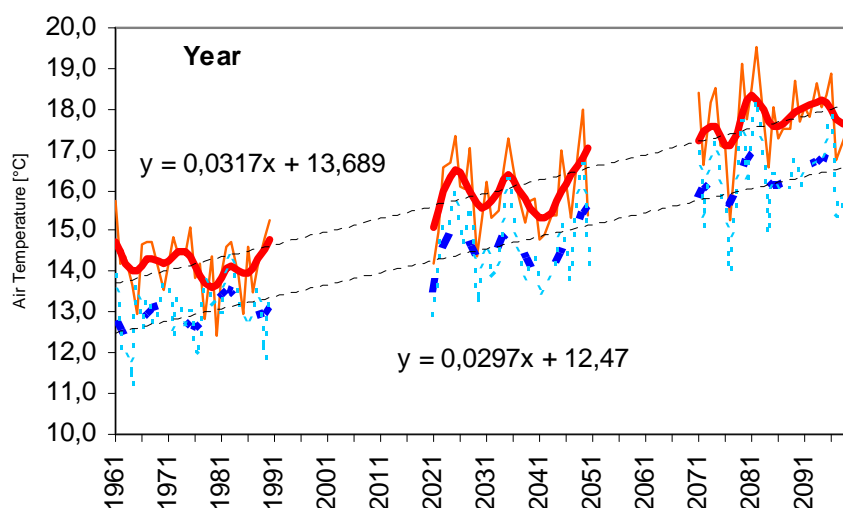


Fig. 6. Corrected and uncorrected maximum temperature [°C] for Czech and Slovak lowland regions in the periods 1961-2100 (solid line – corrected model outputs; dashed line uncorrected outputs)

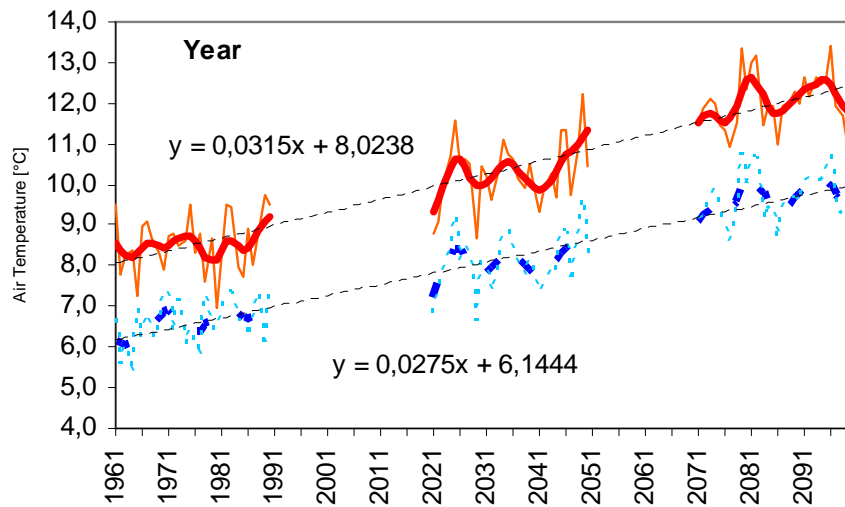


Fig. 7. Corrected and uncorrected maximum temperature [°C] for Czech and Slovak mountainous regions in the periods 1961-2100 (solid line – corrected model outputs; dashed line uncorrected outputs)

### 3) Minimum temperature (index 002)

Table 5. Corrected and uncorrected minimum temperature [°C] for Czech and Slovak lowland and mountainous regions in the periods 1961-1990, 2021-2050 and 2071-2100

Region	Model	Period	YEAR	DJF	MAM	JJA	SON
Lowlands	uncorr	1961-1990	5,1	-3,5	3,5	15,3	5,3
Lowlands	corr	1961-1990	4,5	-3,8	4,4	13,0	5,0
Mountains	uncorr	1961-1990	-0,9	-7,6	-2,8	6,9	-0,4
Mountains	corr	1961-1990	0,2	-7,9	-0,6	7,9	1,2
Lowlands	uncorr	2021-2050	6,7	-2,3	5,0	17,2	7,1
Lowlands	corr	2021-2050	6,2	-1,9	5,7	14,7	6,4
Mountains	uncorr	2021-2050	0,8	-6,1	-1,6	9,4	1,2
Mountains	corr	2021-2050	1,9	-6,0	0,4	10,1	2,4
Lowlands	uncorr	2071-2100	8,4	-1,2	6,8	19,1	8,7

<b>Lowlands</b>	<b>corr</b>	<b>2071-2100</b>	7,8	-0,5	7,4	16,5	7,8
<b>Mountains</b>	<b>uncorr</b>	<b>2071-2100</b>	2,3	-5,0	-0,2	11,5	2,6
<b>Mountains</b>	<b>corr</b>	<b>2071-2100</b>	3,4	-4,8	2,1	12,0	3,7

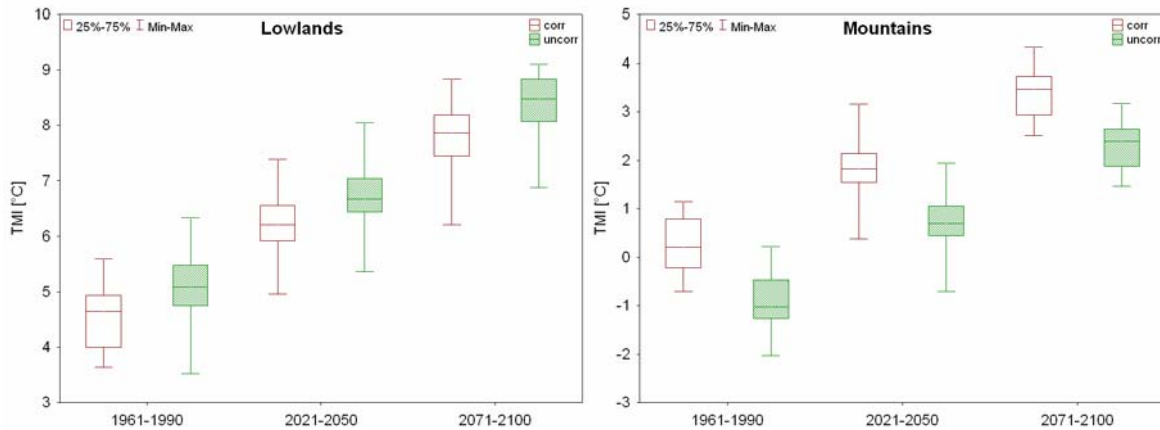


Fig. 8. Corrected and uncorrected minimum temperature [°C] for Czech and Slovak lowland (left) and mountainous regions (right) in the periods 1961-1990, 2021-2050 and 2071-2100.

The results for minimum temperature between corrected and uncorrected outputs are very different for both regions. For lowlands, minimum temperatures are higher by about 0.6°C for uncorrected outputs compared to corrected model outputs, but in mountainous regions the situation is opposite. Corrected minimum temperatures are higher by about 1.1°C.

In the period 2021-2050 both outputs predict higher minimum temperature about by 1.6-1.7°C in lowlands. Different results are obtained for mountainous region. Uncorrected model outputs predict higher minimum temperature by only 1.1°C, while corrected outputs forecast similar results as got for lowlands. Both outputs give the same differences (for lowlands and mountains) for the second time slice compared to the period 1961-1990.

It is shown in Fig. 9 and Fig. 10 that annual linear trend for the whole period 1961-2100 is similar for both outputs and regions. Big differences are found between trends for winter and autumn seasons. Corrected model outputs lead to higher trend values in winter and lower in autumn (see Tab. 6), for uncorrected outputs the result is opposite.

Table 6. Linear trends of the corrected and uncorrected minimum temperature [°C] for Czech and Slovak lowlands and mountains regions in the periods 1961-1990, 2021-2050 and 2071-2100

Region	Model	Period	YEAR	DJF	MAM	JJA	SON
<b>Lowlands</b>	<b>uncorr</b>	<b>1961-2100</b>	0,029	0,022	0,029	0,034	0,030
<b>Lowlands</b>	<b>corr</b>	<b>1961-2100</b>	0,029	0,031	0,026	0,031	0,024

<b>Mountains</b>	<b>uncorr</b>	<b>1961-2100</b>	<b>0,029</b>	<b>0,024</b>	<b>0,023</b>	<b>0,042</b>	<b>0,027</b>
<b>Mountains</b>	<b>corr</b>	<b>1961-2100</b>	<b>0,028</b>	<b>0,030</b>	<b>0,024</b>	<b>0,037</b>	<b>0,022</b>

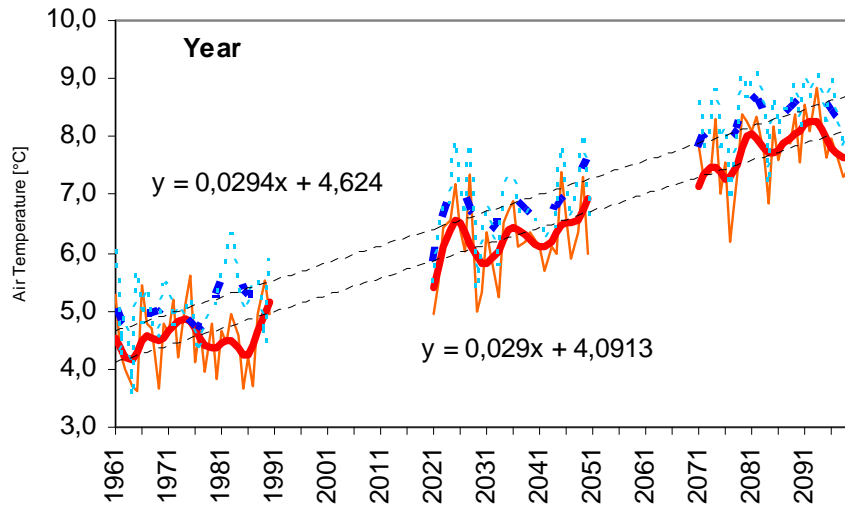


Fig. 9. Corrected and uncorrected minimum temperature [°C] for Czech and Slovak lowland regions in the periods 1961-2100 (solid line – corrected model outputs; dashed line uncorrected outputs)

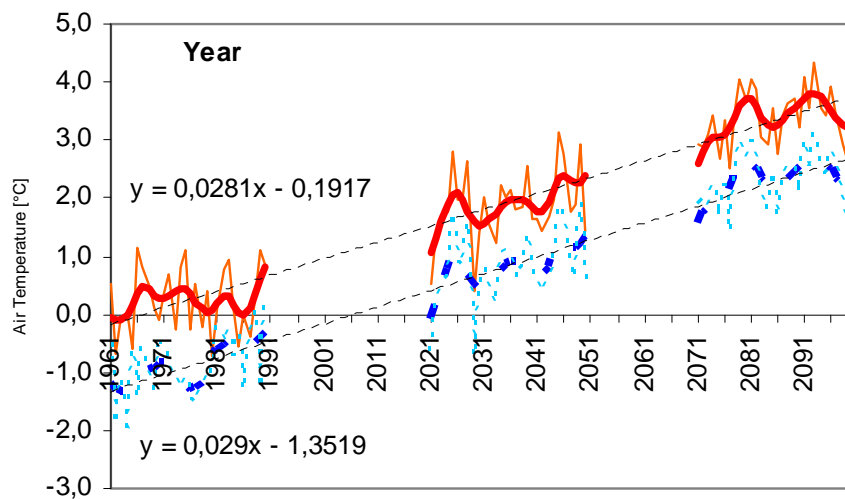


Fig. 10. Corrected and uncorrected minimum temperature [°C] for Czech and Slovak mountainous regions in the periods 1961-2100 (solid line – corrected model outputs; dashed line uncorrected outputs)

#### 4) DTA (index 004)

Table 7. Corrected and uncorrected DTA [°C] for Czech and Slovak lowland and mountainous regions in the periods 1961-1990, 2021-2050 and 2071-2100

Region	Model	Period	YEAR	DJF	MAM	JJA	SON
Lowlands	uncorr	1961-1990	7,9	5,7	9,1	9,4	7,7
Lowlands	corr	1961-1990	9,7	6,2	10,9	12,0	9,5
Mountains	uncorr	1961-1990	7,6	5,5	7,9	9,9	6,9
Mountains	corr	1961-1990	8,2	7,1	8,6	9,4	8,1
Lowlands	uncorr	2021-2050	7,8	6,0	8,7	9,3	7,6
Lowlands	corr	2021-2050	9,7	6,2	10,8	12,3	9,6
Mountains	uncorr	2021-2050	7,4	5,7	7,9	9,0	6,8
Mountains	corr	2021-2050	8,4	7,3	8,5	9,5	8,1
Lowlands	uncorr	2071-2100	8,0	5,9	8,5	9,8	7,9
Lowlands	corr	2071-2100	10,0	6,3	11,0	12,8	10,0
Mountains	uncorr	2071-2100	7,4	5,4	7,8	9,0	7,2
Mountains	corr	2071-2100	8,6	7,2	8,6	10,0	8,7

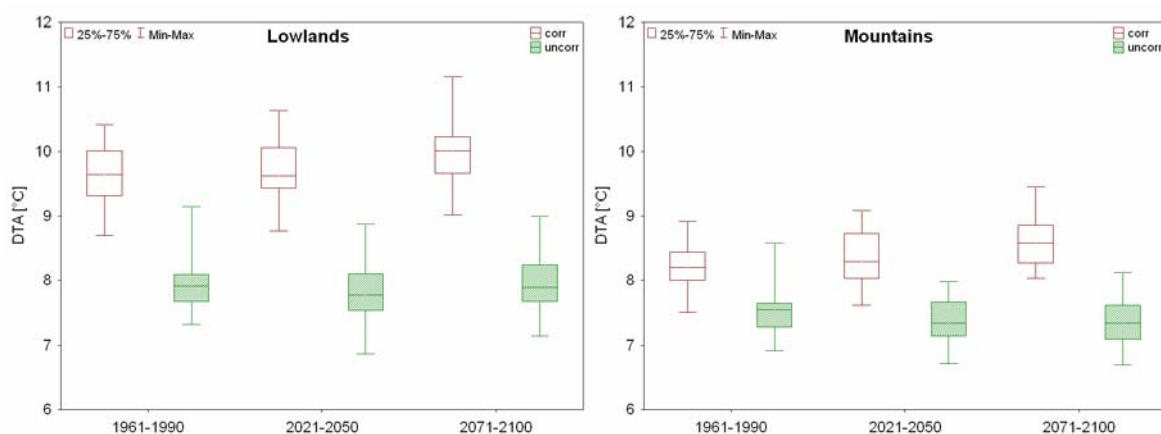


Fig. 11. Corrected and uncorrected DTA [°C] for Czech and Slovak lowland (left) and mountainous regions (right) in the periods 1961-1990, 2021-2050 and 2071-2100

Uncorrected outputs for temperature amplitude are lower for both regions (compared to corrected ones). In Lowlands the difference is quite high, between 1.8°C (1961-1990) and 2.0°C (2071-2100). In mountainous region the difference is lower: from 0.6°C for period 1961-1990 to 1.2°C for the time slice 2071-2100.

Both outputs lead to similar temperature amplitudes as in the reference period 1961-1990. Linear trends are very often very low and non-significant (see Tab. 8).

Table 8. Linear trends of the corrected and uncorrected DTA [°C] for Czech and Slovak lowland and mountainous regions in the periods 1961-1990, 2021-2050 and 2071-2100

Region	Model	Period	YEAR	DJF	MAM	JJA	SON
Lowlands	uncorr	1961-2100	0,000	0,001	-0,006	0,003	0,001
Lowlands	corr	1961-2100	0,003	0,000	0,001	0,006	0,003
Mountains	uncorr	1961-2100	-0,002	-0,001	-0,001	-0,008	0,002
Mountains	corr	1961-2100	0,004	0,002	0,000	0,005	0,005

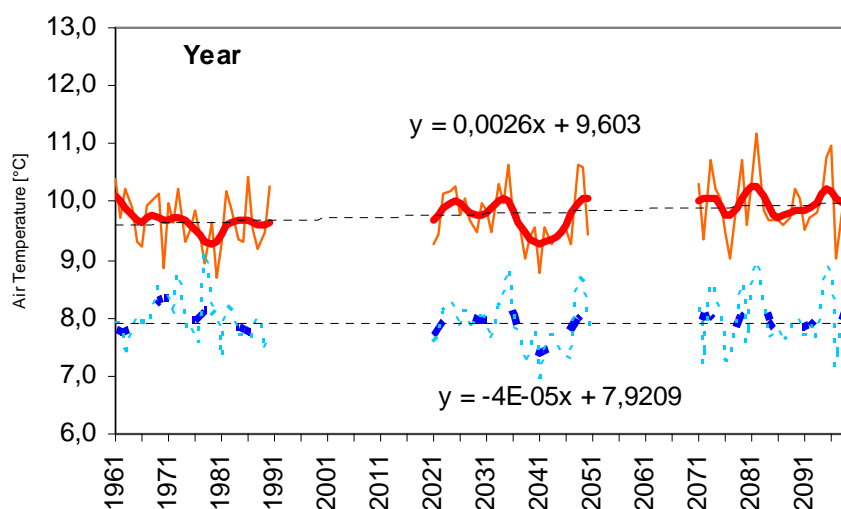


Fig. 12. Corrected and uncorrected DTA [°C] for Czech and Slovak lowland regions in the periods 1961-2100 (solid line – corrected model outputs; dashed line uncorrected outputs)

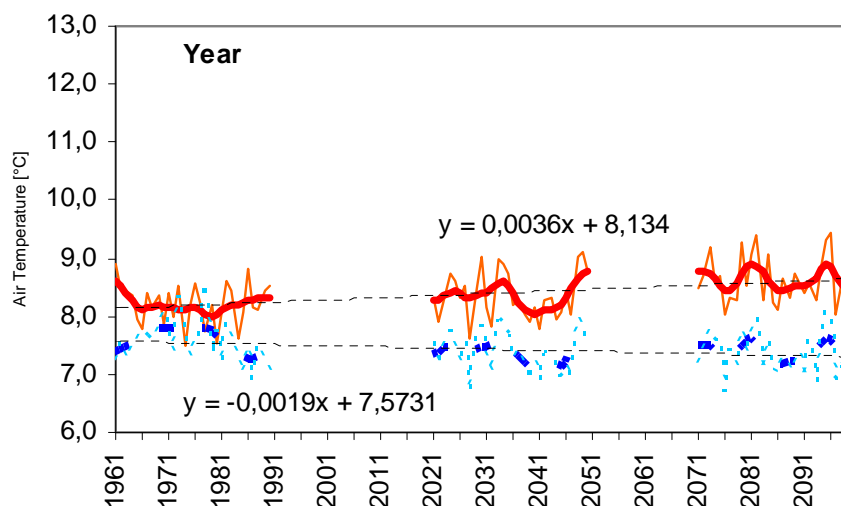


Fig. 13. Corrected and uncorrected DTA [°C] for Czech and Slovak mountainous regions in the periods 1961-2100 (solid line – corrected model outputs; dashed line uncorrected outputs)

### 5) Mean heat wave duration (index 052)

Table 9. Corrected and uncorrected I052 for Czech and Slovak lowland and mountainous regions in the periods 1961-1990, 2021-2050 and 2071-2100

Region	Model	Period	YEAR	DJF	MAM	JJA	SON
Lowlands	uncorr	1961-1990	1,8	0,7	0,7	1,8	3,1
Lowlands	corr	1961-1990	2,8	3,0	5,0	1,7	1,2
Mountains	uncorr	1961-1990	1,2	0,7	1,2	0,2	2,6
Mountains	corr	1961-1990	2,7	2,2	4,6	1,4	2,5
Lowlands	uncorr	2021-2050	2,0	1,3	0,6	3,0	2,5
Lowlands	corr	2021-2050	2,4	1,7	2,8	2,5	2,0
Mountains	uncorr	2021-2050	1,4	0,2	2,1	1,0	1,9
Mountains	corr	2021-2050	2,6	1,6	3,3	1,7	2,6
Lowlands	uncorr	2071-2100	2,4	1,4	2,4	3,4	1,2
Lowlands	corr	2071-2100	2,5	2,8	4,4	1,3	0,8
Mountains	uncorr	2071-2100	1,2	0,0	2,6	1,1	0,6
Mountains	corr	2071-2100	2,1	1,5	3,9	0,6	1,8

Corrected outputs give higher annual mean heat wave duration for both regions. Differences among seasons (between corrected and uncorrected outputs) are quite high. For winter and spring corrected model outputs are higher, but for summer and autumn uncorrected outputs predict higher values.

The change in mean heat wave duration (linear trend) is not significant for the future.

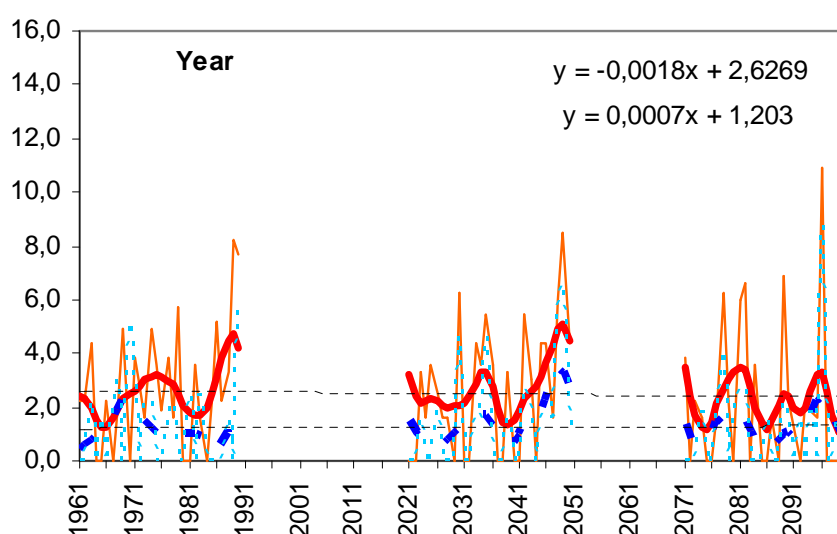


Fig. 14. Corrected and uncorrected I052 for Czech and Slovak mountainous regions in the periods 1961-2100 (solid line – corrected model outputs; dashed line uncorrected outputs)

## 6) Percentage of summer days (index 058) and percentage of hot days (index 066)

Table 10a. Corrected and uncorrected I058 [%] for Czech and Slovak lowlands and mountainous regions in the periods 1961-1990, 2021-2050 and 2071-2100

Region	Model	Period	YEAR	DJF	MAM	JJA	SON
Lowlands	uncorr	1961-1990	13,0	0,0	1,4	42,9	7,3
Lowlands	corr	1961-1990	16,1	0,0	7,9	49,2	6,8
Mountains	uncorr	1961-1990	0,2	0,0	0,0	0,6	0,1
Mountains	corr	1961-1990	0,8	0,0	0,0	3,1	0,2
Lowlands	uncorr	2021-2050	18,4	0,0	5,7	59,0	11,2

<b>Lowlands</b>	<b>corr</b>	<b>2021-2050</b>	21,8	1,1	9,5	68,0	10,4
<b>Mountains</b>	<b>uncorr</b>	<b>2021-2050</b>	1,6	0,0	2,5	5,9	3,1
<b>Mountains</b>	<b>corr</b>	<b>2021-2050</b>	3,4	1,9	3,2	12,2	3,9
<b>Lowlands</b>	<b>uncorr</b>	<b>2071-2100</b>	24,7	0,0	6,2	72,9	20,3
<b>Lowlands</b>	<b>corr</b>	<b>2071-2100</b>	28,4	1,7	13,9	80,3	19,6
<b>Mountains</b>	<b>uncorr</b>	<b>2071-2100</b>	4,1	0,0	1,6	14,6	4,2
<b>Mountains</b>	<b>corr</b>	<b>2071-2100</b>	8,0	1,7	2,0	28,0	5,9

Table 10b. Corrected and uncorrected I066 [%] for Czech and Slovak lowland and mountainous regions in the periods 1961-1990, 2021-2050 and 2071-2100

<b>Region</b>	<b>Model</b>	<b>Period</b>	<b>YEAR</b>	<b>DJF</b>	<b>MAM</b>	<b>JJA</b>	<b>SON</b>
<b>Lowlands</b>	<b>uncorr</b>	<b>1961-1990</b>	2,4	0,0	0,0	7,9	1,4
<b>Lowlands</b>	<b>corr</b>	<b>1961-1990</b>	3,6	0,0	0,3	13,5	0,3
<b>Mountains</b>	<b>uncorr</b>	<b>1961-1990</b>	0,0	0,0	0,0	0,0	0,0
<b>Mountains</b>	<b>corr</b>	<b>1961-1990</b>	0,0	0,0	0,0	0,0	0,0
<b>Lowlands</b>	<b>uncorr</b>	<b>2021-2050</b>	5,6	0,0	0,1	18,5	3,0
<b>Lowlands</b>	<b>corr</b>	<b>2021-2050</b>	7,3	0,0	0,8	25,3	2,2
<b>Mountains</b>	<b>uncorr</b>	<b>2021-2050</b>	0,0	0,0	0,0	0,0	0,0
<b>Mountains</b>	<b>corr</b>	<b>2021-2050</b>	0,0	0,0	0,0	0,0	0,0
<b>Lowlands</b>	<b>uncorr</b>	<b>2071-2100</b>	12,0	0,0	0,1	39,4	8,0
<b>Lowlands</b>	<b>corr</b>	<b>2071-2100</b>	14,4	0,0	1,6	49,1	5,8
<b>Mountains</b>	<b>uncorr</b>	<b>2071-2100</b>	0,4	0,0	0,0	1,6	0,0
<b>Mountains</b>	<b>corr</b>	<b>2071-2100</b>	0,3	0,0	0,0	1,3	0,0

Percentage of hot days (I066) is higher for corrected model outputs. Higher differences are obtained for summer. Percentage of summer days (I058) gives similar results as percentage of hot days. Corrected model outputs lead to higher number of summer days in lowlands regions (by about 3 %). Quite low values are found in the mountainous regions. For the period 2021-2050 both corrected and uncorrected outputs predict higher percentage of summer days by about 5 % in lowlands, for the second time slice the difference is more than 10 %.

For the period 2021-2050 corrected model outputs indicates change + 3.7% of hot days and uncorrected outputs about 3.2% for lowlands compared to reference period 1961-1990. This index can not be calculated for mountains at all in this period. For the period 2071-2100 both outputs give difference

higher than 10% for lowlands. Values increase mainly in summer (see Tab. 10b). Linear trend is about 3% per 10 years (Tab 11). Linear trend for summer days is 1% per 10 years in lowlands (both for corrected and uncorrected outputs).

Table 11. Linear trends of the corrected and uncorrected I066 [%] for Czech and Slovak lowland and mountainous regions in the periods 1961-1990, 2021-2050 and 2071-2100

Region	Model	Period	YEAR	DJF	MAM	JJA	SON
Lowlands	uncorr	1961-2100	0,083		0,000	0,272	0,058
Lowlands	corr	1961-2100	0,095		0,011	0,311	0,049
Mountains	uncorr	1961-2100	0,003			0,014	
Mountains	corr	1961-2100	0,003			0,012	

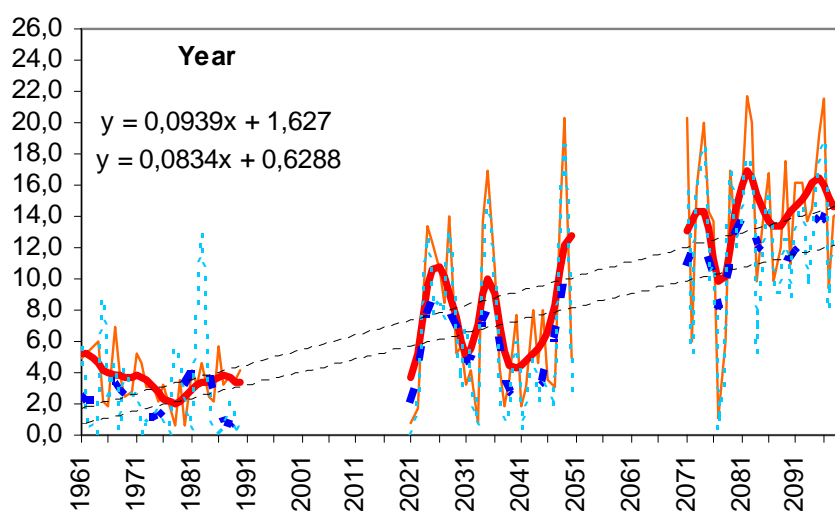


Fig. 15. Corrected and uncorrected I066 [%] for Czech and Slovak lowland regions in the periods 1961-2100 (solid line – corrected model outputs; dashed line uncorrected outputs)

## 7) Mean climatological precipitation (index 076)

Table 12. Corrected and uncorrected I076 [mm] for Czech and Slovak lowland and mountainous regions in the periods 1961-1990, 2021-2050 and 2071-2100

Region	Model	Period	YEAR	DJF	MAM	JJA	SON
Lowlands	uncorr	1961-1990	1,9	1,7	2,2	2,4	1,4
Lowlands	corr	1961-1990	1,5	1,0	1,4	2,0	1,3
Mountains	uncorr	1961-1990	4,7	4,4	5,3	5,3	4,0

<b>Mountains</b>	<b>corr</b>	<b>1961-1990</b>	2,6	1,9	2,4	3,5	2,4
<b>Lowlands</b>	<b>uncorr</b>	<b>2021-2050</b>	2,0	1,5	2,3	2,4	1,6
<b>Lowlands</b>	<b>corr</b>	<b>2021-2050</b>	1,5	0,9	1,5	1,9	1,5
<b>Mountains</b>	<b>uncorr</b>	<b>2021-2050</b>	4,8	3,9	5,6	5,5	4,2
<b>Mountains</b>	<b>corr</b>	<b>2021-2050</b>	2,6	1,7	2,6	3,5	2,5
<b>Lowlands</b>	<b>uncorr</b>	<b>2071-2100</b>	1,8	1,6	2,2	2,1	1,5
<b>Lowlands</b>	<b>corr</b>	<b>2071-2100</b>	1,4	1,1	1,5	1,6	1,4
<b>Mountains</b>	<b>uncorr</b>	<b>2071-2100</b>	4,5	4,2	5,6	4,6	3,8
<b>Mountains</b>	<b>corr</b>	<b>2071-2100</b>	2,5	1,9	2,7	2,9	2,2

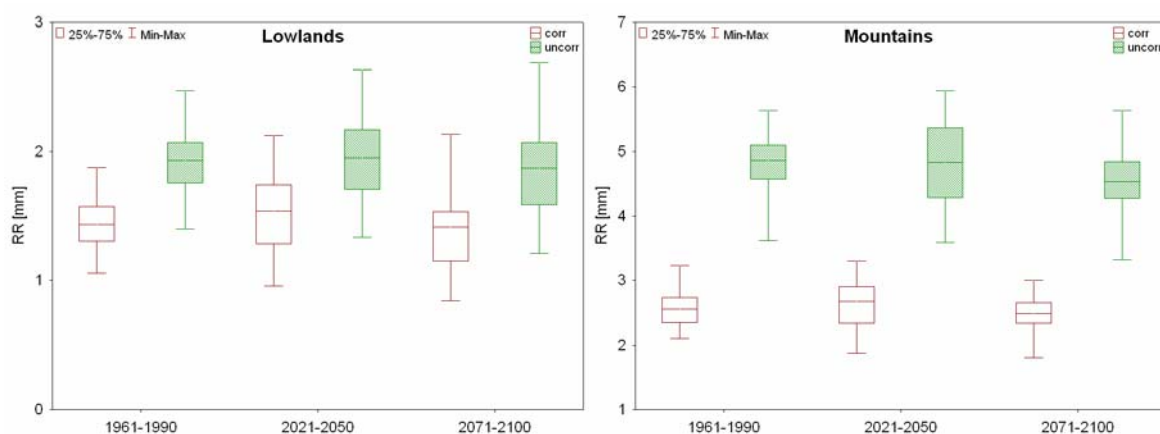


Fig. 16. Corrected and uncorrected I076 [mm] for Czech and Slovak lowland (left) and mountainous regions (right) in the periods 1961-1990, 2021-2050 and 2071-2100

Uncorrected model outputs lead to higher mean climatological precipitation for both regions. Differences are higher for mountains (2 mm; see Fig. 16). In lowlands the difference is only about 0.5 mm. For the future we get no significant change in the mean precipitation, except for summer where we can expect significant decrease 0.03-0.06 % per 10 years according to the model results.

Table 13. Linear trends of the corrected and uncorrected I076 [mm] for Czech and Slovak lowland and mountainous regions in the periods 1961-1990, 2021-2050 and 2071-2100

Region	Model	Period	YEAR	DJF	MAM	JJA	SON
<b>Lowlands</b>	<b>uncorr</b>	<b>1961-2100</b>	0,000	0,000	0,000	-0,003	0,001
<b>Lowlands</b>	<b>corr</b>	<b>1961-2100</b>	-0,001	0,000	0,001	-0,004	0,001

<b>Mountains</b>	<b>uncorr</b>	<b>1961-2100</b>	-0,001	-0,002	0,004	<b>-0,006</b>	-0,001
<b>Mountains</b>	<b>corr</b>	<b>1961-2100</b>	-0,001	0,000	<b>0,003</b>	<b>-0,006</b>	-0,001

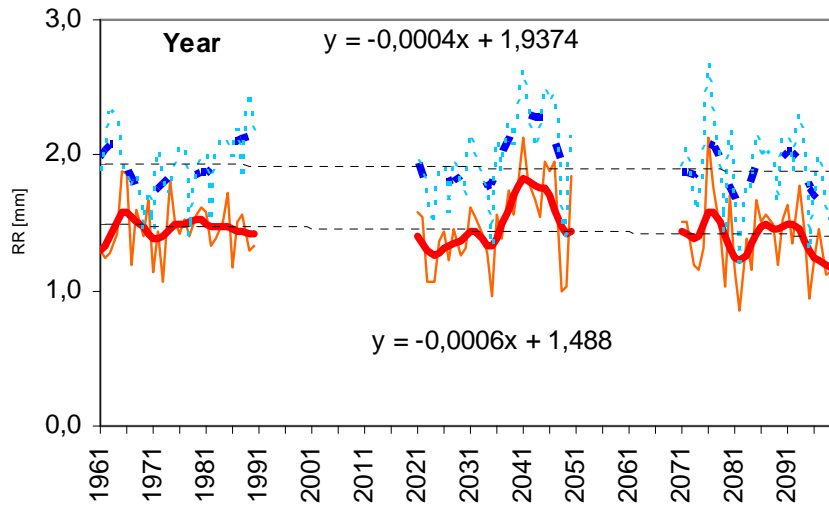


Fig. 17. Corrected and uncorrected I076 [mm] for Czech and Slovak lowland regions in the periods 1961-2100 (solid line – corrected model outputs; dashed line uncorrected outputs)

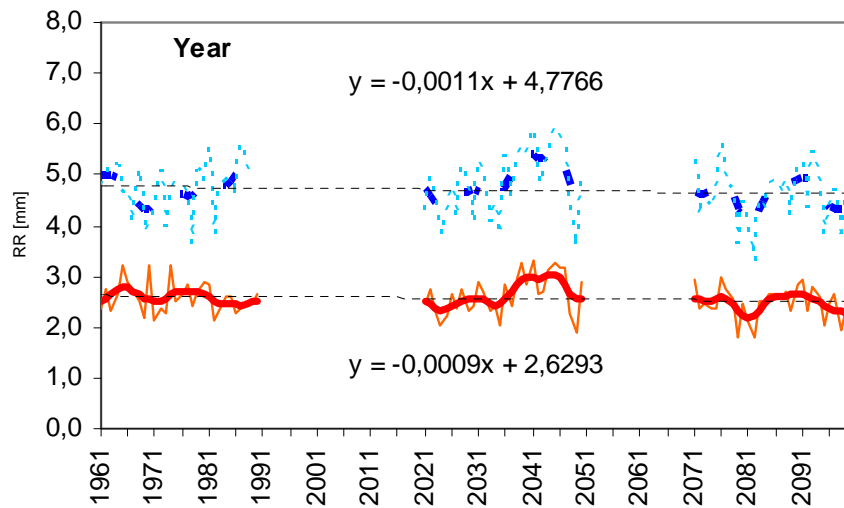


Fig. 18. Corrected and uncorrected I076 [mm] for Czech and Slovak mountainous regions in the periods 1961-2100 (solid line – corrected model outputs; dashed line uncorrected outputs)

## 8) Mean wet-day precipitation (index 077)

Table 14. Corrected and uncorrected I077 [mm] for Czech and Slovak lowland and mountainous regions in the periods 1961-1990, 2021-2050 and 2071-2100

Region	Model	Period	YEAR	DJF	MAM	JJA	SON
Lowlands	uncorr	1961-1990	5,1	5,0	5,1	5,1	5,2
Lowlands	corr	1961-1990	5,5	4,1	5,2	6,6	5,6
Mountains	uncorr	1961-1990	8,6	8,5	9,1	7,6	9,0
Mountains	corr	1961-1990	6,5	4,9	5,7	8,0	6,8
Lowlands	uncorr	2021-2050	5,5	5,0	5,1	5,6	6,1
Lowlands	corr	2021-2050	5,9	4,3	5,3	6,9	6,5
Mountains	uncorr	2021-2050	8,9	8,6	9,2	8,0	9,5
Mountains	corr	2021-2050	6,8	5,1	6,1	7,7	7,4
Lowlands	uncorr	2071-2100	5,5	5,2	5,3	5,5	6,2
Lowlands	corr	2071-2100	5,9	4,3	5,7	6,9	6,5
Mountains	uncorr	2071-2100	9,0	8,8	9,5	7,6	9,9
Mountains	corr	2071-2100	6,6	5,2	6,3	7,4	7,4

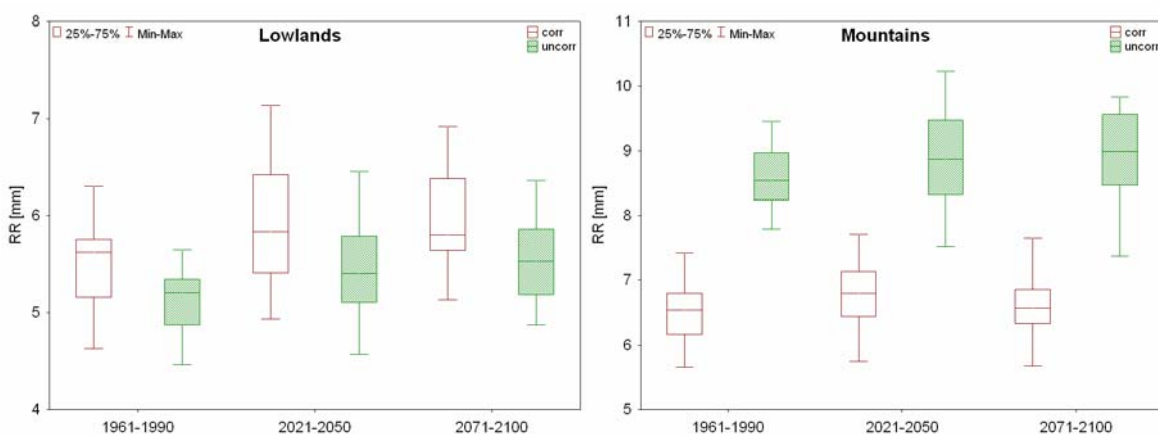


Fig. 19. Corrected and uncorrected I077 [mm] for Czech and Slovak lowland (left) and mountainous regions (right) in the periods 1961-1990, 2021-2050 and 2071-2100

Difference between corrected and uncorrected model outputs is again depending on the region (as I076). Uncorrected model outputs give lower wet-day precipitation for lowlands. Difference is 0.4 mm for each time slice. For corrected values range between lower and upper quartile (grid points) is higher. Another situation we get for mountainous region. Uncorrected model leads to higher annual wet-day precipitation from 2.1 to 2.4 mm compared to corrected values.

Linear trends are significant mainly for annual and autumn precipitation (increasing trend), but the values are low (0.03-0.1 mm per 10 years). Nonetheless, if we take into account fact that mean climatological precipitations (I076) are rather decreasing, it means that more precipitation sums will occur in less days, which should mean increase in frequency of extreme events occurrence.

Table 15. Linear trends of the corrected and uncorrected I077 [mm] for Czech and Slovak lowland and mountainous regions in the periods 1961-1990, 2021-2050 and 2071-2100

Region	Model	Period	YEAR	DJF	MAM	JJA	SON
Lowlands	uncorr	1961-2100	0,004	0,002	0,002	0,004	0,010
Lowlands	corr	1961-2100	0,004	0,002	0,004	0,003	0,009
Mountains	uncorr	1961-2100	0,004	0,003	0,004	0,001	0,009
Mountains	corr	1961-2100	0,001	0,003	0,006	-0,005	0,006

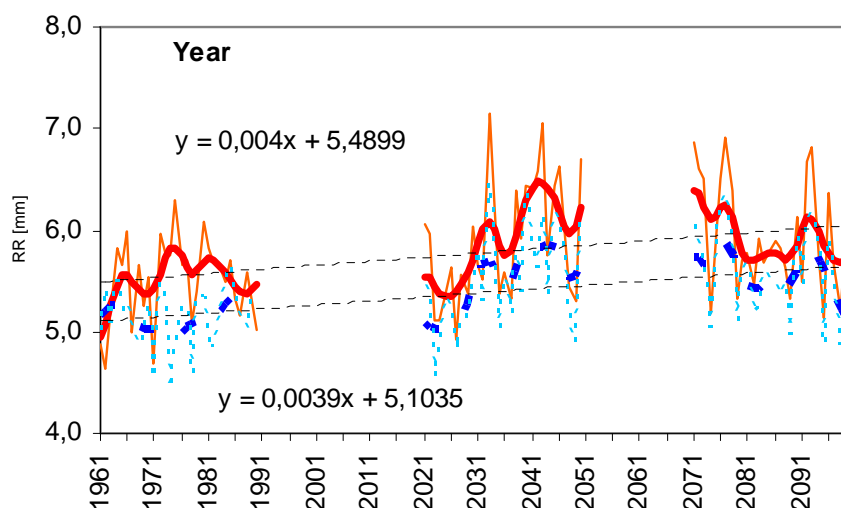


Fig. 20. Corrected and uncorrected I077 [mm] for Czech and Slovak lowland regions in the periods 1961-2100 (solid line – corrected model; dashed line uncorrected model)

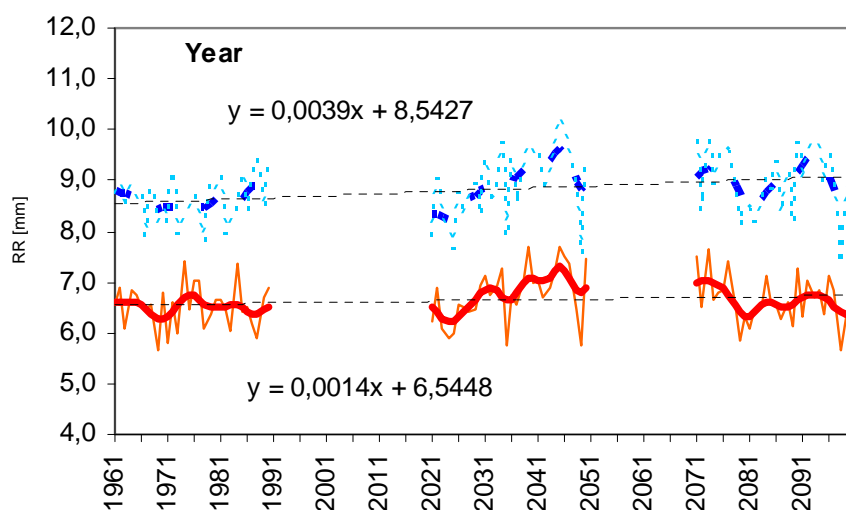


Fig. 21. Corrected and uncorrected I077 [mm] for Czech and Slovak mountainous regions in the periods 1961-2100 (solid line – corrected model; dashed line uncorrected model)

### 9) Greatest 1-day total rainfall (index 113)

Table 16. Corrected and uncorrected I113 [mm] for Czech and Slovak lowland and mountainous regions in the periods 1961-1990, 2021-2050 and 2071-2100

Region	Model	Period	YEAR	DJF	MAM	JJA	SON
Lowlands	uncorr	1961-1990	36,7	18,3	25,6	28,0	21,2
Lowlands	corr	1961-1990	32,6	13,6	20,8	28,9	20,7
Mountains	uncorr	1961-1990	68,6	37,3	49,7	55,3	45,2
Mountains	corr	1961-1990	44,6	20,8	24,8	38,7	28,1
Lowlands	uncorr	2021-2050	40,5	18,3	26,5	31,5	24,6
Lowlands	corr	2021-2050	35,4	14,3	22,0	29,5	24,2
Mountains	uncorr	2021-2050	71,6	37,2	51,0	56,8	47,4
Mountains	corr	2021-2050	48,0	20,7	27,9	40,3	31,5
Lowlands	uncorr	2071-2100	40,7	19,4	26,8	30,6	23,1
Lowlands	corr	2071-2100	35,7	15,1	22,6	28,8	22,7
Mountains	uncorr	2071-2100	69,2	38,3	52,4	52,8	45,3
Mountains	corr	2071-2100	46,1	21,4	28,3	38,3	29,9

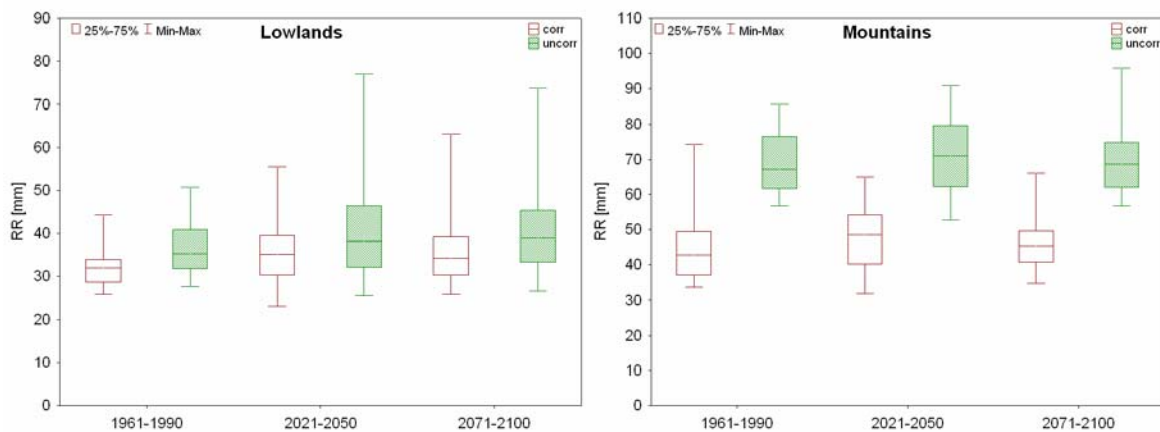


Fig. 22. Corrected and uncorrected I113 [mm] for Czech and Slovak lowland (left) and mountainous regions (right) in the periods 1961-1990, 2021-2050 and 2071-2100

Uncorrected model outputs indicate higher greatest 1-day total rainfall (compared to corrected ones) for lowlands by about 4 mm for the reference period 1961-1990 and 5 mm for the two time slices. For mountainous regions the differences are much higher (more than 20 mm; see Fig. 22). For the corrected values a range between lower and upper quartile (grid points) values is lower in both regions compared to uncorrected outputs.

In the period 2021-2050 both outputs predict higher value of I113 by 2.8 mm in lowlands and 3-3.4 mm in mountains. For the second time slice (2071-2100) and lowlands we see the same values as in the previous one (2021-2050), in mountains we get about 2 mm lower values. Linear trend is low, but statistically significant for annual values and most of the seasons.

Table 17. Linear trends of the corrected and uncorrected I113 [mm] for Czech and Slovak lowland and mountainous regions in the periods 1961-1990, 2021-2050 and 2071-2100

Region	Model	Period	YEAR	DJF	MAM	JJA	SON
Lowlands	uncorr	1961-2100	0,002	0,000	0,000	0,003	0,000
Lowlands	corr	1961-2100	0,002	-0,001	0,001	0,001	0,001
Mountains	uncorr	1961-2100	0,002	0,001	0,003	0,001	0,000
Mountains	corr	1961-2100	0,004	0,001	0,003	0,004	0,002

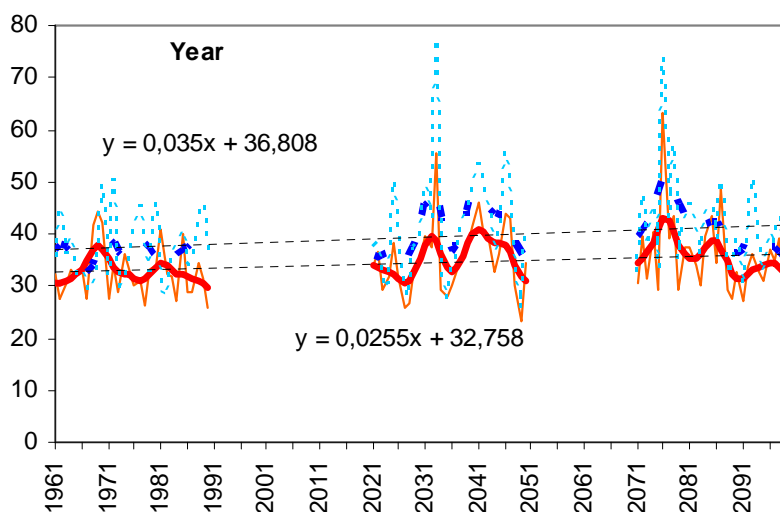


Fig. 23. Corrected and uncorrected I113 [mm] for Czech and Slovak lowland regions in the periods 1961-2100 (solid line – corrected model; dashed line uncorrected model)

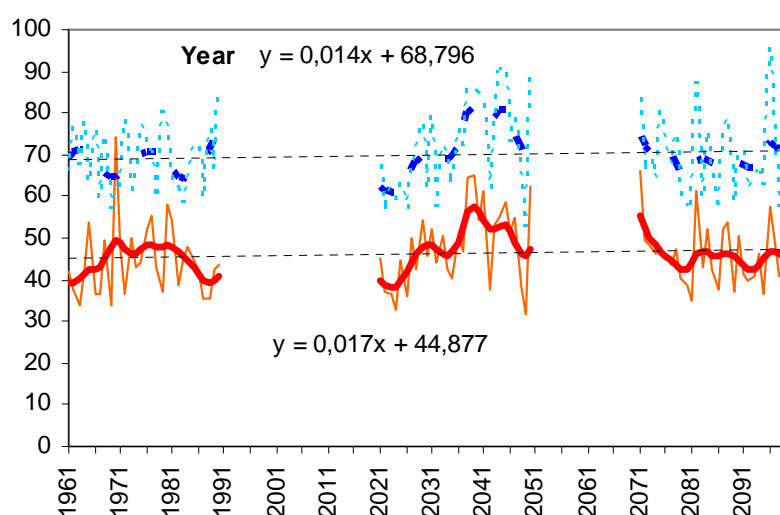


Fig. 24. Corrected and uncorrected I113 [mm] for Czech and Slovak mountainous regions in the periods 1961-2100 (solid line – corrected model; dashed line uncorrected model)

### 10) Greatest 5-day total rainfall (index 115)

Table 18. Corrected and uncorrected I115 [mm] for Czech and Slovak lowland and mountainous regions in the periods 1961-1990, 2021-2050 and 2071-2100

Region	Model	Period	YEAR	DJF	MAM	JJA	SON
Lowlands	uncorr	1961-1990	65,9	36,0	48,2	51,8	37,5

<b>Lowlands</b>	<b>corr</b>	<b>1961-1990</b>	53,8	23,9	33,6	47,3	35,8
<b>Mountains</b>	<b>uncorr</b>	<b>1961-1990</b>	139,4	86,0	102,4	103,7	92,8
<b>Mountains</b>	<b>corr</b>	<b>1961-1990</b>	86,4	45,6	49,4	72,1	58,9
<b>Lowlands</b>	<b>uncorr</b>	<b>2021-2050</b>	70,5	34,6	48,0	54,4	43,8
<b>Lowlands</b>	<b>corr</b>	<b>2021-2050</b>	62,7	25,4	38,3	50,9	42,1
<b>Mountains</b>	<b>uncorr</b>	<b>2021-2050</b>	147,2	80,5	109,6	103,9	98,6
<b>Mountains</b>	<b>corr</b>	<b>2021-2050</b>	92,0	43,1	57,9	72,8	63,7
<b>Lowlands</b>	<b>uncorr</b>	<b>2071-2100</b>	71,0	37,6	49,4	52,0	40,2
<b>Lowlands</b>	<b>corr</b>	<b>2071-2100</b>	61,6	27,8	40,1	47,6	38,6
<b>Mountains</b>	<b>uncorr</b>	<b>2071-2100</b>	141,0	83,5	113,0	96,3	90,8
<b>Mountains</b>	<b>corr</b>	<b>2071-2100</b>	86,3	45,0	59,6	68,5	58,1

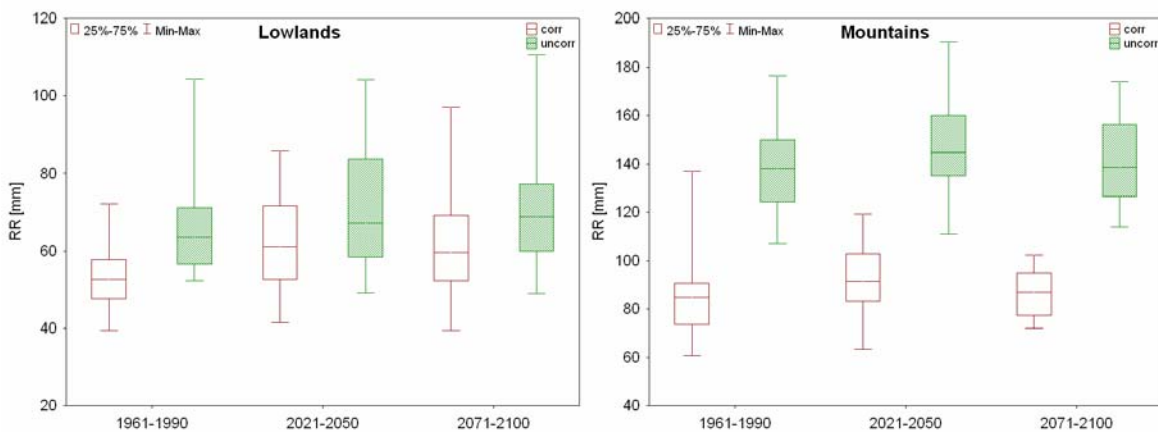


Fig. 25. Corrected and uncorrected I115 [mm] for Czech and Slovak lowland (left) and mountainous regions (right) in the periods 1961-1990, 2021-2050 and 2071-2100

Uncorrected model outputs give higher value of 5-day total rainfall compared to corrected ones for both regions. In lowlands differences vary between 7.8 mm (2021-2050) and 12.1 mm (reference period). In the mountainous regions differences are substantially higher. Highest differences are found for the reference period 1961-1990 (40 mm; see Fig. 25).

Linear trend is statistically significant for all annual values and for most of the seasons. The highest values of the index are predicted in the period 2021-2050. The two last decades in the period 2071-2100 show substantially decreasing trend (see Fig. 22).

Table 19. Linear trends of the corrected and uncorrected I113 [mm] for Czech and Slovak lowland and mountainous regions in the periods 1961-1990, 2021-2050 and 2071-2100

Region	Model	Period	YEAR	DJF	MAM	JJA	SON
Lowlands	uncorr	1961-2100	0,003	-0,001	-0,002	0,004	0,002
Lowlands	corr	1961-2100	0,006	0,002	0,004	0,002	0,000
Mountains	uncorr	1961-2100	0,009	-0,001	0,007	0,007	0,004
Mountains	corr	1961-2100	0,004	0,001	0,007	0,003	0,000

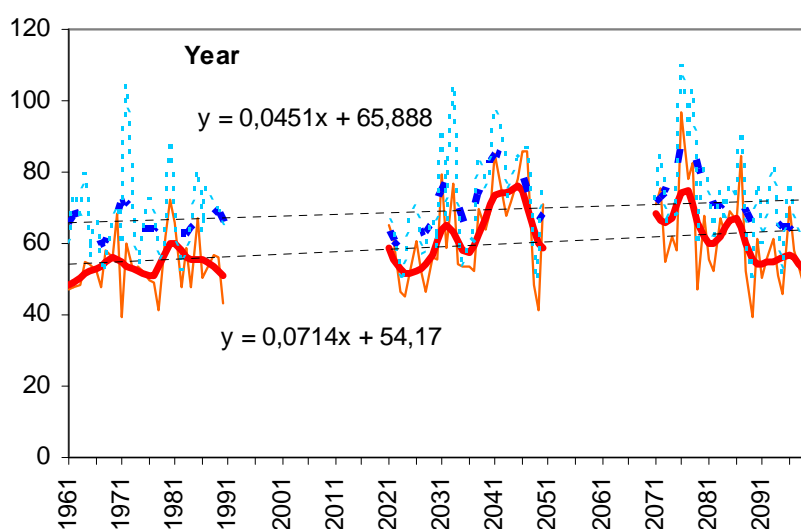


Fig. 26. Corrected and uncorrected I115 [mm] for Czech and Slovak lowland regions in the periods 1961-2100 (solid line – corrected model; dashed line uncorrected model)

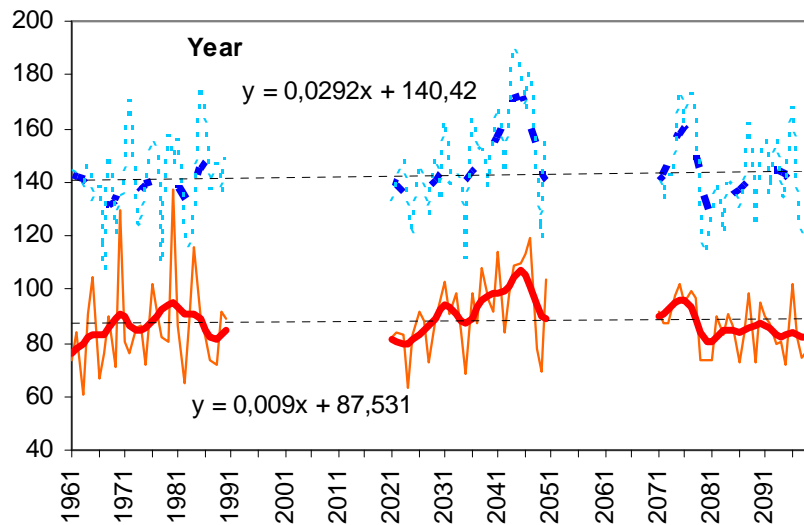


Fig. 27. Corrected and uncorrected I115 [mm] for Czech and Slovak mountainous regions in the periods 1961-2100 (solid line – corrected model; dashed line uncorrected model)

## 11) Conclusions

It was shown on example of processing extreme indices for the ALADIN-Climate CZ outputs (the area of the Czech and Slovak Republic), that there exist differences between results for corrected and uncorrected RCM outputs. The comparison was done separately for mountainous and lowland regions. Found discrepancies in the results (e.g. making corrected temperatures too high and precipitations too low for mountainous regions compared to lowlands) probably follow from the way of the technical series calculation (station measurements to model grid points) which are then used for validation and correction of model outputs. There was a presumption that using model orography will lead to better results (since model is tuned to that “wrong” orography), but it seems it would have been better to use real orography since then the corrected outputs would not be lowered to such extend and would seem more realistic (in case of temperature and also precipitation). Thus we recommend to recalculate station data to model grid points (for model validation and correction) using “real” orography, because RCMs, even with wrong orography, are capable to handle the altitude bias to some extent.

If we would analyze only corrected simulations of ALADIN-Climate/CZ RCM for air temperature and precipitation with special focus on differences between lowland and mountainous regions of the Czech and Slovak Republic, we would found no significant changes between the two regions neither for near (2051-2070) nor far future (2071-2100). The regions show similar values of change and trends. For uncorrected outputs we can see the differences but the problem is that the results are biased to some extend because of model errors. With current state (used way of model outputs correction) we recommend to apply, for analysis of trends, uncorrected model outputs, but in case we need to work with variance and higher statistical moments, it seems better to work with corrected results even if we need to

take into account that absolute values, mainly for higher elevations, are lower than expected (see previous paragraph for explanation).

It is needed to continue working on the issue of correction method evaluation in the future and to compare results from more models. Such cooperation has been already established between CHMI, CUNI and BOCU and will continue even beyond scope (end) of the CECILIA project.

## References

- Déqué, M., Frequency of precipitation and temperature extremes over France in an anthropogenic scenario: model results and statistical correction according to observed values. *Global and Planetary Change*, 57, 16-26, 2007.
- Farda, A., Štěpánek, P., Halenka, T., Skalák, P. and Belda, M., Model ALADIN in climate mode forced with ERA-40 reanalysis (coarse resolution experiment). *Meteorological journal*, 10, 123-130, 2007.
- Farda, A., Dynamical downscaling of Air Temperature in the Central Europe (PhD. thesis, in Czech with extended abstract in English). Faculty of Mathematics and Physics, Charles University in Prague, 2008.
- Skalák, P., Štěpánek, P., Farda, A., Validation of ALADIN-Climate/CZ for present climate (1961–1990) over the Czech Republic. *Időjárás*, Vol. 112, No. 3-4, pp. 191-201, 2008.
- Štěpánek, P., ProClimDB – software for processing climatological datasets, CHMI, !! HYPERLINK "http://www.climahom.eu" <http://www.climahom.eu>, 2008
- Štěpánek, P., Zahradníček, P. a Skalák, P., 2009, Data quality kontrol and homogenization of air temperature and precipitation series in the area of the Czech Republic in the period 1961–2007. *Advances in Science and Research*, 3, 23–26, 2009 <http://www.adv-sci-res.net/3/23/2009/>.

## **D4.4 a1.2 Selected extreme indices for the area of the Czech Republic: spatial comparison of results applying station data and RCM output**

Petr Štěpánek (CHMI), Pavel Zahradníček (CHMI), Petr Skalák (CHMI), Aleš Farda (CHMI),

Jan Kyselý (IAP)

In the following text we compare selected extreme indices calculated for the area of the Czech Republic either from station data or from outputs of RCM ALADIN-Climate/CZ outputs at 10 km resolution (driven by GCM ARPEGE). RCM description can be found e.g. in Farda et al. (2007) or Farda (2008). All input station observations were quality controlled, homogenized in daily scale and gaps in data were filled (details can be found e.g. in Štěpánek et al., 2009). Spatial distribution of the used stations (268) can be seen in Fig. 1. Maps of indices calculated from station data are part of Deliverable D4.2 (Appendix B). Unfortunately it was not possible to use also outputs of RCM ALADIN-Climate/CZ at 25 km resolution from project ENSEMBLES for further comparison in this analysis due to technical problems at CHMI (breakdown of PC with stored ENSEMBLES data) so that calculations were not available for this deliverable.

All data processing was done by ProClimDB database software (free download from <http://www.climahom.eu/>) for processing of climatological datasets (Štěpánek, 2008). Interpolation was carried out applying approach adopted at CHMI utilizing local linear regression (dependence of given meteorological element on altitude) and universal kriging interpolation method.

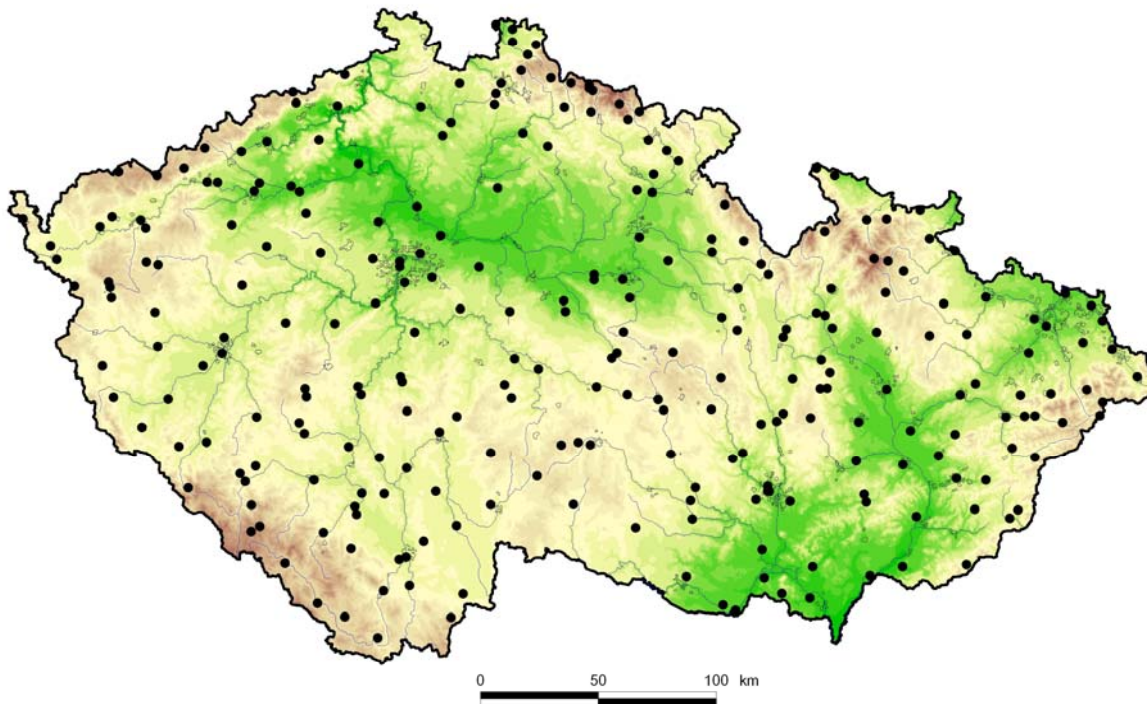


Fig. 1. Climatological station network used for indices calculation

### **1) Maximum temperature (index 001)**

For winter (DJF) time frame, differences between RCM ALADIN @10 km outputs and station data are only 0,2°C (in average for the whole Czech Republic) but spatial differences are quit high, values span from -3,7°C to 2,8°C. The most negative biases are obtained for eastern and north-eastern parts of the Czech Republic (Zlin and Moravskoslezsky region), in average by 0.7°C. On the contrary for western parts of the Czech Republic (Karlovarský region) temperatures are higher by 1°C in spatial average. Another warmer region is Českomoravská vrchovina (region Vysočina).

Maximum temperatures for summer time frame are according to RCM ALADIN @10 km outputs smaller by -0,99°C. Values (differences) span from -3,67 to 3,85°C, but majority of the area is negatively biased. Greatest differences are obtained for NW and central Bohemia (in average up to 1,2°C). Minimum differences are found in southern Moravia. Positively biased are areas of Krkonoše and Beskydy mountains.

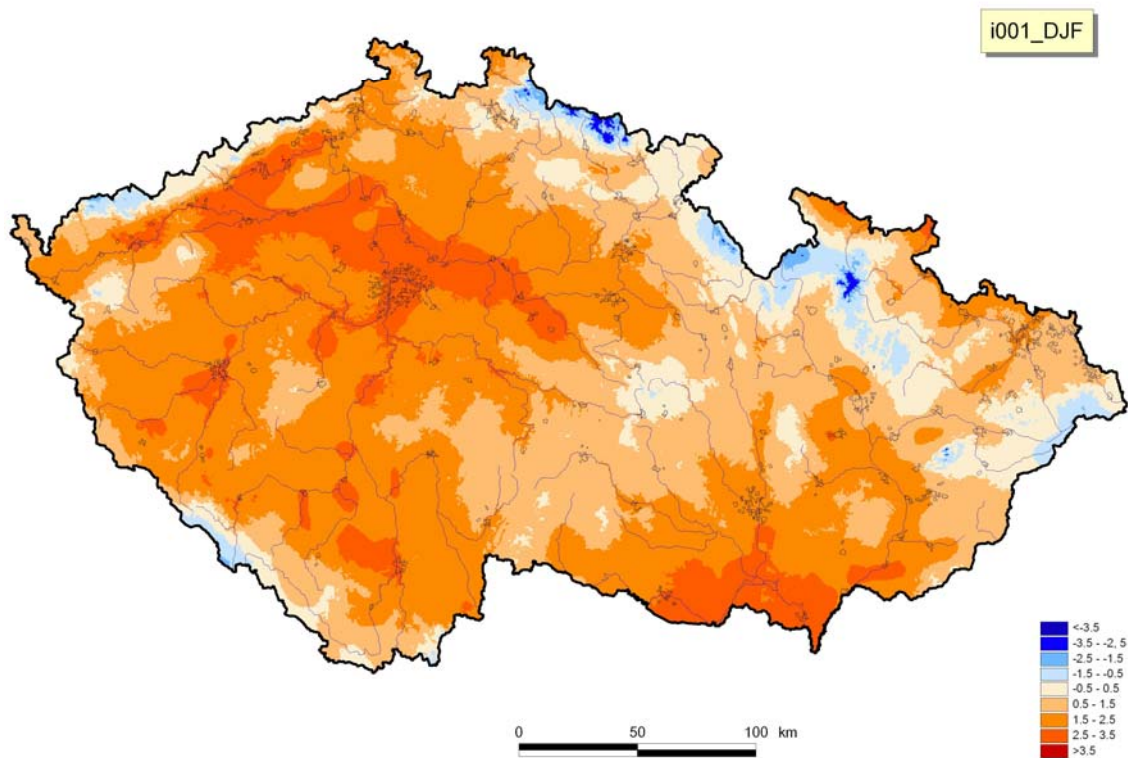


Fig. 2a. Maximum temperature [°C] for the area of the Czech Republic from outputs of ALADIN-Climate/CZ (driven by GCM ARPEGE) in the period 1961-1990. DJF

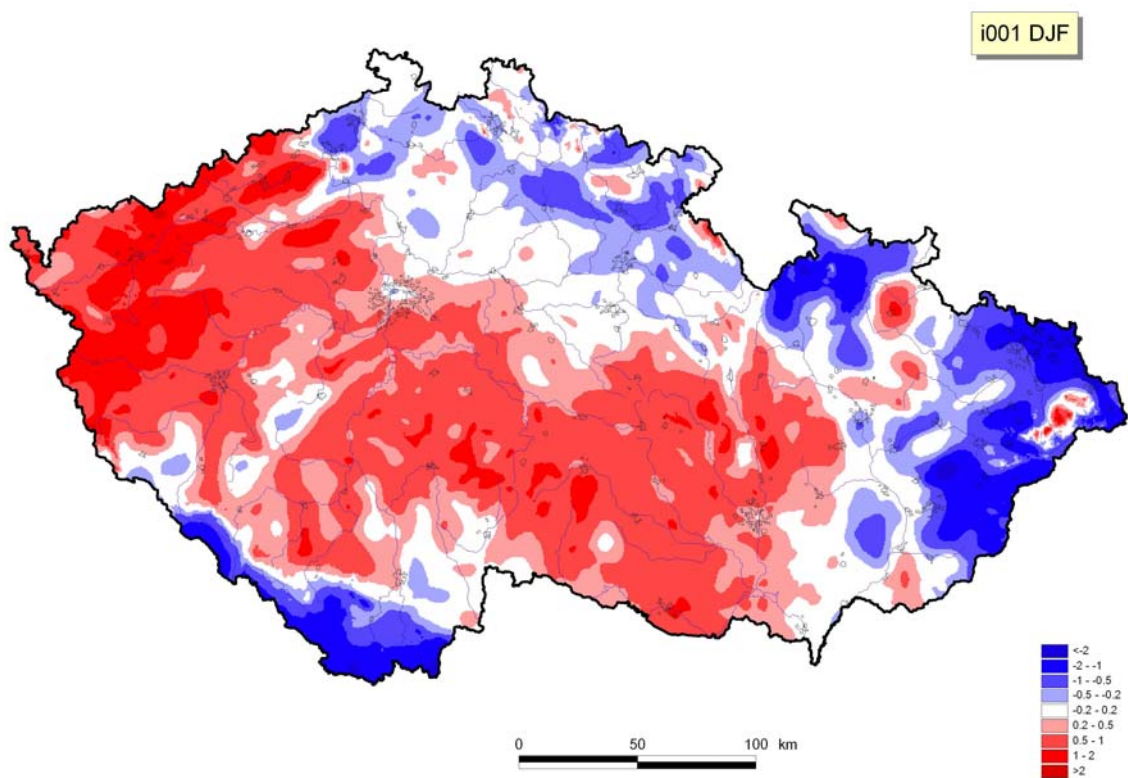


Fig. 2b. Differences between RCM ALADIN @10 km outputs and station data for the area of the Czech Republic in the period 1961-1990. DJF.

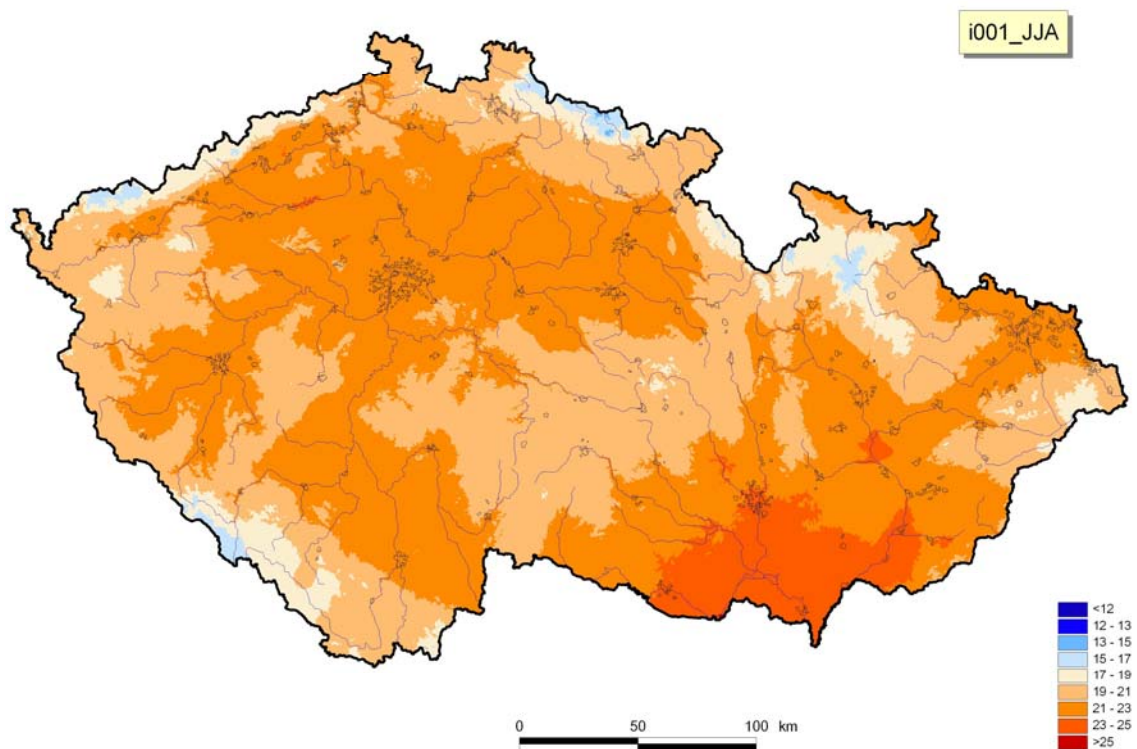


Fig. 3a. Maximum temperature [ $^{\circ}\text{C}$ ] for the area of the Czech Republic from outputs of ALADIN-Climate/CZ (driven by GCM ARPEGE) in the period 1961-1990. JJA

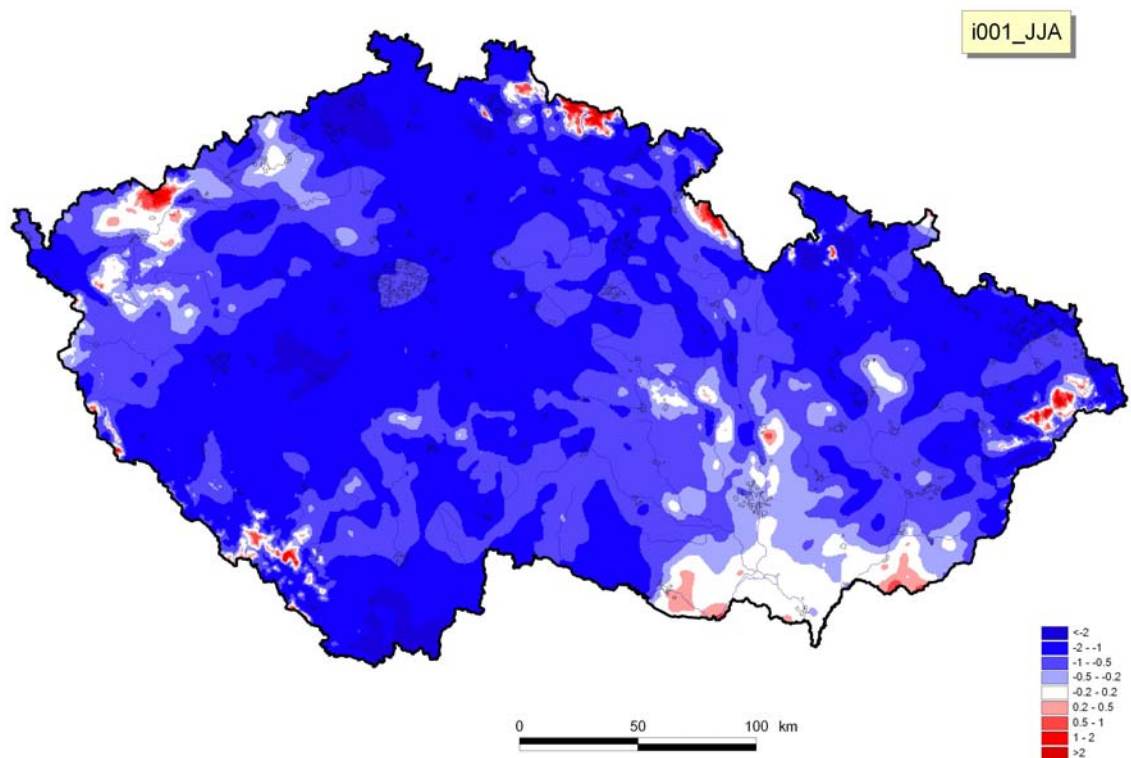


Fig. 3b. Differences between RCM ALADIN @10 km outputs and station data for the area of the Czech Republic in the period 1961-1990. JJA.

## 2) Minimum temperature (index 002)

Variance for minimum air temperature in winter is smaller for the model outputs than for stations data. Moreover model outputs are positively biased for this index, in average for the whole Czech Republic they are higher by 0,61°C. Greatest differences occur in southern and south-western Bohemia (Jihočeský and Plzeňský region). Model outputs agree with station data mainly in Moravia (Zlínský, Olomoucký and Jihomoravský region) and in eastern Bohemia (Královehradecký region). Model strongly overestimates minimum temperature in Krkonoše mountains and on the contrary for Prague it gives markedly lower temperatures.

For summer time frame, index i002 for the whole Czech Republic is higher in the model by 1,47°C compared to station data. Differences span from -2,12 to 3,87°C. Similarly as for winter, model outputs are overestimated for most of the area. Southern Moravia is the warmest part of the Czech Republic and the model ALADIN estimates minimum temperatures to be even more higher by 2,12°C.

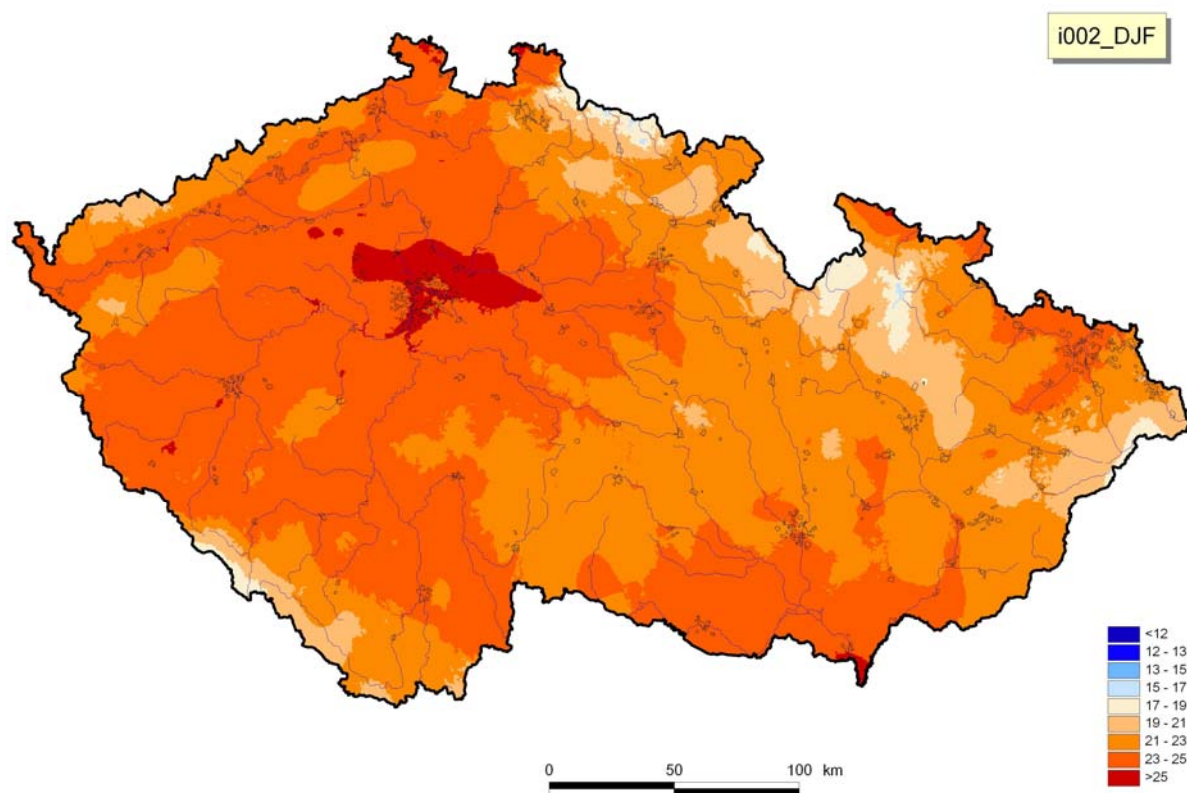


Fig. 4a. Minimum temperature [°C] for the area of the Czech Republic from outputs of ALADIN-Climate/CZ (driven by GCM ARPEGE) in the period 1961-1990. DJF

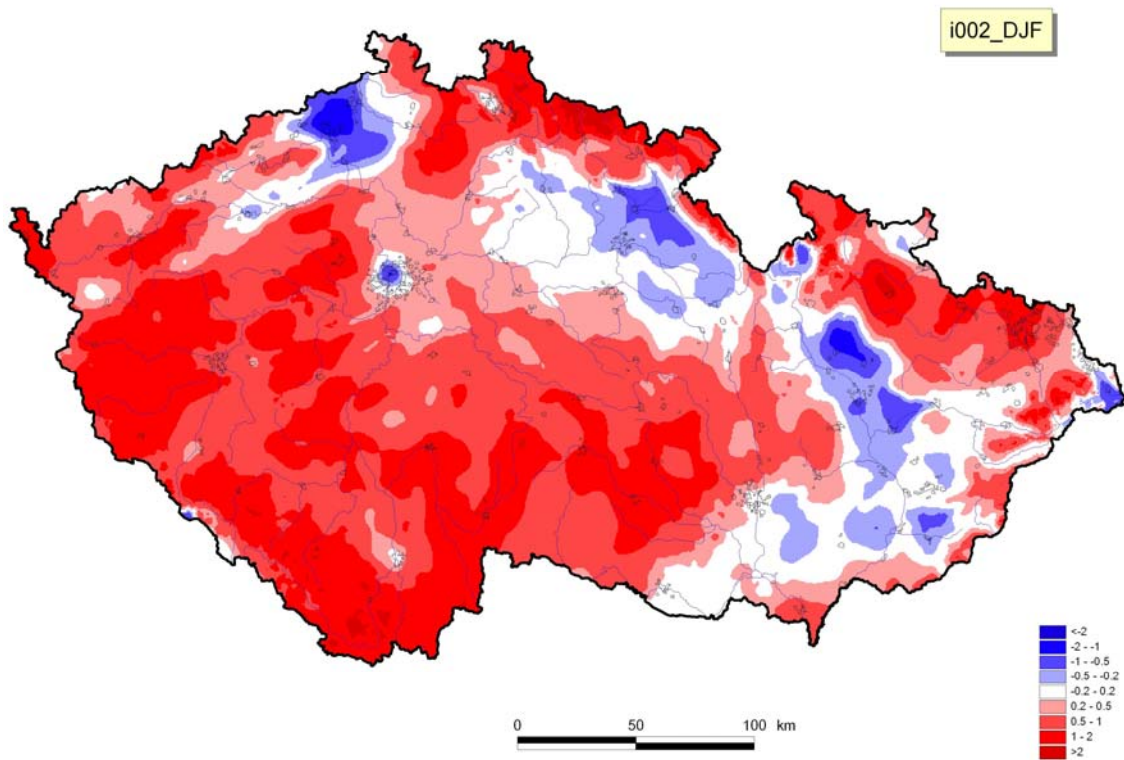


Fig. 5b. Differences between RCM ALADIN @10 km outputs and station data for the area of the Czech Republic in the period 1961-1990. DJF.

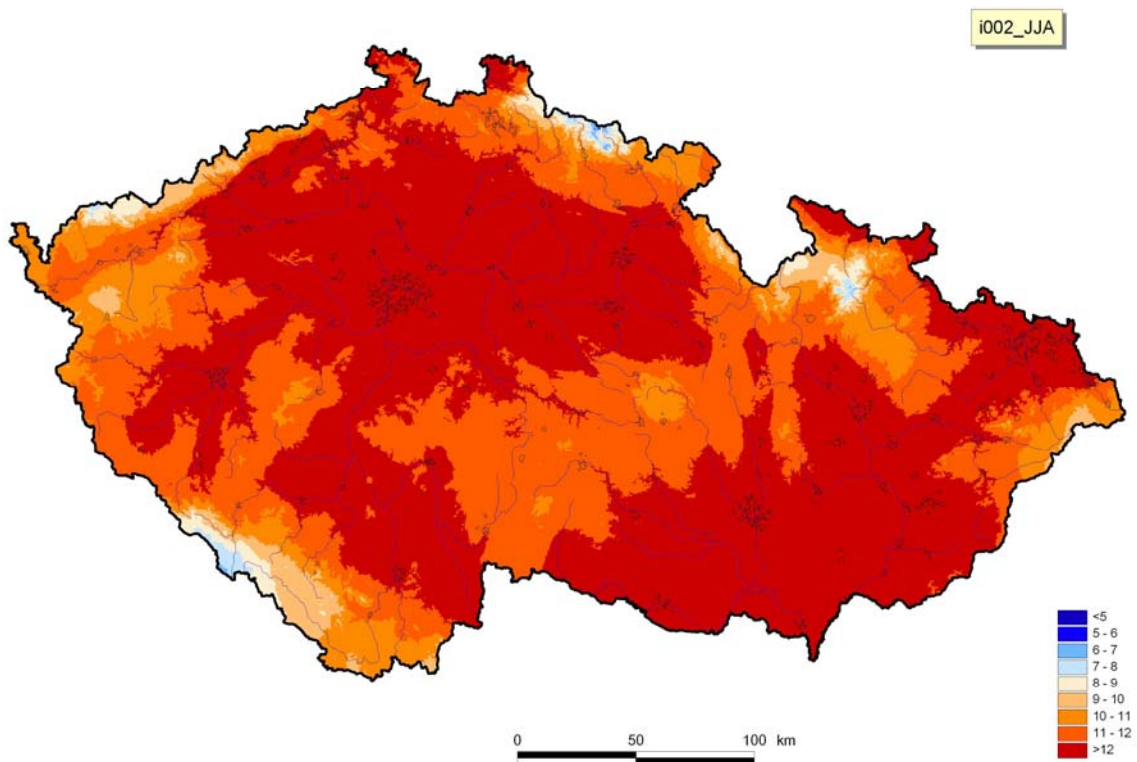


Fig. 4a. Minimum temperature [°C] for the area of the Czech Republic from outputs of ALADIN-Climate/CZ (driven by GCM ARPEGE) in the period 1961-1990. JJA

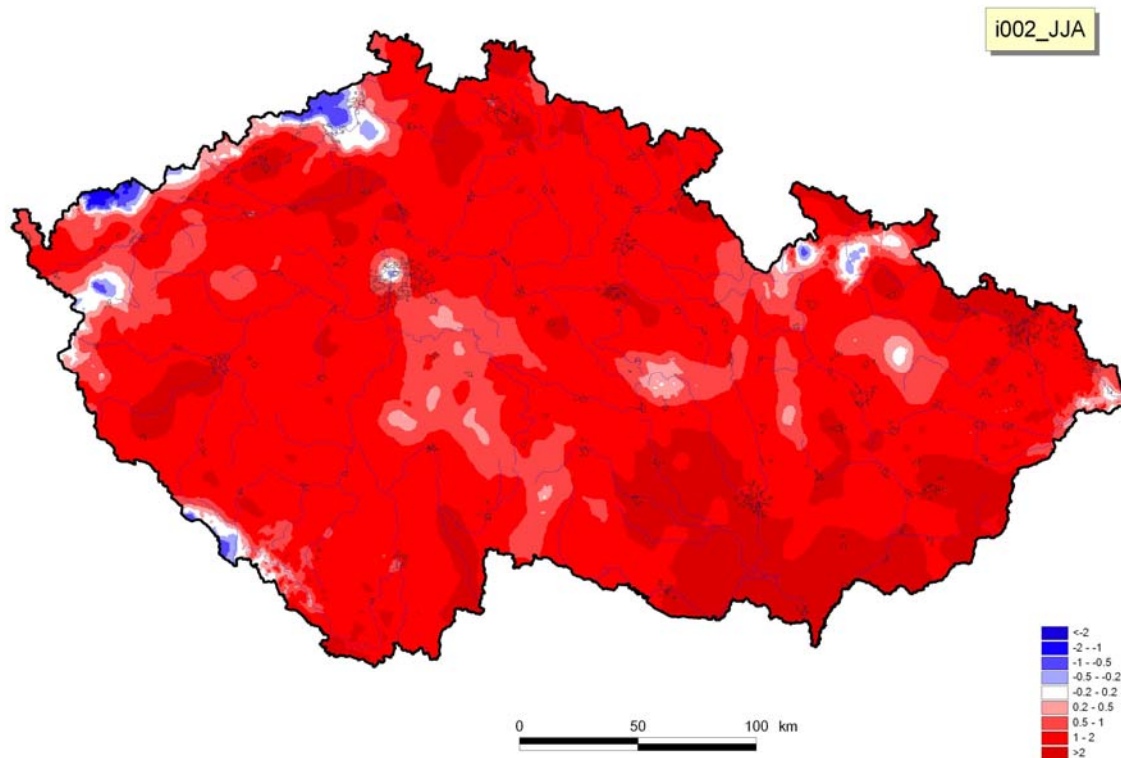


Fig. 5b. Differences between RCM ALADIN @10 km outputs and station data for the area of the Czech Republic in the period 1961-1990. JJA.

### 3) Air temperature (index 003)

Mean air temperature for winter time frame are according to ALADIN 10 km higher by  $0,41^{\circ}\text{C}$  for the whole are of the Czech Republic. Differences span from  $-1,62^{\circ}\text{C}$  to  $3,10^{\circ}\text{C}$ . Spatial distribution of differences between model and station data is similar to index 001 (maximum temperature). Western part of Bohemia (Karlovarský a Plzeňský region) and Vysočina are the most overestimated. Results for most of Moravia and western Bohemia (Polabí) are in agreement in both datasets.

In case of summer time frame, model outputs give mean temperatures higher by  $0,85^{\circ}\text{C}$  (for the whole are of the Czech Republic). Difference vary between  $-1,36^{\circ}\text{C}$  and  $4,98^{\circ}\text{C}$ . The highest differences are obtained for southern and eastern Moravia ( $+1,25^{\circ}\text{C}$  in average for the whole region).

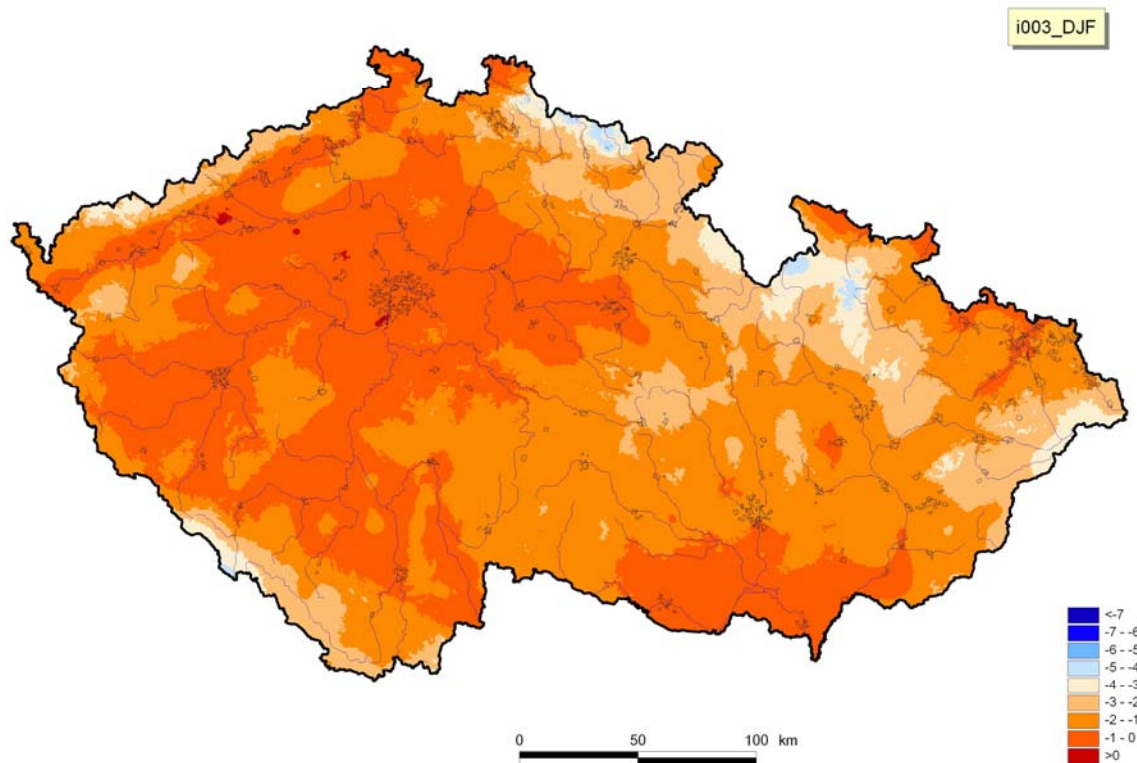


Fig. 6a. Mean air temperature [ $^{\circ}$ C] for the area of the Czech Republic from outputs of ALADIN-Climate/CZ (driven by GCM ARPEGE) in the period 1961-1990. DJF

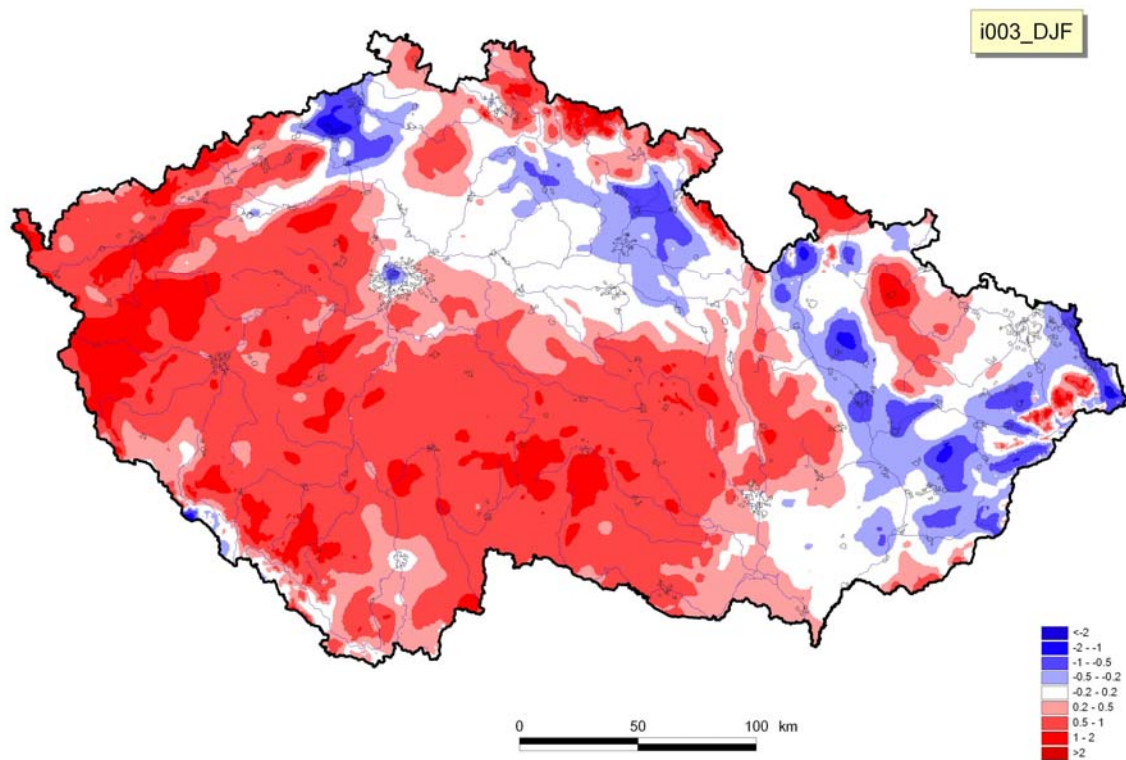


Fig. 6b. Differences between RCM ALADIN @10 km outputs and station data for the area of the Czech Republic in the period 1961-1990. DJF.

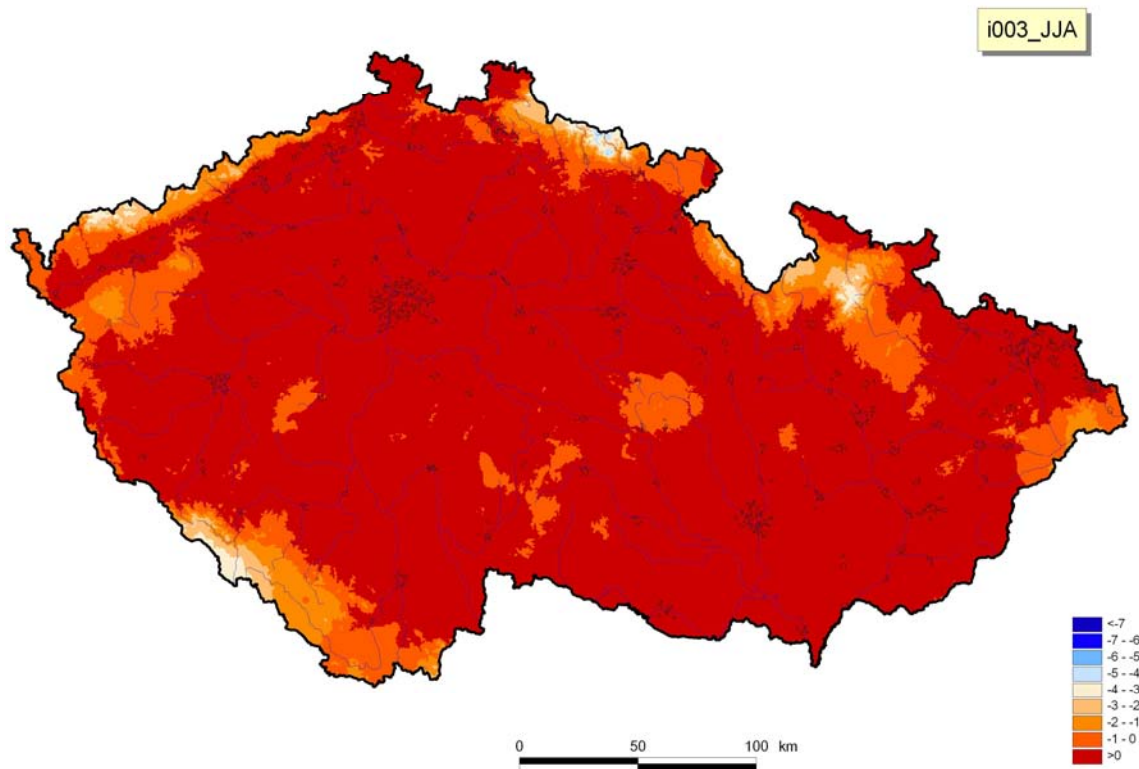


Fig. 7a. Mean air temperature [°C] for the area of the Czech Republic from outputs of ALADIN-Climate/CZ (driven by GCM ARPEGE) in the period 1961-1990. JJA

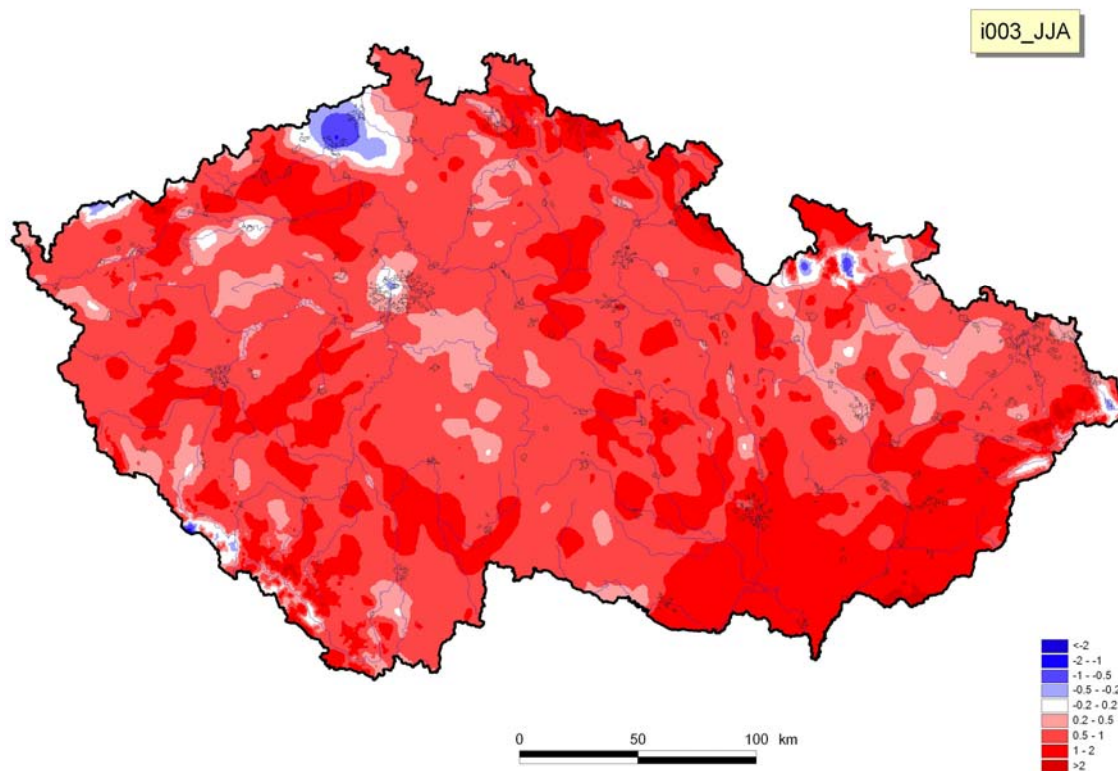


Fig. 8b. Differences between RCM ALADIN @10 km outputs and station data for the area of the Czech Republic in the period 1961-1990. JJA.

#### 4) Percentage of summer days (index 058)

Percentage of summer days is overestimated by the model ALADIN @ 10 km by 4,98% (average for the whole area of the Czech Republic). Differences between model and station data vary from -9,72 to 2,51%. Highest differences are found in central and north-western Bohemia. On the contrary minimum differences occur in the highly elevated parts of the Czech Republic. These results are caused by minimum occurrence of summer days in these areas. For the rest of the republic, the lowest differences are found in southern Moravia.

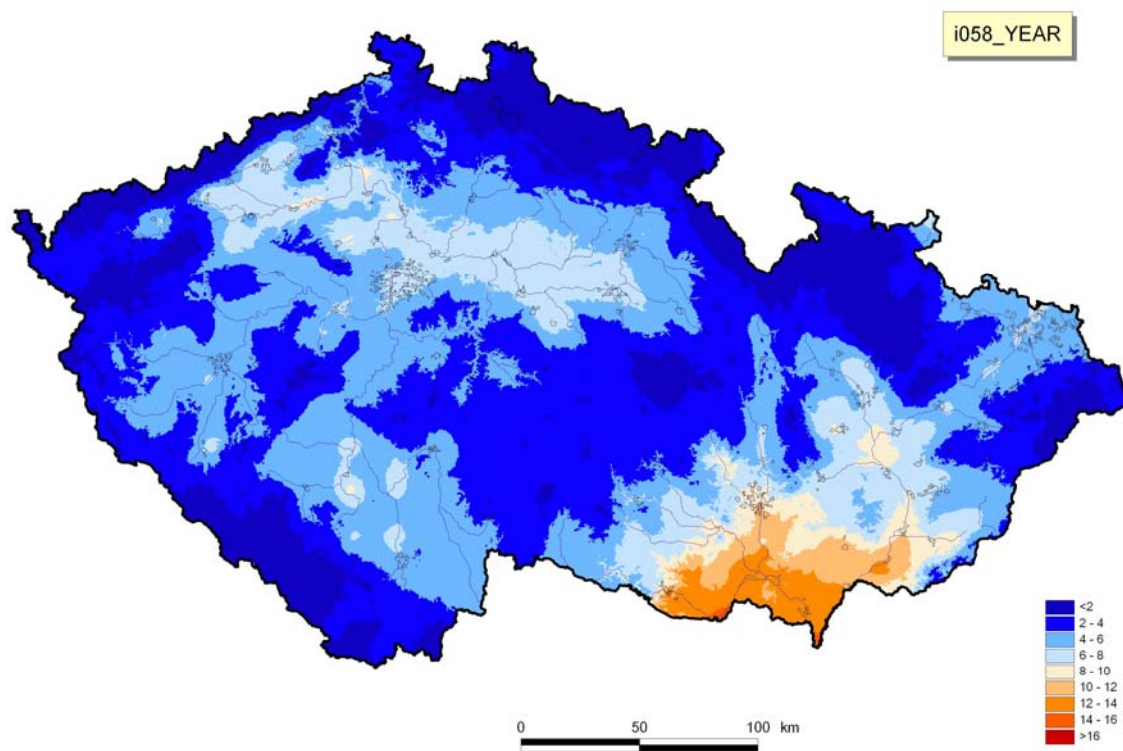


Fig. 8a. Percentage of summer days for the area of the Czech Republic from outputs of ALADIN-Climat/CZ (driven by GCM ARPEGE) in the period 1961-1990. Year

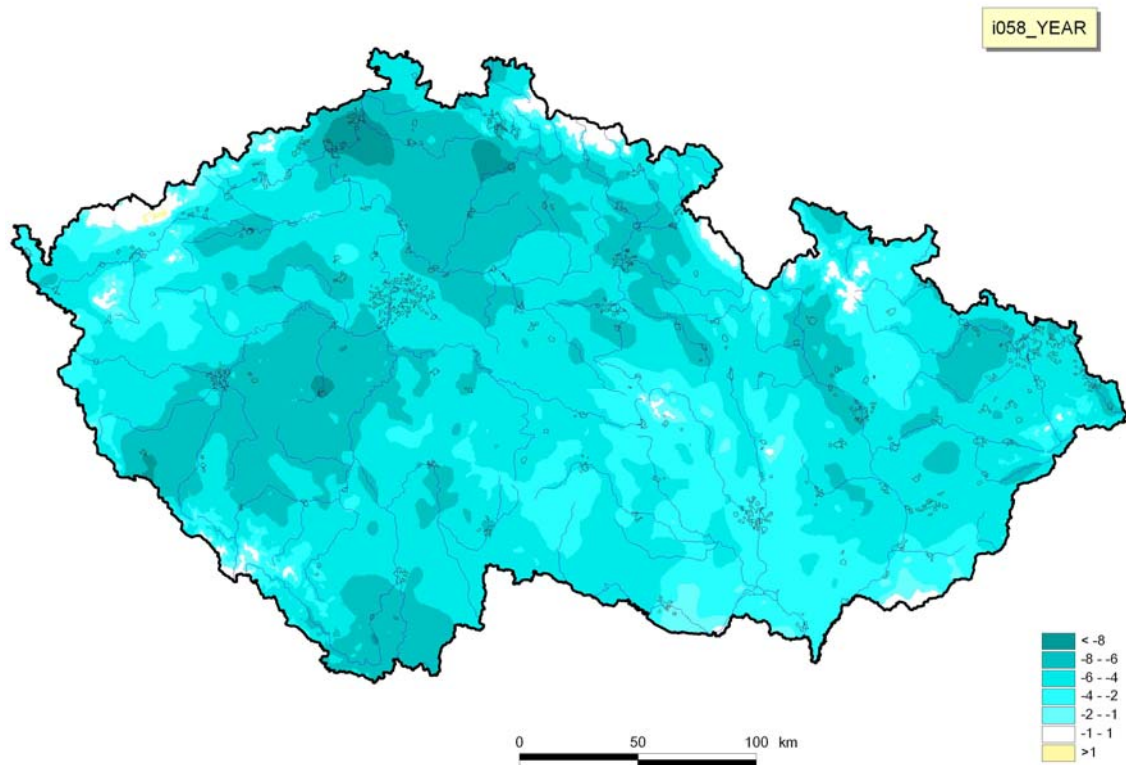


Fig. 8b. Differences between RCM ALADIN @10 km outputs and station data for the area of the Czech Republic in the period 1961-1990. Year.

### **5) Percentage of hot days (index 066)**

Occurrence of hot days is not frequent in the area of the Czech Republic. Average for the whole area is only 1,41%, for the model outputs it is even by 0,95% less. Differences span from -2,91 to 1,78%. Similar to index 58 (percentage of summer days), mountainous areas coincides the best because of zero values in these areas. Spatial distribution of differences is the same as for index i058.

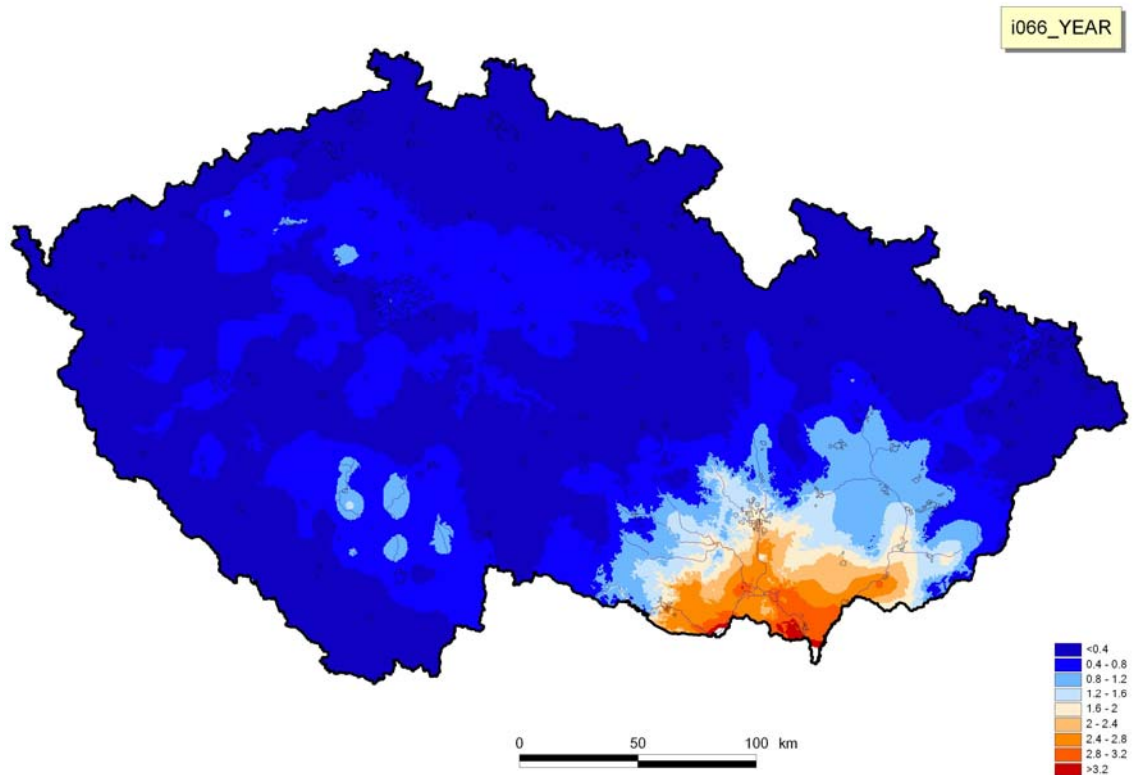


Fig. 9a. Maximum temperature [°C] for the area of the Czech Republic from outputs of ALADIN-Climate/CZ (driven by GCM ARPEGE) in the period 1961-1990. Year

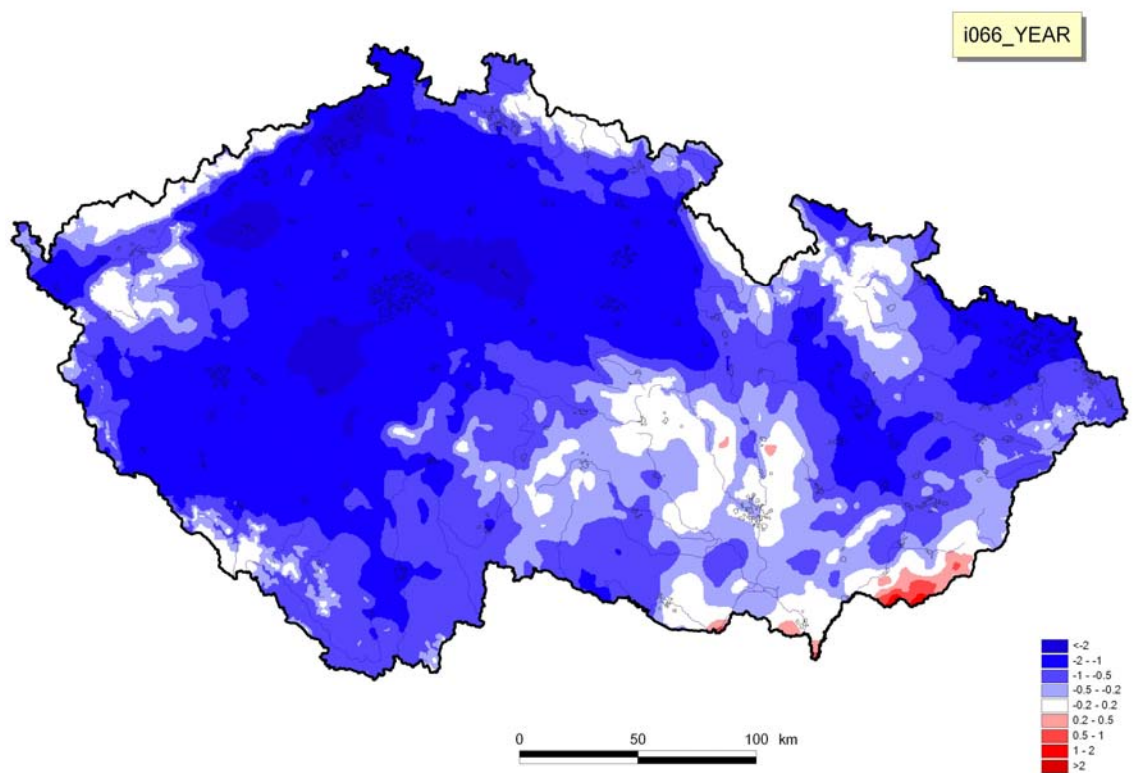


Fig. 9b. Differences between RCM ALADIN @10 km outputs and station data for the area of the Czech Republic in the period 1961-1990. Year

## 6) Mean climatological precipitation (index 076)

Mean climatological precipitation in winter time frame is according to the model outputs higher by 0,63 mm compared to station data. Differences between the two datasets are quite high, they vary from -2,72 up to 6,66 mm. Greater differences are found in Bohemia. Model underestimates markedly mean precipitation in Šumava Mountains. Smaller difference between model and station data is found in southern Moravia.

For summer time frame the model calculates values of mean climatological precipitation higher by 0,75 mm (for the whole are of the Czech Republic). Differences vary less than in winter, from -1,04 to 4,61 mm. Spatial distribution of differences is similar to winter months. Greater differences are found for area of Bohemia, the best agreement is achieved in eastern parts of the Czech Republic.

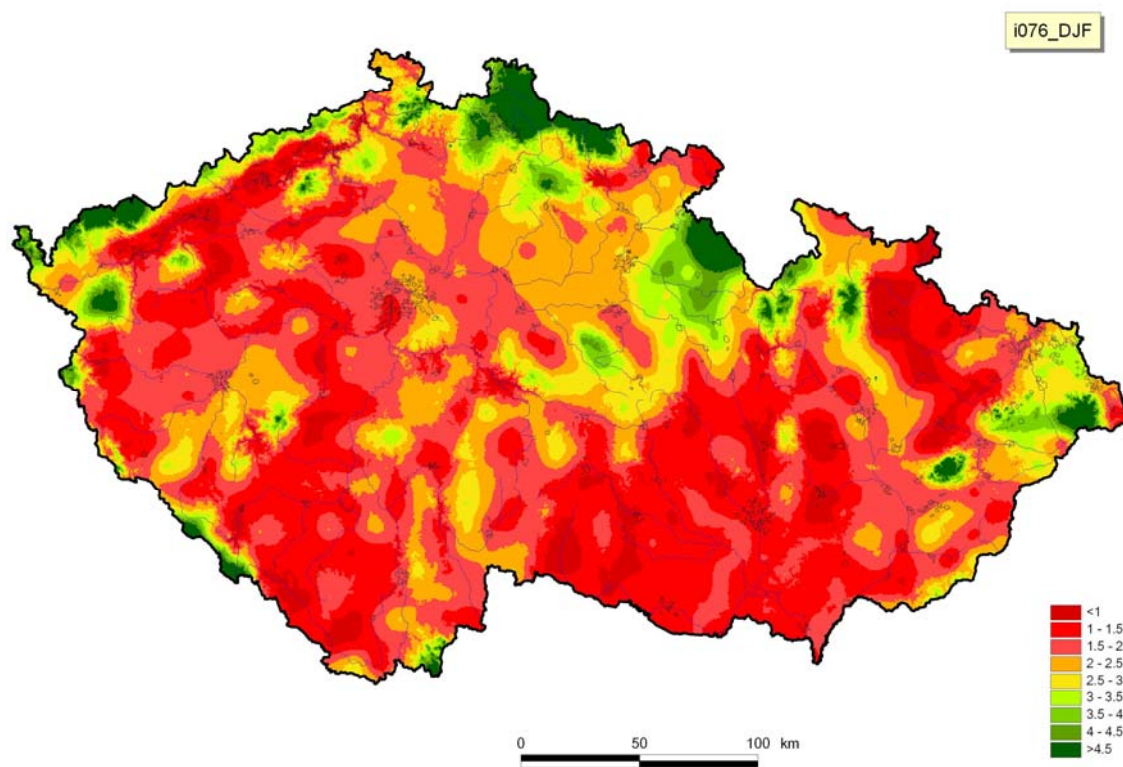


Fig. 10a. Mean climatological precipitation [mm] for the area of the Czech Republic from outputs of ALADIN-Climate/CZ (driven by GCM ARPEGE) in the period 1961-1990. DJF

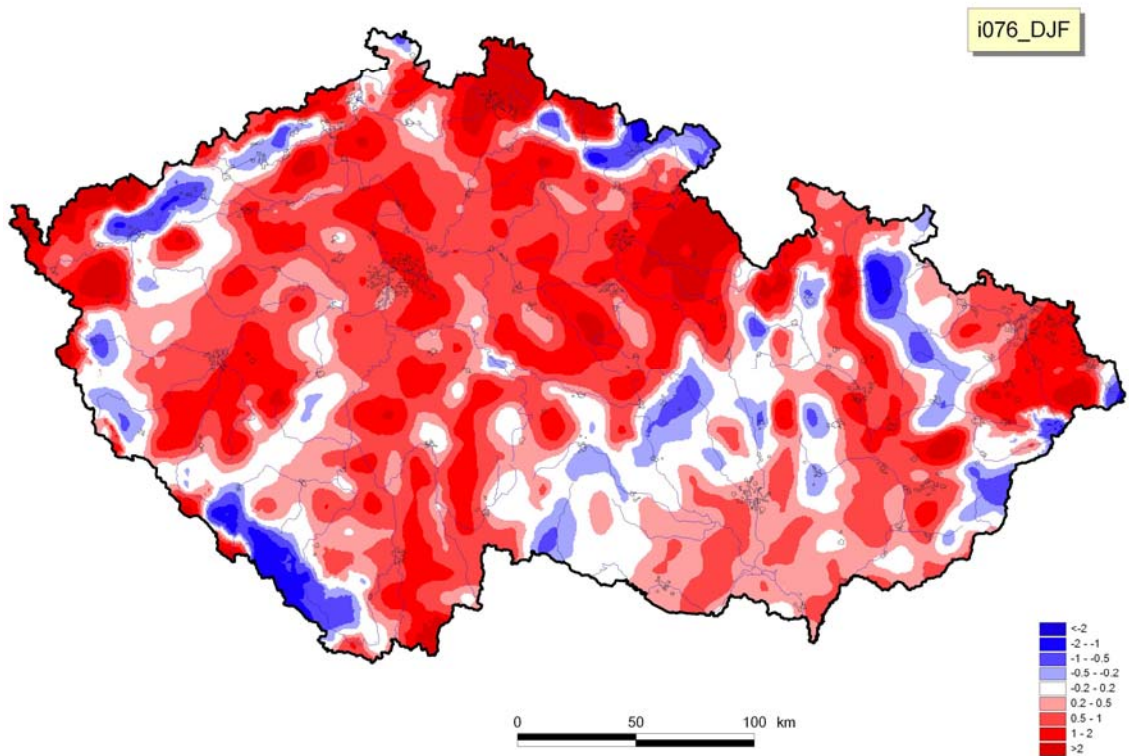


Fig. 10b. Differences between RCM ALADIN @10 km outputs and station data for the area of the Czech Republic in the period 1961-1990. DJF.

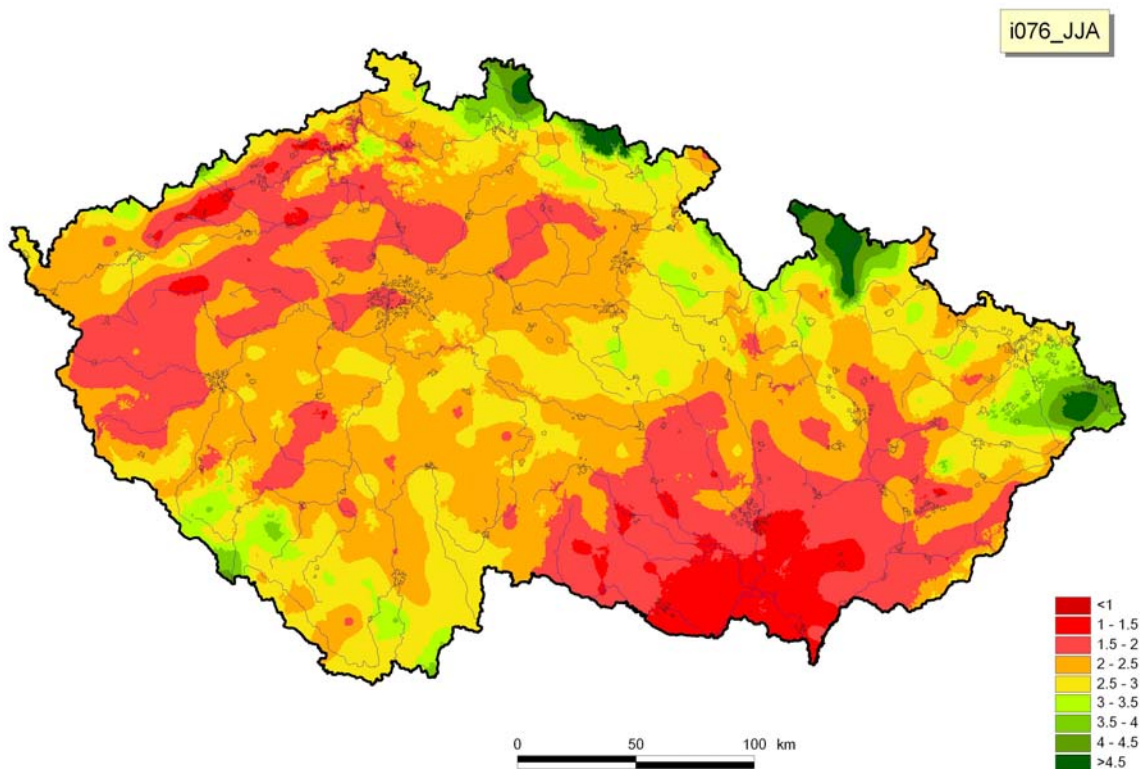


Fig. 11a. Mean climatological precipitation [mm] for the area of the Czech Republic from outputs of ALADIN-Climate/CZ (driven by GCM ARPEGE) in the period 1961-1990. JJA

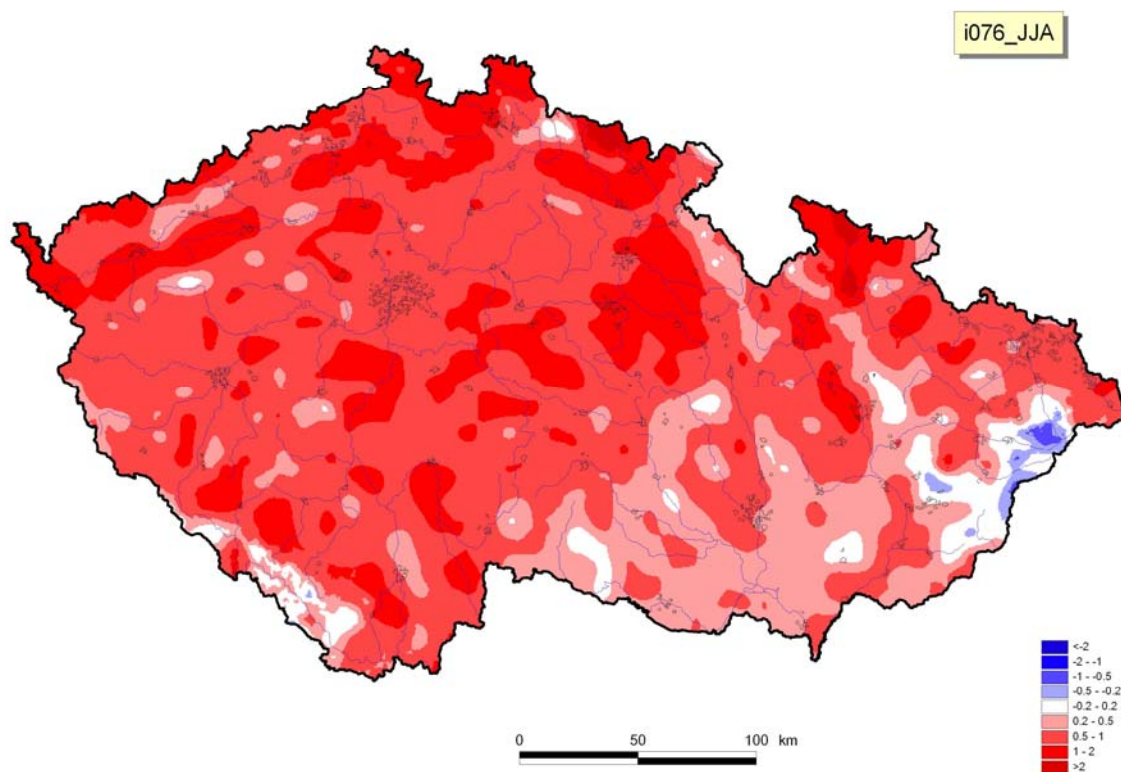


Fig. 11b. Differences between RCM ALADIN @10 km outputs and station data for the area of the Czech Republic in the period 1961-1990. JJA.

## 7) Mean wet-day precipitation (index 077)

Similar to the previous index, mean wet-day precipitation in winter time frame is overestimated by the model ALADIN 10 km by 0,98 mm. Differences span between 8,89 and 13,49 mm. Spatial distribution of differences is similar to mean climatological precipitation.

Summer months give quite different results. Model results are negatively biased by -2,04 mm (for the whole area of the Czech Republic). Maximum negative difference is -5,75 mm and maximum positive one is 1,11 mm. Greatest differences are found in north-eastern (Moravskoslezský region) and eastern (Zlínský region) parts of the Czech Republic.

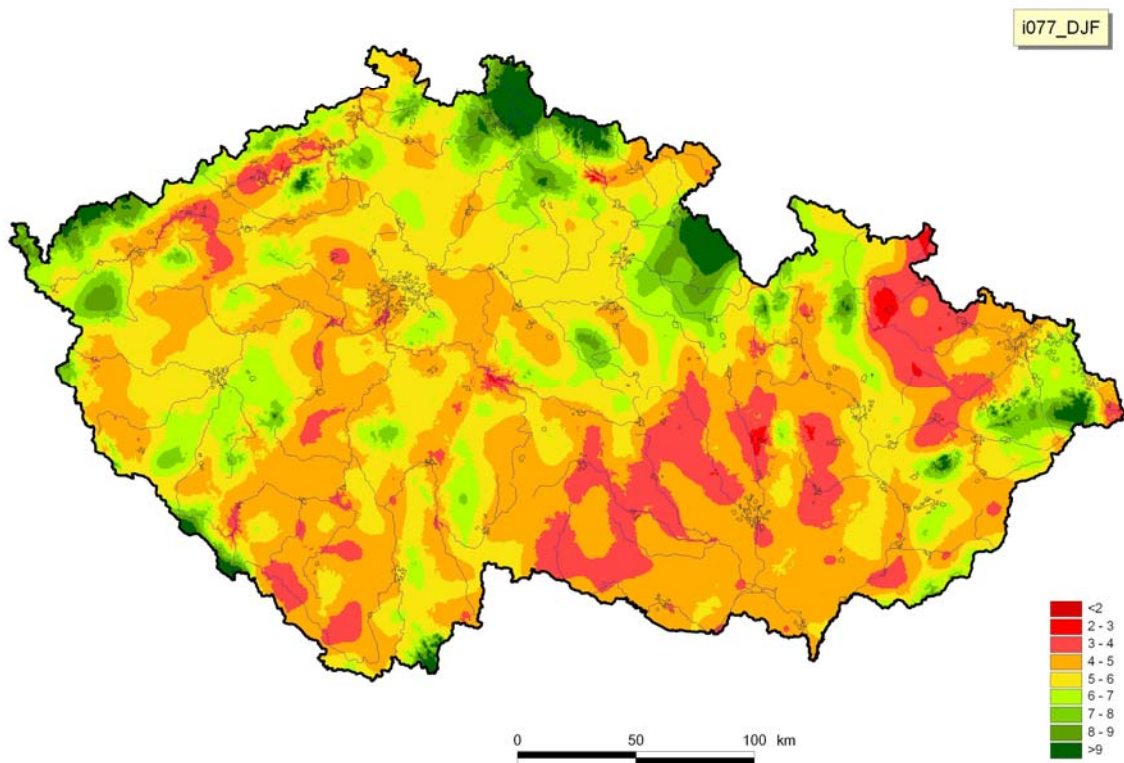


Fig. 12a. Mean wet-day precipitation [mm] for the area of the Czech Republic from outputs of ALADIN-Climate/CZ (driven by GCM ARPEGE) in the period 1961-1990. DJF

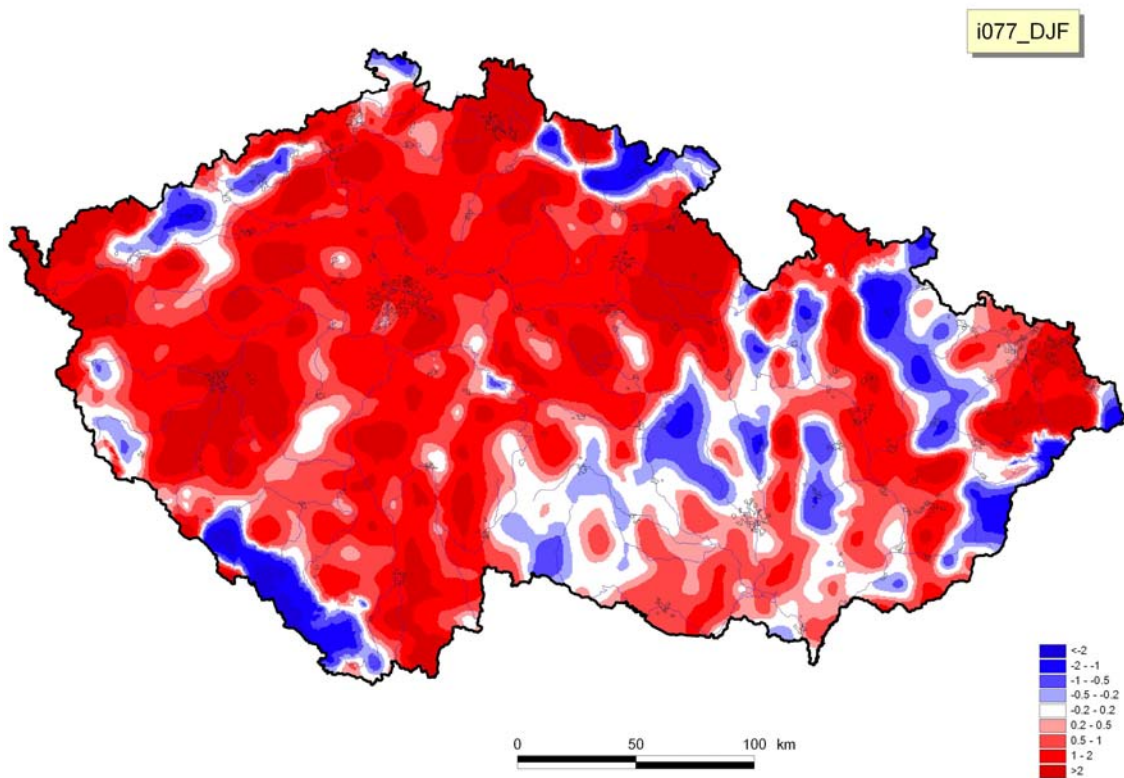


Fig. 12b. Differences between RCM ALADIN @10 km outputs and station data for the area of the Czech Republic in the period 1961-1990. DJF.

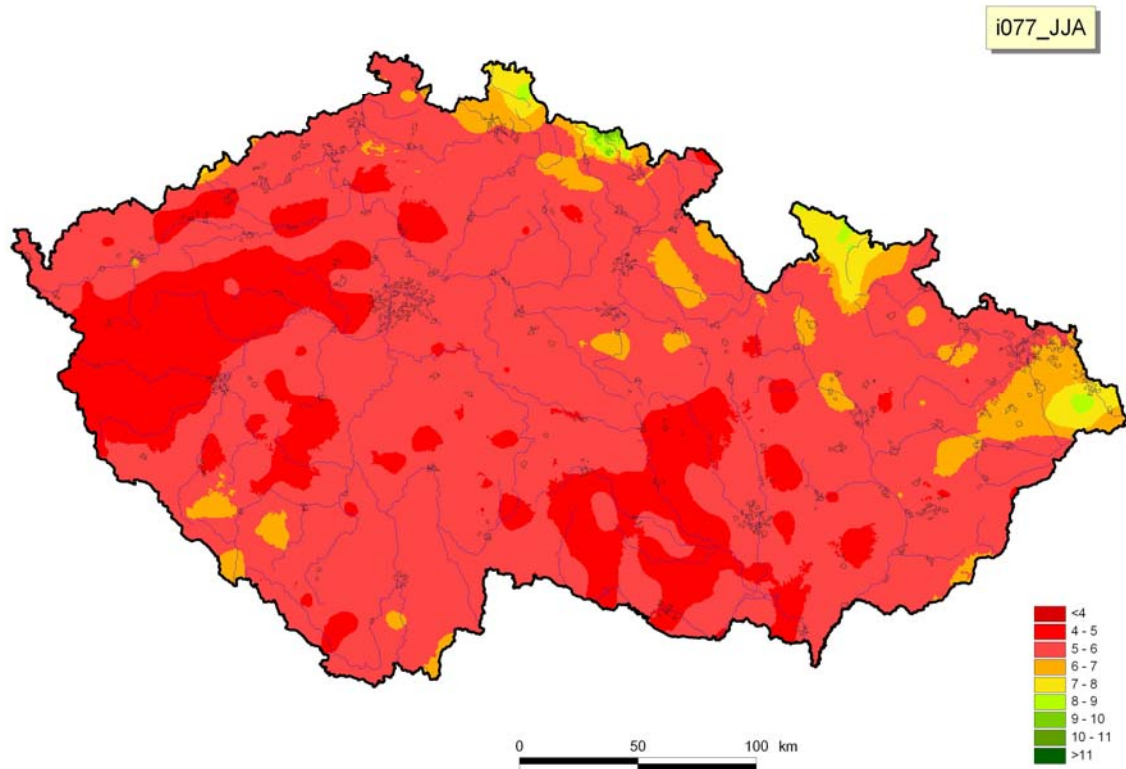


Fig. 13a. Mean wet-day precipitation [mm] for the area of the Czech Republic from outputs of ALADIN-Climate/CZ (driven by GCM ARPEGE) in the period 1961-1990. JJA

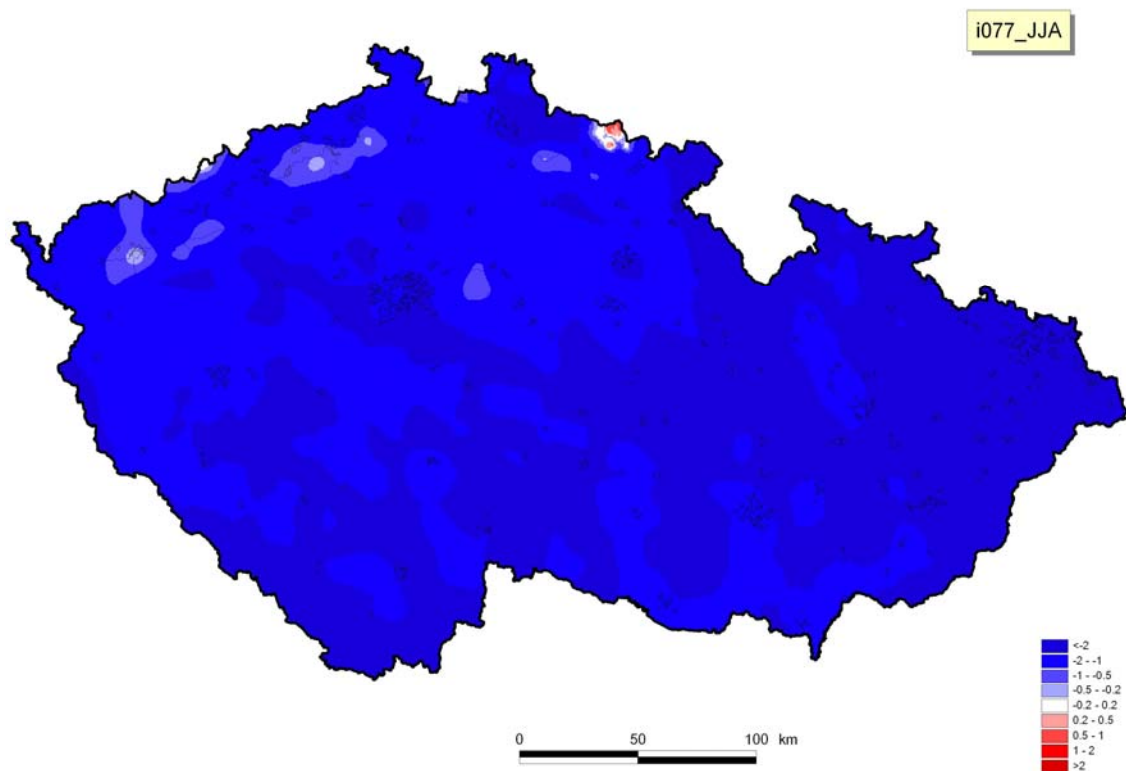


Fig. 13b. Differences between RCM ALADIN @10 km outputs and station data for the area of the Czech Republic in the period 1961-1990. JJA.

## 8) Percentage of wet days (index 078)

Percentage of wet days for winter time frame given by the model ALADIN 10 km is overestimated by 4,65% (for the whole area of the Czech Republic). Spread of differences is very large, from -25,85 to 46,08%. For most of the area the model gives positively biased values. The highest increase is found for central Bohemia, mainly for Prague and also for eastern Bohemia (Pardubický region). On the contrary, model underestimates markedly area of Šumava Mountains.

For summer months the differences are even greater. Model overestimates by 25,84% (for the whole area of the Czech Republic). Differences vary from 11,58 to 42,06%. The least overestimated percentage of wet-days is obtained in southern Moravia and relatively also in Krušné hory mountains.

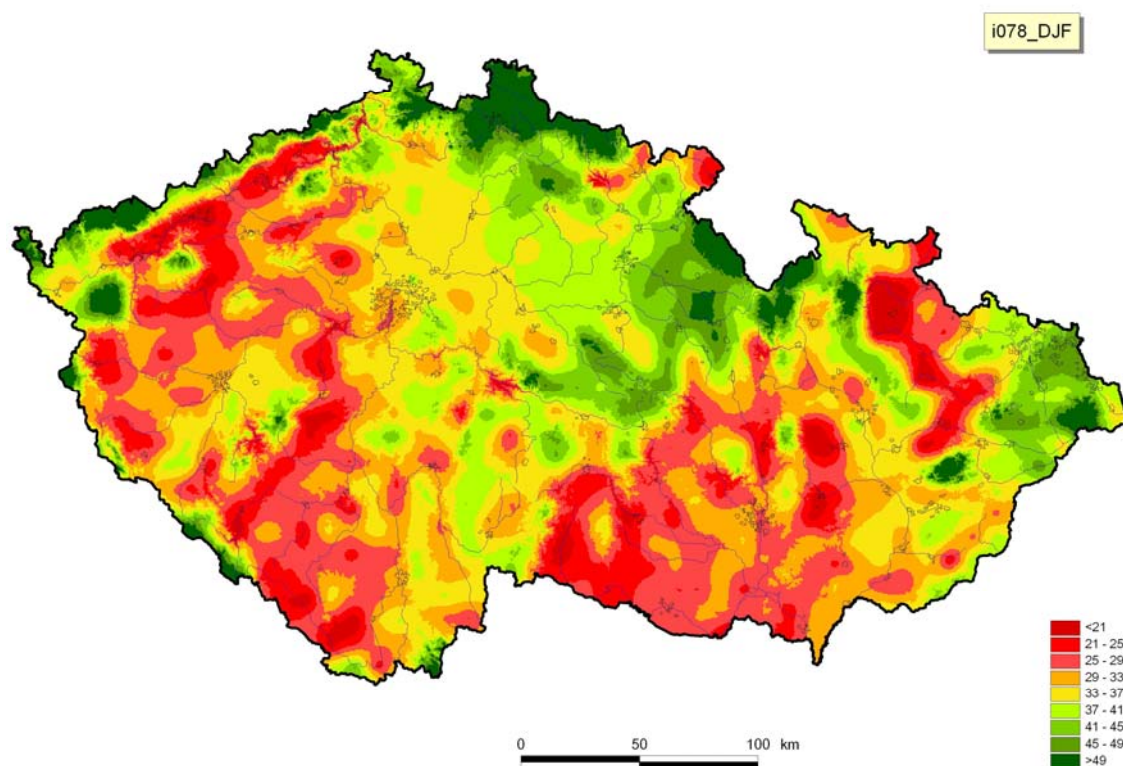


Fig. 14a. Percentage of wet days for the area of the Czech Republic from outputs of ALADIN-Climate/CZ (driven by GCM ARPEGE) in the period 1961-1990. DJF

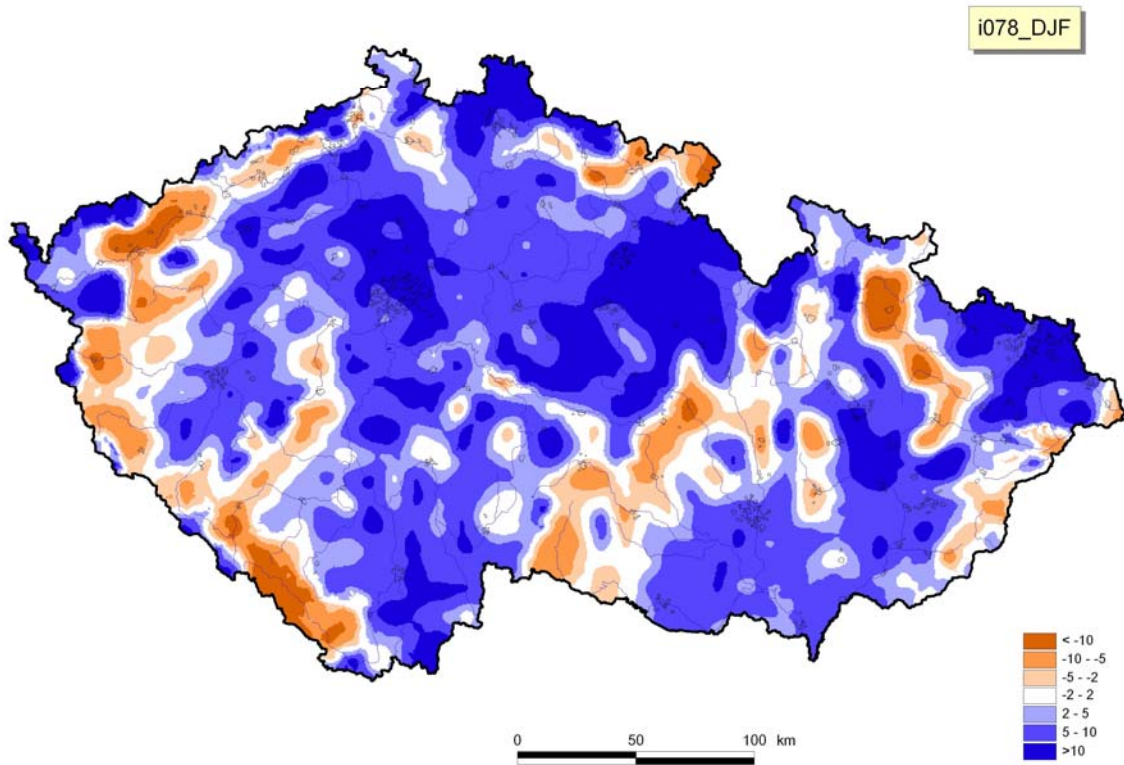


Fig. 14b. Differences between RCM ALADIN @10 km outputs and station data for the area of the Czech Republic in the period 1961-1990. DJF.

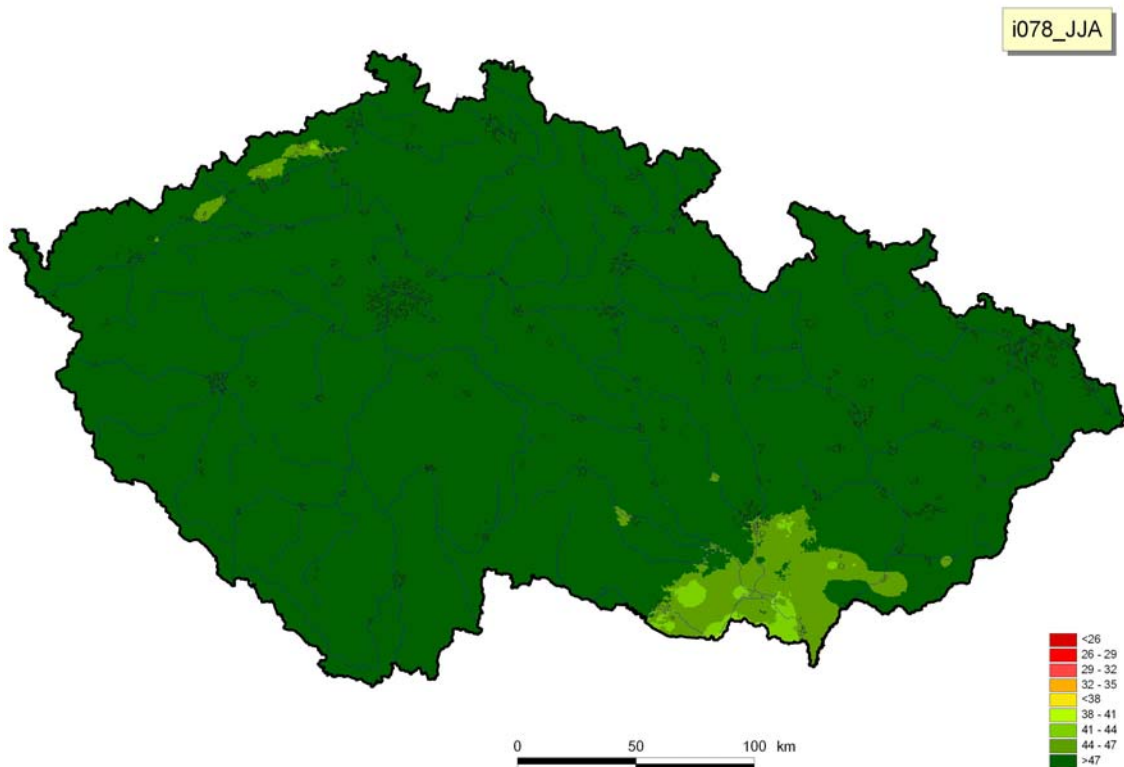


Fig. 15a. Percentage of wet days for the area of the Czech Republic from outputs of ALADIN-Climate/CZ (driven by GCM ARPEGE) in the period 1961-1990. JJA

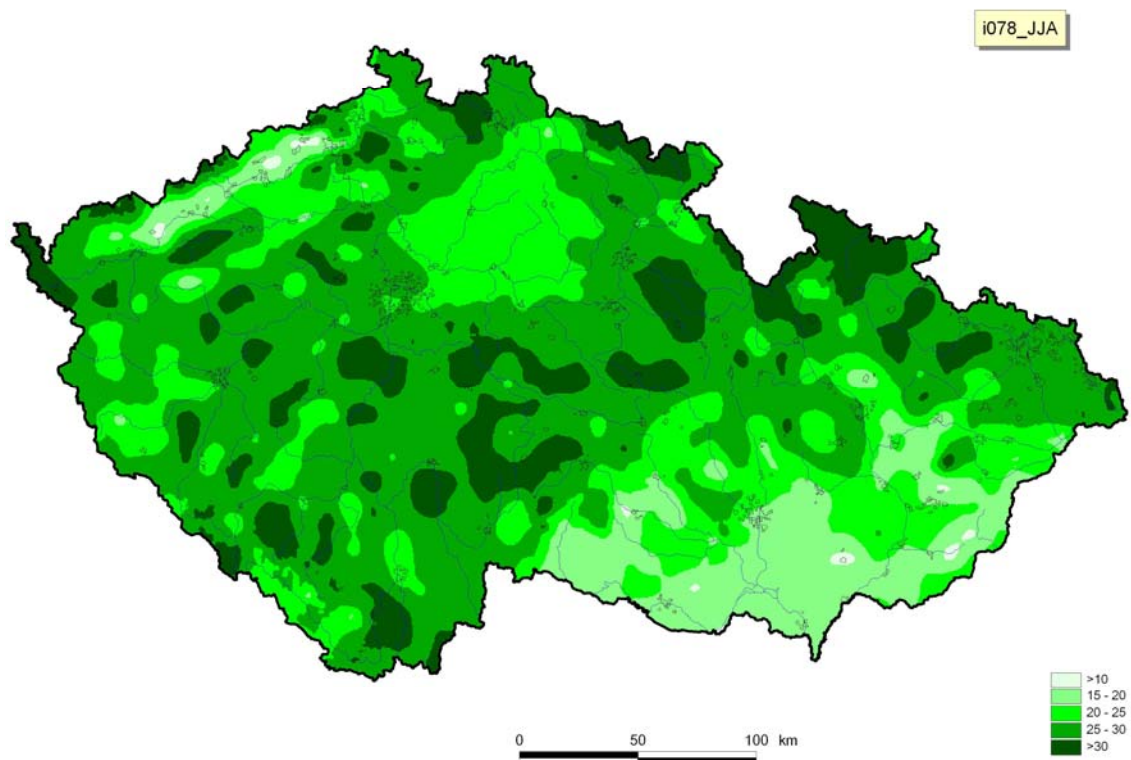


Fig. 15b. Differences between RCM ALADIN @10 km outputs and station data for the area of the Czech Republic in the period 1961-1990. JJA.

### **9) Greatest 1-day total rainfall (index 113)**

For winter time frame, the model ALADIN 10 km gives greatest 1-day total rainfall smaller by -8,68 mm compared to station data (for the whole area of the Czech). Differences span from -60,79 to 23,38 mm. Almost entire area is underestimated by the model, particularly mountainous regions.

Similarly as for previous indexes (index 078), also for this one and summer months we get great differences between the model ALADIN 10 km and station data. Average difference for the whole area of the Czech Republic is -44,46 mm, maximum difference is up to -181,38 mm. Great differences are found mainly in mountainous regions. The datasets agree the best in southern Moravia. The model outputs are underestimated for entire area.

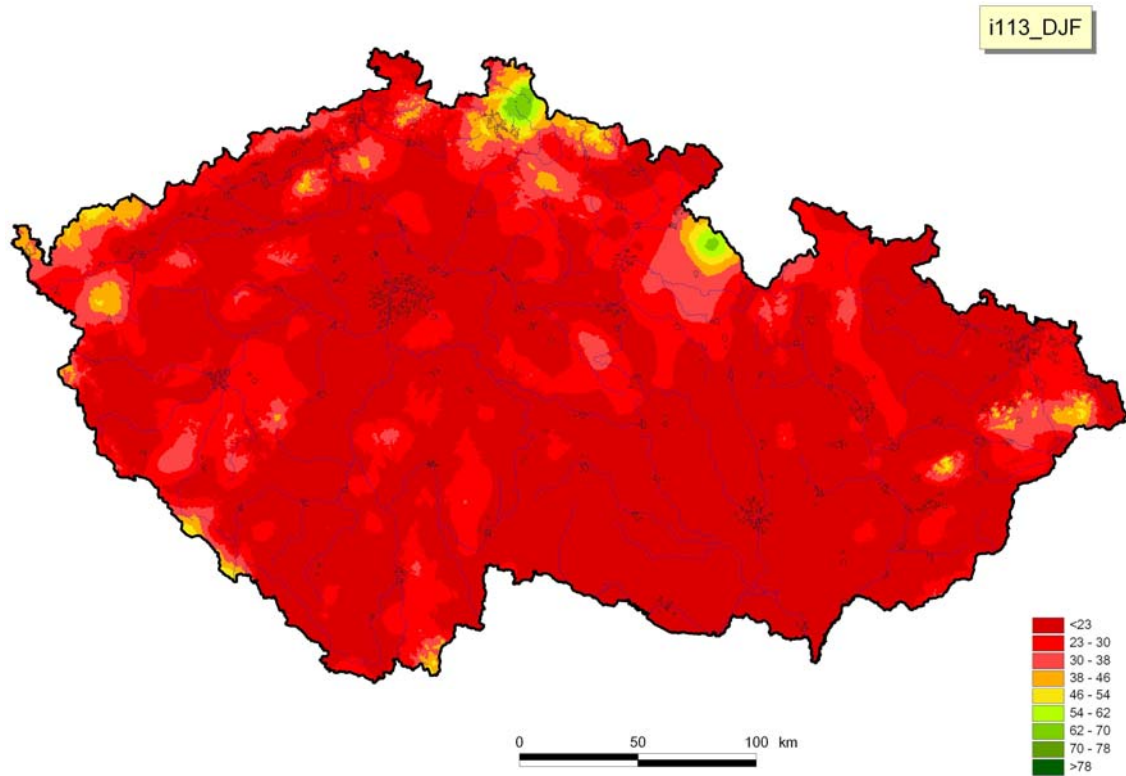


Fig. 16a. Greatest 1-day total rainfall [mm] for the area of the Czech Republic from outputs of ALADIN-Climate/CZ (driven by GCM ARPEGE) in the period 1961-1990. DJF

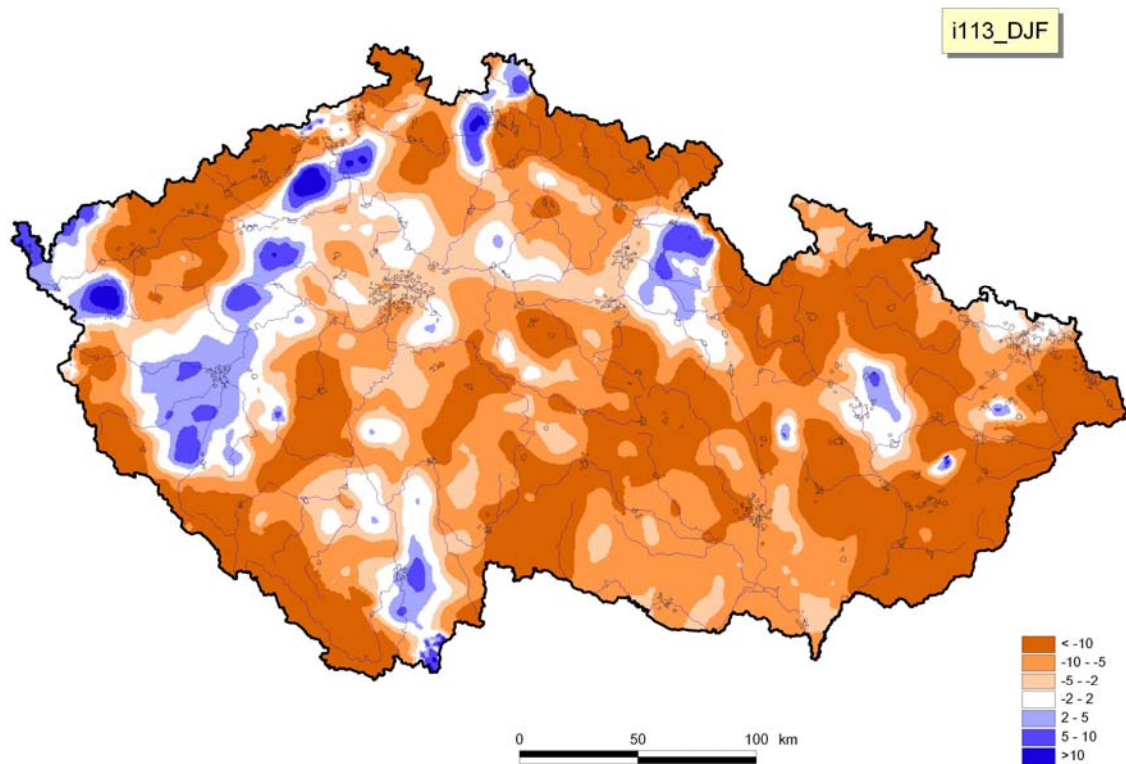


Fig. 16b. Differences between RCM ALADIN @10 km outputs and station data for the area of the Czech Republic in the period 1961-1990. DJF.

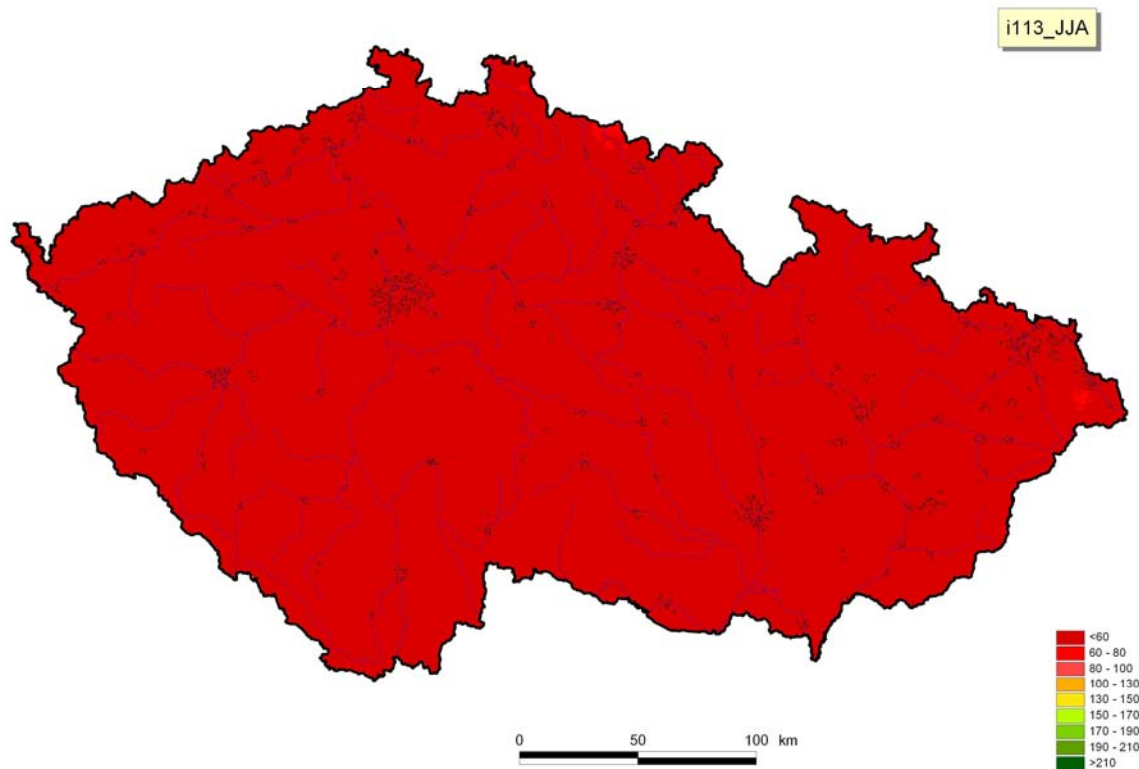


Fig. 17a. Greatest 1-day total rainfall [mm] for the area of the Czech Republic from outputs of ALADIN-Climate/CZ (driven by GCM ARPEGE) in the period 1961-1990. JJA

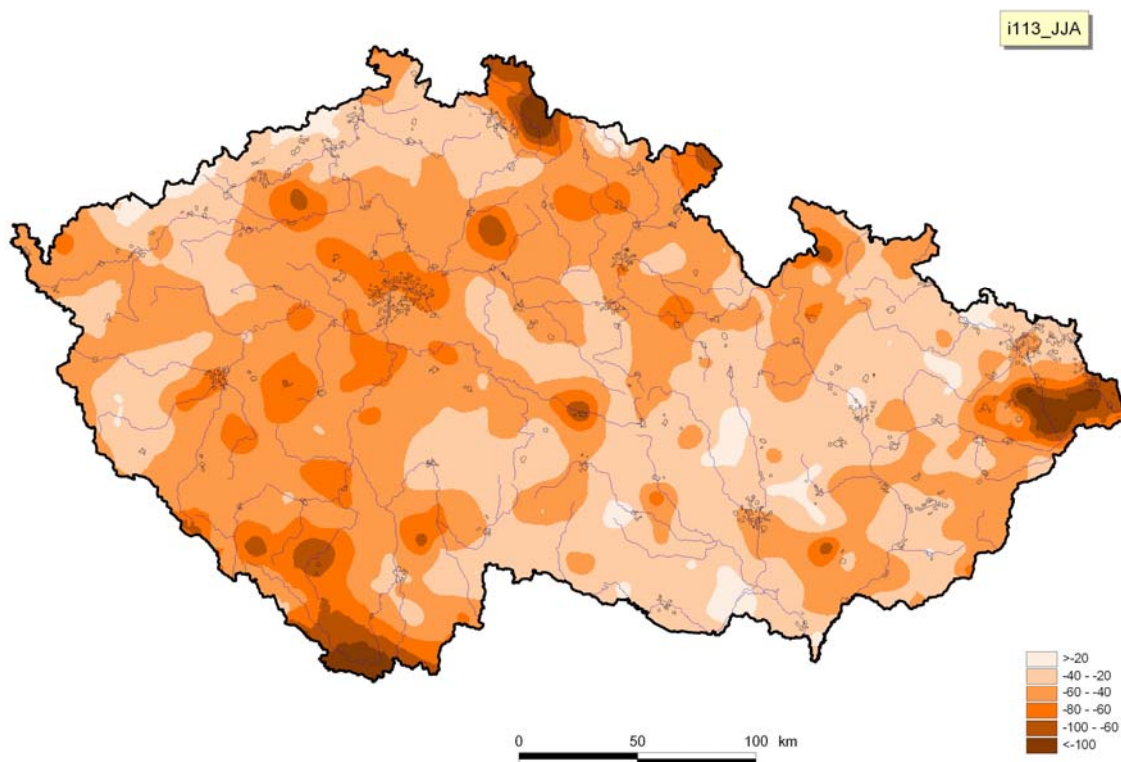


Fig. 17b. Differences between RCM ALADIN @10 km outputs and station data for the area of the Czech Republic in the period 1961-1990. JJA.

## 10) *Greatest 5-day total rainfall (index 115)*

The model 10 km outputs overestimate greatest 5-day total rainfall in winter by 25,99 mm (for the whole area of the Czech). Differences vary from -86,71 mm to 199,51 mm. Greatest differences are found in north-western and western Bohemia. In average results agree best in Vysočina region (central part of the Czech Republic). For mountainous regions values are generally underestimated.

For summer, average difference between model and station data for the whole area of the Czech Republic is only 9,44 mm, but great spatial differences exist, both negative and positive ones (from -234,7 mm to 158,29 mm). The most underestimated area is situated around Prague and Beskydy mountains, while great positive biases of the model are found for southern Moravia.

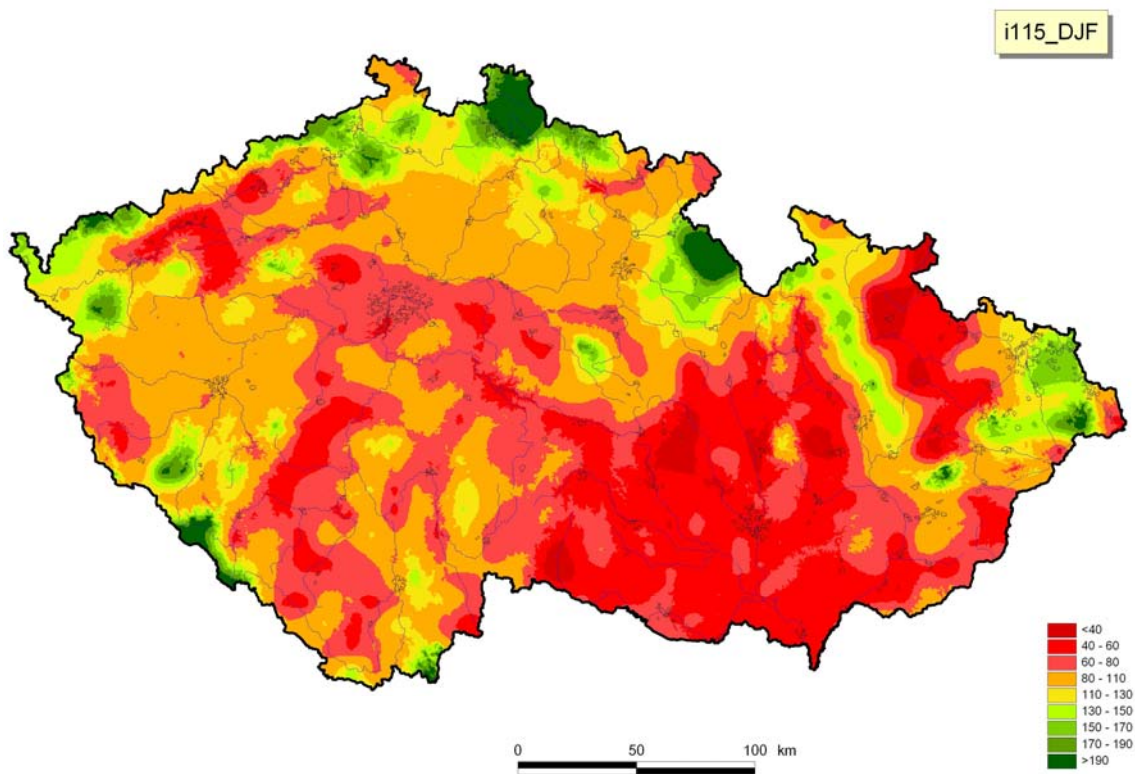


Fig. 18a. Greatest 5-day total rainfall [mm] for the area of the Czech Republic from outputs of ALADIN-Climat/CZ (driven by GCM ARPEGE) in the period 1961-1990. DJF

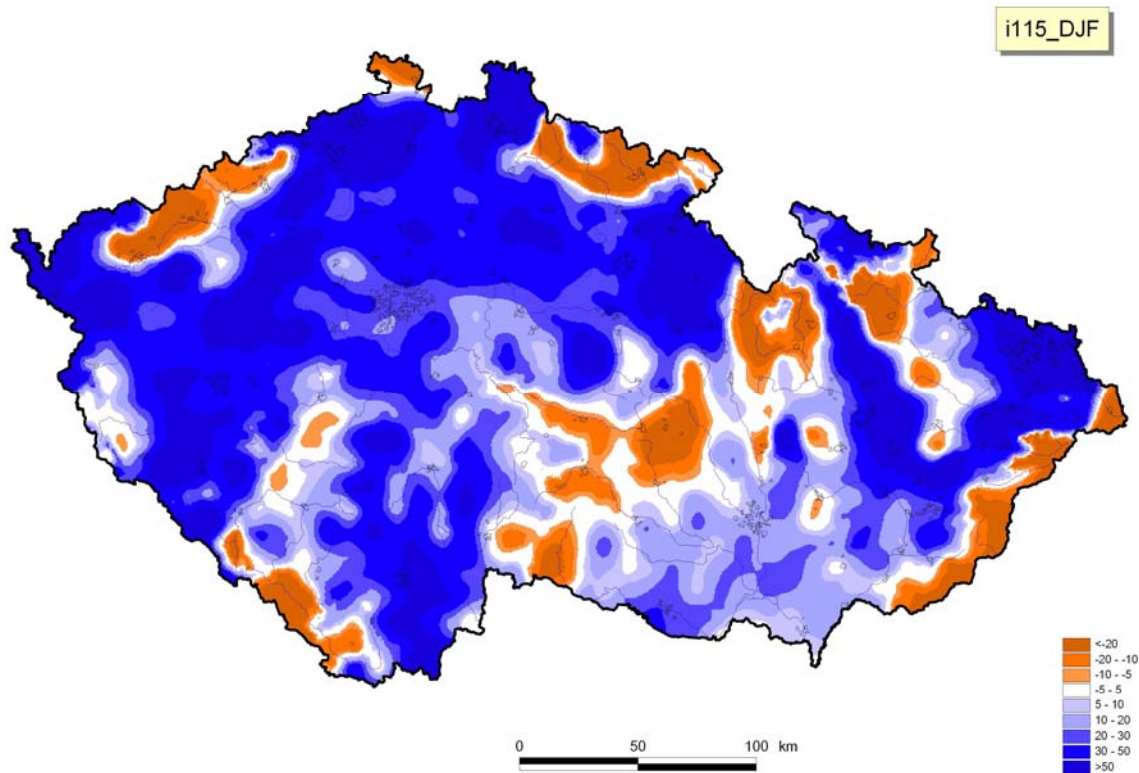


Fig. 18b. Differences between RCM ALADIN @10 km outputs and station data for the area of the Czech Republic in the period 1961-1990. DJF.

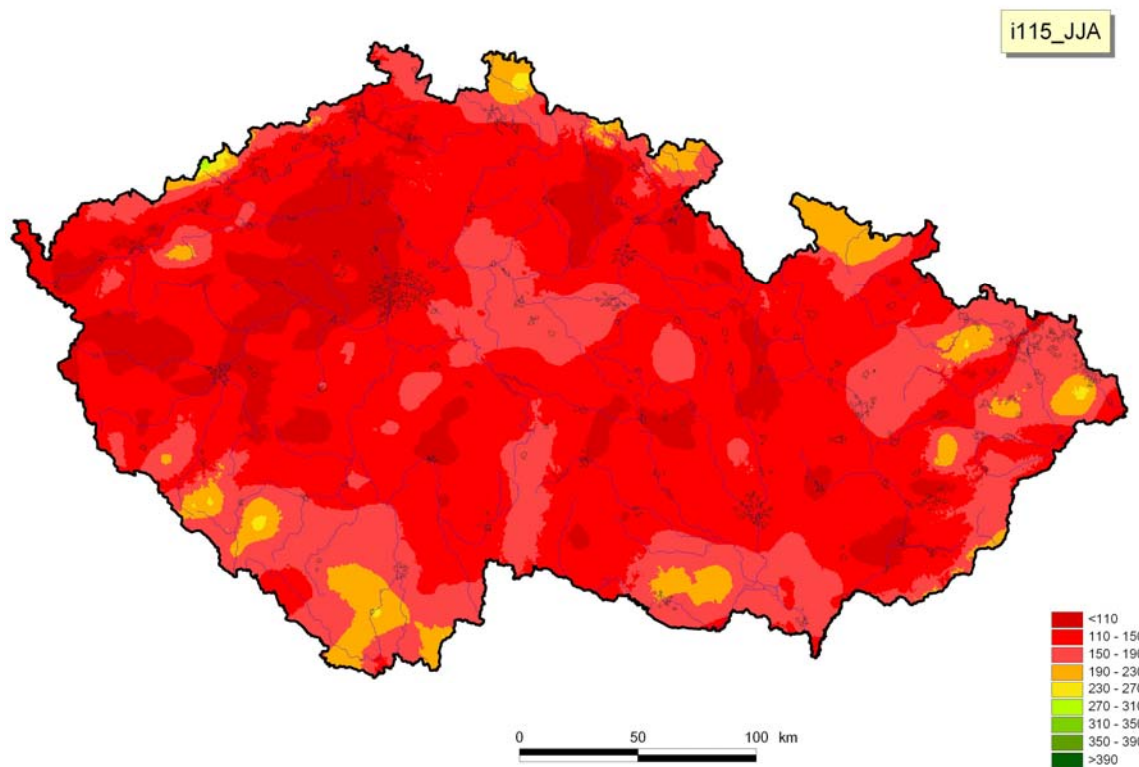


Fig. 19a. Greatest 5-day total rainfall [mm] for the area of the Czech Republic from outputs of ALADIN-Climate/CZ (driven by GCM ARPEGE) in the period 1961-1990. JJA

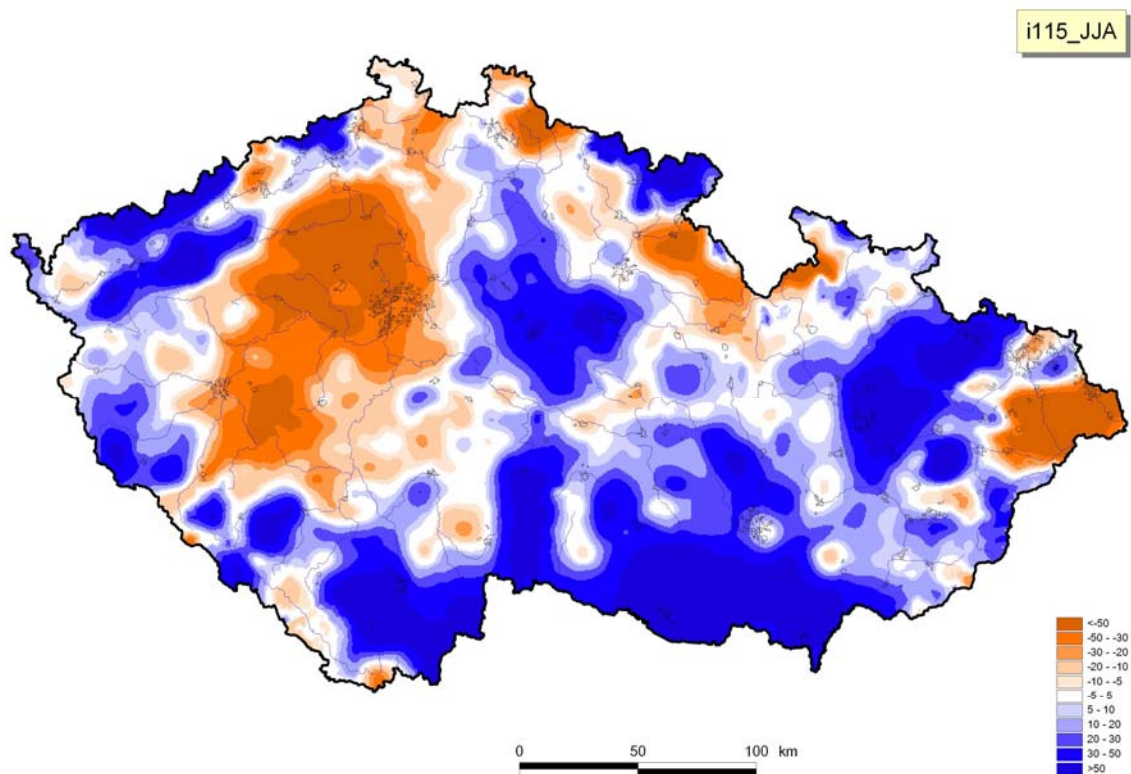


Fig. 19b. Differences between RCM ALADIN @10 km outputs and station data for the area of the Czech Republic in the period 1961-1990. JJA.

## 11) **Conclusions**

It was shown on selected extreme indices that even if in spatial averages differences between station data and RCM outputs (ALADIN-Climate/CZ outputs at 10 km resolution driven by GCM ARPEGE in this case) are acceptable, spatial differences between model and station data can be quite big in certain regions. On the other hand, compared to results of RCM at 25 km resolution, results from 10 km are more realistic.

While winter temperatures (maximum, minimum and mean) are positively biased for western and central part of the Czech Republic and negatively biased for the rest of the area, in case of summer, maximum temperatures are negatively biased while minimum and mean temperatures are positively biased (for almost entire Czech Republic). This also means that model outputs have lower variability compared to reality. Model outputs then give also less number (percentage) of summer or hot days (model outputs are negatively biased again for the whole area).

Precipitation indices are more spatially heterogeneous than temperature ones. In case of winter, for most of the area model outputs for both climatological and wet-day precipitations are positively biased

(mainly for eastern part, i.e. Bohemia). In case of summer, we find positive bias for mean climatological precipitation but negative bias for mean wet-day precipitation. As effect, percentage of wet days is positively biased for summer and the whole area, while for winter most of the area is positively biased but there are many regions with negative bias. Greatest 1-day total rainfall in summer is again negatively biased for the whole area (like mean wet-day precipitation) while for winter differences vary from negative to positive ones within the area of the Czech Republic. Greatest 5-day total rainfall is in average overestimated both for summer and winter even if great spatial differences exist.

## References

- Farda, A., Štěpánek, P., Halenka, T., Skalák, P. and Belda, M., Model ALADIN in climate mode forced with ERA-40 reanalysis (coarse resolution experiment). *Meteorological journal*, 10, 123-130, 2007.
- Farda, A., Dynamical downscaling of Air Temperature in the Central Europe (PhD. thesis, in Czech with extended abstract in English). Faculty of Mathematics and Physics, Charles University in Prague, 2008.
- Skalák, P., Štěpánek, P., Farda, A., Validation of ALADIN-Climate/CZ for present climate (1961–1990) over the Czech Republic. *Időjárás*, Vol. 112, No. 3-4, pp. 191-201, 2008.
- Štěpánek, P., ProClimDB – software for processing climatological datasets, CHMI, !! HYPERLINK "<http://www.climahom.eu>" <http://www.climahom.eu>, 2008
- Štěpánek, P., Zahradníček, P. a Skalák, P., 2009. Data quality kontrol and homogenization of air temperature and precipitation series in the area of the Czech Republic in the period 1961–2007. *Advances in Science and Research*, 3, 23–26, 2009 <http://www.adv-sci-res.net/3/23/2009/>.

## D4.4.a2 Analysis for Czech republic – RegCM (led by CUNI)

In this section, illustrative results are presented for the outputs of the RegCM model, run at CUNI, over the area of the Czech Republic. In the first subsection, the model data are validated against direct measurements representing the period 1961-1990. In the second subsection, the changes simulated for the periods 2021-2050 (near future) and 2071-2100 (far future) are given. For details on the regional climate model, see deliverable D2.1. The statistics used for the validation were selected from the list in deliverable D4.1, where more details on their definition can be found; the numbers of the indices refer to Table 1 in deliverable D4.1.

### CUNI.1

The validation results here are presented in the form of maps comparing the model outputs to a set of site-specific observations, gathered for the period 1961-1990 at Czech weather stations. The list of stations is available from the CECILIA databases. For other validation results regarding the RegCM model at CUNI (as well as of other CECILIA simulations), see, e.g., deliverables D2.6 (areal averages of mean temperature and precipitation for various regions and models), D3.3 (comparison of the outputs of statistical and dynamical downscaling) or D3.2 (validation of raw and postprocessed RCM outputs).

In general, the RegCM model tends to underestimate the amplitude of the annual cycle of the temperature characteristics. This is especially evident for maximum daily temperature (Fig. CUNI.1), and somewhat less so for minimum (Fig. CUNI.2) and mean temperature (Fig. CUNI.3).

In case of precipitation, there is a very strong wet bias (Fig. CUNI.4) and the model systematically and substantially overestimates the amount of wet days (Fig. CUNI.6). As both these effects combine, the simulated mean intensity of precipitation is actually close to reality in winter, and even somewhat underestimated in the summer season (Fig. CUNI.5). Despite the wet bias of the precipitation totals, the model is able to reproduce the highest 1-day precipitation events relatively realistically, especially in summer (Fig. CUNI.7), though overestimation reappears for 5-day maximum totals, particularly in winter (Fig. CUNI.8).

Because of the profound cold bias in summer, the simulated number of summer days ( $T_{\max} \geq 25$  °C) is substantially lower than in reality (Fig. CUNI.9), and tropical days ( $T_{\max} \geq 30$  °C) are almost nonexistent in the RegCM outputs in the control period over the Czech Republic (Fig. CUNI.10). Similarly, due to the warm bias of minimum daily temperature in winter, the number of frost days is underestimated as well (not shown).

From the presented examples (and outcomes of other validation procedures undertaken), it is apparent that the examined run of the RegCM model suffers from serious systematic errors. These prevent the raw model-generated data from being directly usable for the impact studies. To cope with this problem, climate change scenarios can be employed, based on differences of the target statistics between the future and control period. Another possible approach is the application of statistical postprocessing, aimed at reduction of biases and other systematic errors – see deliverables D3.2-5 for details and examples.

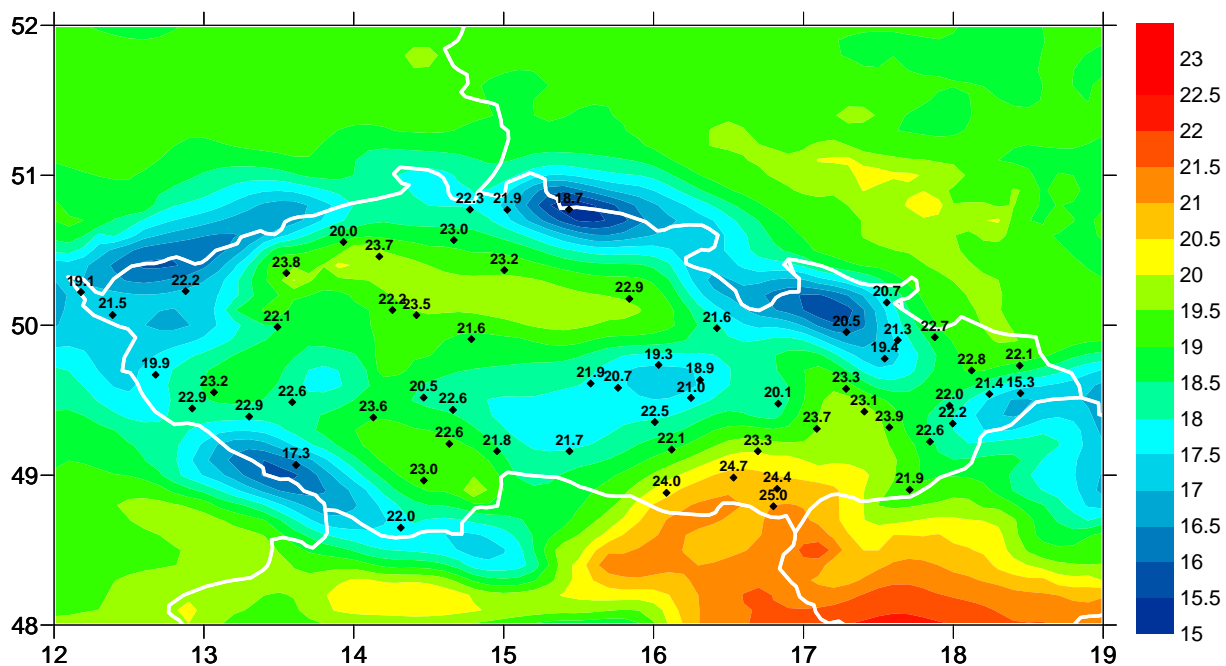
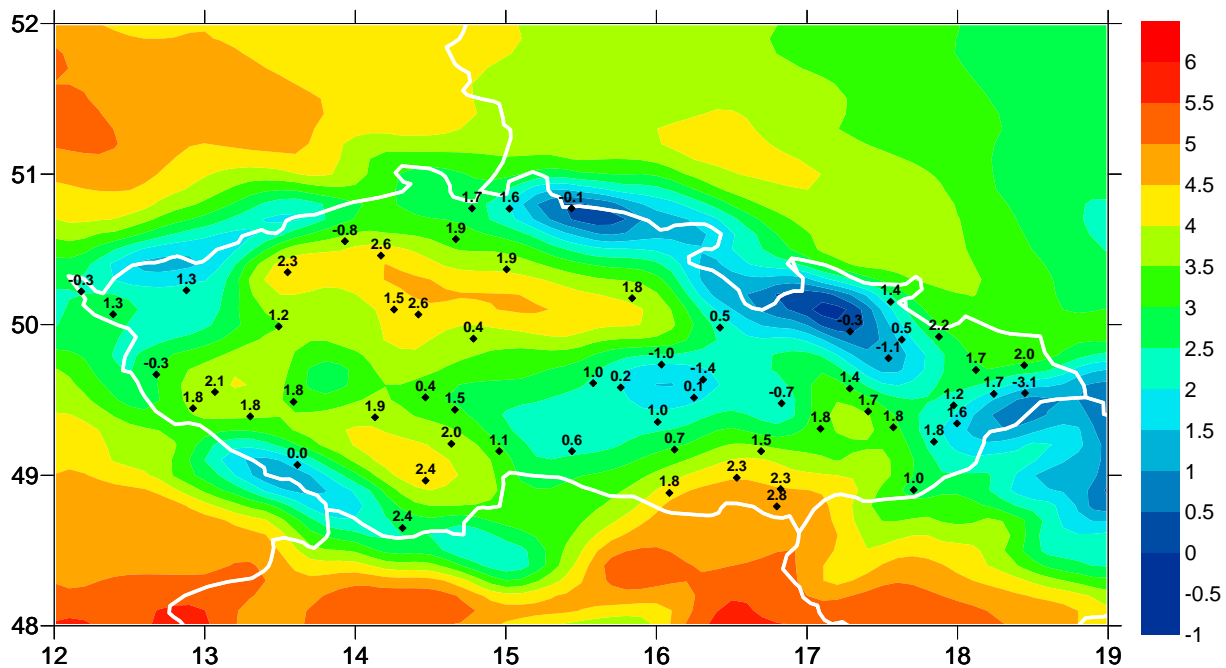


**Fig. CUNI.1.** Values of index 001 (**mean of daily maximum temperature**, °C) simulated by the RegCM model (background) and derived from data measured in the Czech Republic, for DJF (**top**) and JJA (**bottom**) seasons. The amplitude of the annual cycle of  $T_{\max}$  is distinctly reduced compared to the observed data – the values are significantly underestimated in summer, but overestimated in winter.

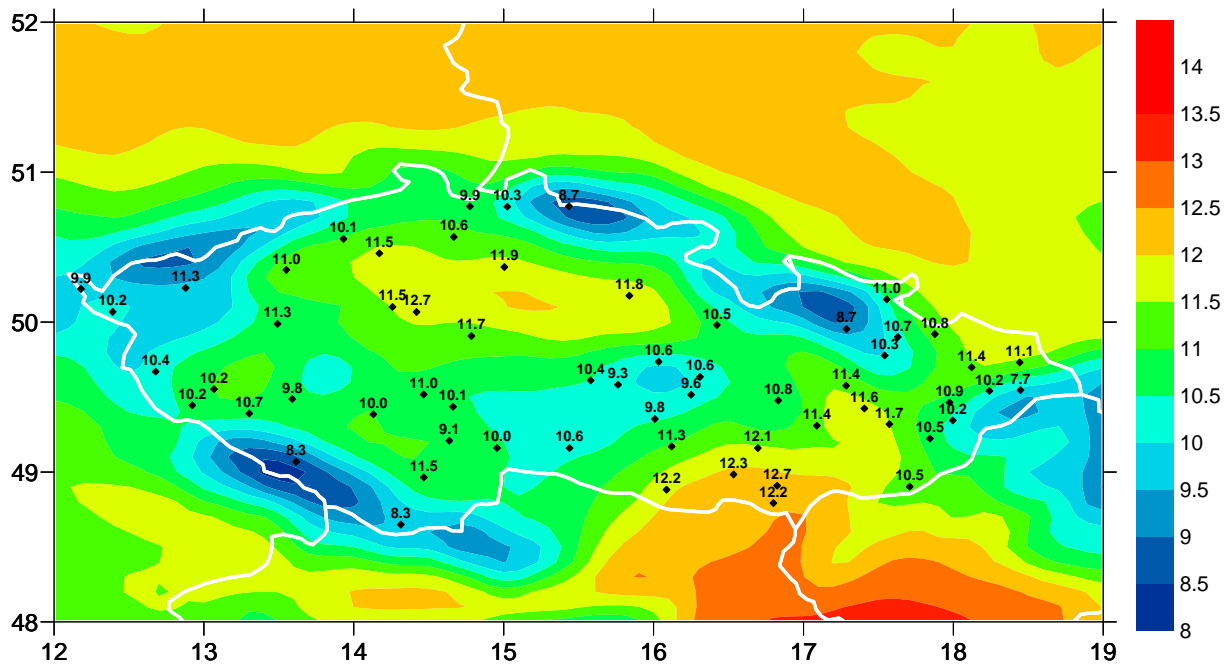
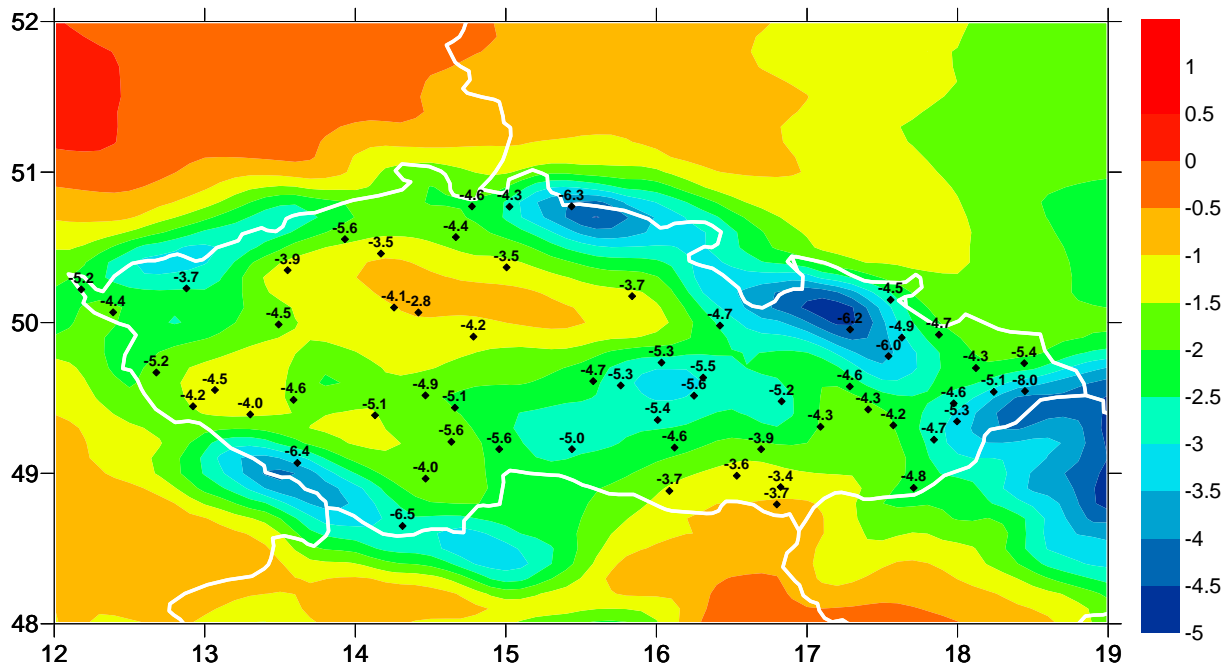


**Fig. CUNI.2.** Values of index 002 (mean of daily minimum temperature, °C) simulated by the RegCM model (background) and derived from data measured in the Czech Republic, for DJF (**top**) and JJA (**bottom**) seasons. While there is a distinct overestimation of minimum temperature in winter, its values are reproduced more realistically in summer.

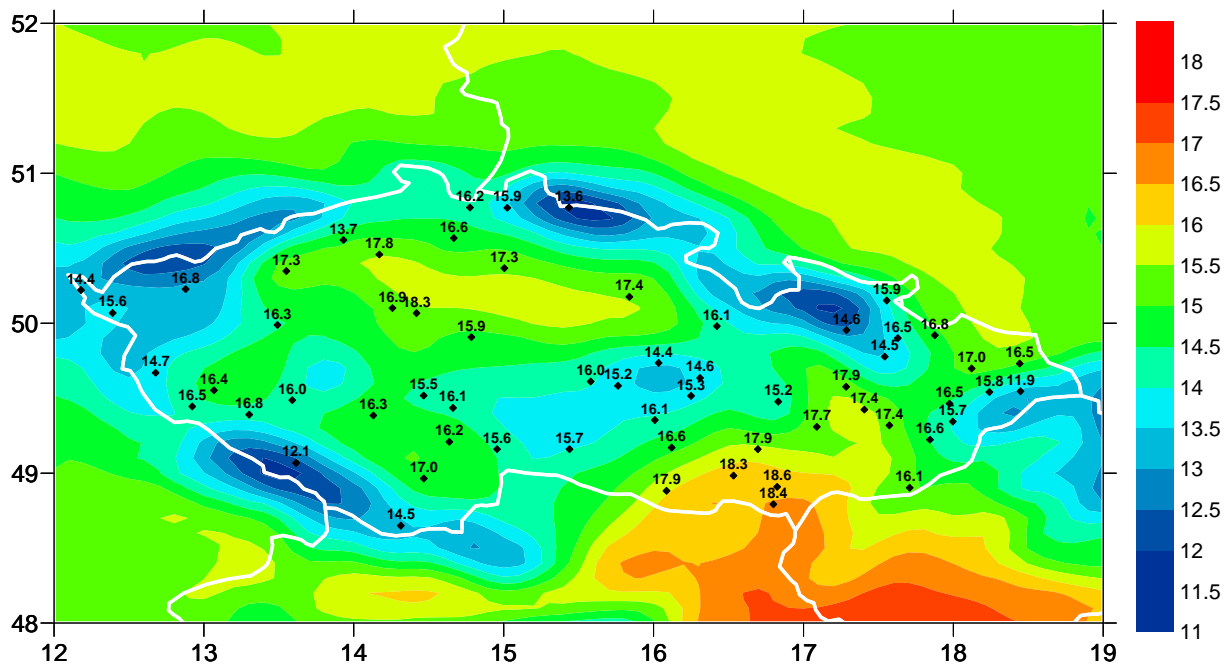
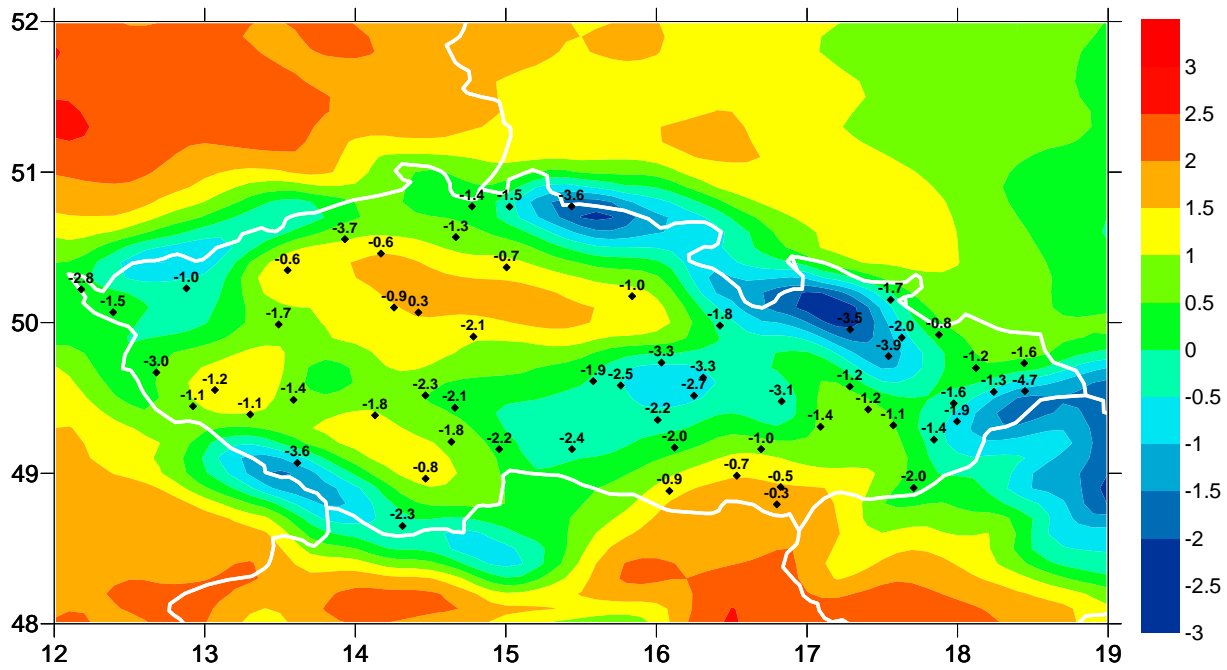


**Fig. CUNI.3.** Values of index 003 (**daily mean temperature**, °C) simulated by the RegCM model (background) and derived from data measured in the Czech Republic, for DJF (**top**) and JJA (**bottom**) seasons. Similarly to maximum temperature, the model tends to be warmer than reality during winter, but colder during summer.

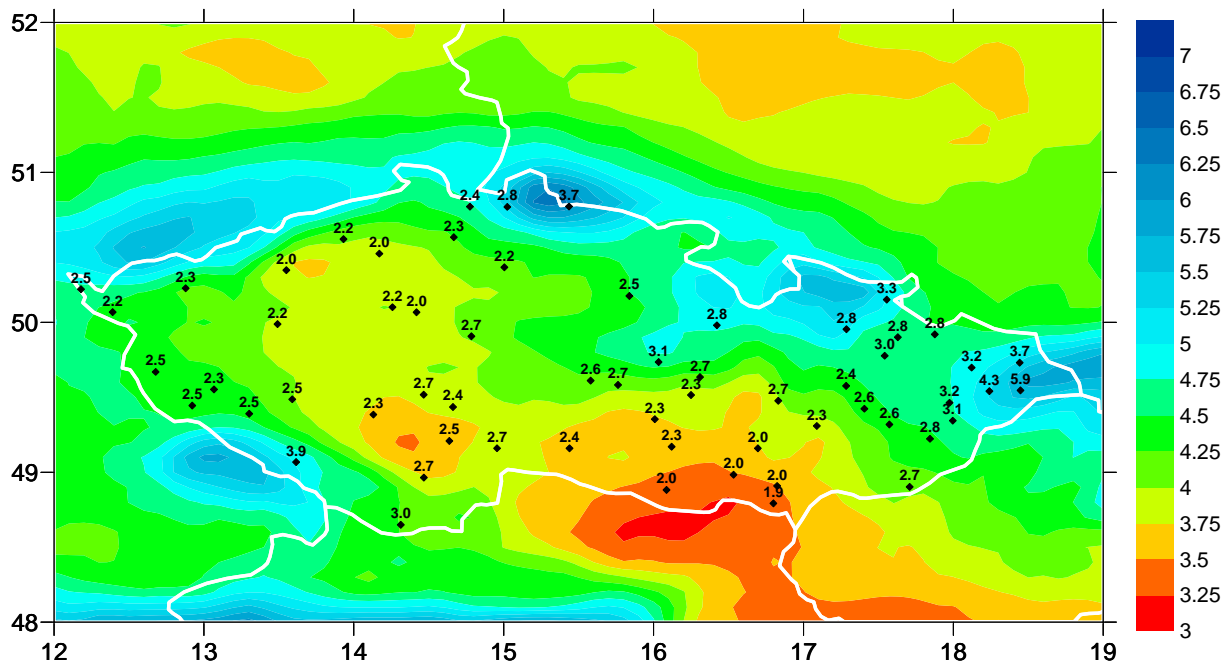
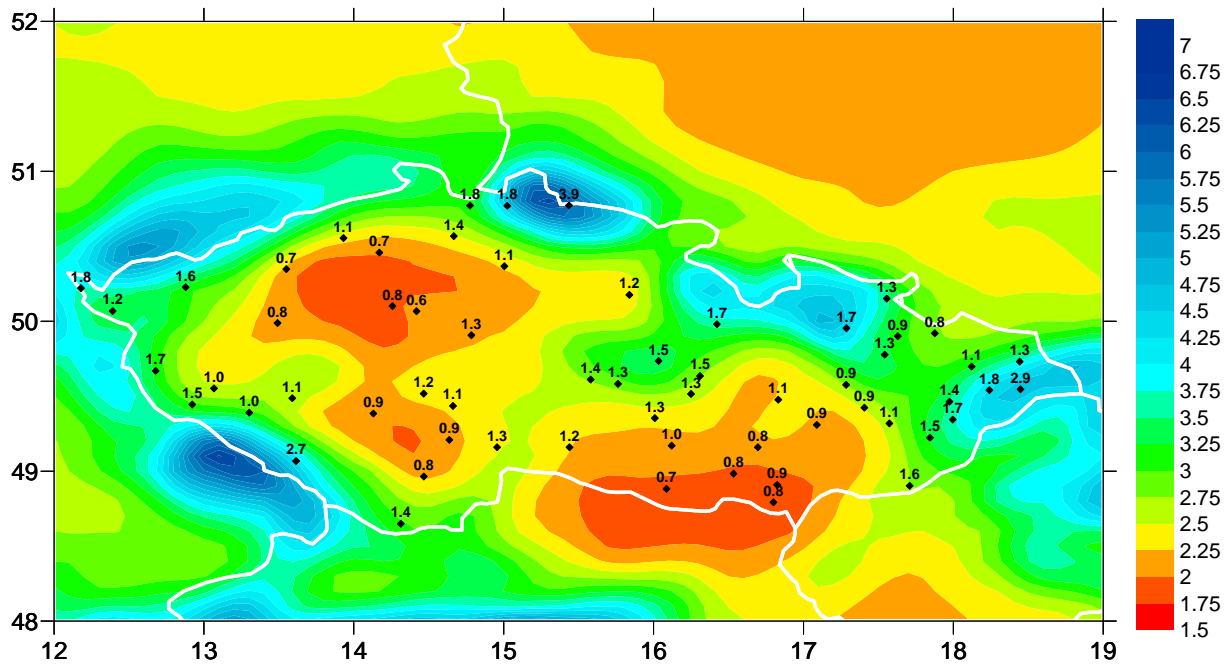


**Fig. CUNI.4.** Values of index 076 (**mean precipitation**, mm/day) simulated by the RegCM model (background) and derived from data measured in the Czech Republic, for DJF (**top**) and JJA (**bottom**) seasons. A very strong wet bias is typical for all seasons, usually almost doubling the amount of precipitation throughout the entire Czech Republic. Despite of the bias, the spatial patterns of precipitation are captured rather well, especially for winter.

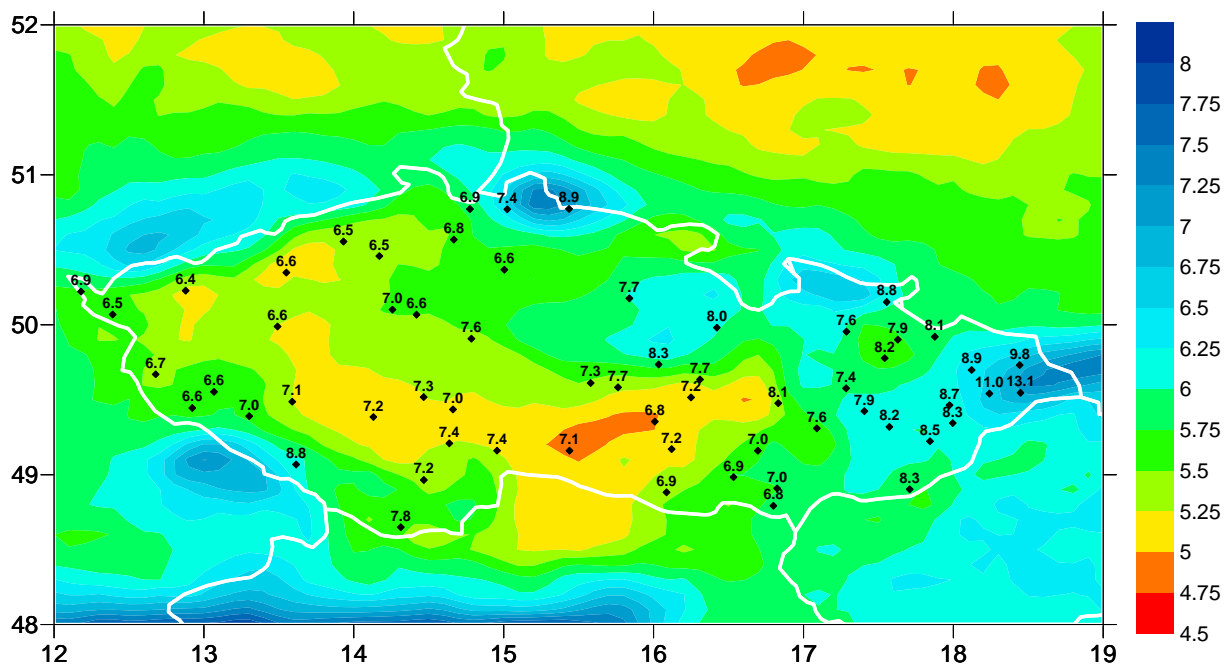
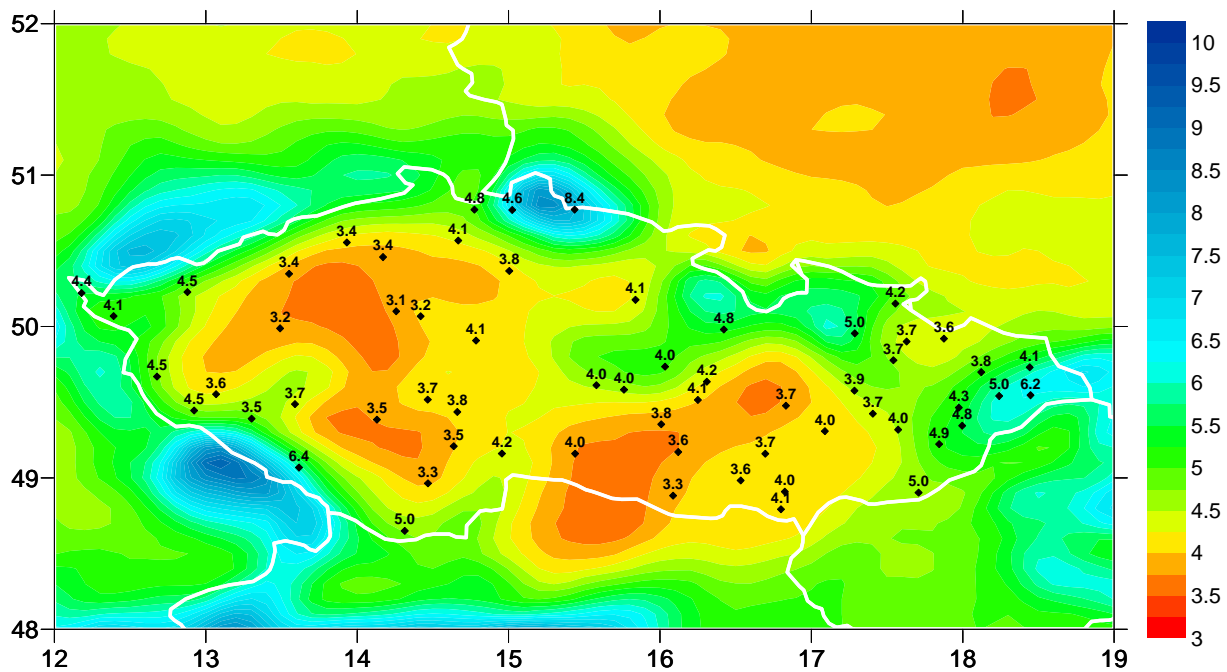


**Fig. CUNI.5.** Values of index 077 (**mean intensity of precipitation**, mm/day) simulated by the RegCM model (background) and derived from data measured in the Czech Republic, for DJF (**top**) and JJA (**bottom**) seasons. Due to a higher-than-real number of wet days in the outputs of the RegCM model, mean intensity of precipitation is simulated with lower error than mean precipitation itself in winter. In summer, the tendency is actually reversed and mean intensity of precipitation is generally somewhat lower than in the measured data.

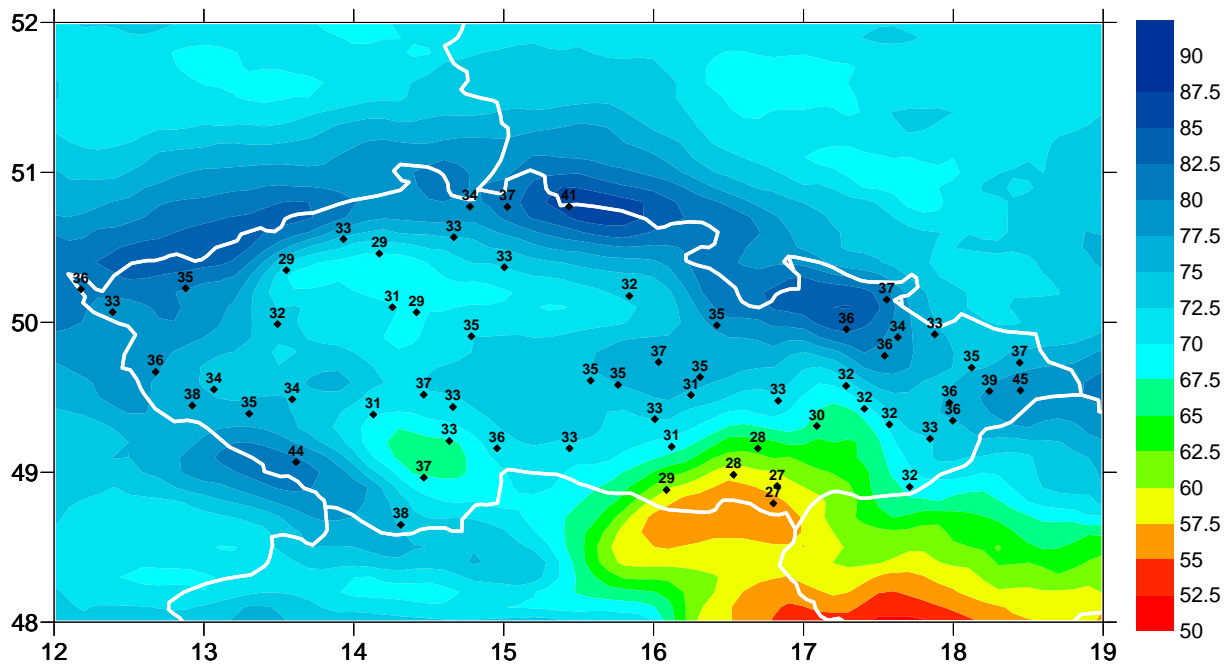
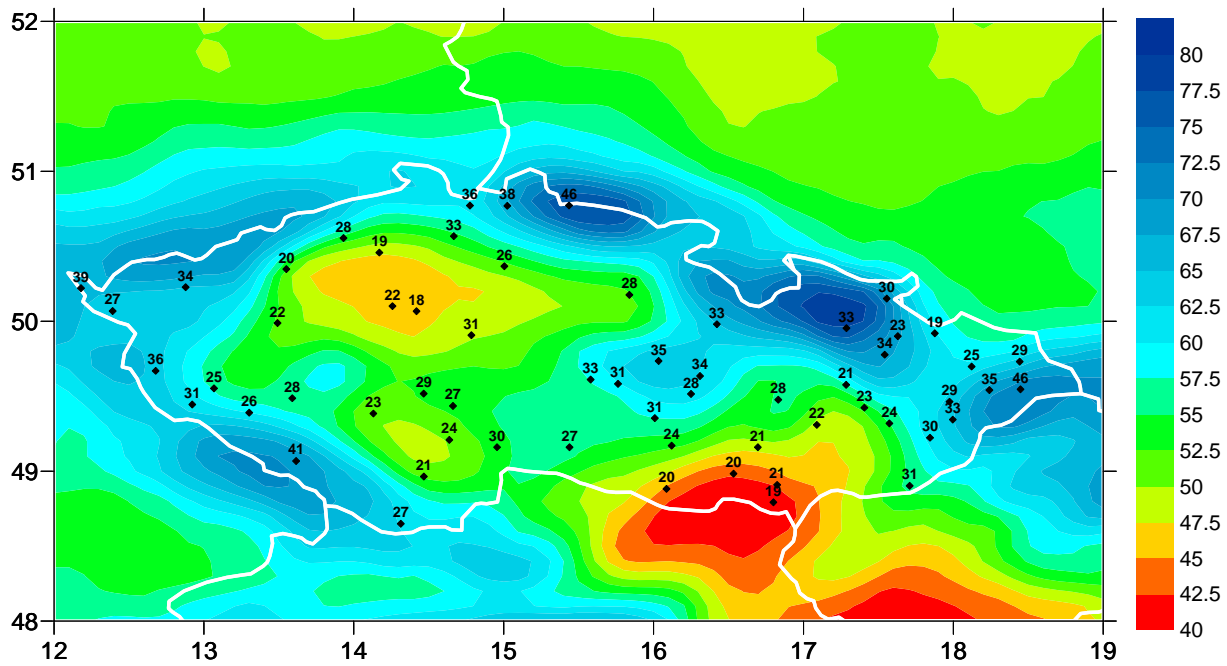


**Fig. CUNI.6.** Values of index 078 (**fraction of wet days, %**) simulated by the RegCM model (background) and derived from data measured in the Czech Republic, for DJF (**top**) and JJA (**bottom**) seasons. The number of days with precipitation  $\geq 1$  mm is greatly overestimated by the RegCM model, regardless of the season.

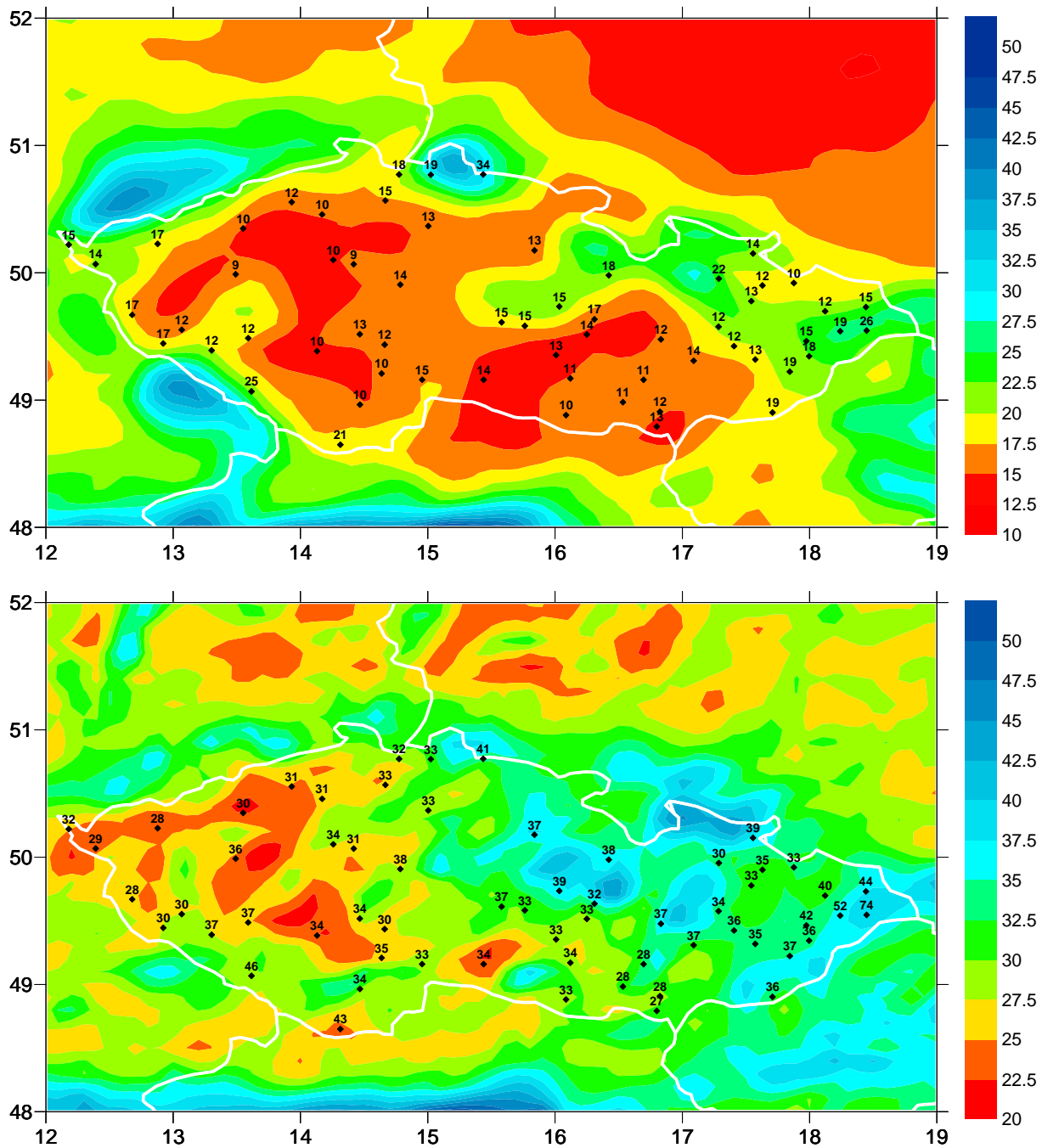


**Fig. CUNI.7.** Values of index 113 (mean value of the greatest 1-day total rainfalls in each year, mm/day) simulated by the RegCM model (background) and derived from data measured in the Czech Republic, for DJF (**top**) and JJA (**bottom**) seasons. While there is some overestimation during winter, the summer maximum precipitations are captured rather well on average by the model, although the strong stochastic component of the high precipitation sums during the warm part of year (and thus high spatial variability) makes point-wise validation problematic.

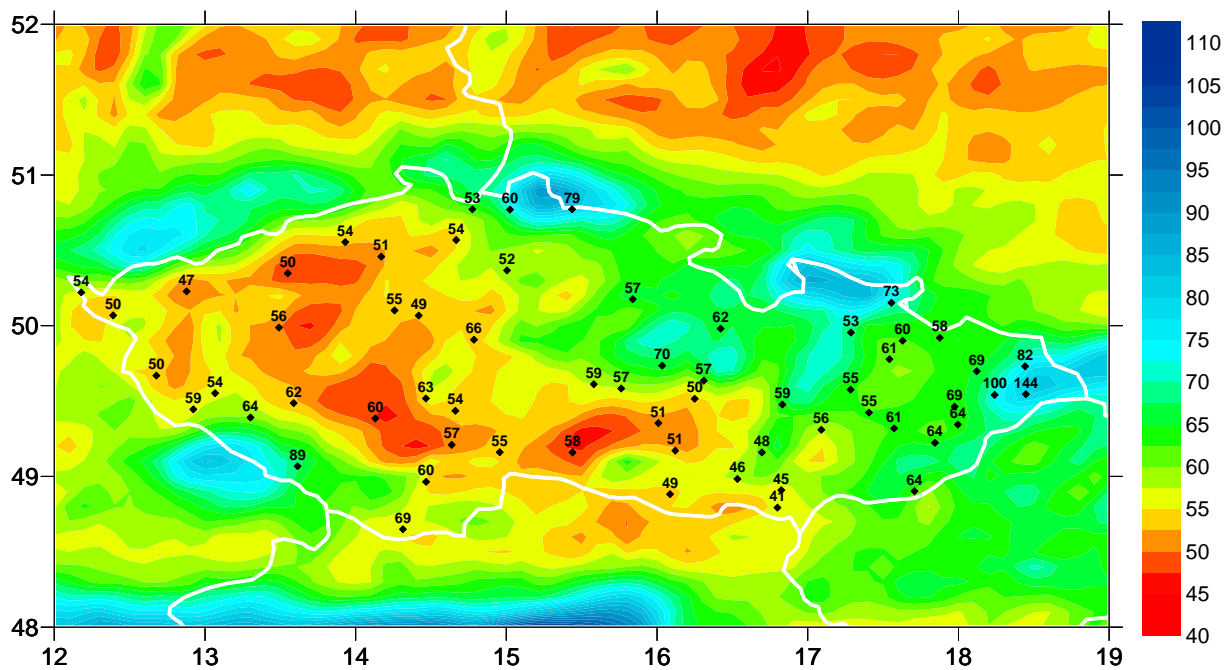
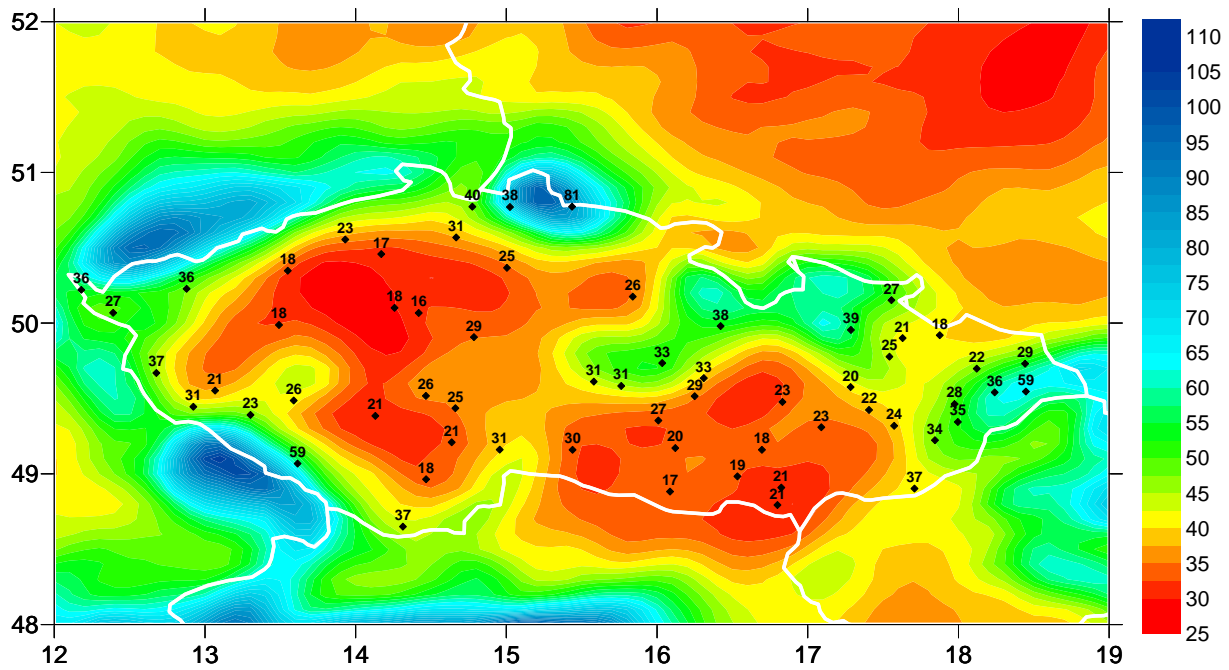


**Fig. CUNI.8.** Values of index 115 (mean value of the greatest 5-day total rainfalls in each year, mm/5 days) simulated by the RegCM model (background) and derived from data measured in the Czech Republic, for DJF (**top**) and JJA (**bottom**) seasons. The 5-day precipitation totals are clearly overestimated in the RegCM outputs in winter; in summer, the values are more realistic.

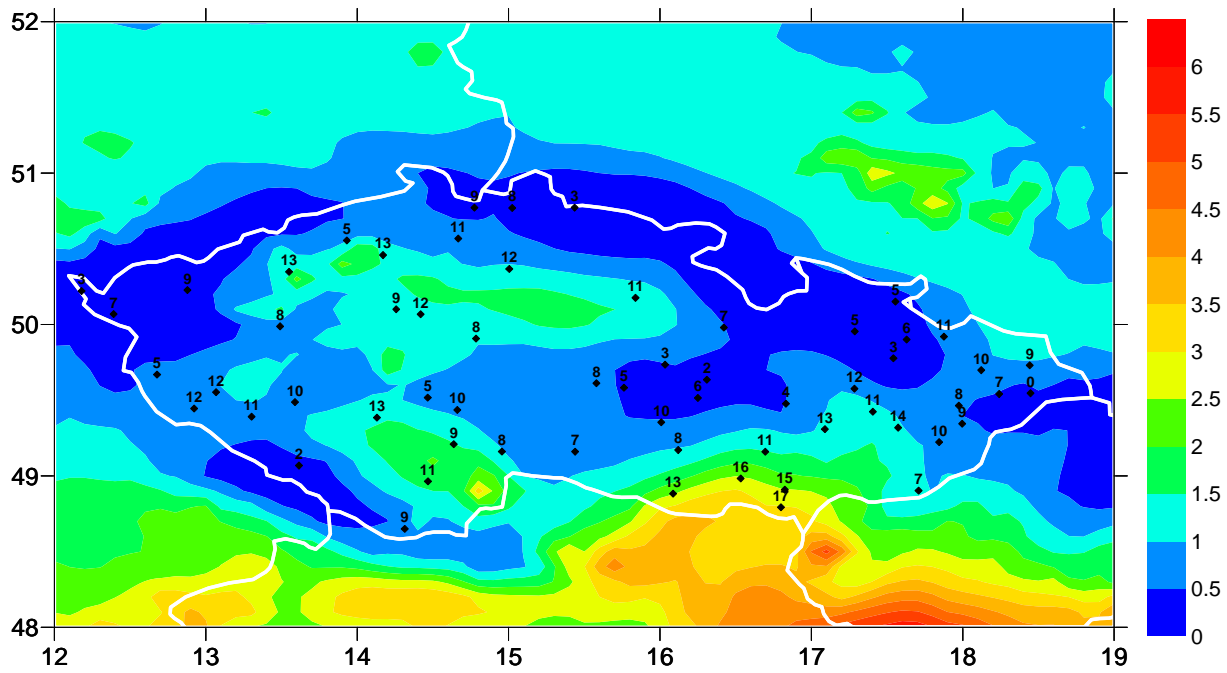


**Fig. CUNI.9.** Values of index 058 (**fraction of summer days, %**) simulated by the RegCM model (background) and derived from data measured in the Czech Republic. Because of the strong cold bias of maximum temperature in summer, the number of days with  $T_{\max} \geq 25 \text{ }^{\circ}\text{C}$  is unrealistically low.

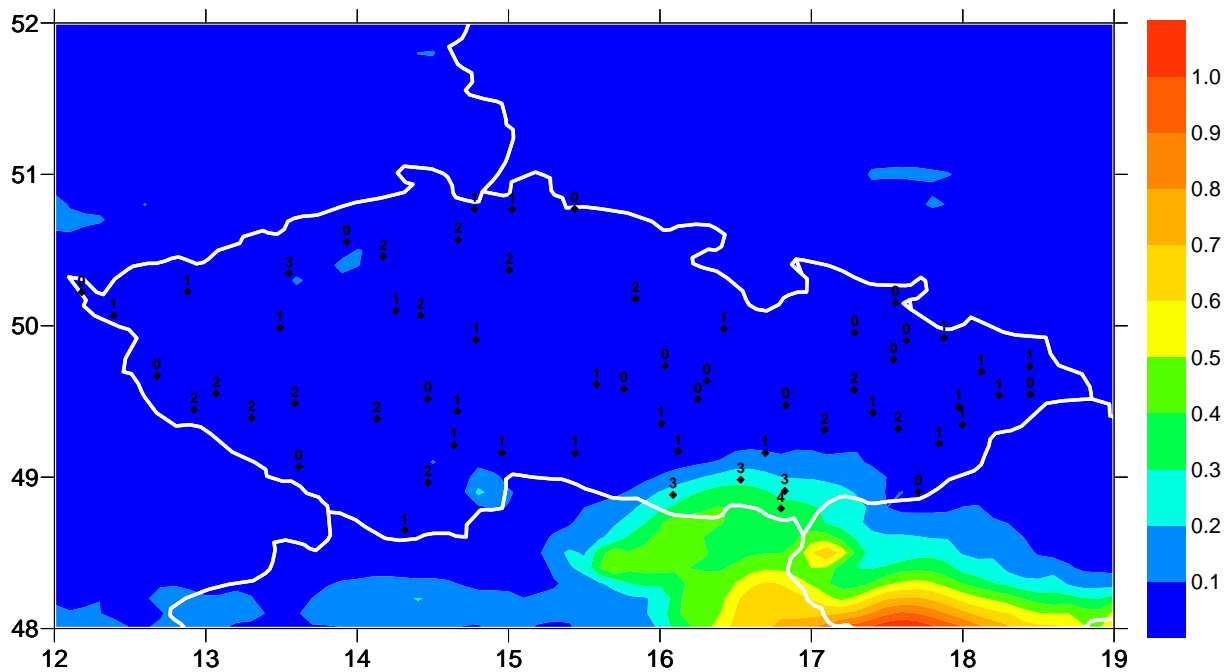


**Fig. CUNI.10.** Values of index 066 (**fraction of tropical days, %**) simulated by the RegCM model (background) and derived from data measured in the Czech Republic. Only very small number of days with  $T_{\max} \geq 30 \text{ }^{\circ}\text{C}$  can be found in the model outputs, mostly in the SE region of the examined area.

## CUNI.2 Projected changes

Projected changes of seasonal means of daily mean (Index003), minimum (Index002) and maximum (Index001) air temperatures between the future period 2021-2050 (2071-2100) and the reference period 1961-1990 are shown in figures CUNI.11-16. The projected changes are slightly larger in DJF than in JJA, for both future periods. The spatial variability of the changes is low, but in DJF the changes are growing towards east (northeast) while in JJA, a reverse pattern was found.

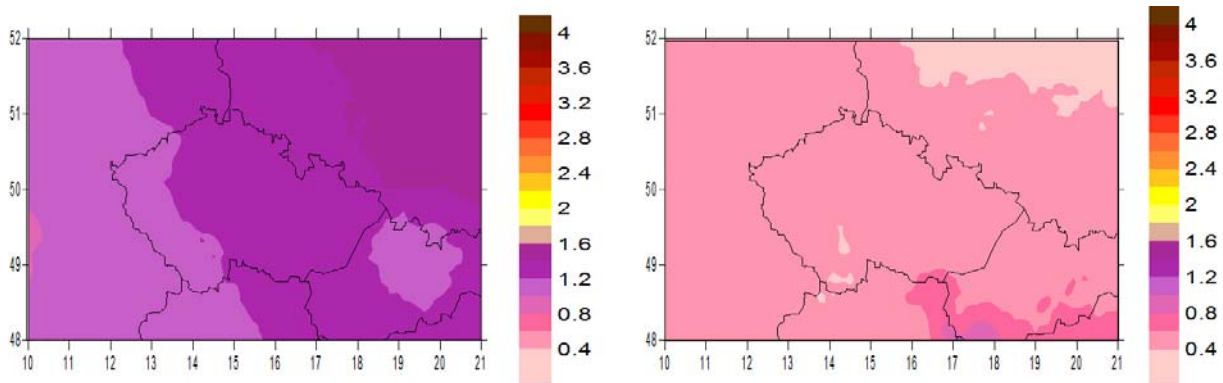


**Fig. CUNI.11.** Index 001 (mean of daily maximum temperature) – difference between the seasonal means in 2021-2050 and 1961-1990 [°C]. DJF season on the left, JJA on the right.

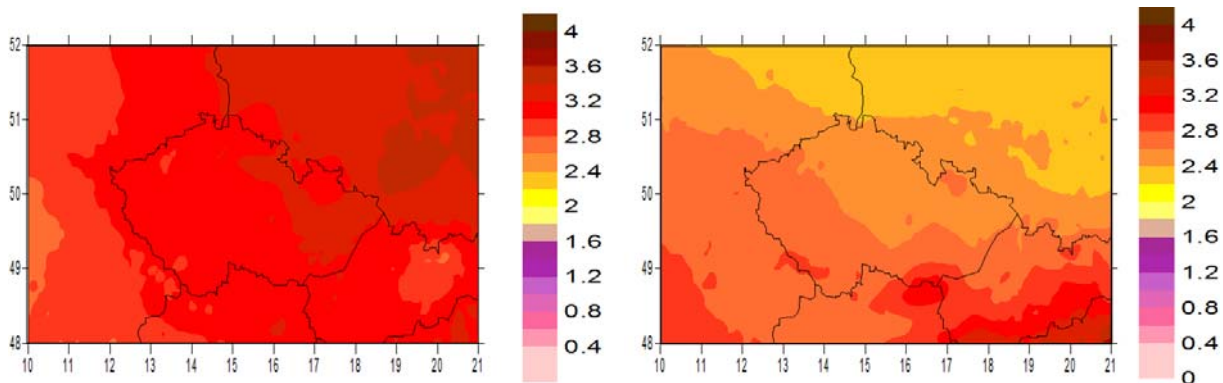


**Fig. CUNI.12.** Index 001 (mean of daily maximum temperature) – difference between the seasonal means in 2071-2100 and 1961-1990 [°C]. DJF season on the left, JJA on the right.

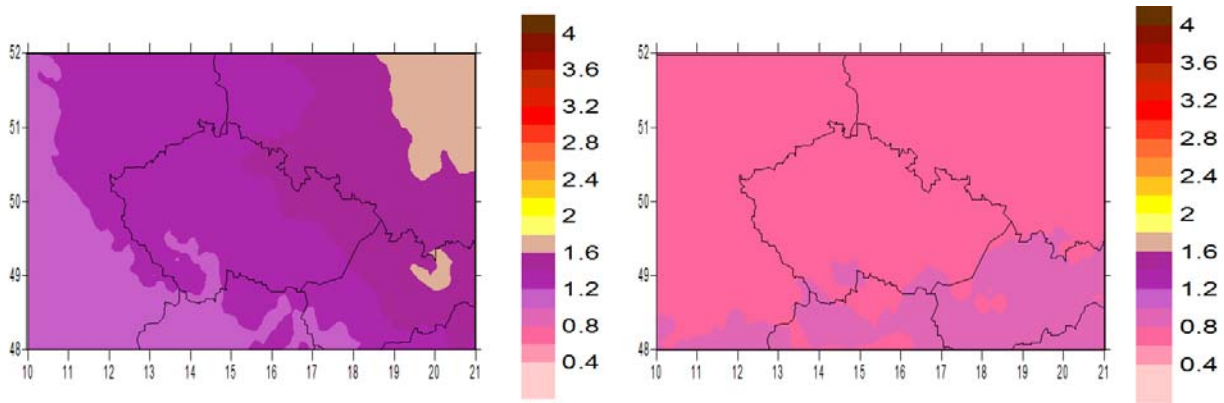


**Fig. CUNI.13.** Index 002 (mean of daily minimum temperature) – difference between the seasonal means in 2021-2050 and 1961-1990 [°C]. DJF season on the left, JJA on the right.

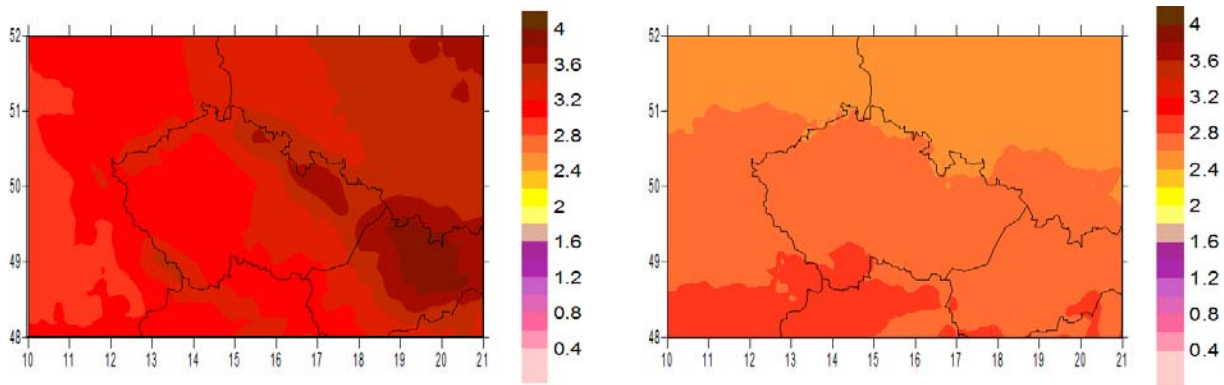


**Fig. CUNI.14.** Index 002 (mean of daily minimum temperature) – difference between the seasonal means in 2071-2100 and 1961-1990 [°C]. DJF season on the left, JJA on the right.

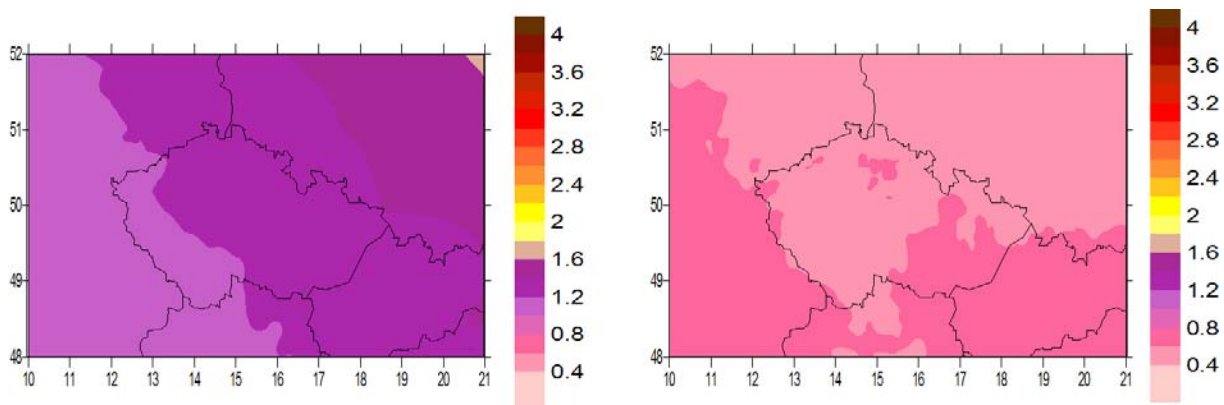


**Fig. CUNI.15.** Index 003 (mean temperature) – difference between the seasonal means in 2021-2050 and 1961-1990 [°C]. DJF season on the left, JJA on the right.

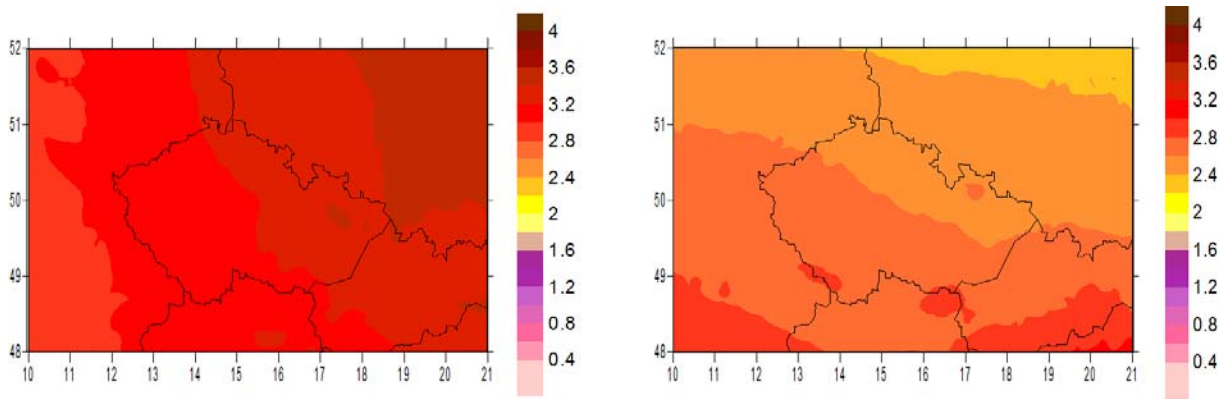


**Fig. CUNI.16.** Index 003 (**mean temperature**) – difference between the seasonal means in 2071-2100 and 1961-1990 [°C]. DJF season on the left, JJA on the right.

Rates of precipitation-based indices 076 and 077 simulated in future and reference periods are illustrated in the figures CUNI.17-20. Mean precipitation is not expected to change by more than 10 % in 2021-2050. The change in 2071-2100 is higher, DJF precipitation is projected to increase by 10-30 % over the most of the area, with largest change over Slovakia. Over the Czech Republic, the precipitation change is 10-20 %. In summer (JJA), the mean precipitation is expected to decrease, but the change is smaller than in DJF. Concerning the mean wet-day precipitation, similarly to mean climatological precipitation, the change is lower than 10% in 2021-2050. In 2071-2100, the mean wet day precipitation in JJA is expected to rise by 5-10% in the western part of the Czech Republic, and to decrease by 5% in the east. In DJF, increased wet-day precipitation is expected in the south-eastern part of studied area. The change is less than 10% over the area of the Czech Republic.

The change of the percentage of wet days is expected to be quite small in both future periods. In 2071-2100, the percentage of wet days is expected to increase in DJF, but to decrease in JJA (Figs. CUNI.21 and CUNI.22).

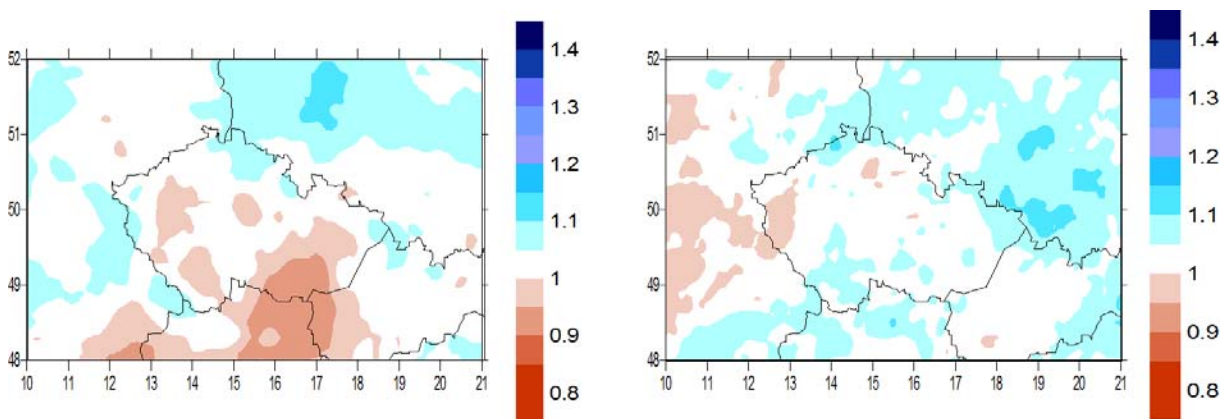


**Fig. CUNI.17.** Index 076 (**mean precipitation**) – relative difference between the seasonal means in 2021-2050 and 1961-1990. DJF season on the left, JJA on the right.

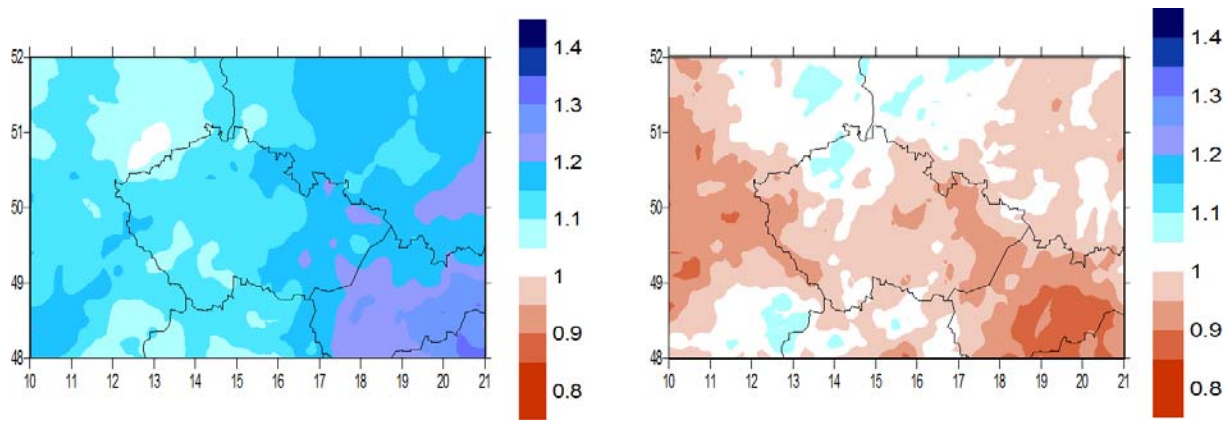


**Fig. CUNI.18.** Index 076 (mean precipitation) – relative difference between the seasonal means in 2071-2100 and 1961-1990. DJF season on the left, JJA on the right.

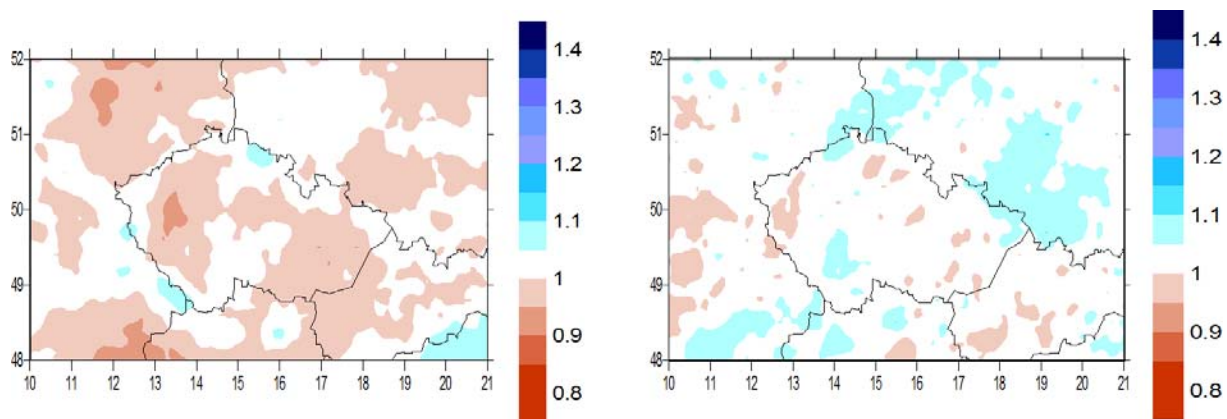


**Fig. CUNI.19.** Index 076 (mean precipitation intensity) – relative difference between the seasonal means in 2021-2050 and 1961-1990. DJF season on the left, JJA on the right.

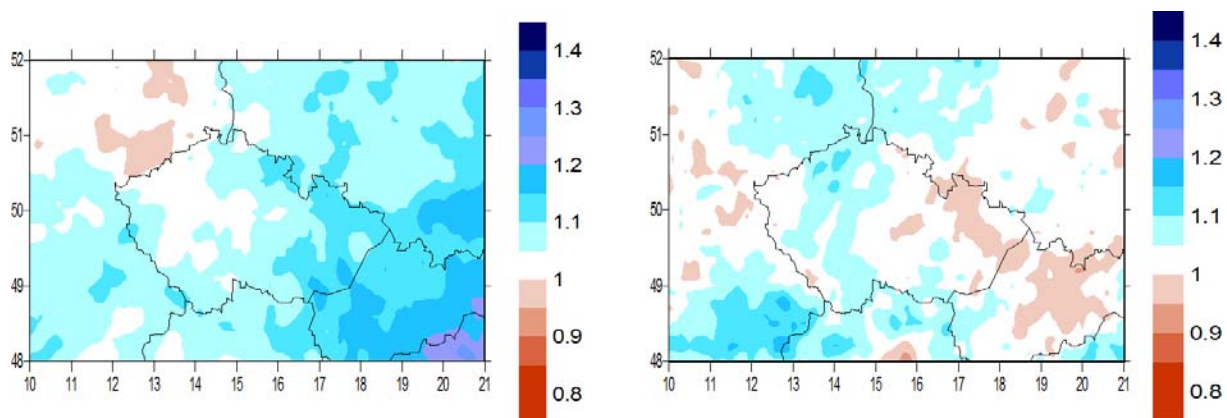


**Fig. CUNI.20.** Index 076 (mean precipitation intensity) – relative difference between the seasonal means in 2071-2100 and 1961-1990. DJF season on the left, JJA on the right.

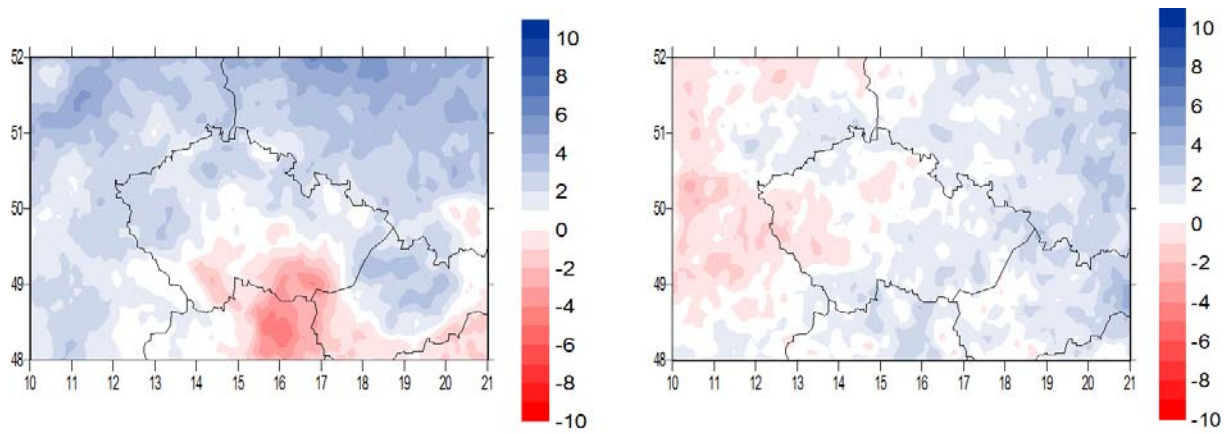


**Fig. CUNI.21.** Index 078 (**wet day fraction**) – difference between the seasonal means in 2021-2050 and 1961-1990 [%]. DJF season on the left, JJA on the right.

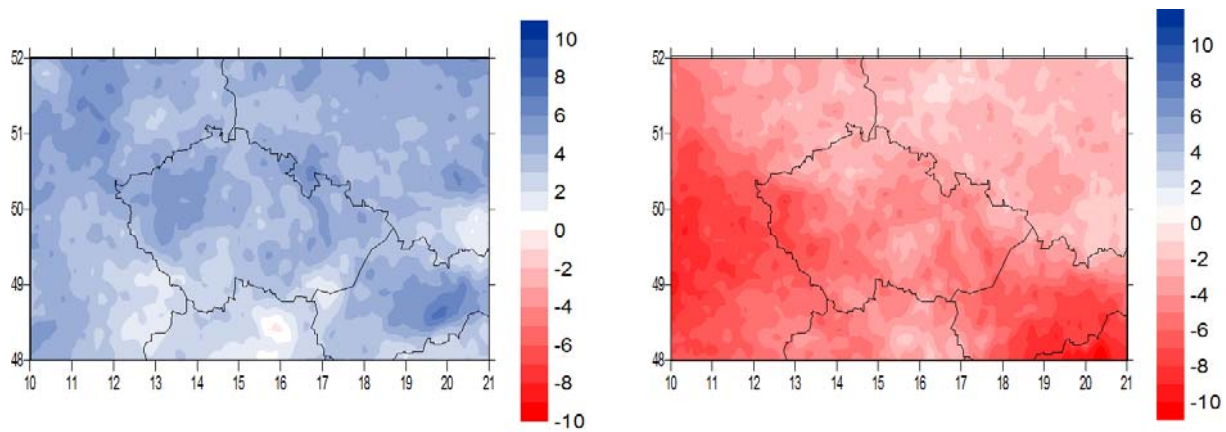


**Fig. CUNI.22.** Index 078 (**wet day fraction**) – difference between the seasonal means in 2071-2100 and 1961-1990 [%]. DJF season on the left, JJA on the right.

The changes of the mean of maximum 1-day (index 113) and 5-day (index 115) precipitation are very spatially variable, especially in JJA. For 2021-2050, the change in both indices is less than 10%. In DJF, the sign of change of index 113 is unambiguous, index 115 is expected to decrease slightly. For the period 2071-2100, there is a tendency for increase of both indices in DJF; in JJA, the fields are dominated by spatial variability, though an increase was simulated in a majority of grid points (Figs. CUNI.23-26).

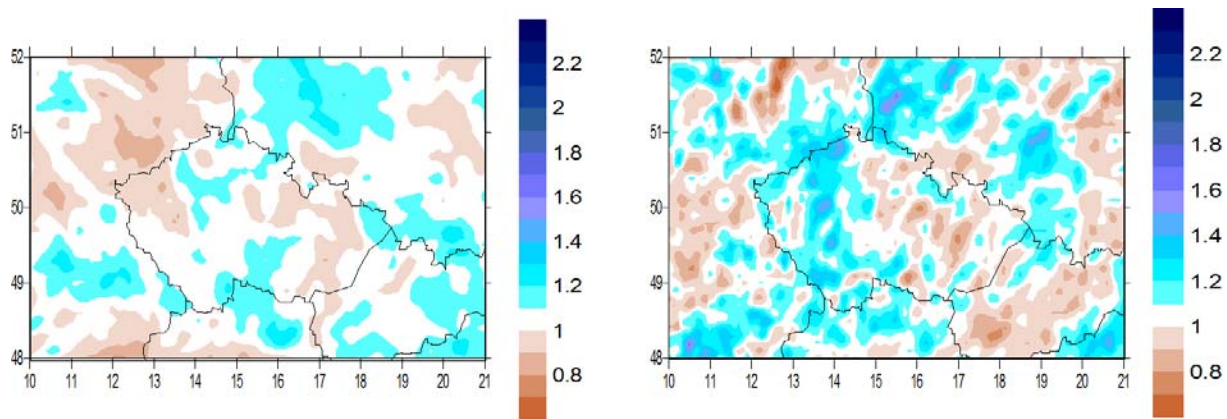


**Fig. CUNI.23.** Index 113 (mean maximum 1-day precipitation) – relative difference between the seasonal means in 2021-2050 and 1961-1990. DJF season on the left, JJA on the right.

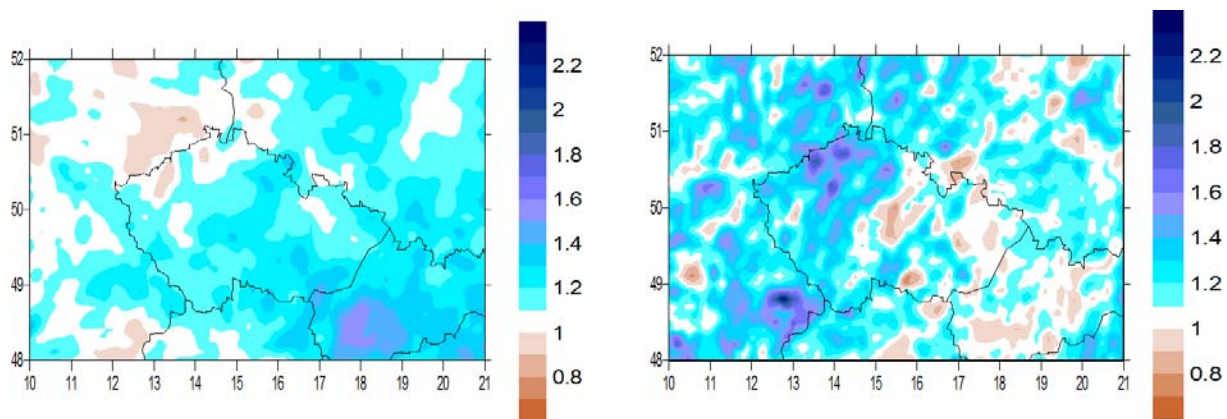


**Fig. CUNI.24.** Index 113 (mean maximum 1-day precipitation) – relative difference between the seasonal means in 2071-2100 and 1961-1990. DJF season on the left, JJA on the right.

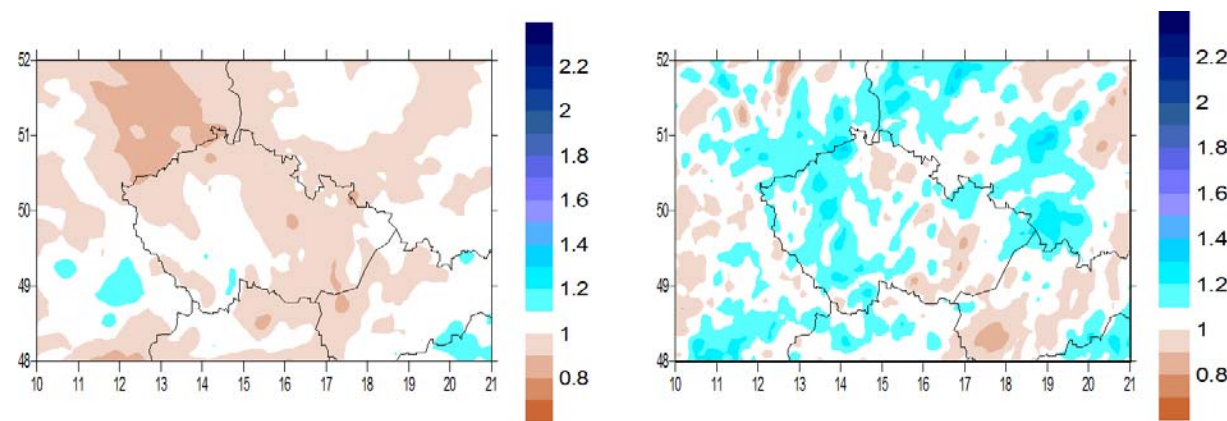


**Fig. CUNI.25.** Index 115 (mean maximum 1-day precipitation) – relative difference between the seasonal means in 2021-2050 and 1961-1990. DJF season on the left, JJA on the right.

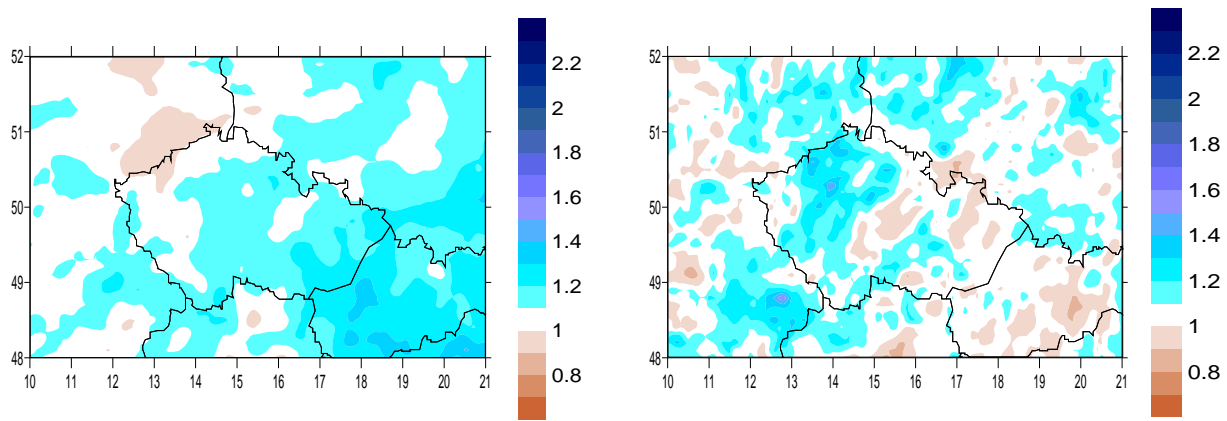


**Fig. CUNI.26.** Index 115 (mean maximum 1-day precipitation) – relative difference between the seasonal means in 2071-2100 and 1961-1990. DJF season on the left, JJA on the right.

Numbers of summer and tropical days generally increase for both future periods, following the rise of maximum daily temperature (Figs. CUNI.27-28). The actual values of this change can however be misleading, due to the aforementioned cold bias of maximum temperatures in summer.

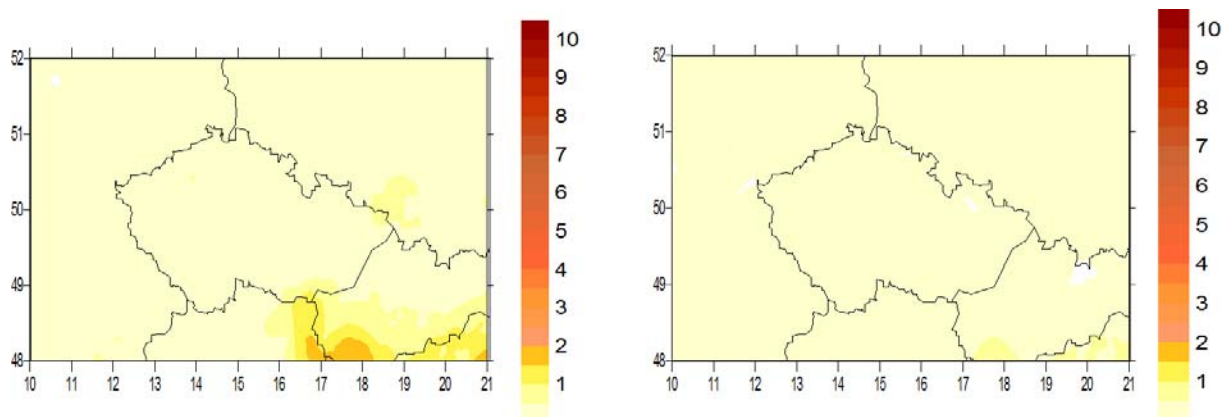


**Fig. CUNI.27.** Difference between the seasonal means of index 058 (**number of summer days**, left) and 066 (**number of tropical days**, right) in 2021-2050 and 1961-1990.

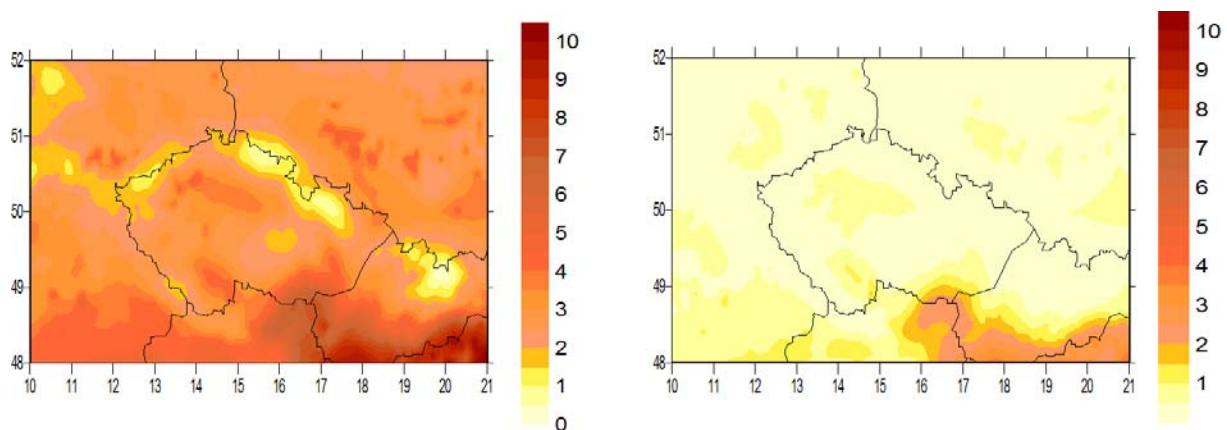


**Fig. CUNI.28.** Difference between the seasonal means of index 058 (**number of summer days**, left) and 066 (**number of tropical days**, right) in 2021-2050 and 1961-1990.

## **D4.4.b Analysis for Carpathian basin**

### **D4.4.b1 (led by ELU)**

Department of Meteorology, Eötvös Loránd University

#### **1. RCM description and calculated extreme indices**

- Model version: **RegCM3 (Beta)**
- Domain: **Carpathian Basin** (using  $120 \times 100$  gridpoints)
- Horizontal resolution: **10 km**
- Evaluation period: **1961-1990; 2021-2050; 2071-2100**
- LBC: **ECHAM driven RegCM (25 km)**
  
- Extreme indices calculated:  
**as agreed in D4.1**  
**(131 indices – from which 75 indices are related to temperature, and 56 indices are related to precipitation)**
- Extreme indices mapped:  
**30-year averages (1961-1990, 2021-2050, 2071-2100),**  
**changes between 2021-2050 and 1961-1990, and between 2071-2100 and 1961-1990**  
**(as simple difference, and relative change also),**  
**annual and four seasonal**
- Extreme indices included in this document: **as agreed**

for winter (DJF) and summer (JJA) seasons:

- 001 - mean Tmax**
- 002 - mean Tmin**
- 003 - mean Tmean**
- 076 - mean climatological precipitation**
- 077 - mean wet-day precipitation**
- 078 - percentage of wet days**
- 113 - greatest 1-day total rainfall**
- 115 - greatest 5-day total rainfall**

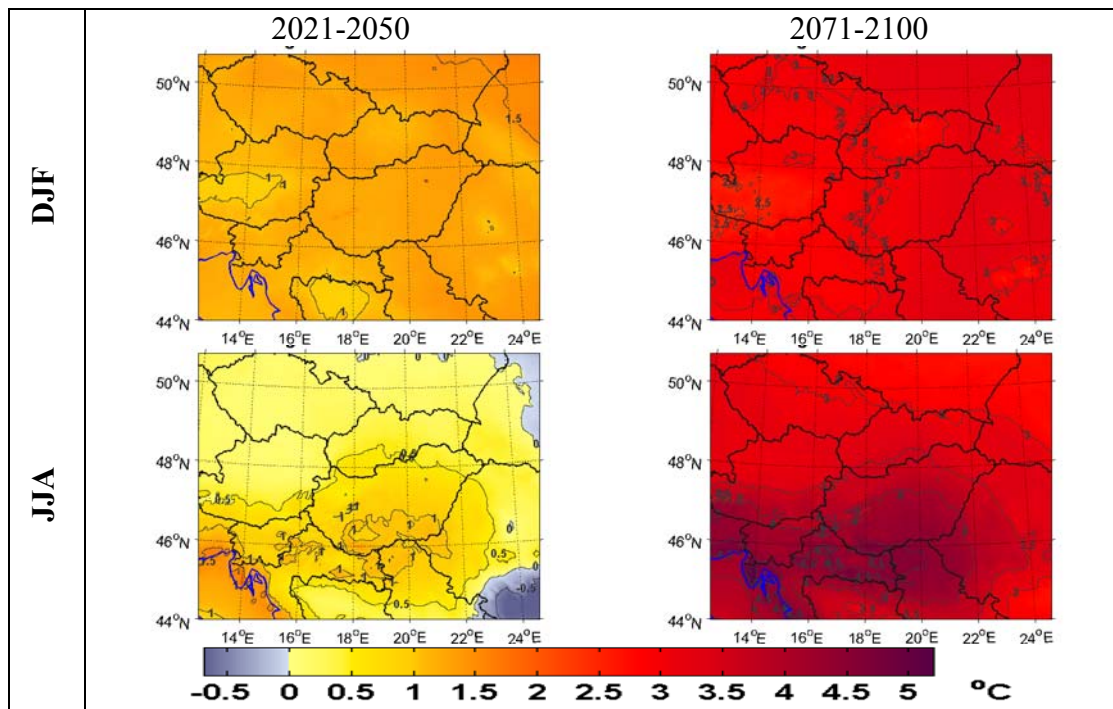
for annual scale:

- 058 - percentage of summer days ( $T_{\max} \geq 25 \text{ }^\circ\text{C}$ )**
- 066 - percentage of hot days ( $T_{\max} \geq 30 \text{ }^\circ\text{C}$ )**

## 2. RESULTS

### 2.1. Temperature related indices

#### Seasonal change of mean Tmax

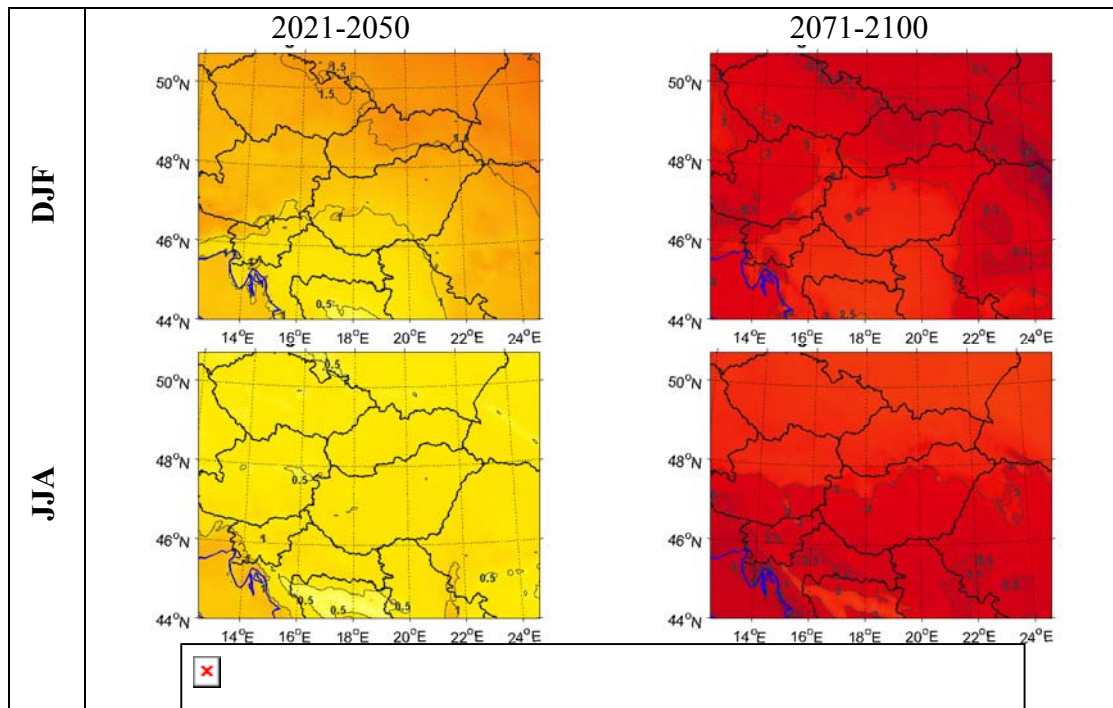


Simulated changes for Hungary:

Season	2021-2050 vs. 1961-1990	2071-2100 vs. 1961-1990
DJF	1.0-1.5 °C	2.8-3.2 °C
JJA	0.3-1.2 °C	3.3-4.8 °C

Simulated winter and summer daily maximum temperature are projected to increase by both time slices (2021-2050, 2071-2100) relative to the reference period (1961-1990). In Hungary the projected changes are about 1 °C by the middle of the 21st century, about 3 °C in winter and 4 °C in summer by the end of the 21st century. The projected winter warming is larger than the summer warming for the 2021-2050 period, while for the far future it is smaller.

## Seasonal change of mean Tmin

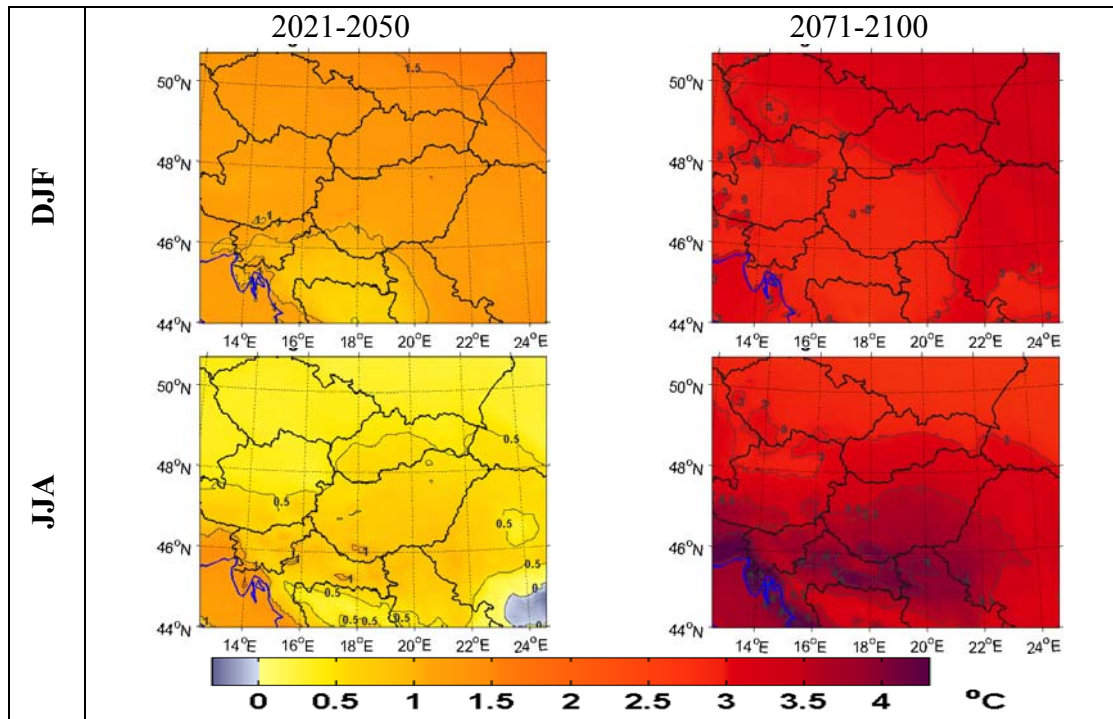


Simulated changes for Hungary:

Season	2021-2050 vs. 1961-1990	2071-2100 vs. 1961-1990
DJF	0.7-1.5 °C	2.7-3.4 °C
JJA	0.5-1.0 °C	2.8-3.5 °C

Similarly to the daily maximum temperature, simulated winter and summer daily minimum temperature are projected to increase by both time slices (2021-2050, 2071-2100) relative to the reference period (1961-1990). Also, similarly to the maximum temperature, the projected winter warming is larger than the summer warming for the 2021-2050 period, while for the 2071-2100 period it is slightly smaller. The projected changes in Hungary are also similar to that of the daily maximum temperature.

## Seasonal change of mean Tmean

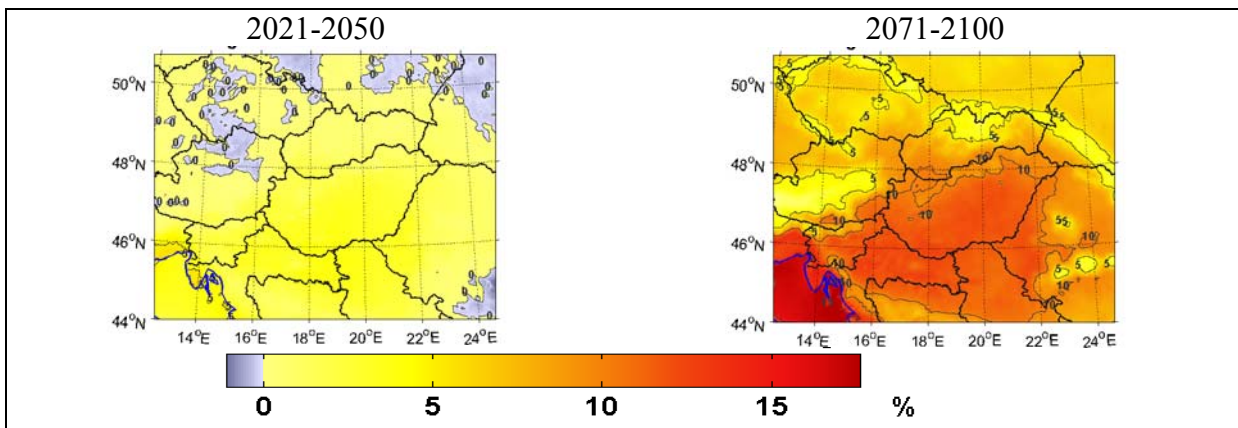


Simulated changes for Hungary:

Season	2021-2050 vs. 1961-1990	2071-2100 vs. 1961-1990
DJF	0.7-1.4 °C	2.7-3.2 °C
JJA	0.5-1.0 °C	3.0-4.2 °C

Similar conclusions can be drawn in case of the simulated daily mean temperature changes to those found in case of daily maximum and minimum temperature. Daily mean temperature is projected to increase, the winter warming is larger than the summer warming for the 2021-2050 period, while for the 2071-2100 period it is smaller. The projected changes in Hungary are about 1 °C by the middle of the 21st century, about 3 °C in winter and 3.5 °C in summer by the end of the 21st century.

## Annual change of percentage of summer days

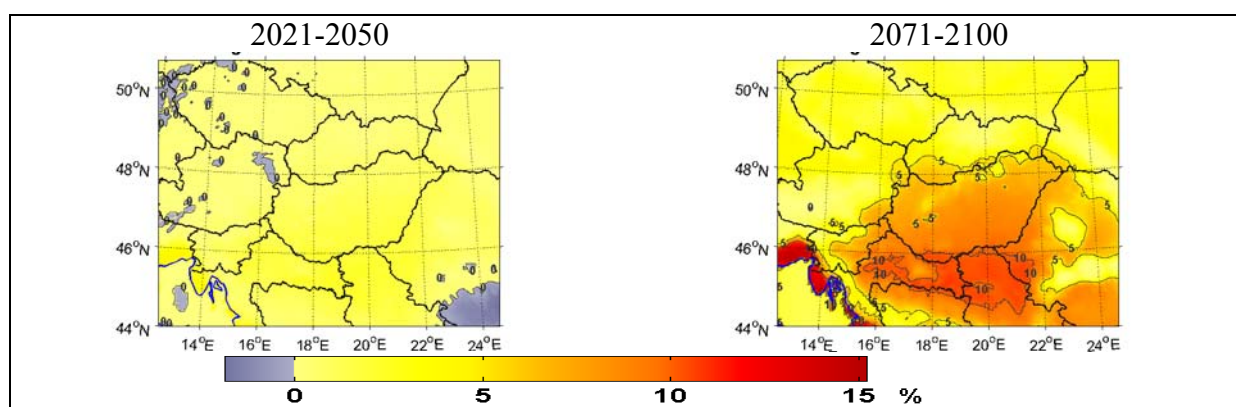


Simulated changes for Hungary:

	1961-1990	2021-2050	2071-2100
Annual ratio	6-20%	8-22%	15-33%
Simulated change	-	1-3%	7-14%

Summer days (when the  $T_{max}$  is larger than  $25\text{ }^{\circ}\text{C}$ ) may occur mainly in May-September in Hungary. In the reference period 6-20% of the total days are simulated as summer days, which means about 22-73 days in a year. By the near future (2021-2050) it is not likely to change too much in Hungary (the increase is only about a week), however, by the end of the century (2071-2100) the annual number of summer days is projected to exceed 110 days in a year in the southern part of the country, and may even reach as much as 120 days per year.

## Annual change of percentage of hot days



Simulated changes for Hungary:

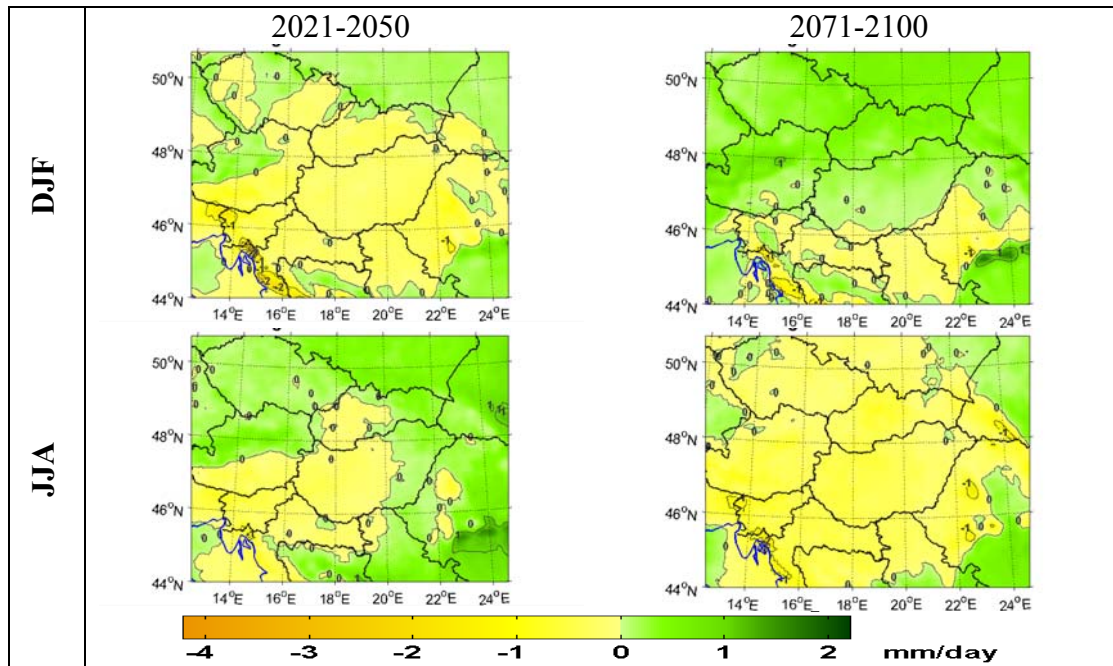
	1961-1990	2021-2050	2071-2100
Annual ratio	2-8%	3-11%	6-17%
Simulated change	-	1-3%	4-12%

Hot days (when the Tmax is larger than 30 °C) may occur mainly in June-August in Hungary.

In the reference period less than 8% of the total days are simulated as hot days, which means less than 30days/year on average. Similarly to the percentage of summer days, the simulated changes by 2071-2100 in Hungary are much larger than the changes by 2021-2050. Also similarly to the summer days, the large frequency changes are projected to occur in the southern part of the country (where according to the RegCM simulations about 62 days will be considered hot days yearly).

## 2.2. Precipitation related indices

### Seasonal change of mean climatological precipitation

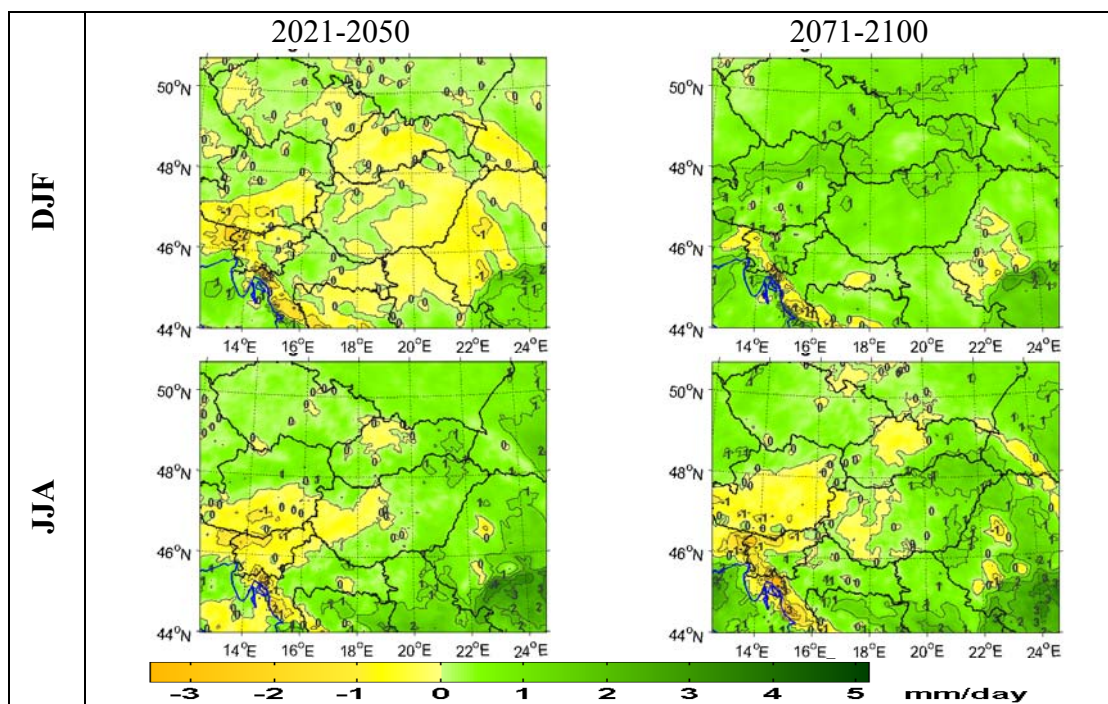


Simulated changes for Hungary:

Season	2021-2050 vs. 1961-1990	2071-2100 vs. 1961-1990
DJF	(-0.5; 0) mm/day (-20%; 0%)	(-0.2; 0.8) mm/day (0%; +20%)
JJA	(-0.5; 0.6) mm/day (-25%; +20%)	(-0.6; 0) mm/day (-30%; 0%)

In general, simulated winter and summer daily mean precipitation are projected to decrease in Hungary by 2021-2050. However, in summer, the eastern part of the country may expect a slightly wetter climate compared to the reference period (1961-1990). Opposite changes are projected for Hungary by 2071-2100 in case of winter and summer. The climate is likely to become wetter in winter and drier in summer. The largest changes are about +20%, and -30% respectively.

## Seasonal change of mean wet-day precipitation

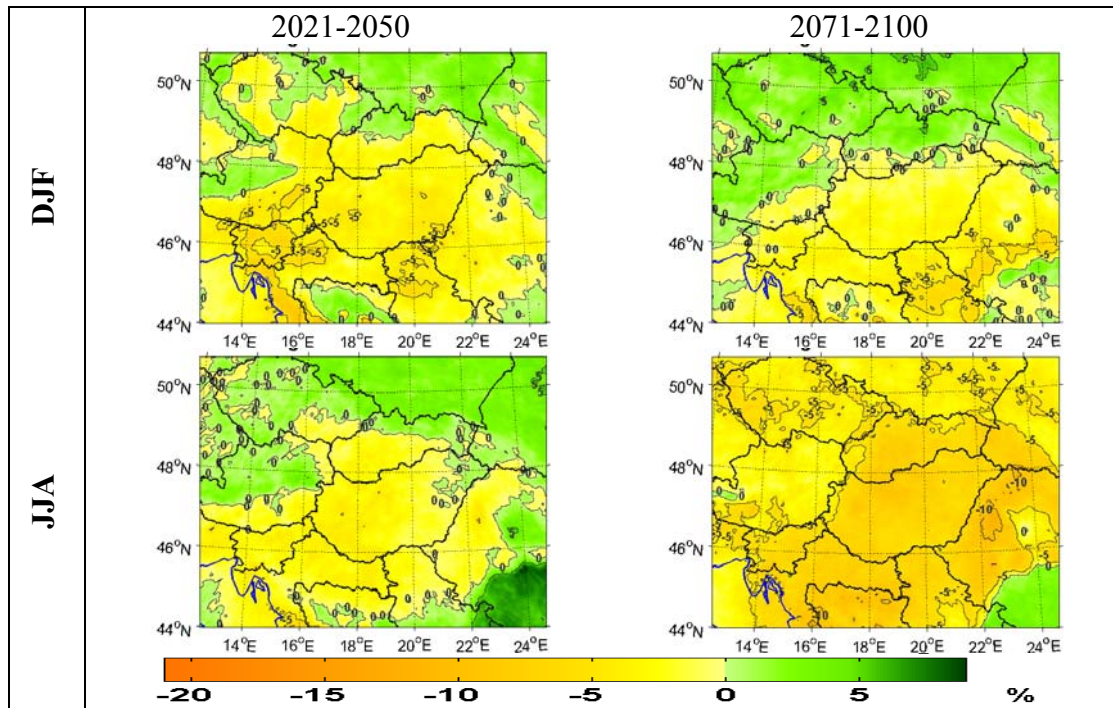


Simulated changes for Hungary:

Season	2021-2050 vs. 1961-1990	2071-2100 vs. 1961-1990
DJF	(-0.5; +0.5) mm/day (-10%; +10%)	(0; 1.2) mm/day (0%; +20%)
JJA	(-1; +1.2) mm/day (-10%; +22%)	(-0.5; +2) mm/day (-7%; +30%)

Simulated winter wet-day mean precipitation is projected mostly to decrease in eastern Hungary and increase in western Hungary by 2021-2050. In summer, large portion of the country (especially in east) may expect an increase of mean wet-day precipitation amount, decrease is projected only around the lake Balaton. The simulations show similar changing pattern by the end of the century for summer. In winter, the wet-day mean precipitation is projected to increase in the entire country. The largest increase is about 30% in the northern mountainous region.

## Seasonal change of percentage of wet days

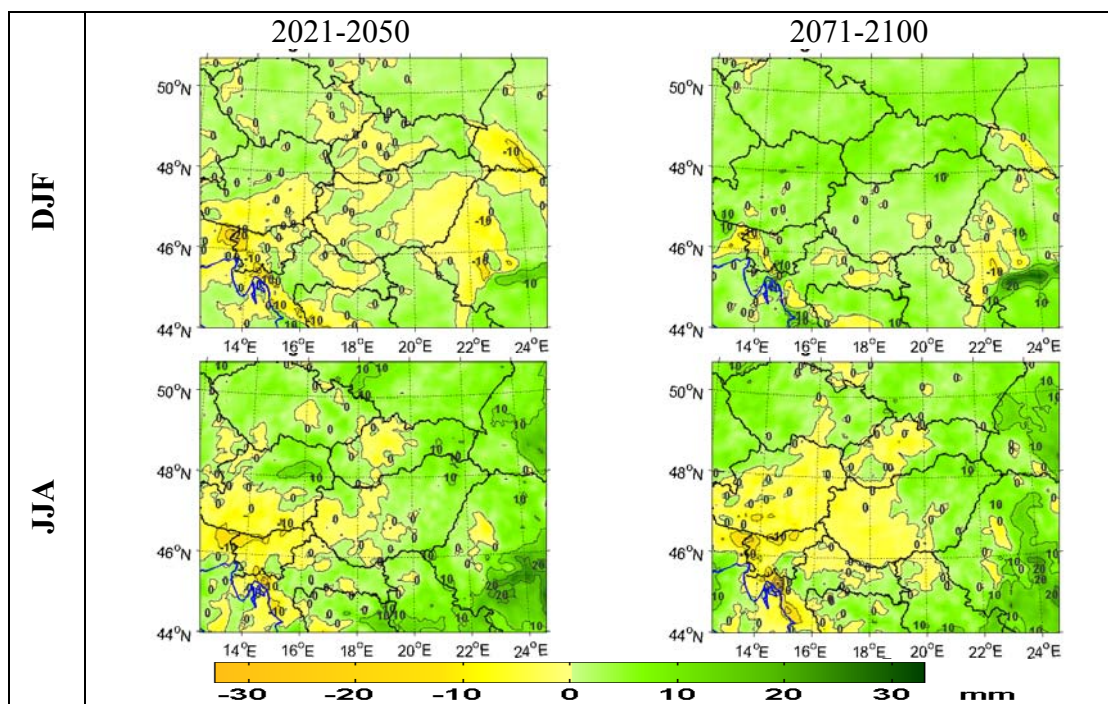


Simulated changes for Hungary:

	1961-1990	2021-2050	2071-2100
DJF ratio	25-43%	22-45%	25-45%
Simulated change	-	(-5%; 0%)	(-3%; 0%)
JJA ratio	25-40%	20-40%	15-30%
Simulated change	-	(-5%; +2%)	(-10%; -5%)

The percentage of wet days is projected to decrease for both winter and summer, and for both future time slices. The simulated changes are larger by 2071-2100 than 2021-2050. The largest changes are projected for summer by the end of the 21st century, when the percentage is likely to decrease by as much as 10%, which means about 9 days less wet day in a season.

## Seasonal change of the greatest 1-day total rainfall

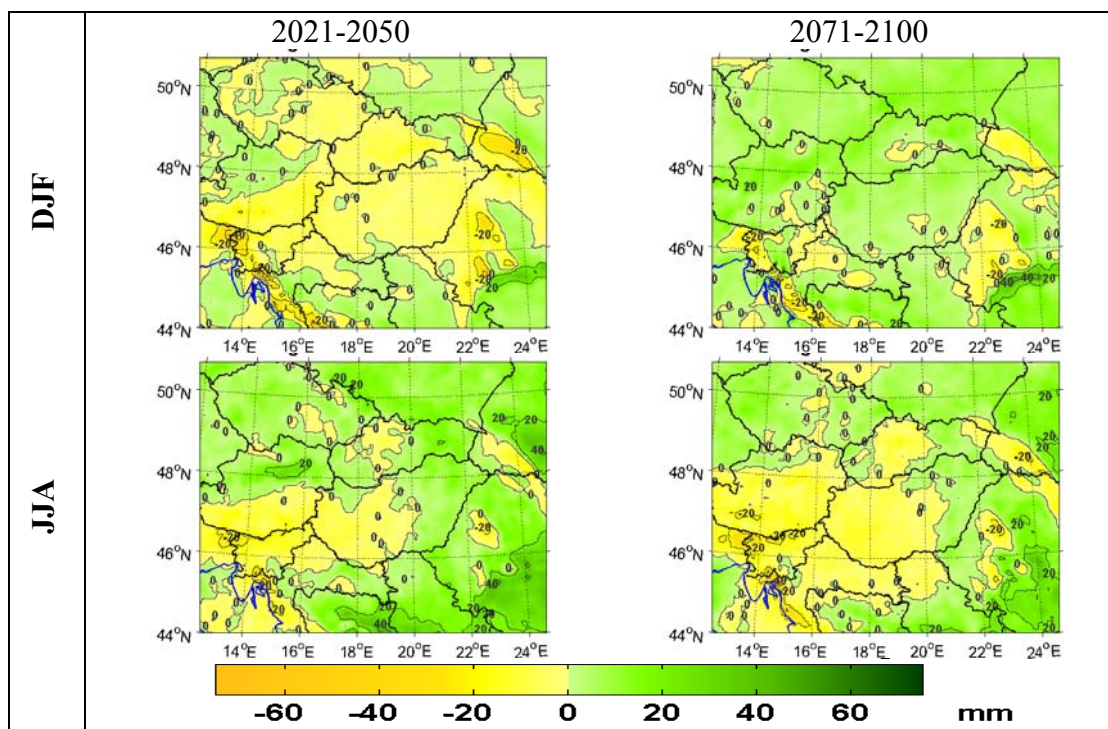


Simulated changes for Hungary:

	1961-1990	2021-2050	2071-2100
DJF	15-30 mm	15-35 mm	18-40 mm
Simulated change	-	(-5 mm; +5 mm) (-20%; +25%)	(0 mm; +10 mm) (0%; +40%)
JJA	20-30 mm	30-40 mm	20-30 mm
Simulated change	-	(-5 mm; +10 mm) (-20%; +50%)	(-5 mm; +10 mm) (-25%; +50%)

The simulated greatest 1-day total rainfall is projected to increase in Hungary by 2071-2100 in winter, the largest changes are expected in the northern mountainous region where it may increase as much as by 40% compared to the reference period. Similar changes are projected in summer for the eastern part of the country, while for the western part the greatest 1-day total rainfall a decrease is expected on the base of the RegCM simulations.

## Seasonal change of the greatest 5-day total rainfall



Simulated changes for Hungary:

	1961-1990	2021-2050	2071-2100
DJF	30-50 mm	30-50 mm	30-60 mm
Simulated change	-	(-10 mm; +5 mm) (-15%; +10%)	(0 mm; +15 mm) (-5%; +25%)
JJA	30-55 mm	30-60 mm	30-55 mm
Simulated change	-	(-10 mm; +15 mm) (-20%; +30%)	(-15 mm; +10 mm) (-30%; +30%)

Similarly to the greatest 1-day total rainfall, the simulated greatest 5-day total rainfall is projected to increase in Hungary by 2071-2100 in winter, and in the northern and eastern regions of the country in summer. This parameter is likely to decrease in the western and central parts of Hungary. By 2021-2050 the pattern of the winter simulated change in Hungary is very different from that of the 2071-2100, namely, the greatest 5-day total rainfall is projected to decrease in Hungary. The pattern of the summer simulated change in Hungary by 2021-2050 is similar to that of the 2071-2100 change, but the decreasing trend is projected for less area in the country.

## **D4.4.b2 Extreme core indices for Hungary simulated with Aladin Climate scenarios vs control (led by OMSZ)**

Monika Lakatos Hungarian Meteorological Service

The expected future change of the extreme temperature and precipitation core indices defined in the WP4 deliverable 4.2 are characterized by the difference maps of the averaged indices values. The daily temperature and precipitation indices resulting from Aladin-Climate simulations for two time slices: 2021-2050 and 2071-2100 versus control run forced by ERA40 were analysed for Hungary.

### **Temperature indices**

The changes of the percentage of “summer days, where  $T_{max} > 25^{\circ}C$ ” and “hot days, where  $T_{max} \geq 30^{\circ}C$ ” are illustrated on annual scale (*Fig. 1-4*). According to the result maps positive change is expected in the warm temperature indices. The increasing of summer days comparing to the control period are between 16.5% and 11.5% in the grid points located in Hungary. The far future change is 16.2 % at least, but there are regions where the increasing exceeds the 22%. The rate of “hot days” increasing is expected more than 10% in the period 2021-2050 on the Great Plain and it is more than 20% almost on the whole territory, excluding the mountainous area, in the period 2071-2100.

The expected change of mean daily maximum and mean daily minimum temperatures were analysed on seasonal scale (*Fig. 5-12*). Both imply warming also in winter and in summer in both projected period. The degree of warming in the near future in the case of daily maximum is higher than in the case of daily minimum in winter. The South Trans Danubian region shows a significant daily minimum increasing in 2021-2050 in winter season. The largest warming, 5.5 °C - 8.1°C, appeared in summer in daily maximum temperatures in the 2071-2100 time interval in Hungary. The middle and southern parts are the hottest according to the far future simulations.

### **Precipitation indices**

Regarding the percentage of wet days (number of days where daily sum  $\geq 1$ mm / total number of days) index (*Fig. 13-16*); there is an obvious decreasing in summer in projections versus the control run, especially in the 2071-2100 period. The order of negative change in summer is larger, around -25% on the extended part of the country, in the far future. The negative change in winter is around -15%, the spatial distribution shows a north eastern growth in both projections and season.

There is no substantive change in the greatest one day total precipitation (*Fig. 17-20*) in winter, none of projections, excluding the eastern border and mid Trans Daubian regions. Maps, concerning summer season are more variable, the change of the one day total precipitation are between 10.8 mm- and -14.2 mm in the period 2021-2050; and 2.3 mm and -15.5 mm in 2071-2100. The decreasing tendency is rather typical than increasing in the future time periods. In the greatest five day total (*Fig. 21-24*) a weak (4-12 mm) increasing is declared in the eastern boundary region in winter, a strong decreasing (12-24 mm) is showed on extended territories of Hungary in summer. The difference between the two future intervals is not considerable.

### Annual maps

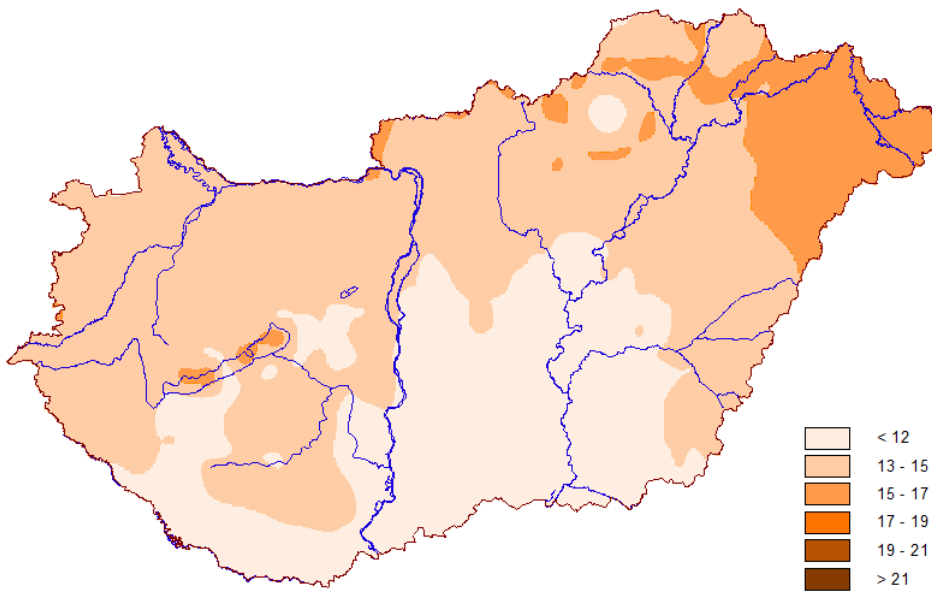


Fig.1. 058 %age of days where  $T_{max} > 25^{\circ}\text{C}$  AA(2021-2050)-AE(1961-1990)

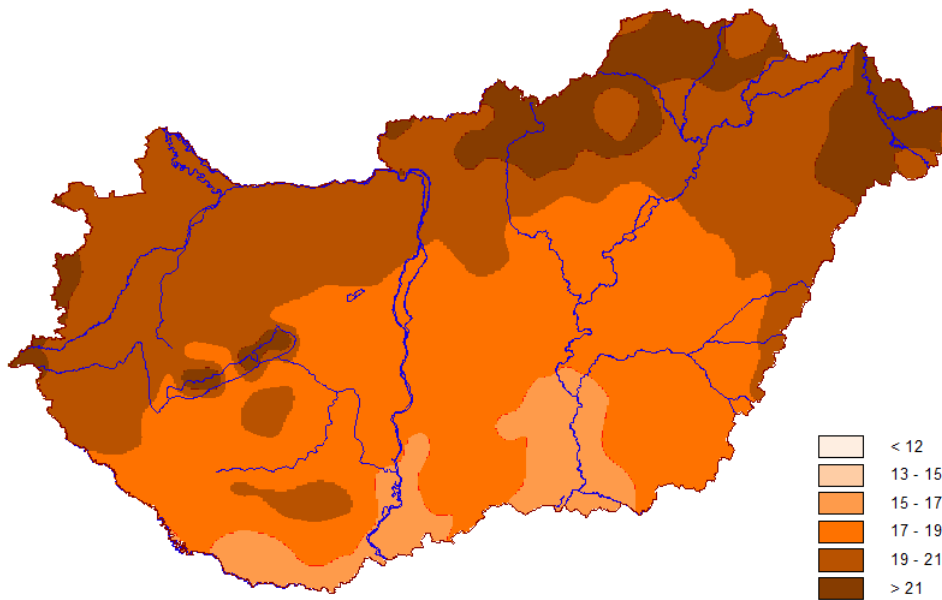


Fig. 2. 058 %age of days where  $T_{max} > 25^{\circ}\text{C}$  AA(2071-2100)-AE(1961-1990)

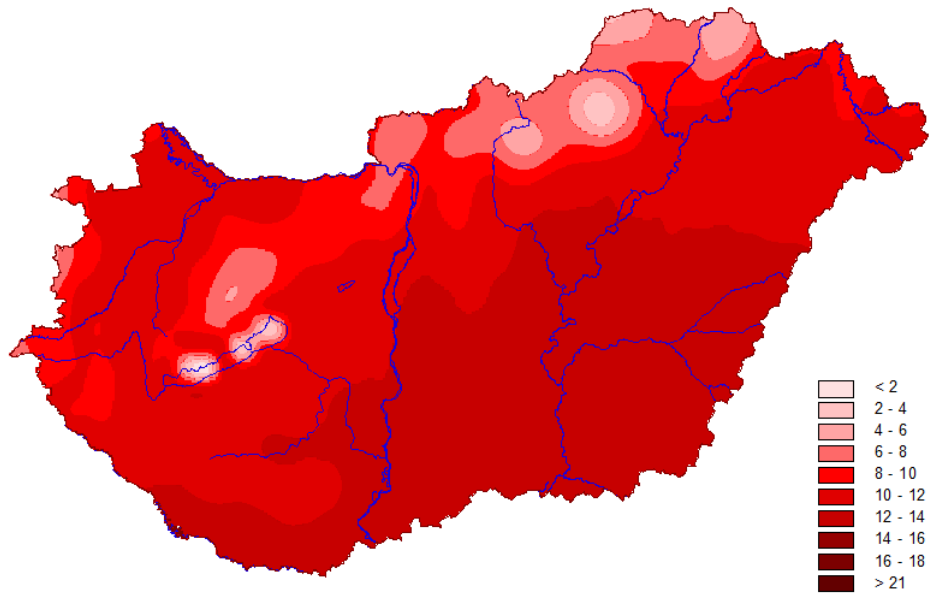


Fig. 3. 066 %age of days with  $T_{max} \geq 30^{\circ}\text{C}$  AA(2021-2050)-AE(1961-1990)

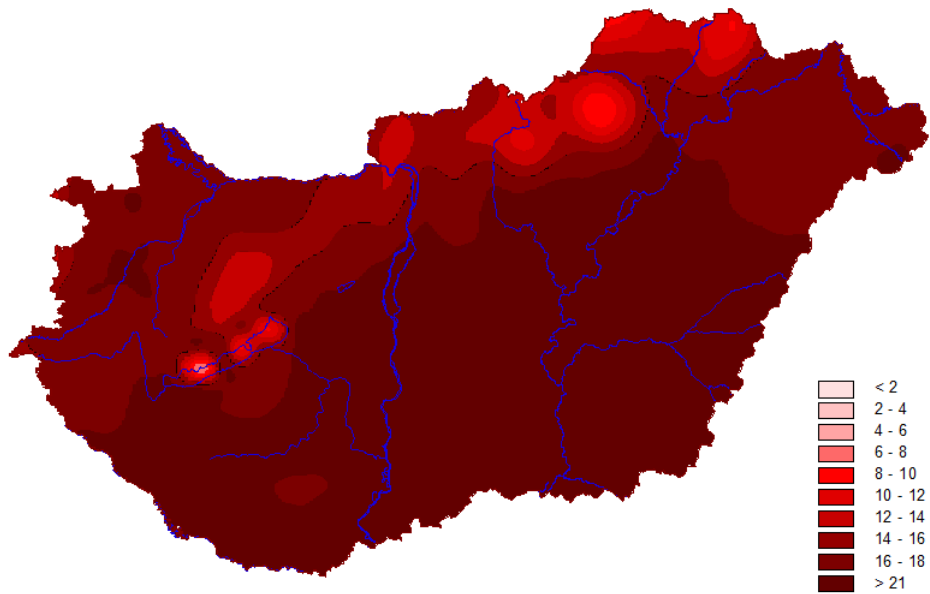


Fig.4. 066 %age of days with  $T_{max} \geq 30^{\circ}\text{C}$  AA(2071-2100)-AE(1961-1990)

### Winter DJF, Summer JJA maps

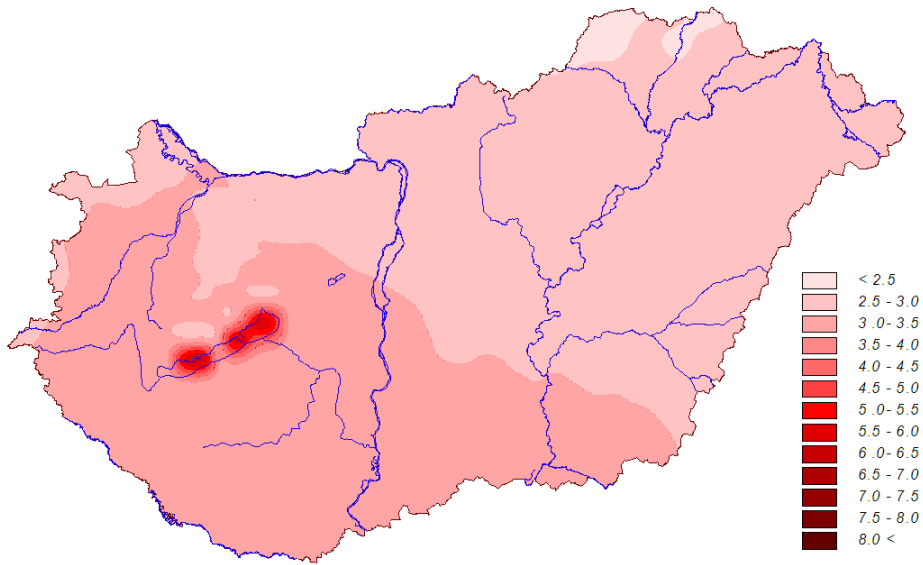


Fig. 5. 001 Mean Tmax DJF AA(2021-2050)-AE(1961-1990)

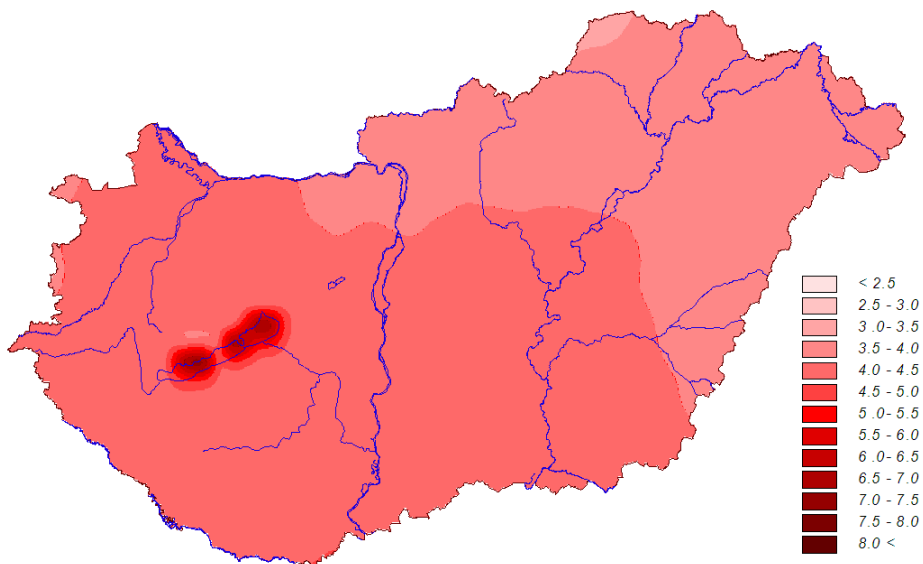
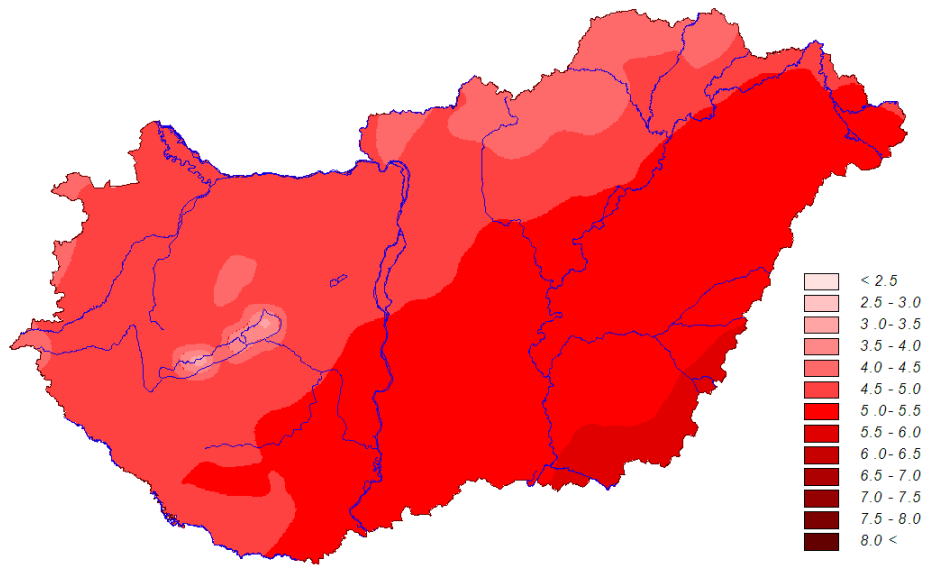
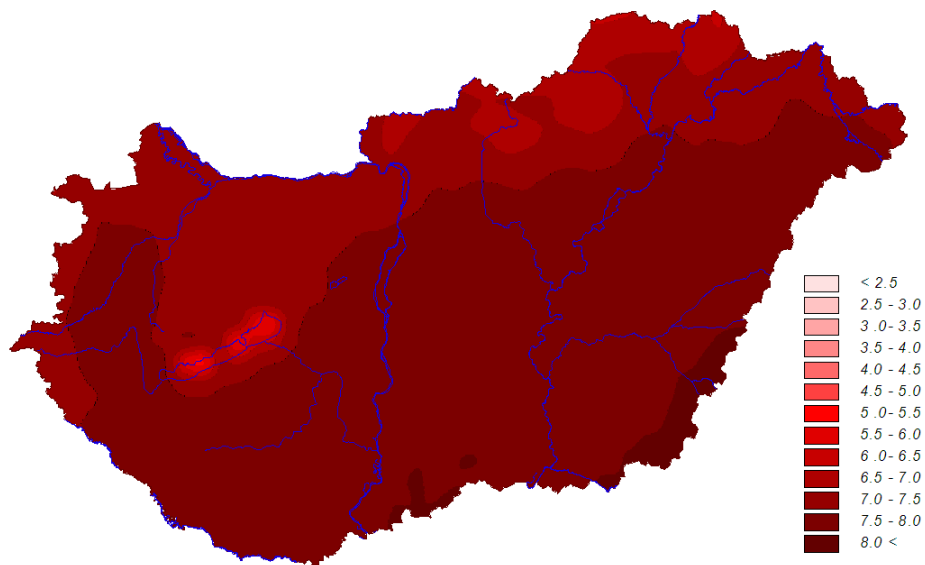


Fig. 6. 001 Mean Tmax DJF AA(2071-2100)-AE(1961-1990)



*Fig. 7. 001 Mean Tmax JJA AA(2021-2050)-AE(1961-1990)*



*Fig. 8. 001 Mean Tmax JJA AA(2071-2100)-AE(1961-1990)*

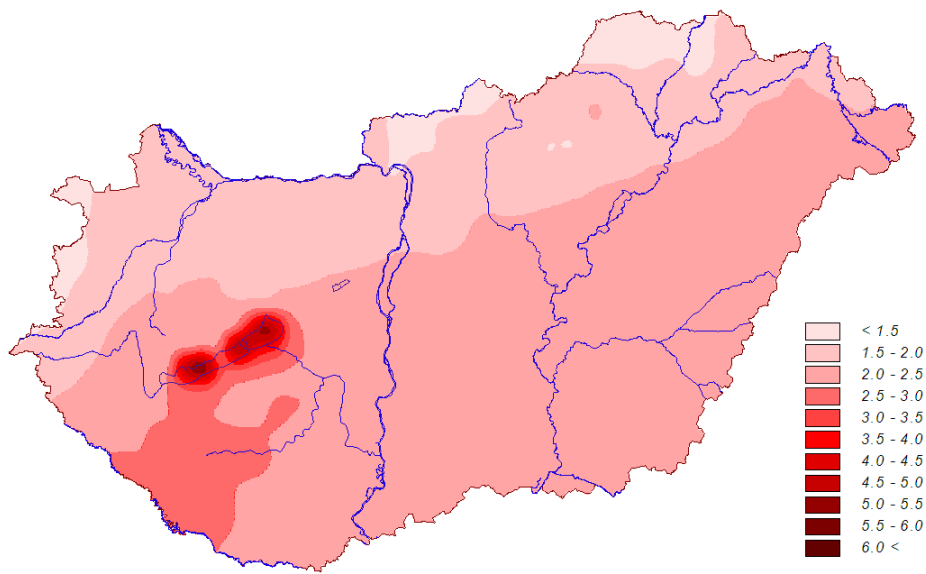


*Fig. 9. 002 Mean Tmin DJF AA(2021-2050)-AE(1961-1990)*

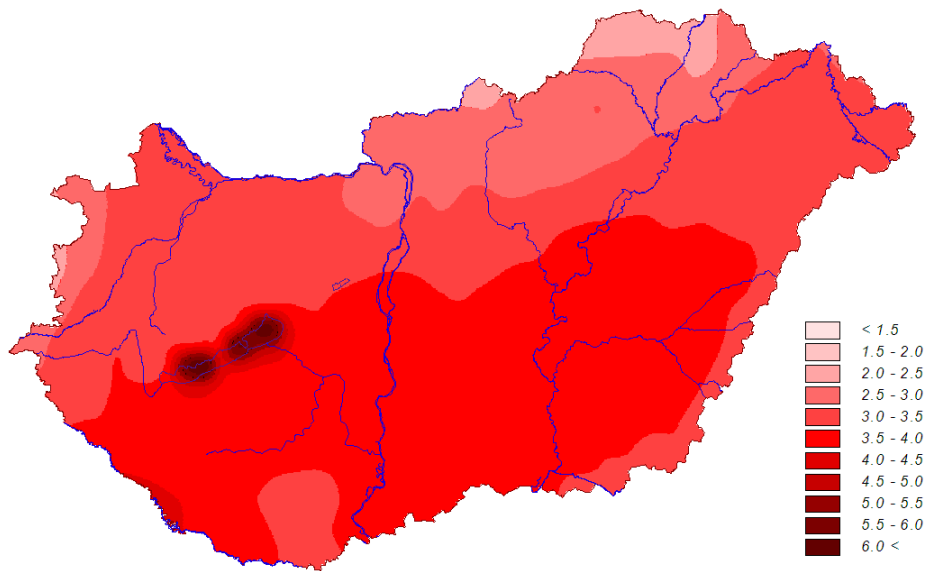


*Fig. 10. 002 Mean Tmin DJF AA(2071-2100)-AE(1961-1990)*

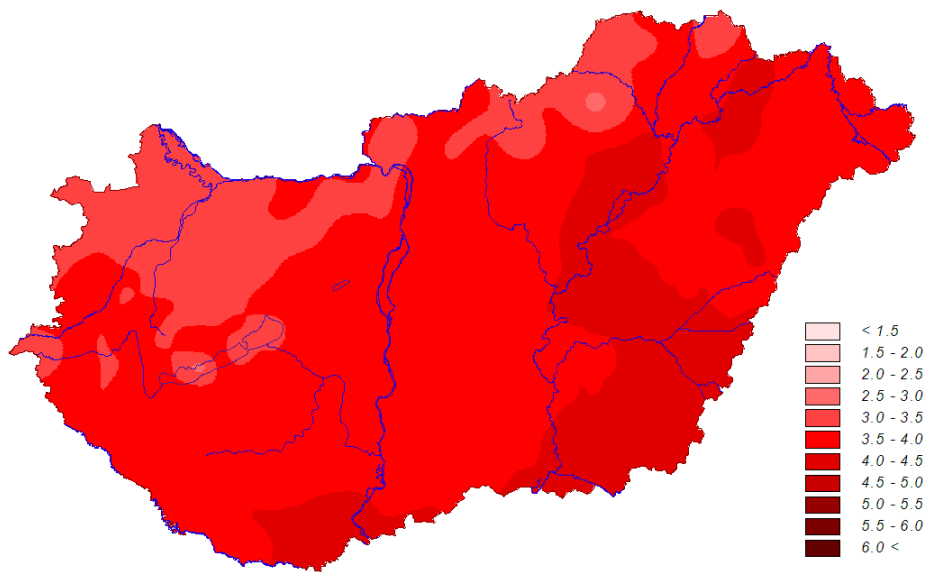


*Fig. 11. 002 Mean Tmin JJA AA(2021-2050)-AE(1961-1990)*

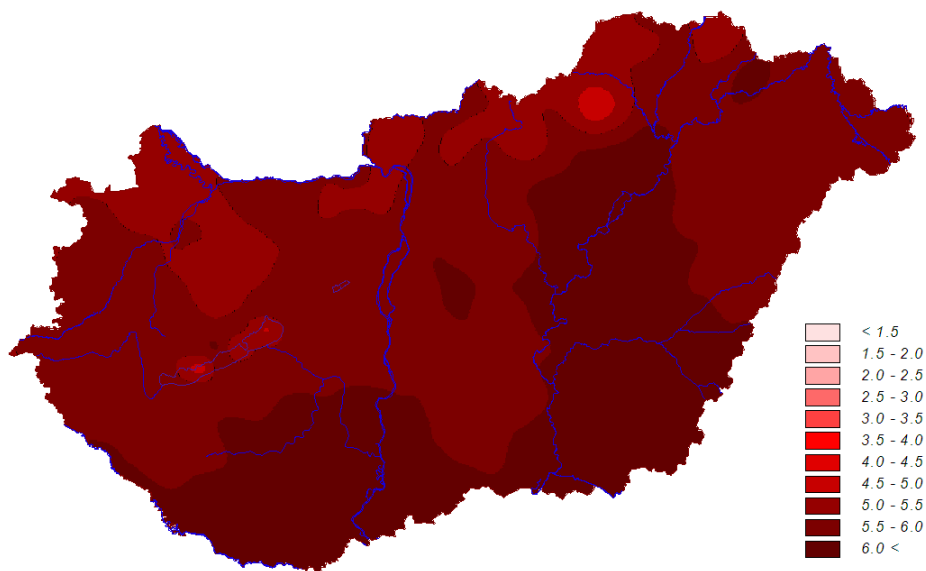


*Fig. 12. 002 Mean Tmin JJA AA(2071-2100)-AE(1961-1990)*

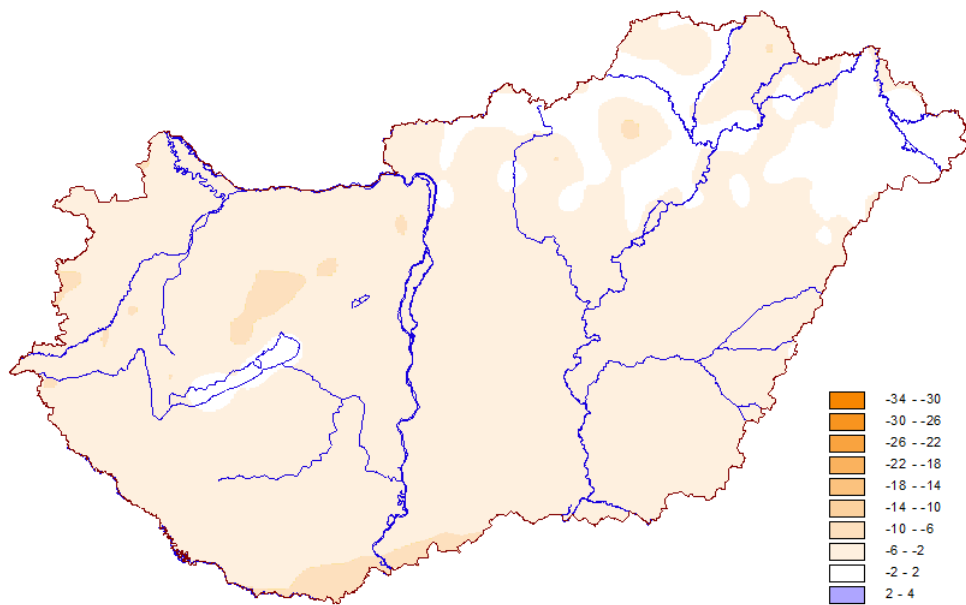


*Fig. 13. 078 Perc of wet days DJF AA(2021-2050)-AE(1961-1990)*

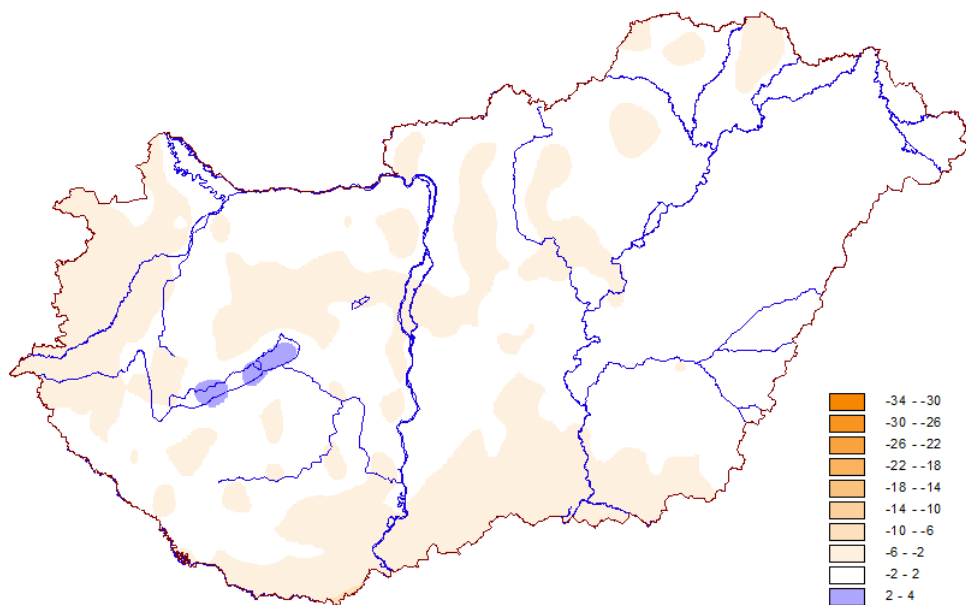


*Fig. 14. 078 Perc of wet days DJF AA(2071-2100)-AE(1961-1990)*

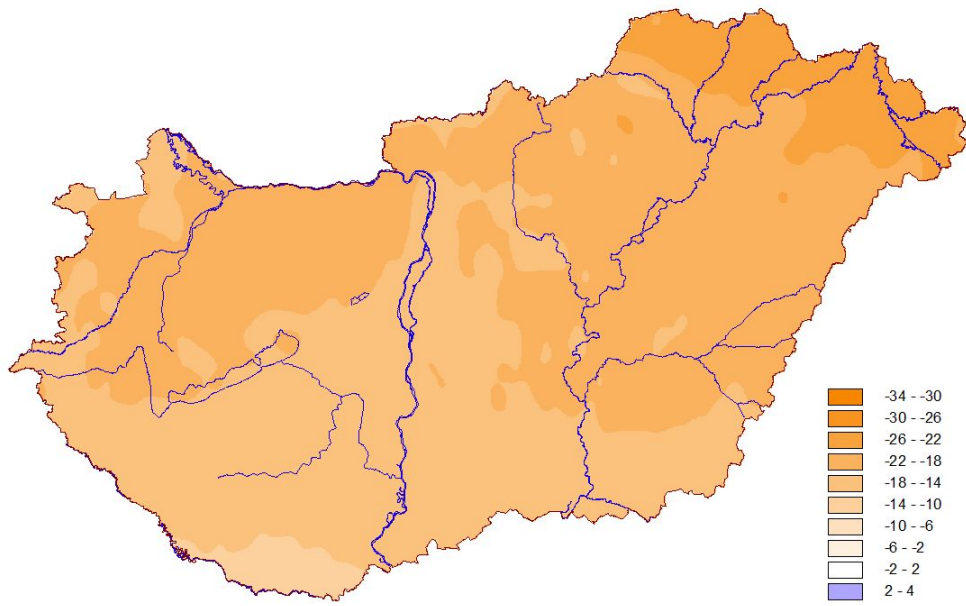


*Fig. 15. 078 Perc of wet days JJA AA(2021-2050)-AE(1961-1990)*

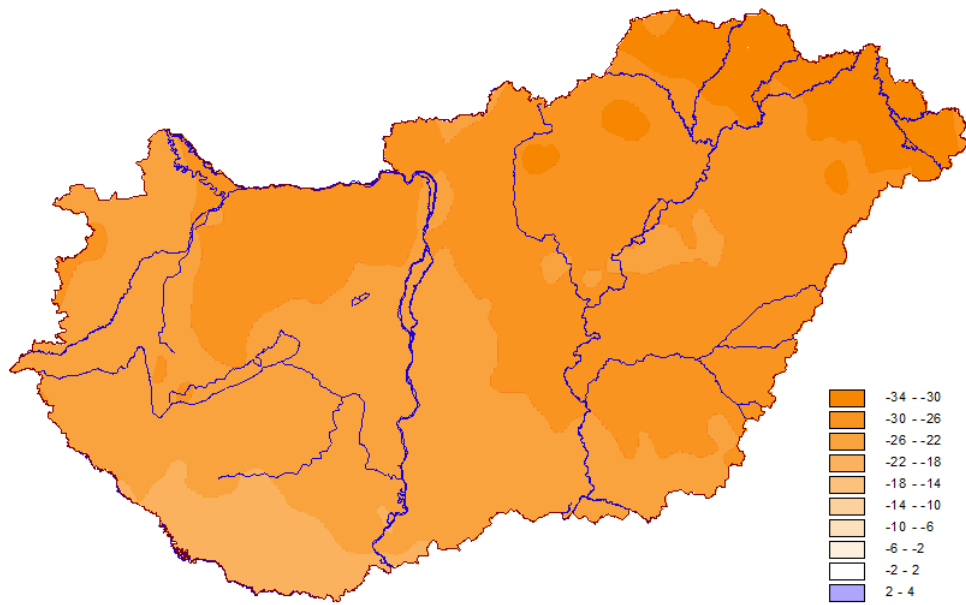


*Fig. 16. 078 Perc of wet days JJA AA(2071-2100)-AE(1961-1990)*

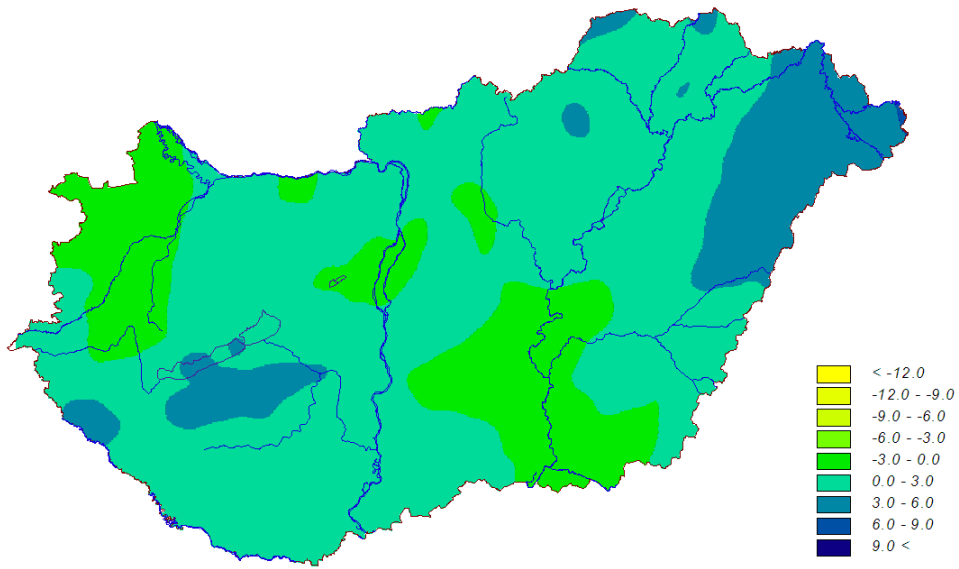


Fig. 17. 113 Greatest 1-day total rainfall DJF AA(2021-2050)-AE(1961-1990)

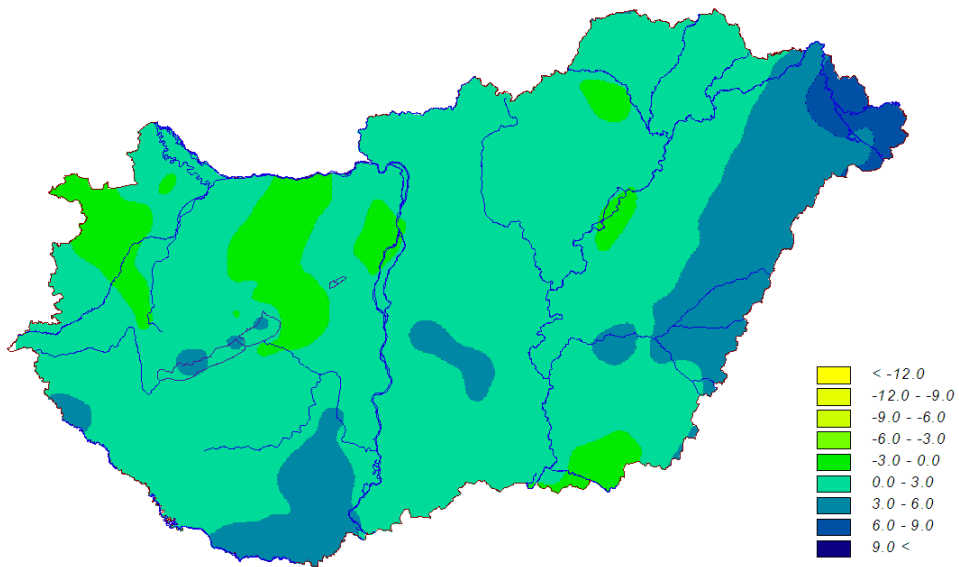
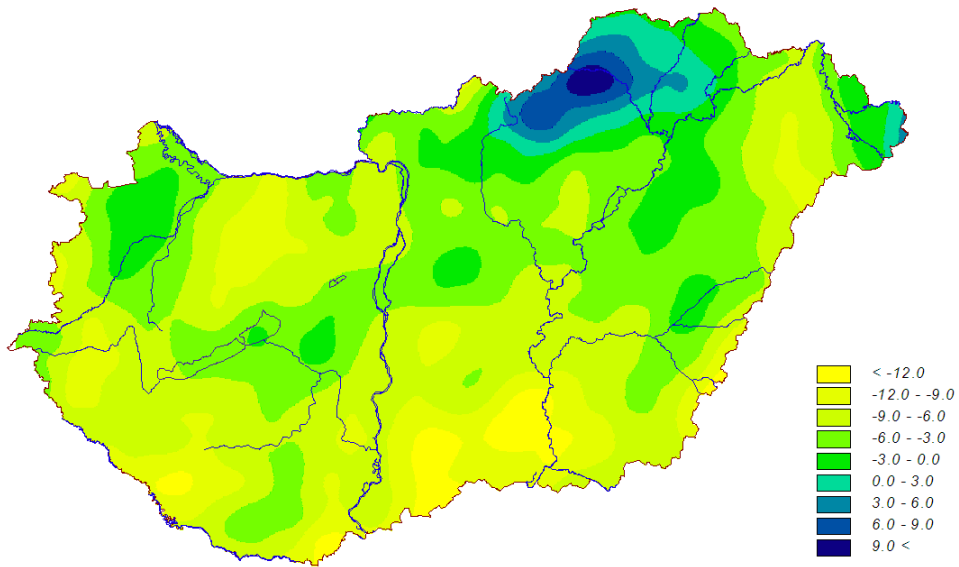
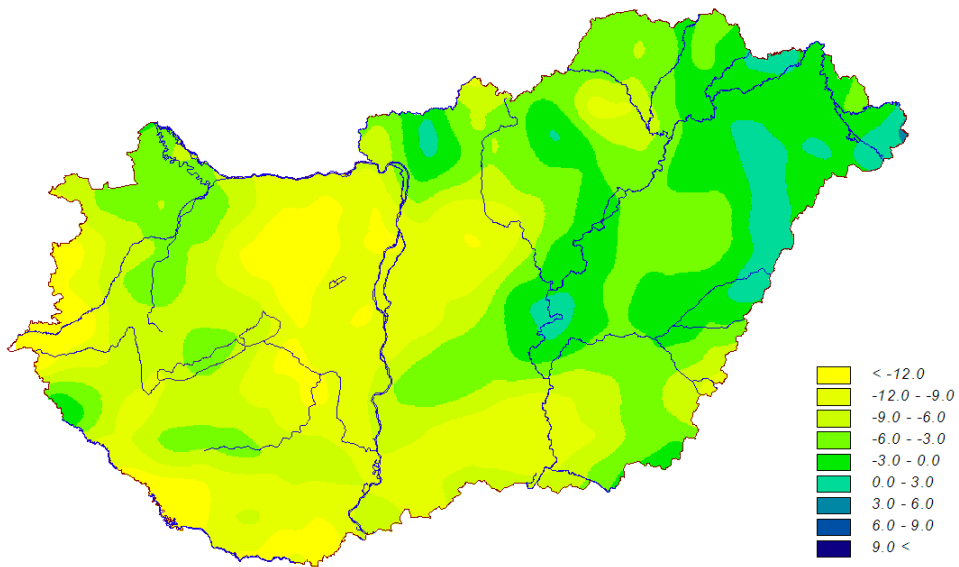


Fig. 18. 113 Greatest 1-day total rainfall DJF AA(2071-2100)-AE(1961-1990)



*Fig. 19. 113 Greatest 1-day total rainfall JJA AA(2021-2050)-AE(1961-1990)*



*Fig. 20. 113 Greatest 1-day total rainfall JJA AA(2071-2100)-AE(1961-1990)*

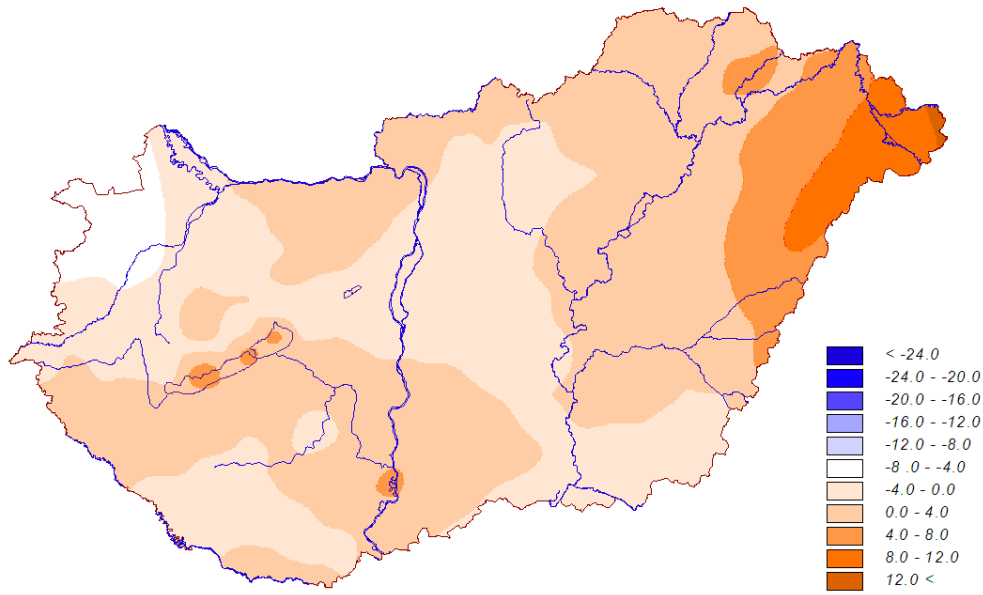


Fig. 21. 115 Greatest 5-day total rainfall DJF AA(2021-2050)-AE(1961-1990)

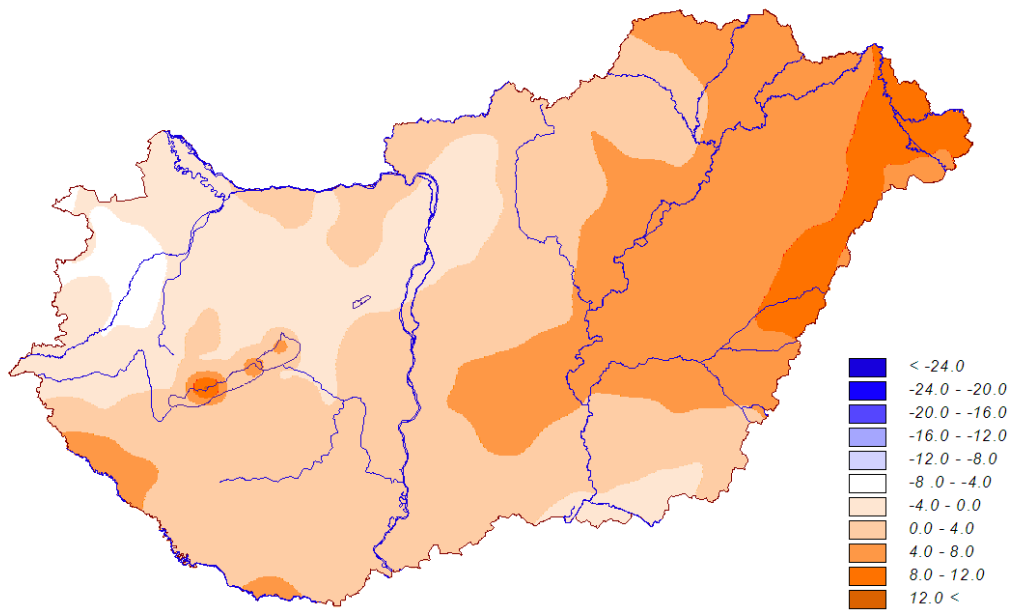


Fig. 22. 115 Greatest 5-day total rainfall DJF AA(2071-2100)-AE(1961-1990)

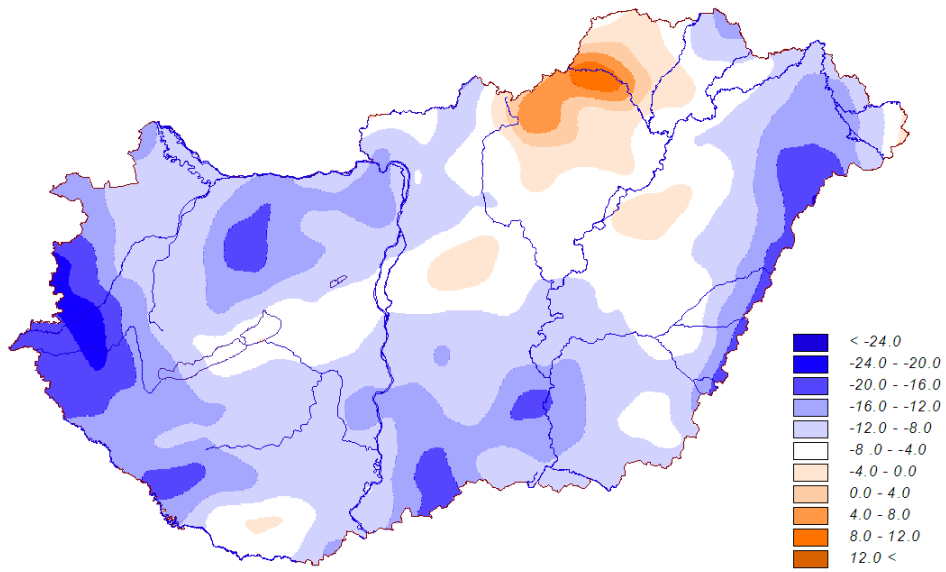


Fig. 23. 115 Greatest 5-day total rainfall JJA AA(2021-2050)-AE(1961-1990)

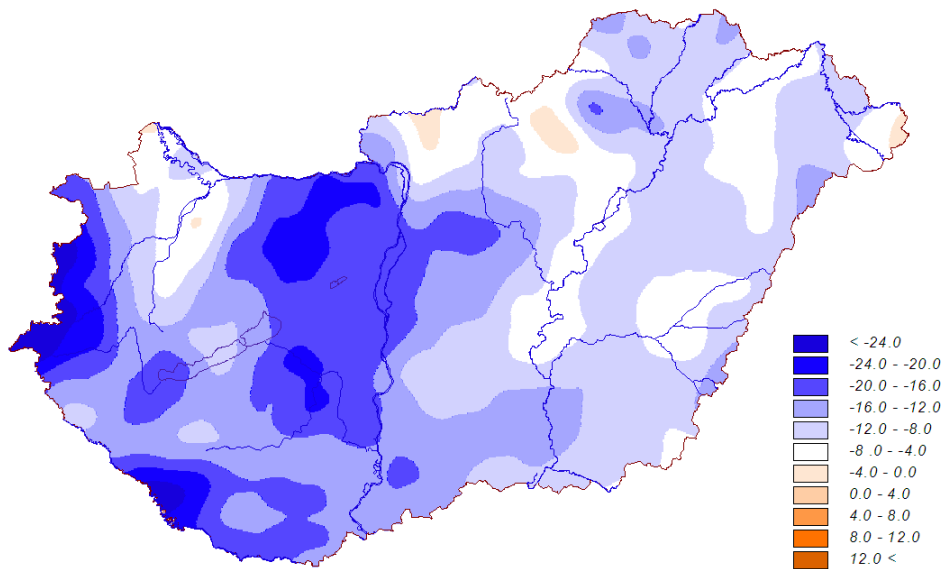


Fig. 24. 115 Greatest 5-day total rainfall JJA AA(2071-2100)-AE(1961-1990)

## 50 years return levels

Asymptotical extreme value distribution fitting was performed using homogenized, gridded observations and Aladin-Arpege in reference period 1961-1990 and also for two future time slices. Maxima of sample series at each grid point were described by Gumbel distribution. The method of moments we used for the parameter estimation. Presentation of the model results as a rate of the observations allows to impact people an easy evaluation the outcomes of simulations.

Maps of the 50 years return levels of the daily maximum temperatures (*Fig. 25-27*) indicate increasing tendency in the near future. The values are much higher relative to observations in the base period than using the control run forced by Aladin-Arpege. The largest increase appears in the mountainous regions in the far future.

In the case of greatest one day total precipitation in the near future there is no significant difference between return level maps using observations or using model (*Fig. 28-30.*). The 50 years return levels of daily precipitation sums exceeds by 50% at least the base period characteristics in extended region of Hungary in both future time slices.

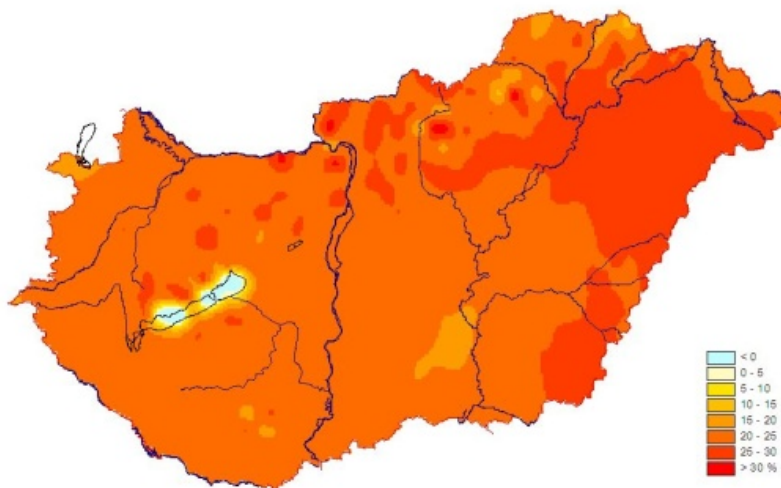


*Fig. 25. 50 year return levels of the daily maximum temperature, Aladin-Arpege 2021-2050 relative to gridded, homogenized Observations 1961-1990*

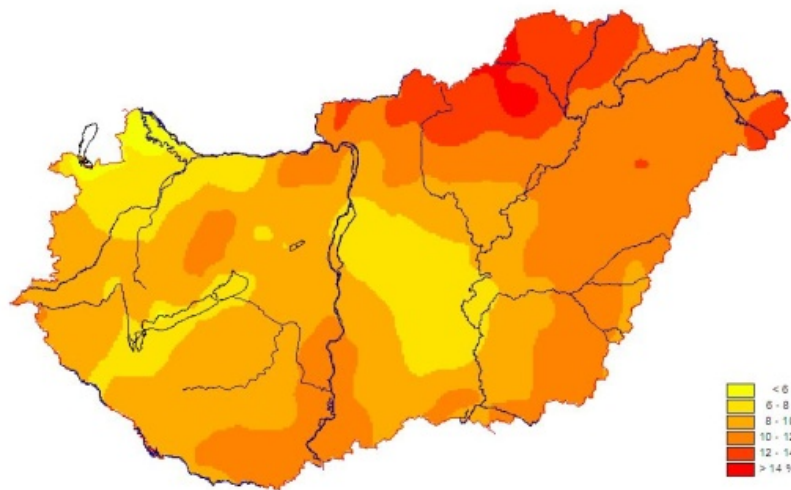


*Fig.26. 50 year return levels of the daily maximum temperature, Aladin-Arpege 2021-2050 relative to Aladin-Arpege 1961-1990*

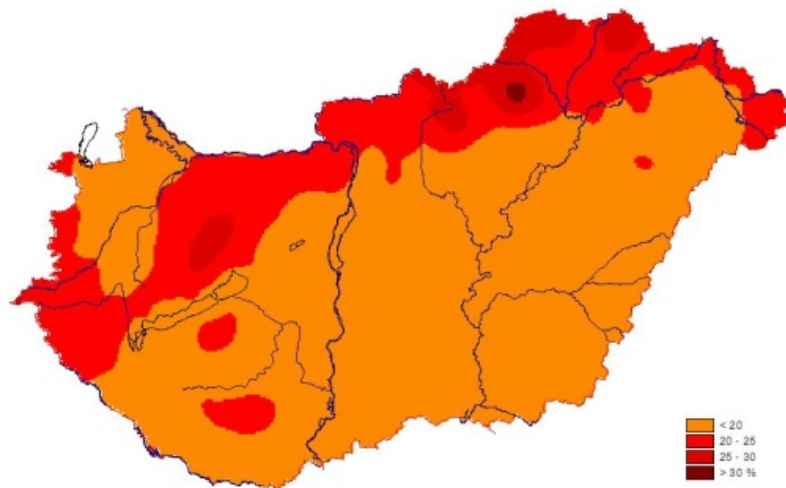


*Fig.27. 50 year return levels of the daily maximum temperature, Aladin-Arpege 2071-2100 relative to Aladin-Arpege 1961-1990*

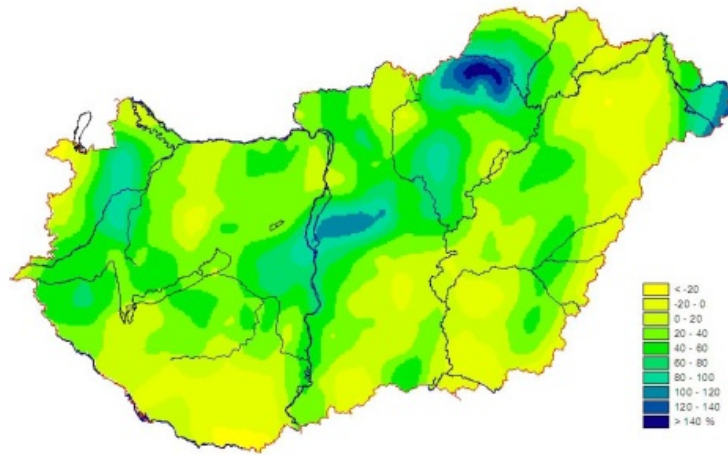


Fig. 28. 50 year return levels of the greatest 1 day total precipitation (Index No. 113.), Aladin-Arpege 2021-2050 relative to gridded, homogenized Observations 1961-1990

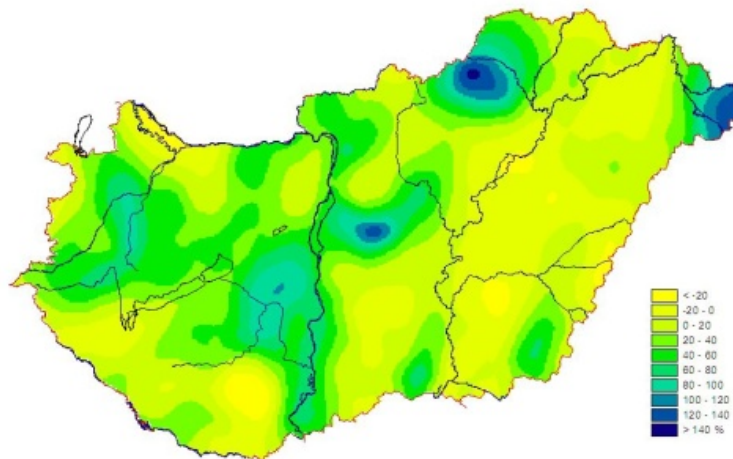
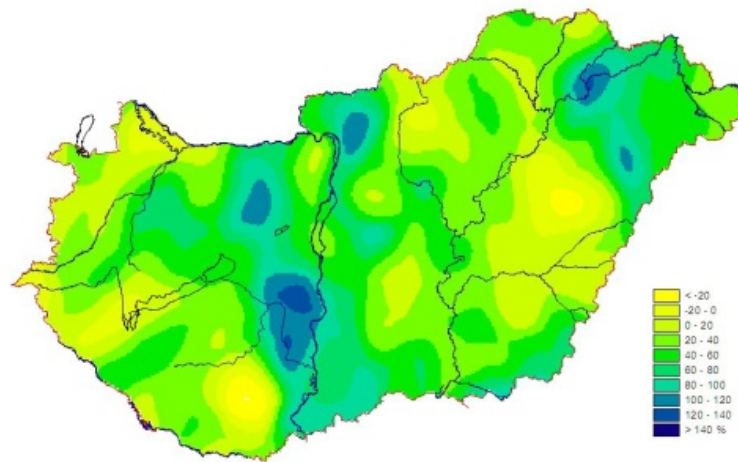


Fig. 29. 50 year return levels of the greatest 1 day total precipitation (Index No. 113.), Aladin-Arpege 2021-2050 relative to Aladin-Arpege 1961-1990



*Fig.30. 50 year return levels of the greatest 1 day total precipitation (Index No. 113.), Aladin-Arpege 2071-2100 relative to Aladin-Arpege 1961-1990*

## **D4.4.c Extreme core indices for Romanian domain simulated with RegCM - Climate scenarios vs control (led by NMA)**

**Constanța Boroneanț**

**National Meteorological Administration, Bucharest, Romania**

### **RCM description and calculated extreme indices**

- Model version: **RegCM3 (Beta)**
- Domain: **Romania and Black Sea** (using  $156 \times 102$  gridpoints), which can be characterized by the following four corners, and the central point of the domain:

	Latitude	Longitude
SW	41.0275°N	15.627°E
SE	41.016°N	34.495°E
NW	50.175°N	14.095°E
NE	50.150°N	36.192°E
Center point	46.0°N	25.0°E

- Horizontal resolution: **10 km**
- Evaluation period: **1961-1990; 2021-2050; 2071-2100**
- LBC: **ECHAM driven RegCM (25 km)**
- Extreme indices calculated:  
**as agreed in D4.1**  
**(131 indices – from which 75 indices are related to temperature, and 56 indices are related to precipitation)**
- Extreme indices mapped:  
**30-year averages (1961-1990, 2021-2050, 2071-2100),**  
**changes between 2021-2050 and 1961-1990, and between 2071-2100 and 1961-1990**  
**(as simple difference, and relative change also),**  
**annual and four seasonal**
- Extreme indices included in this document: **as agreed**

for winter (DJF) and summer (JJA) seasons:

**001 - mean Tmax**

**002 - mean Tmin**

**003 - mean Tmean**

**076 - mean climatological precipitation**

**078 - percentage of wet days**

**113 - greatest 1-day total rainfall**

**115 - greatest 5-day total rainfall**

for annual scale:

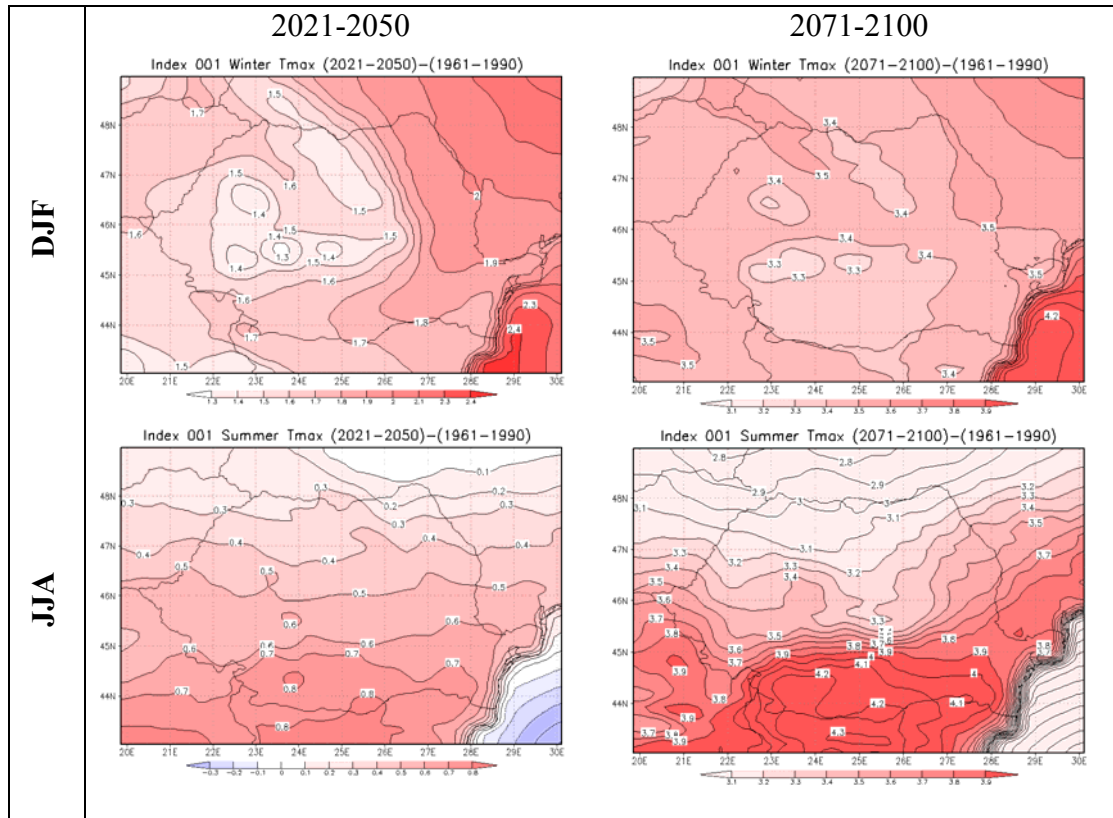
**058 - percentage of summer days ( $T_{max} \geq 25 \text{ }^\circ\text{C}$ )**

**066 - percentage of hot days ( $T_{max} \geq 30 \text{ }^\circ\text{C}$ )**

### 3. RESULTS

#### 2.1. Temperature related indices

##### Seasonal change of mean Tmax

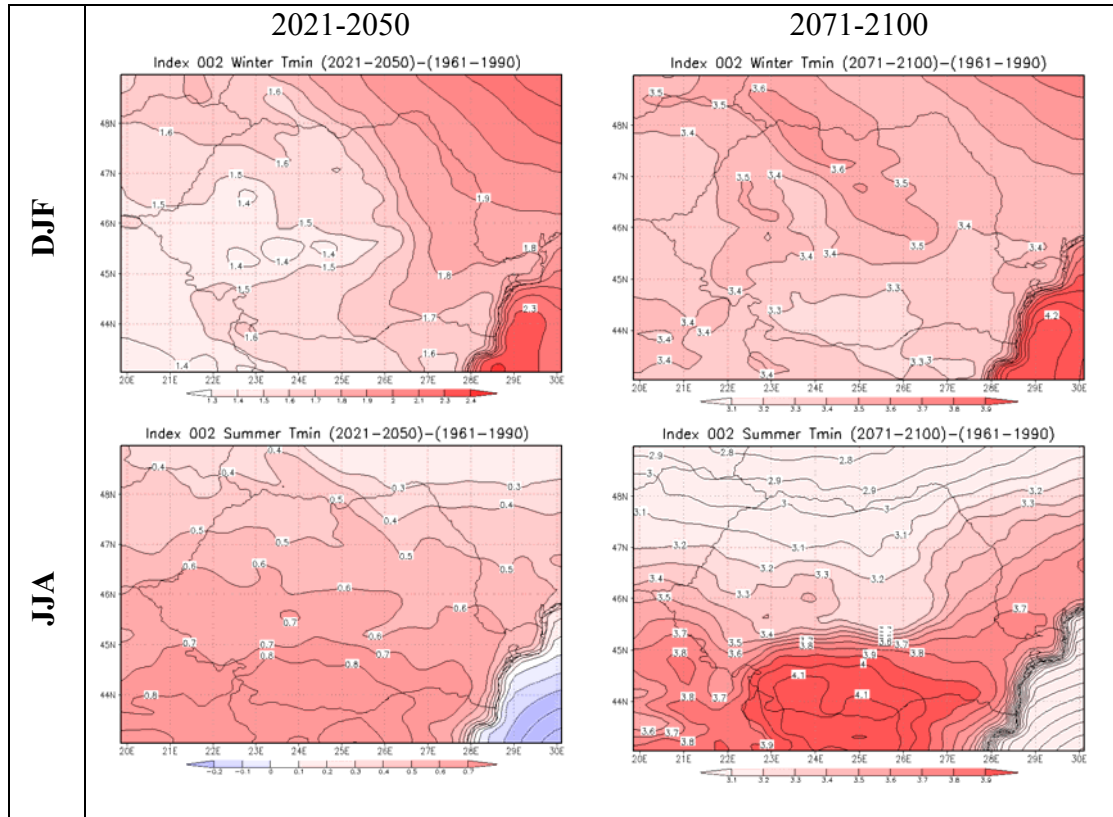


Simulated changes for Romania:

Season	2021-2050 vs. 1961-1990	2071-2100 vs. 1961-1990
DJF	1.4-24.5 °C	3.1-4.2 °C
JJA	0.3-0.8 °C	3.1-4.3 °C

Simulated winter and summer daily maximum temperature are projected to increase by both time slices (2021-2050, 2071-2100) relative to the reference period (1961-1990). In Romania the projected changes in winter are about 2-2.4 °C in the eastern part of the country and over the Black Sea by the middle of the 21st century and about 3.4-4.2 °C by the end of the 21st century. During summer, the projected changes are more enhanced over the southern part of the country ranging 0.5 to 0.8°C by the mid 21st century and 3.4 to 4.3°C by the end of the 21st century.

## Seasonal change of mean Tmin



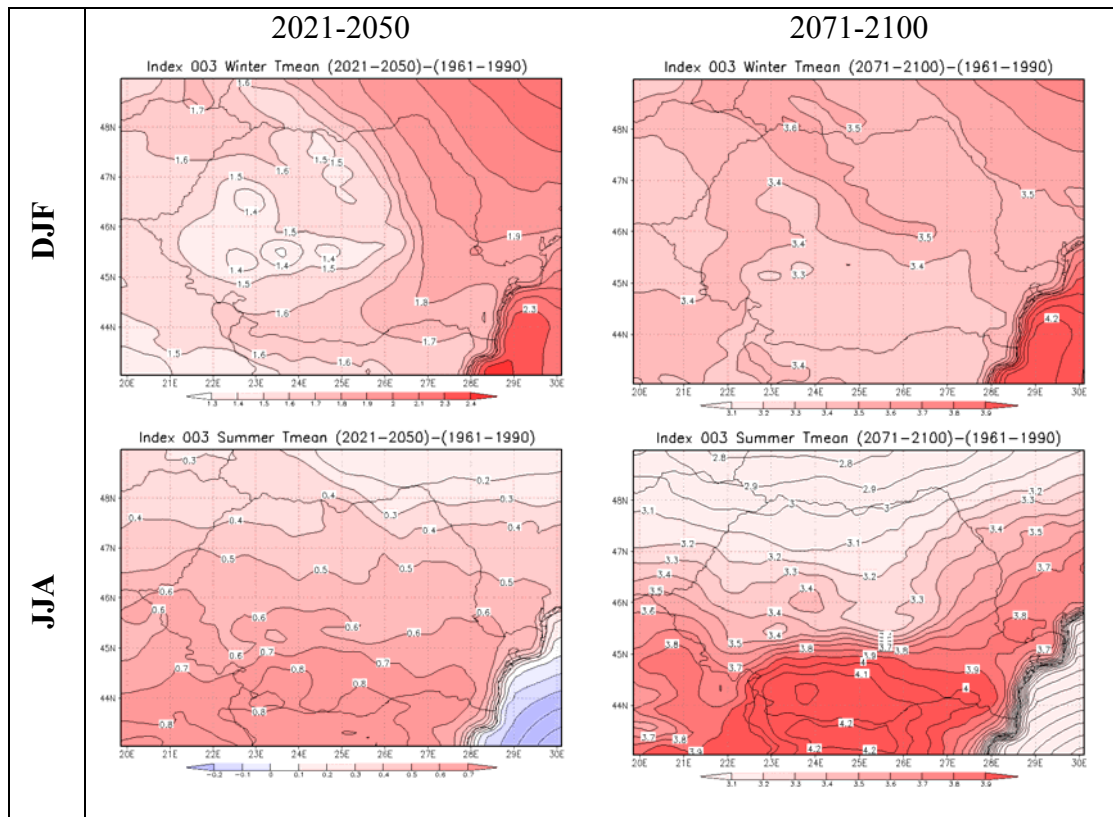
Simulated changes for Romania:

Season	2021-2050 vs. 1961-1990	2071-2100 vs. 1961-1990
DJF	1.3-2.4 °C	3.1-4.2 °C
JJA	-0.2-0.7 °C	3.1-4.1 °C

Similarly to the daily maximum temperature, simulated winter and summer daily minimum temperature are projected to increase by both time slices (2021-2050, 2071-2100) relative to the reference period (1961-1990). Also, similarly to the maximum temperature, the projected winter warming is larger than the summer warming for both periods (1.6°C to 2.3 °C in the eastern part of the country and over the Black Sea by mid 21<sup>st</sup> century and, about 3.4°C over the northern half of the country and 4.2 °C over the Black Sea by the end of the 21<sup>st</sup> century.

During summer the projected changes are expected to be larger in the southern half of the country ranging between 0.6 to 0.8°C by the mid 21<sup>st</sup> century and between 3.4°C and 4.1°C by the end of 21<sup>st</sup> century.

## Seasonal change of mean Tmean

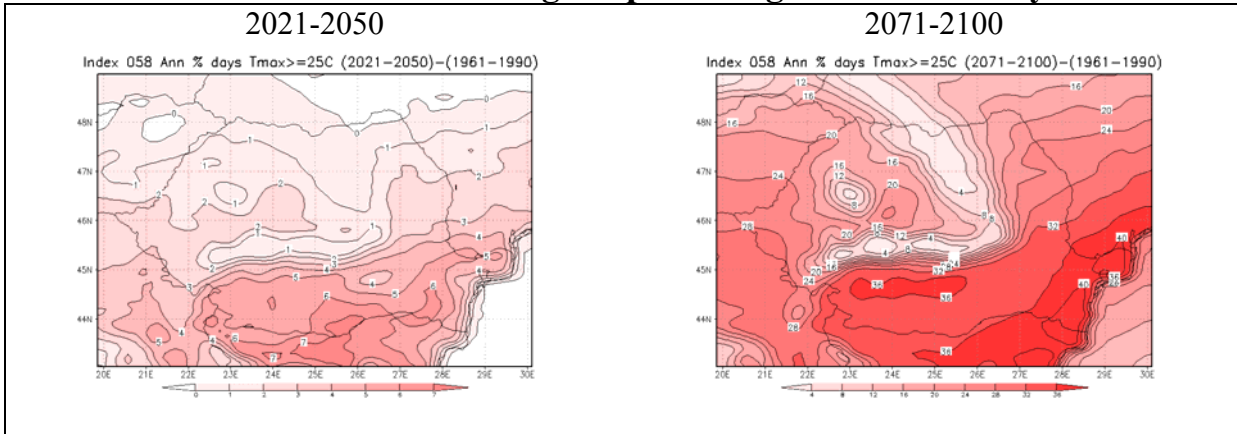


Simulated changes for Romania:

Season	2021-2050 vs. 1961-1990	2071-2100 vs. 1961-1990
DJF	1.3-2.3 °C	3.2-4.2 °C
JJA	-0.2-0.7 °C	3.2-4.2 °C

Similar conclusions can be drawn in case of the simulated daily mean temperature changes to those found in case of daily maximum and minimum temperature. Daily mean temperature is projected to increase, the winter warming is larger than the summer warming for the 2021-2050 period while for the 2071-2100 the range of increase is the same but the distribution of patterns is different (3.4°C in the northern part during winter and 3.4 to 4.2 °C in the southern part of the country during summer). The patterns of projected changes over Romania are similar to that of the daily maximum and daily minimum for both time slices.

## Annual change of percentage of summer days

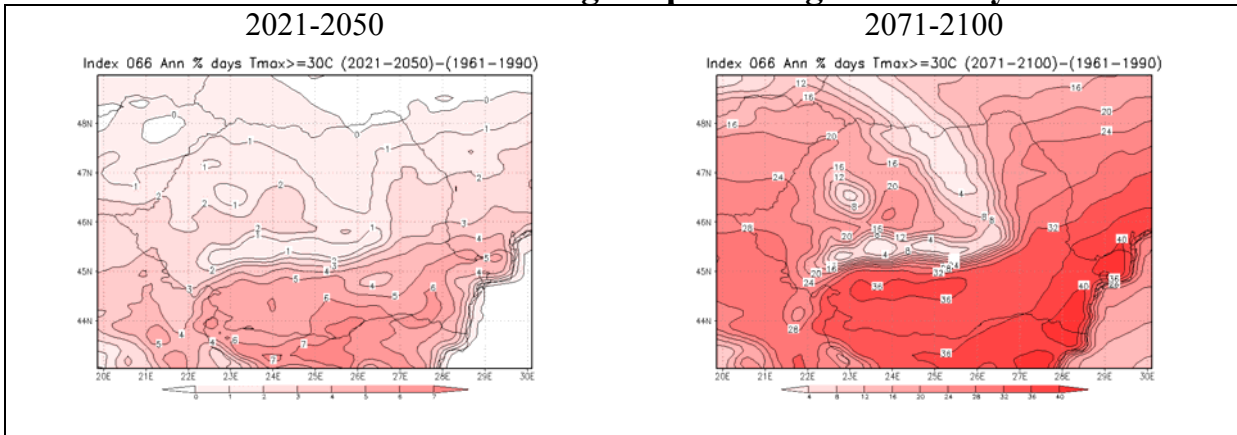


Simulated changes for Romania:

	2021-2050 vs 1961-1990	2071-2100 vs 1961-1990
Simulated change	1-7%	4-40%

Summer days (when the Tmax is larger than 25 °C) may occur mainly during June-September but they can occur in May and October as well in Romania. By the near future period (2021-2050) it is likely increase the number of summer days mostly in the southern half of the Romanian territory; by the end of the century (2071-2100) the annual number of summer days is expected to increase up to the percentage of 40% in the southern part of the country.

## Annual change of percentage of hot days



Simulated changes for Romania:

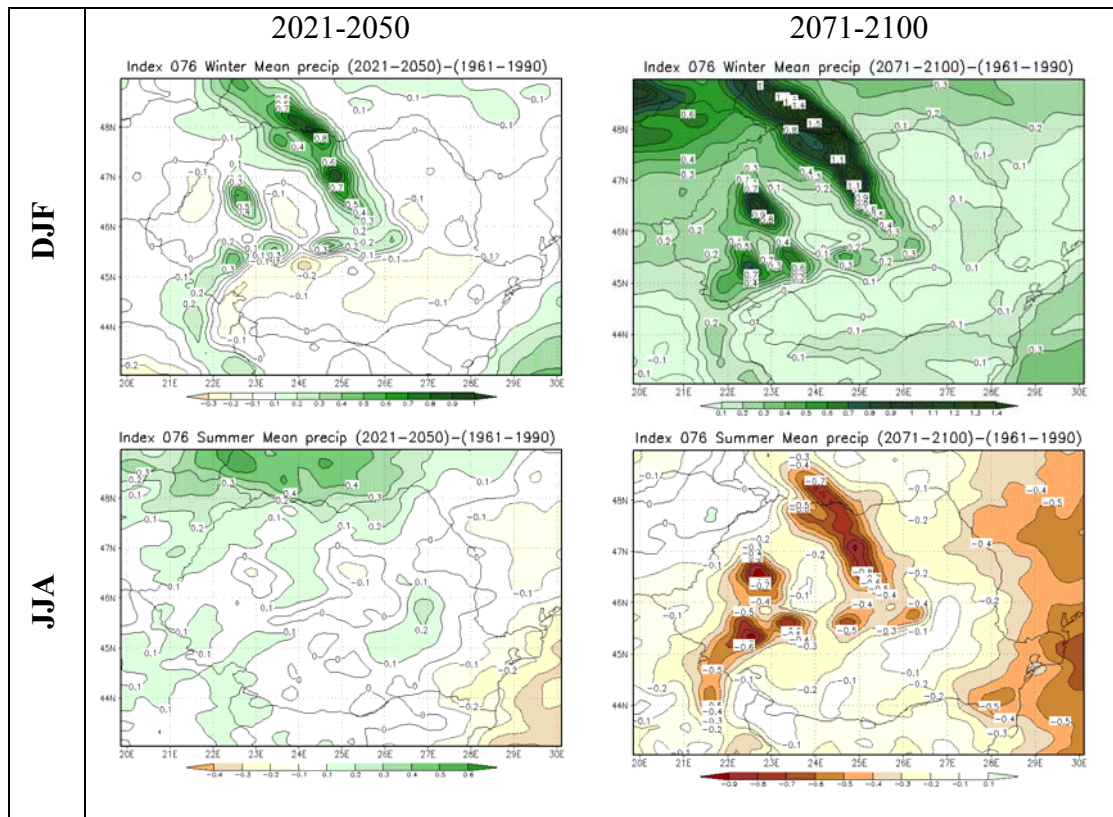
	2021-2050 vs 1961-1990	2071-2100 vs 1961-1990
Simulated change	0-7%	4-40%

Hot days (when the Tmax is larger than 30 °C) occur mainly in June-August but they can occur in May and September in Romania.

Comparing to the reference period and increase of the percentage of hot days up to 7% of the total days are expected by the middle of the 21<sup>st</sup> century and up to 40% by the end of the 21<sup>st</sup> century, in the southern part of the country.

## 2.2. Precipitation related indices

### Seasonal change of mean climatological precipitation

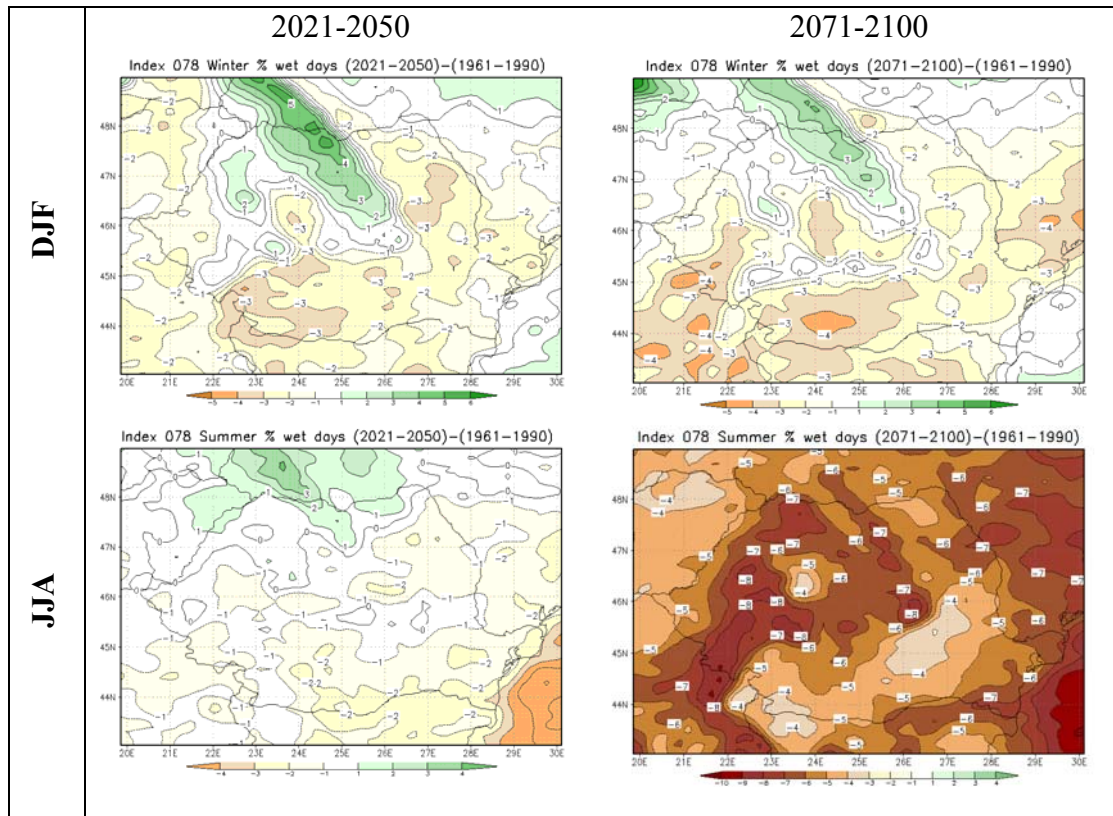


Simulated changes for Romania:

Season	2021-2050 vs. 1961-1990	2071-2100 vs. 1961-1990
DJF	(-0.3; 1) mm/day	(-0.1; 1.4) mm/day
JJA	(-0.1; 0.6) mm/day	(-0.9; 0.1) mm/day

In general, simulated winter daily mean precipitation is projected to increase in Romania in the north-western part of the country and at high altitudes during both periods. By the middle of the 21<sup>st</sup> century the daily mean precipitation is expected to slightly decrease mostly in the south-eastern part of the country while by the end of the century the decrease in daily mean precipitation is expected to be enhanced up to -0.9 mm/day as compared to the reference period. The climate is likely to become wetter in the north-western part of the country in winter and drier over most of the territory but more enhanced in the north western part of the country and at high altitudes.

## Seasonal change of percentage of wet-days



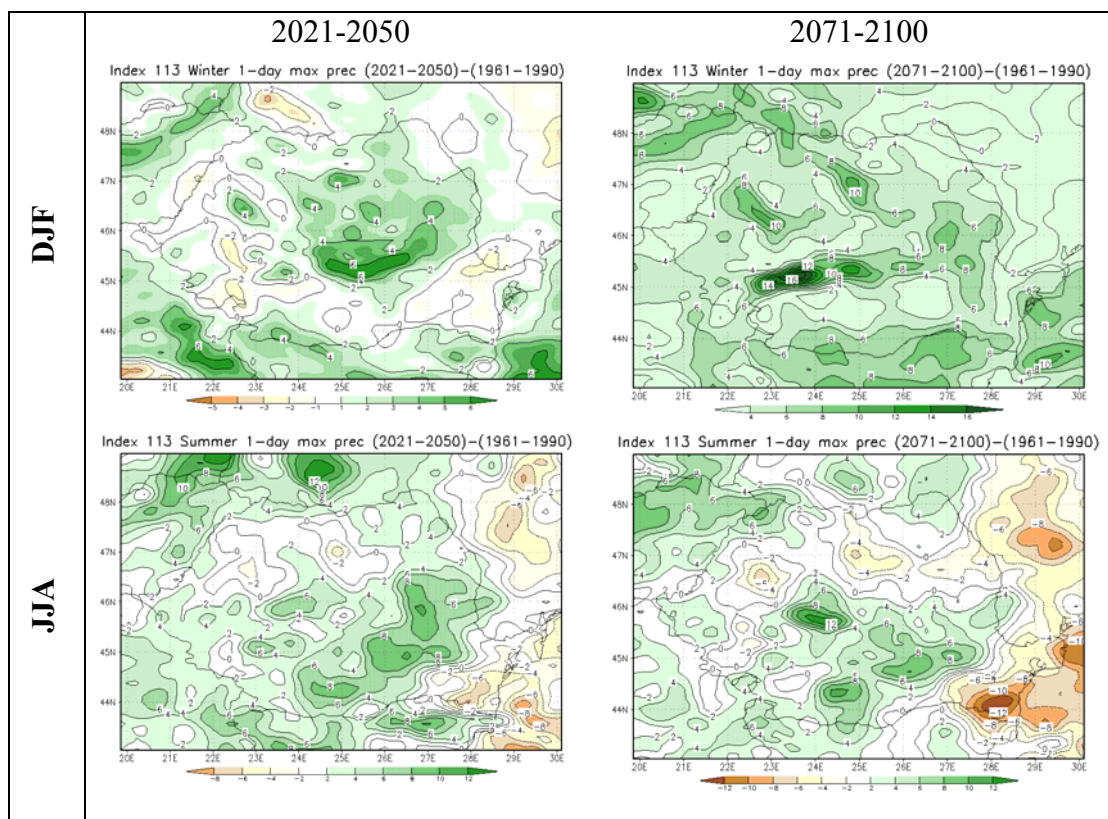
Simulated changes for Romania:

	2021-2050 vs 1961-1990	1961-1990 vs 2071-2100
DJF	-3%; 5%	-4%; 4%
JJA	-4%; 4%	-9%; -4%

The percentage of wet days during winter is projected to decrease in the extra Carpathian regions up to -3% being more enhanced in the south-western part of the country. In the north-western part of the country the percentage of wet days will increase as compared to the reference period 196-1990 up to 5% by middle 21<sup>st</sup> century and up to 3% by the end of the century.

During summer, the percentage of wet days will decrease all over the country up to -2%, excepting a small area in the north-western part of the country where it will increase up to 3% by mid of the 21<sup>st</sup> century. The decrease of the percentage of wet days is expected over the whole territory of Romania by the end of the century, being more enhanced in the western and south western part of the country up to -8%

## Seasonal change of the greatest 1-day total rainfall



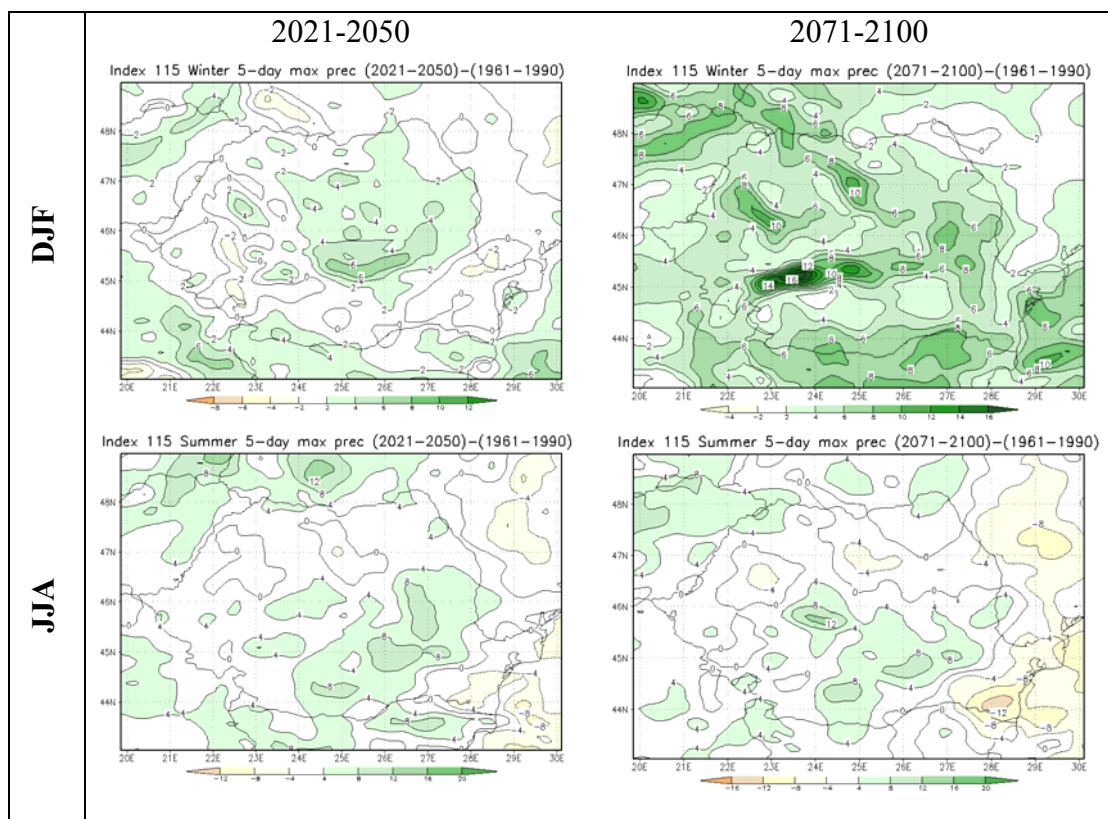
Simulated changes for Romania:

	2021-2050 vs 1961-1990	2071-2100 vs 1961-1990
DJF	-2-6 mm/day	4-16 mm/day
JJA	-8-12 mm/day	-12-12 mm/day

During winter the simulated greatest 1-day total rainfall is projected to slightly decrease locally in the western and eastern part of the country and to increase with up to 6 mm/day in the mountains and the central plateau by the middle of 21<sup>st</sup> century. By the end of the century the simulated greatest 1-day total rainfall is projected to increase all over the country during winter with an average of 4 mm/day both intra and extra Carpathians while at high altitudes this index will increase with up to 16 mm/day.

During summer the greatest 1-day total rainfall is projected to increase up to 8 mm/day in the extra Carpathians and central plateau and to decrease in the eastern part of the country along the western coast of the Black Sea and adjacent regions by the middle of 21<sup>st</sup> century. Similar patterns of changes are projected in summer by the end of the century when the increase of this index is expected with up to 12 mm/day and the decrease of this index up to 12 mm/day.

## Seasonal change of the greatest 5-day total rainfall



Simulated changes for Romania:

	2021-2050 vs 1961-1990	2071-2100 vs 1961-1990
DJF	0-6 mm	4-16 mm
JJA	-8-8 mm	-12-12 mm

Similarly to the greatest 1-day total rainfall, the simulated greatest 5-day total rainfall is projected to increase in Romania both by middle 21<sup>st</sup> century and by the end of the century. The patterns of changes are similar to those for greatest 1-day total rainfall for both seasons. This parameter is likely to increase in the central plateau up to 6 mm by the middle of 21<sup>st</sup> century and up to 16 mm by the end of the century during winter.

The pattern of the summer simulated change in Romania by 2021-2050 is similar to that of the 2071-2100 change, but the decreasing trend is projected for less area in the country.

## **D4.4.d Extreme core indices for Bulgaria simulated with Aladin Climate scenarios vs control**

Vesselin Alexandrov and Ekaterina Koleva

### **INTRODUCTION**

- *At the first stage of the project NIMH computed the common WP4 extreme indices based on daily data in Bulgaria. A trend analysis was applied. Relationships between NAO and some extreme events in Bulgaria were considered.*
- *At this stage NIMH provides an analysis of the high-resolution 10-km CECILIA simulations over Bulgaria with a special focus on extremes. The following aspects are considered for the country: analysis of expected changes in extreme events, relative to the current climate;*

### **DATA AND METHODS**

- *Data: Observed (1961-1990) daily weather (air temperature and precipitation) data from near 60 weather stations across Bulgaria were used ( fig. 1)*
- *Data: 10 km ALADIN simulated weather outputs for the future climate conditions in Bulgaria (2021-2050; 2071-2100): air temperature and precipitation data from ca 50 weather stations across Bulgaria*
- *Method: Stepanek's, STARDEX, and R software were applied in this case study*

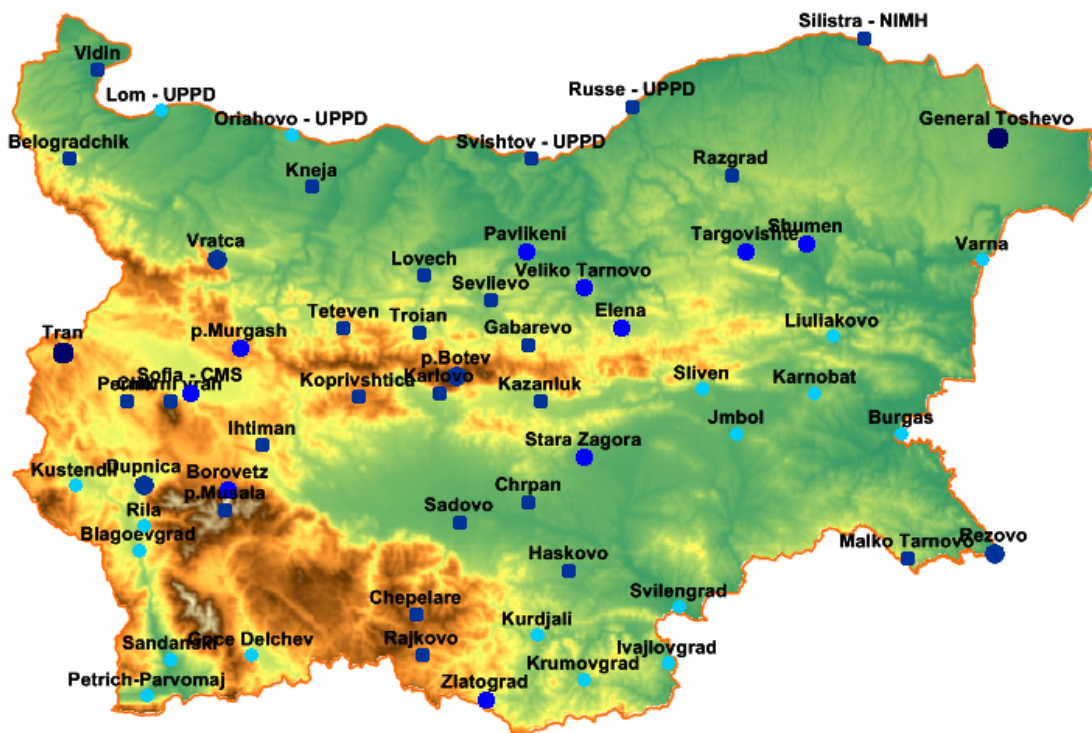
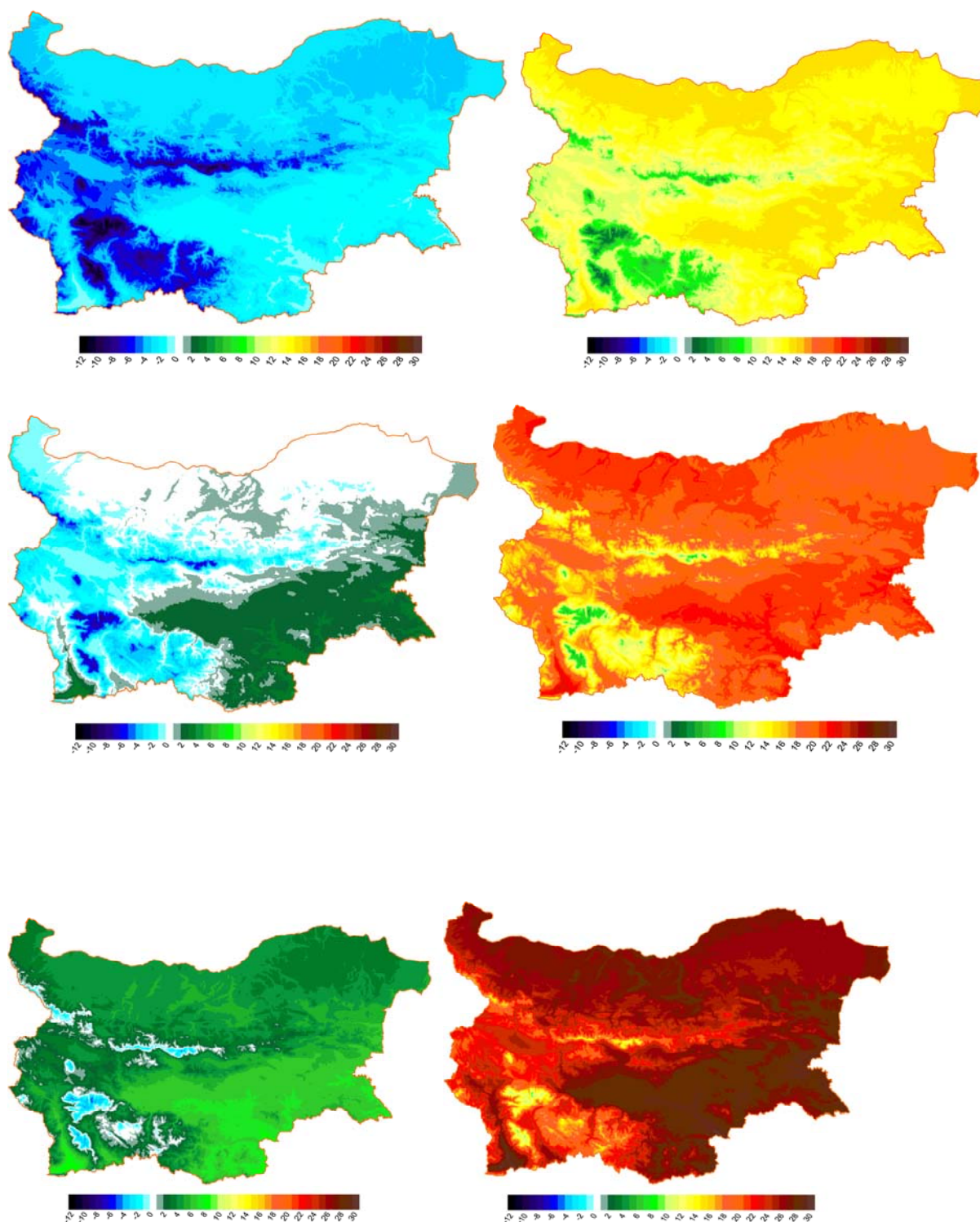


Fig. 1. Weather stations used in the study

- Core temperature indices such as:
- *Maximum, minimum and average air temperature in winter and summer*
- *Summer days ( $T_{max} > 25^{\circ}C$ )*
- *Tropical nights ( $T_{min} > 20^{\circ}C$ )*
- *Hot days ( $T_{max} > 30^{\circ}C$ )*
- *Extremely hot days ( $T_{max} > 35^{\circ}C$ )*
- *Severe cold days ( $T_{min} < -10^{\circ}C$ )*
- Core precipitation indices such as:
- *precipitation in winter and summer*
- *Mean wet day precip in winter and summer*
- *% of wet day precip in winter and summer*
- *Max precip in winter and summer*
- *5-days max precip in winter and summer*

## RESULTS



**Fig. 2. Minimum (top), average (middle) and maximum (down) temperature in winter (left) and summer (right) during current climate**

Fig. 2 represents Minimum, average and maximum temperature in winter and summer during current climate. It is interesting to see how the changes will be eventually observed under the expected climate change scenarios for the 21<sup>st</sup> century. For this purpose the ALADIN model outputs were applied. Fig. 3 and 4 are giving the tendencies of the future air temperature change – toward warming ca by 3-5°C depending on the period and location.

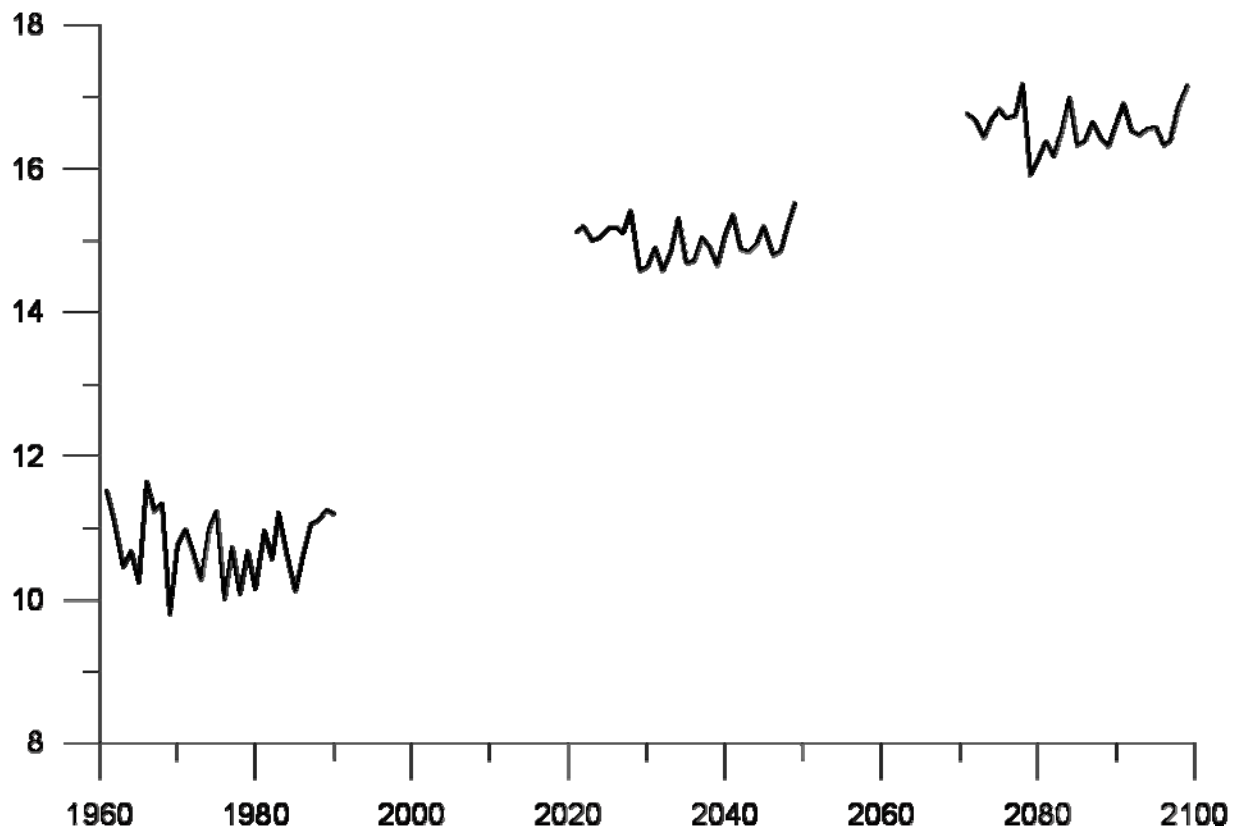


Fig. 3 annual temperature in a station for the observed period 1961-90 and simulated by ALADIN time slices, 2021-50, 2071-2100

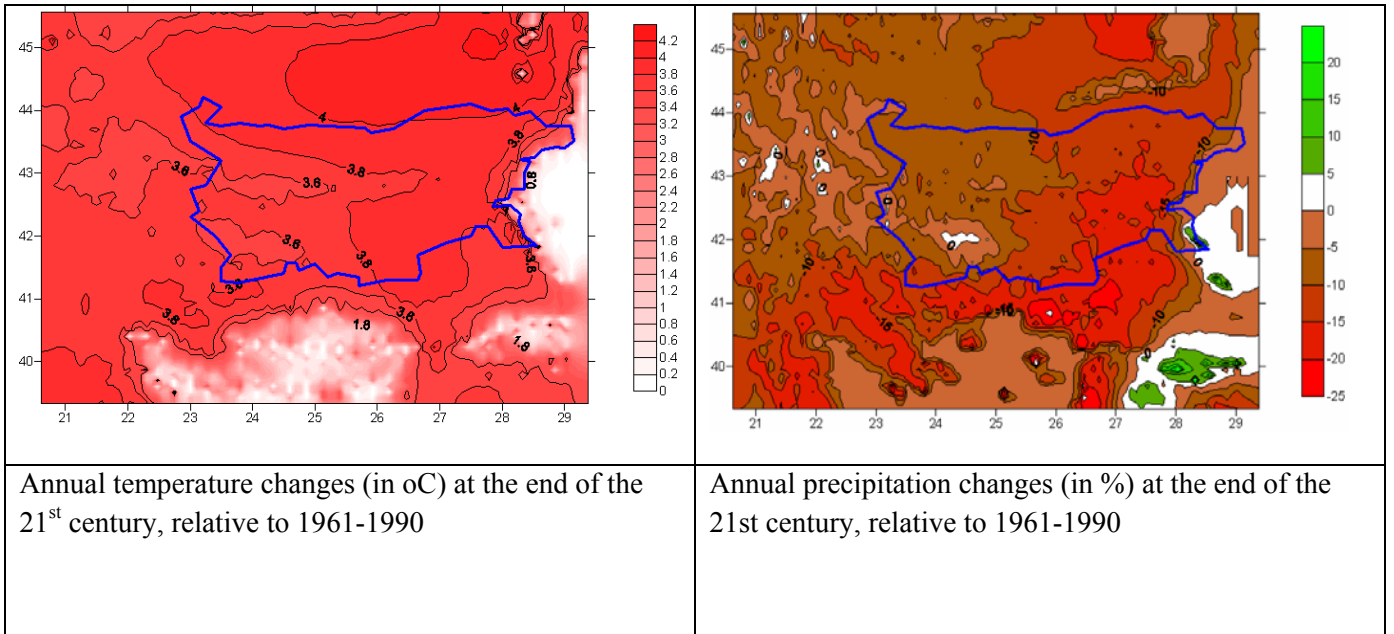
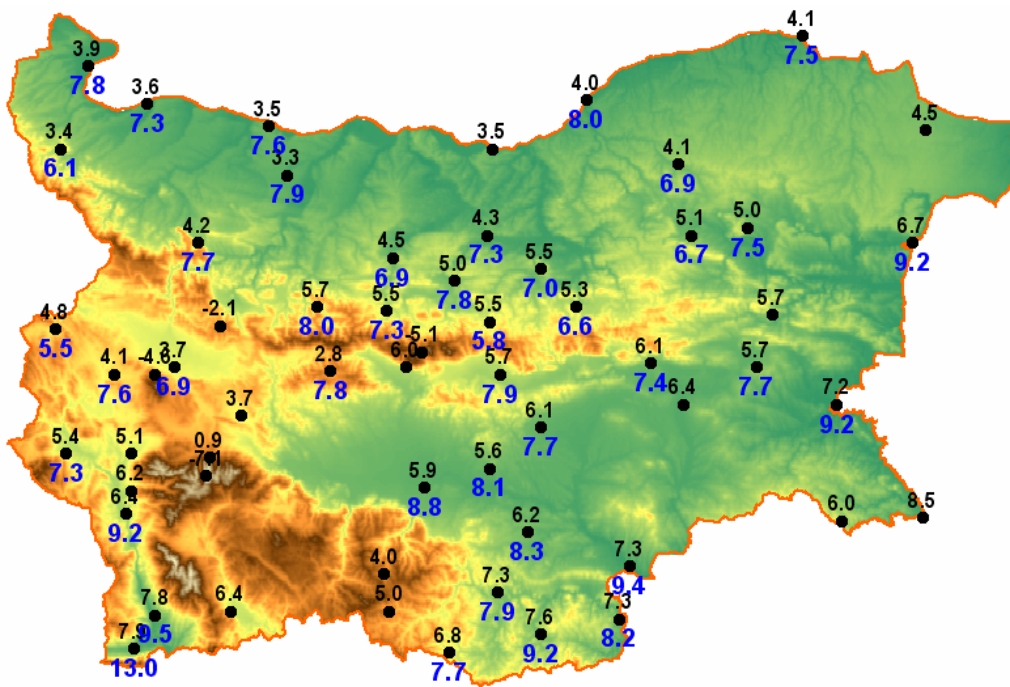


Fig.4 ALADIN climate change scenarios for the period 2071-2100, relative to the current climate



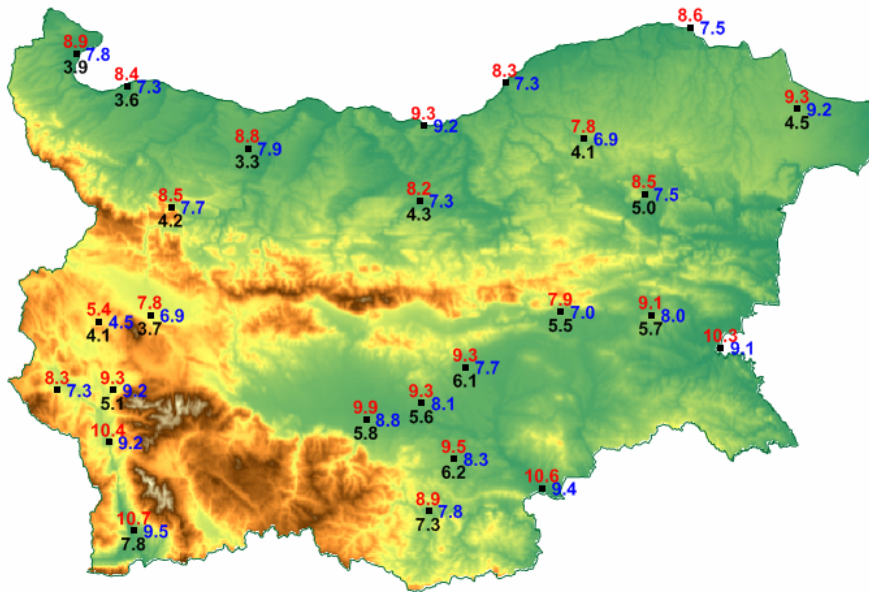
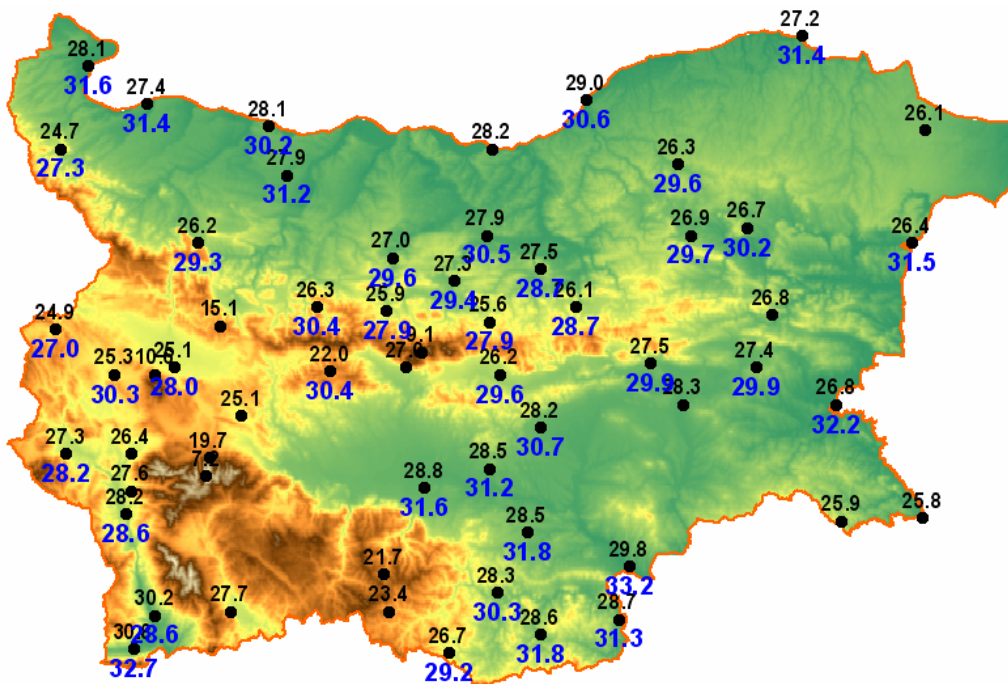


Fig 5. Maximum air temperature in winter, 1961-1990, 2021-2050, 2071-2100

- Obviously winters will be milder in the next decades reaching up to 10oC and even more in some areas





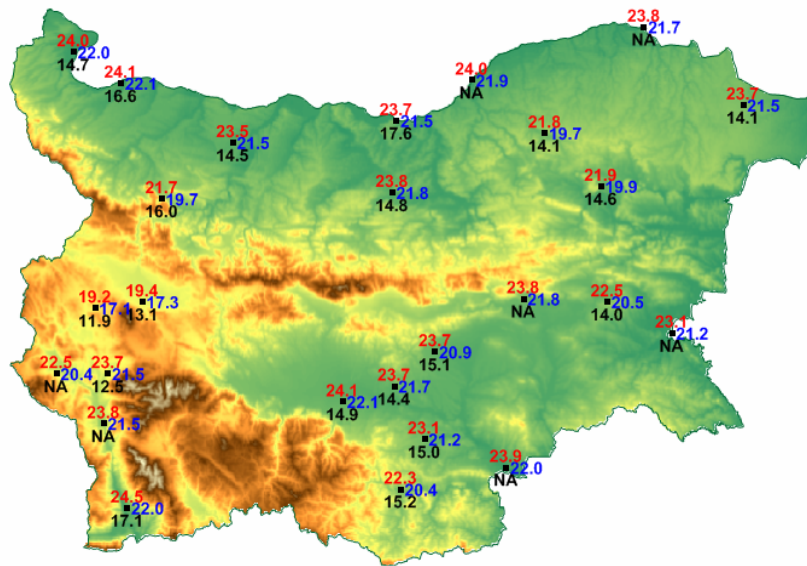
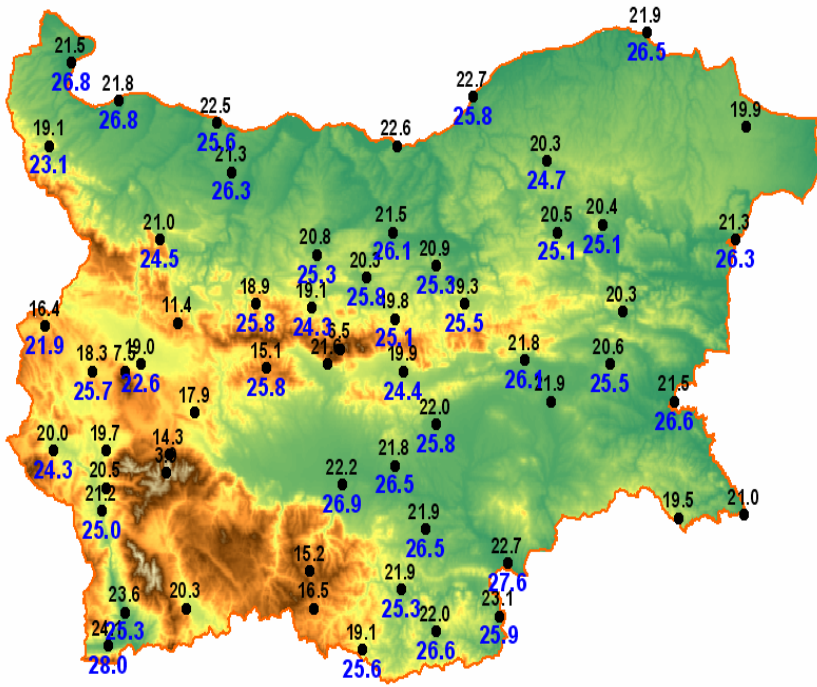
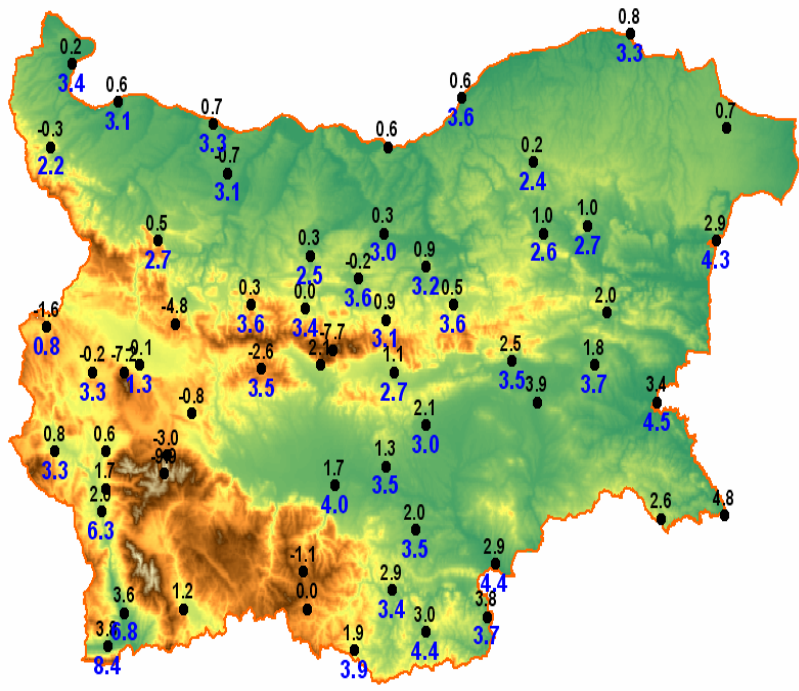


Fig 7. minimum air temperature in winter and summer, 1961-1990, 2021-2050, 2071-2100

Ice days will decrease, higher min temperature will affect the period of vernalisation in winter and crop growth in summer



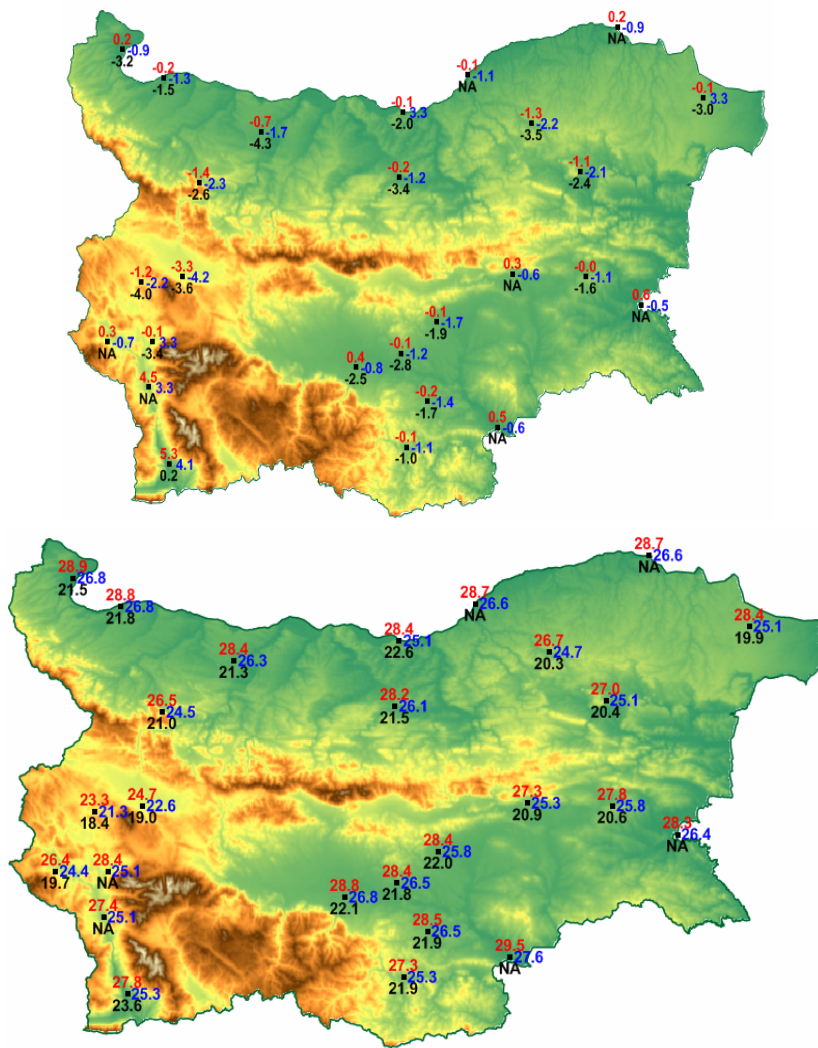


Fig 8. mean air temperature in winter and summer, 1961-1990, 2021-2050, 2071-2100

It is clear that by increasing maximum and minimum air temperatures will caused respective increase of mean air temperature both in winter and summer

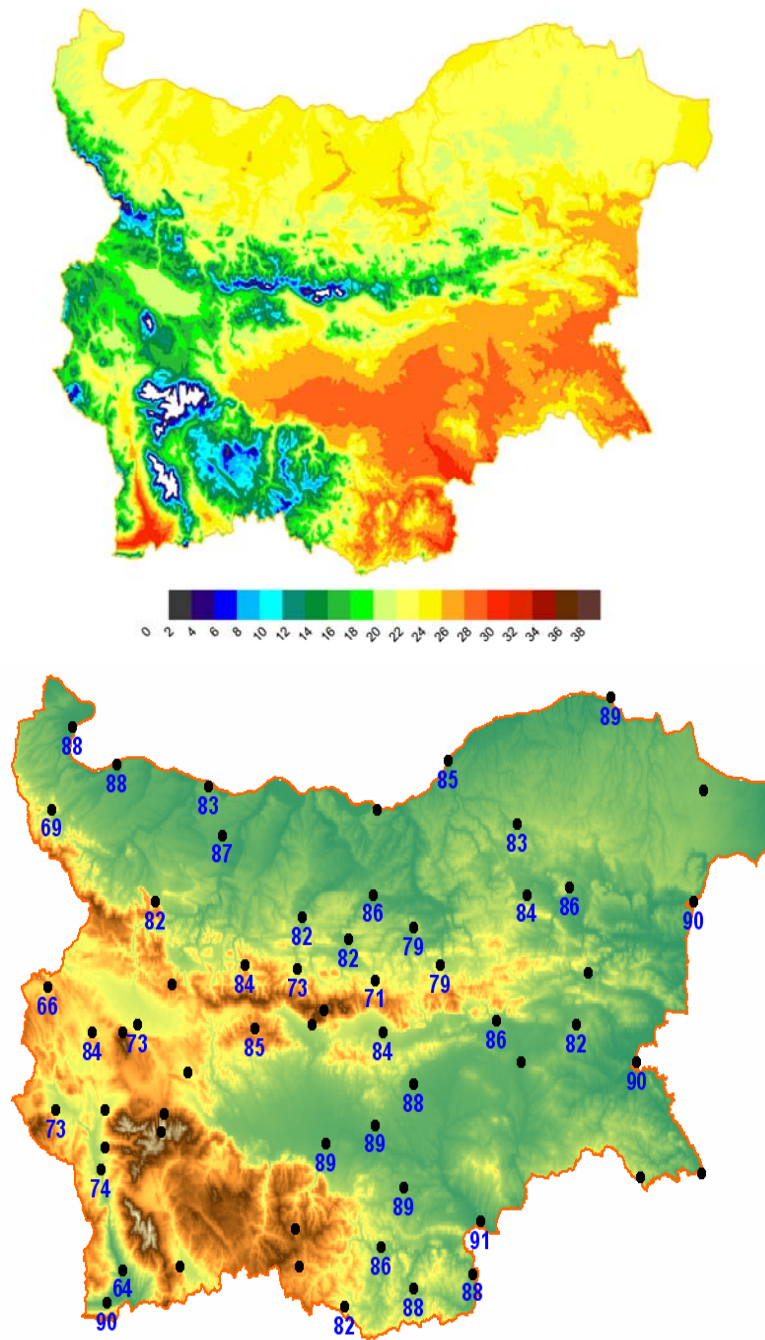


Fig. 9 Summer days (Tmax>25oC) , 1961-1990. 2021-2050

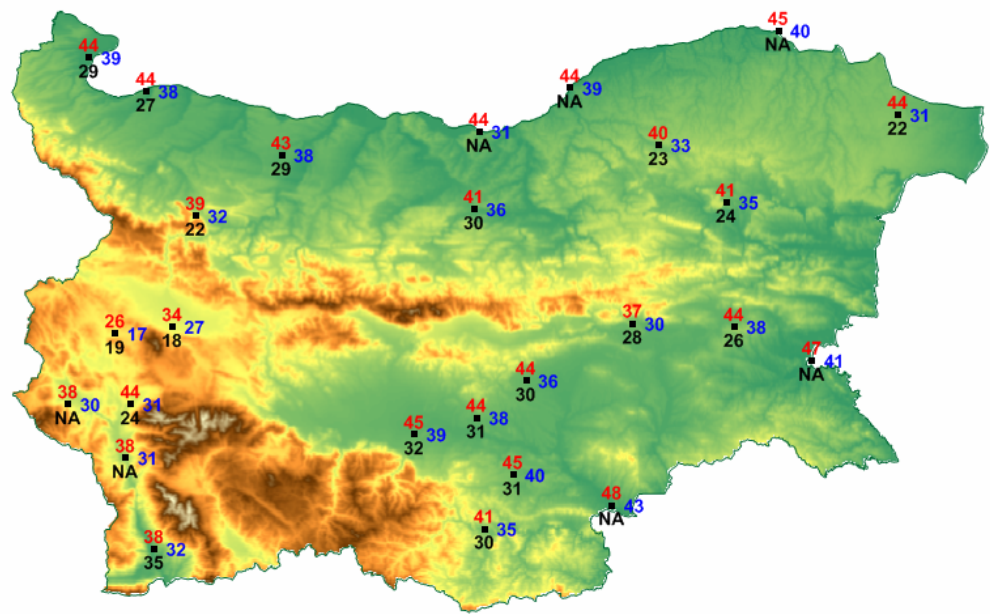
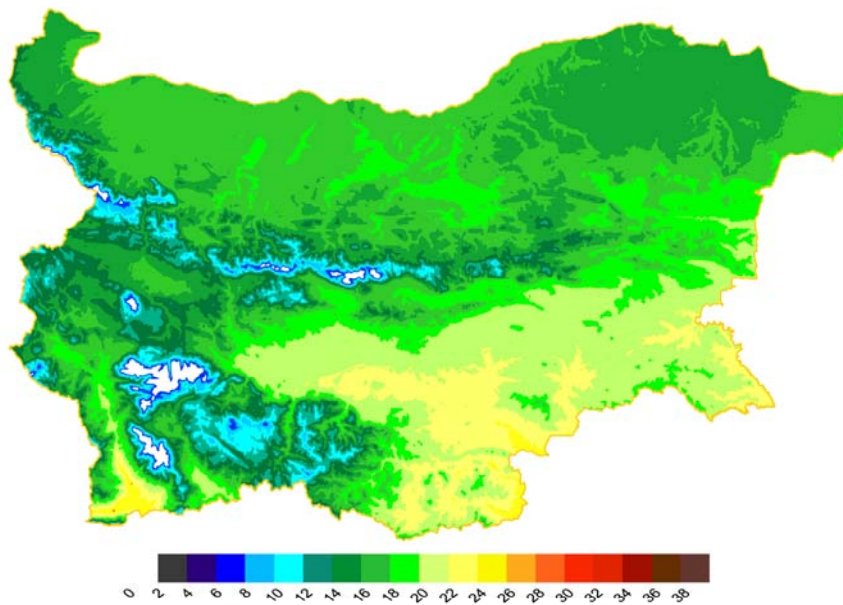


Fig 10. Percentage of “summer days (%age of days where  $T_{max} > 25C$ ), 1961-1990, 2021-2050, 2071-2100

- The number of summer days increases up to 90 days in the period 2021-2050. Percentage of summer days is projected to rise from 18-20 % nowadays to more than 40 % in most flat locations in south Bulgaria



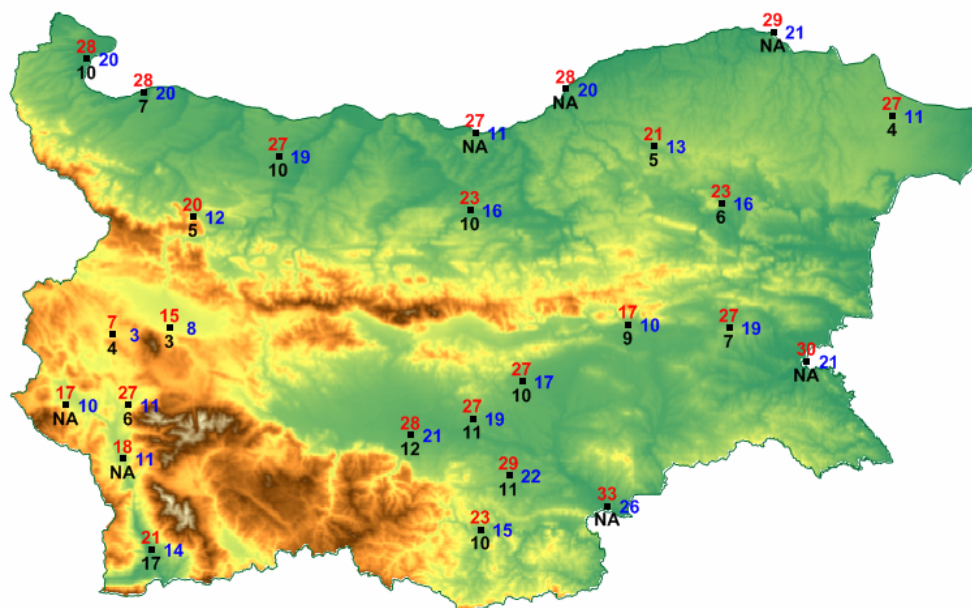
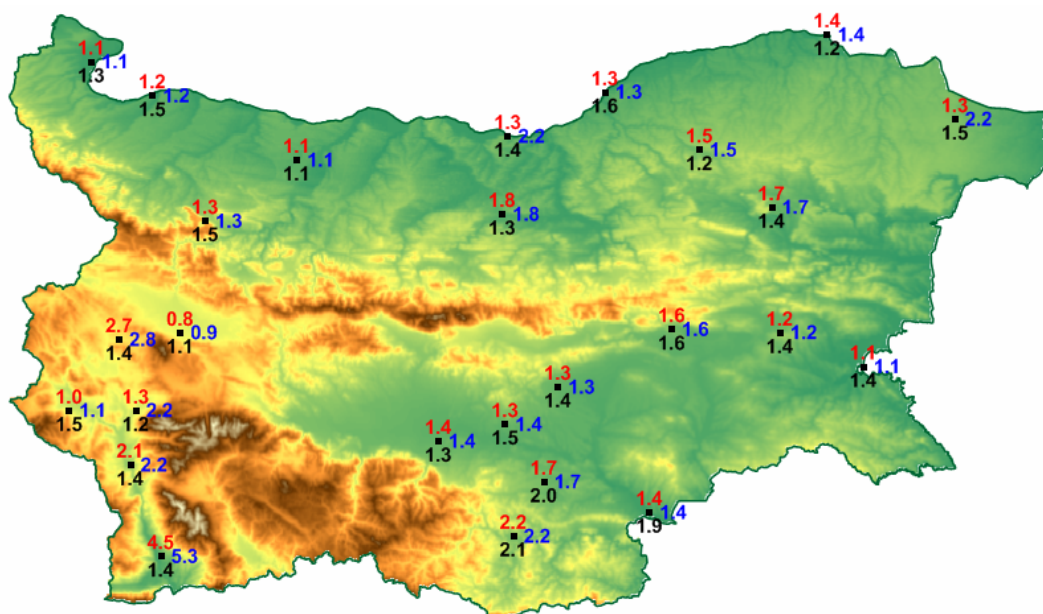


Fig. 11. Number (above) and percentage (below) of hot days ( %age of days with  $T_{max} \geq 30C$ ). 1961-1990, 2021-2050, 2071-2100

- The hot days would increase as well , up to 30 % till the end of the 21<sup>st</sup> century



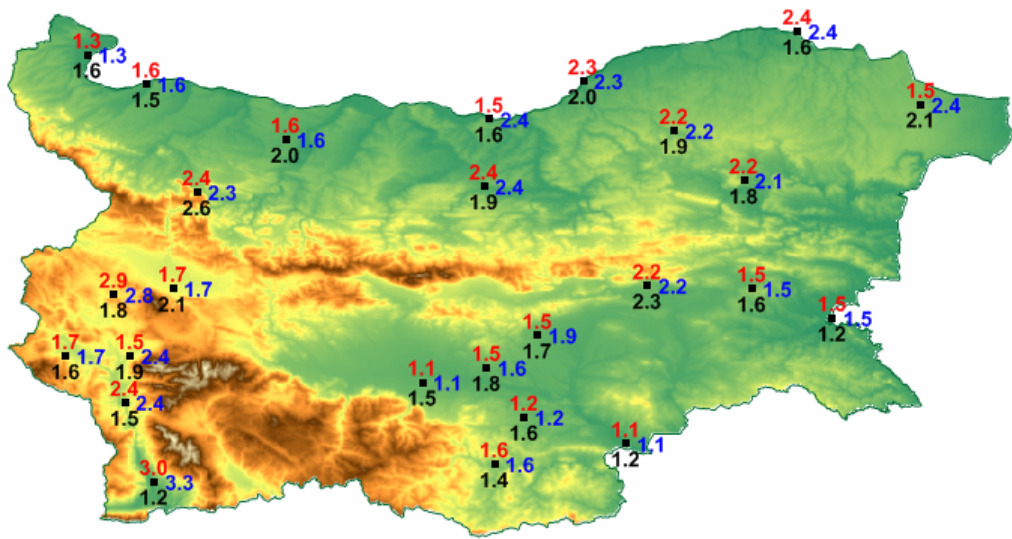
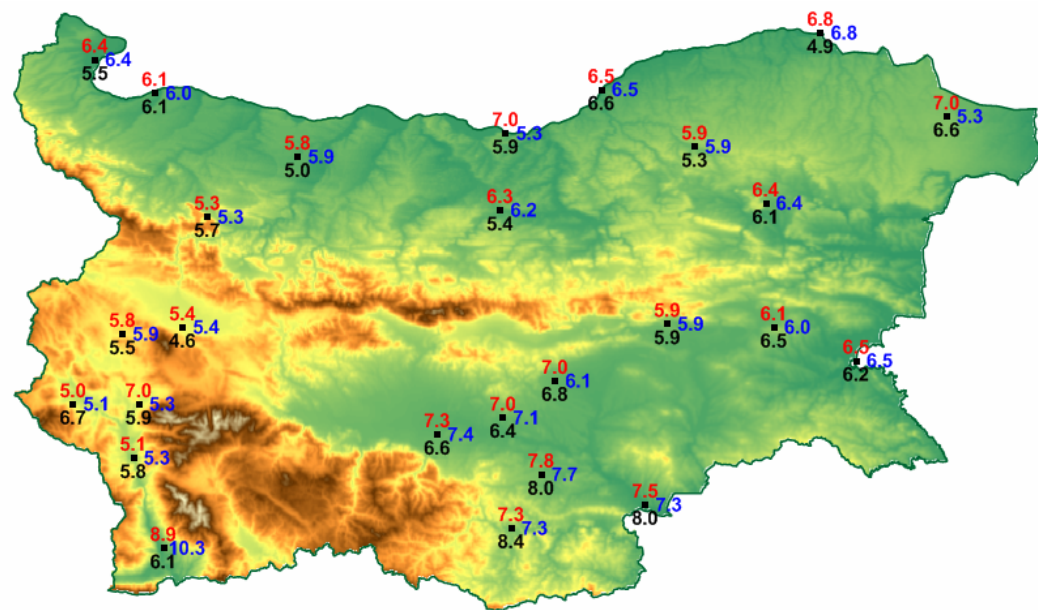


Fig.12 Mean climatological precipitation (mean precipitation including both wet and dry days) in winter and summer (down)1961-1990, 2021-2050, 2071-2100



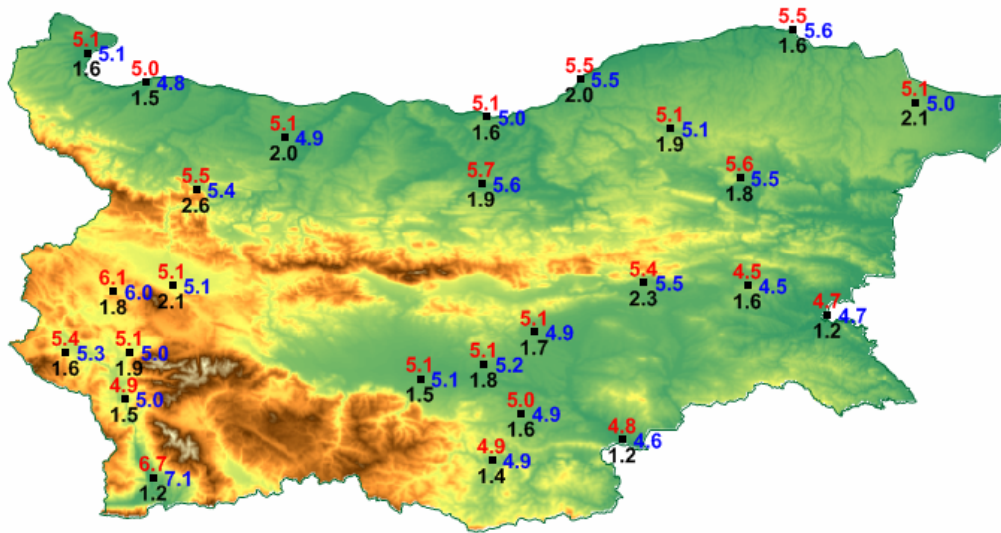
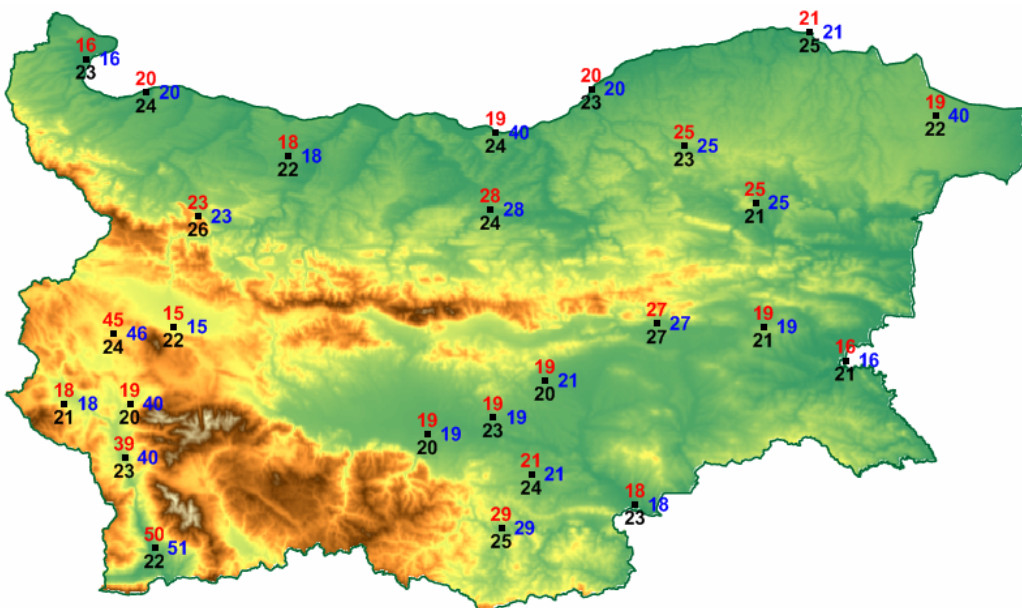


Fig.13 Mean wet-day precipitation (mean wet-day precipitation (equivalent to “simple daily intensity”))



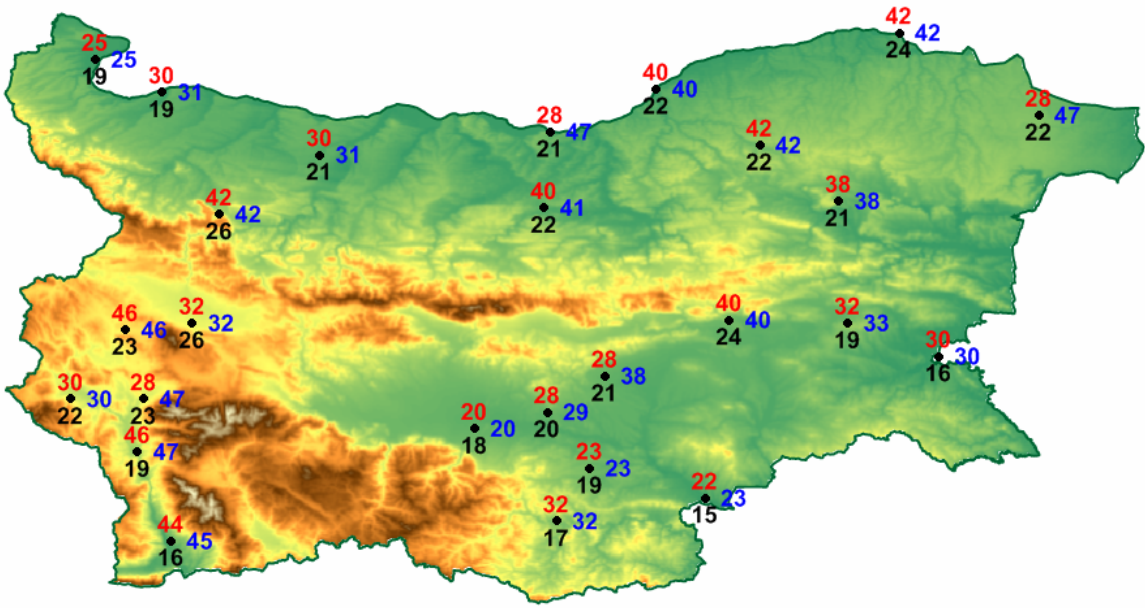
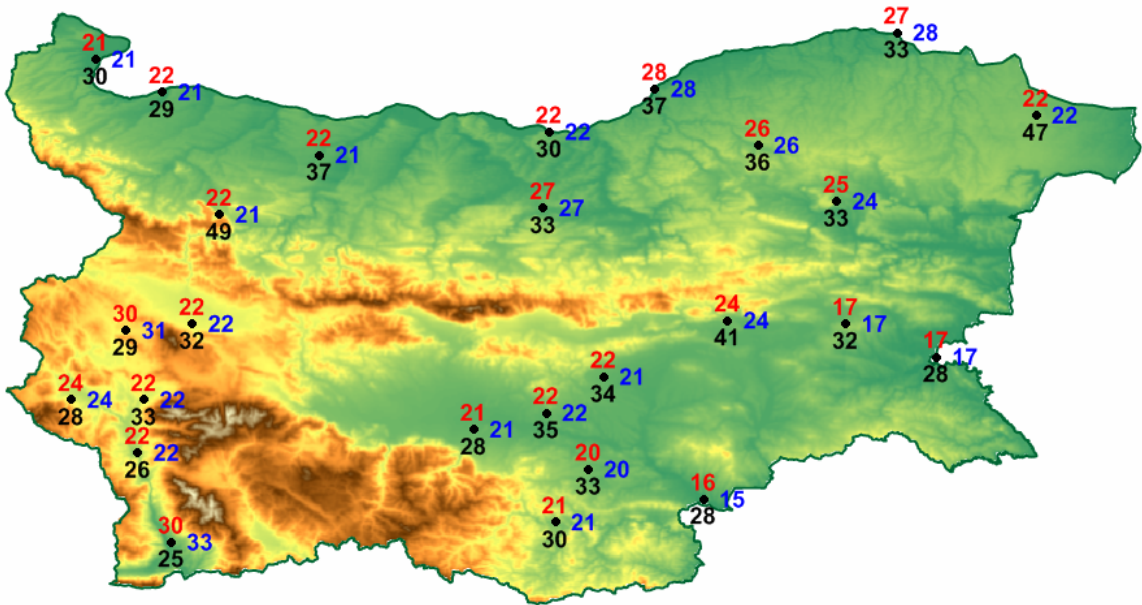


Fig.14 Percentage of wet days



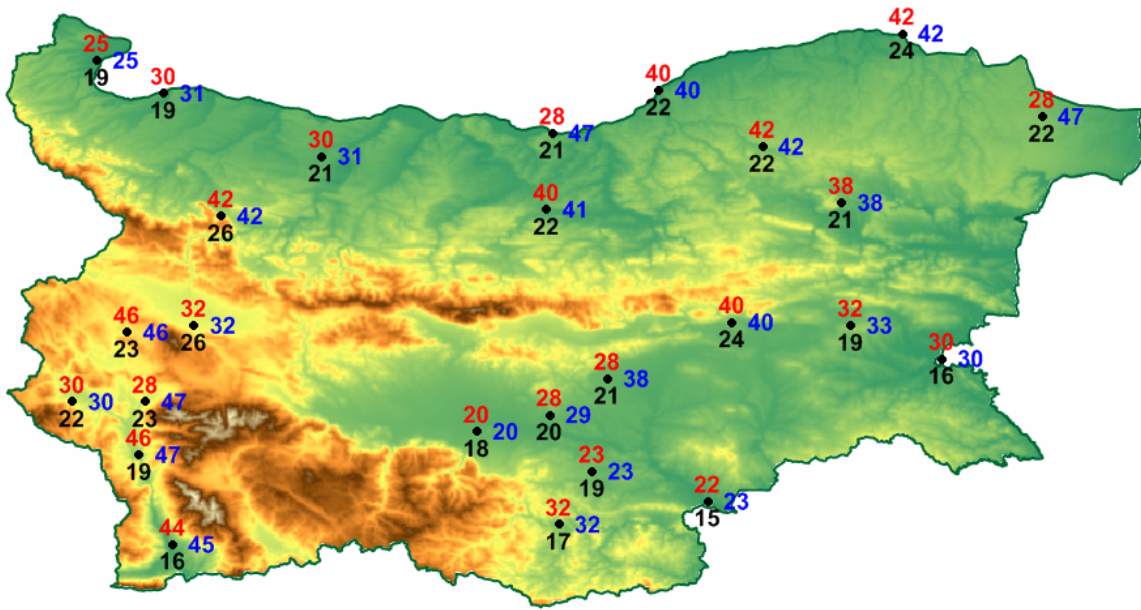
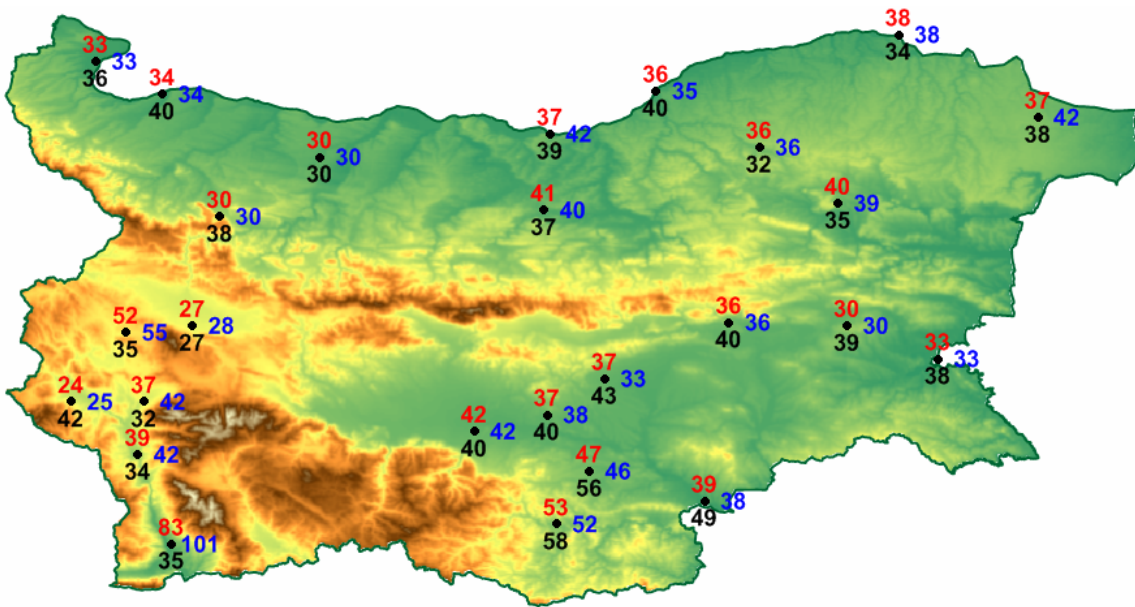


Fig.15 Greatest 1-day total rainfall in winter (top) and summer (down)





## **D4.4.e Synthesis for whole region and intercomparison with pre-existing RCM data sets (led by ETHZ and DMI)**

### **D4.4.1 ETHZ and DMI**

The aim of this deliverable is the provision of a synthesis of the results for the whole Central and Eastern European region and an inter-comparison of the high-resolution simulations with pre-existing RCM (PRUDENCE, ENSEMBLES) simulations and the observational datasets analyzed in D4.2. The latter include the station observations from the local partners, the ECA&D station data (Klein Tank et al. 2002; <http://eca.knmi.nl/>), and the E-Obs gridded observations from the ENSEMBLES project (Haylock et al. 2008).

In addition to D4.3, also the CECILIA transient driving run from ICTP, as well as the CECILIA 10-km high-resolutions simulations from the partners are now available for the analysis.

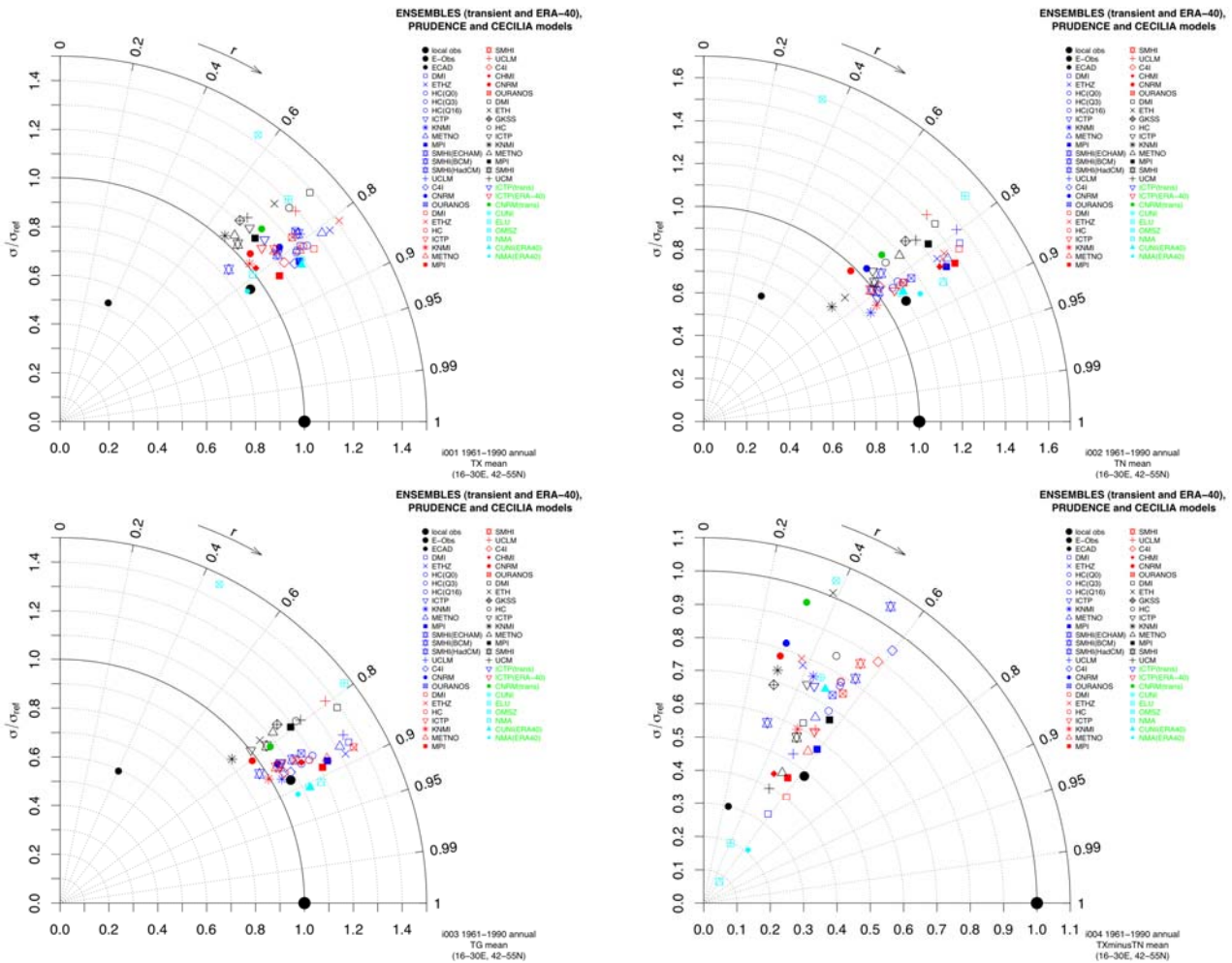
The following two subsections present results from the validation and the model inter-comparison separately for selected temperature and precipitation indices.

#### **D4.4.1.1 Temperature indices**

Figure 1 displays Taylor plots (Taylor 2001) showing the spatial standard deviations  $\sigma$  (normalized by the standard deviation of the reference observations) and the spatial correlation coefficients  $r$  of the PRUDENCE, the ENSEMBLES and the CECILIA driving (CNRM, ICTP) and high-resolution (CUNI, ELU, NMA, OMSZ) simulations, compared against the local station observations (reference). For comparison, also the ECA&D and the E-Obs observations are included in the plots (also relative to the local observations). The statistics are derived from the annual indices values of the period 1961–1990 and for the East European domain (16°E–30°E, 42°N–55°N). Note that the CECILIA runs from ICTP coincide with the respective ENSEMBLES runs (thus sharing the same symbol and color). Moreover, note that the CECILIA high-resolution runs do not cover the whole region and thus might not be fully representative for the analyzed domain.

Generally, the spatial agreement between the models and the local station observations is good for mean, maximum and minimum temperature (Figure 1, top and bottom left panels). This is the case both in terms of the spatial variability, which is however often overestimated in the models; and in terms of the spatial correlation with the local observations, which varies mostly between 0.6 and 0.9 for these indices. The spread between the models becomes larger for the daily temperature range (bottom right), with most models showing lower spatial variability compared to the local observations. Moreover, the spatial correlation between the local observations and the models decreases to below 0.6. Note the

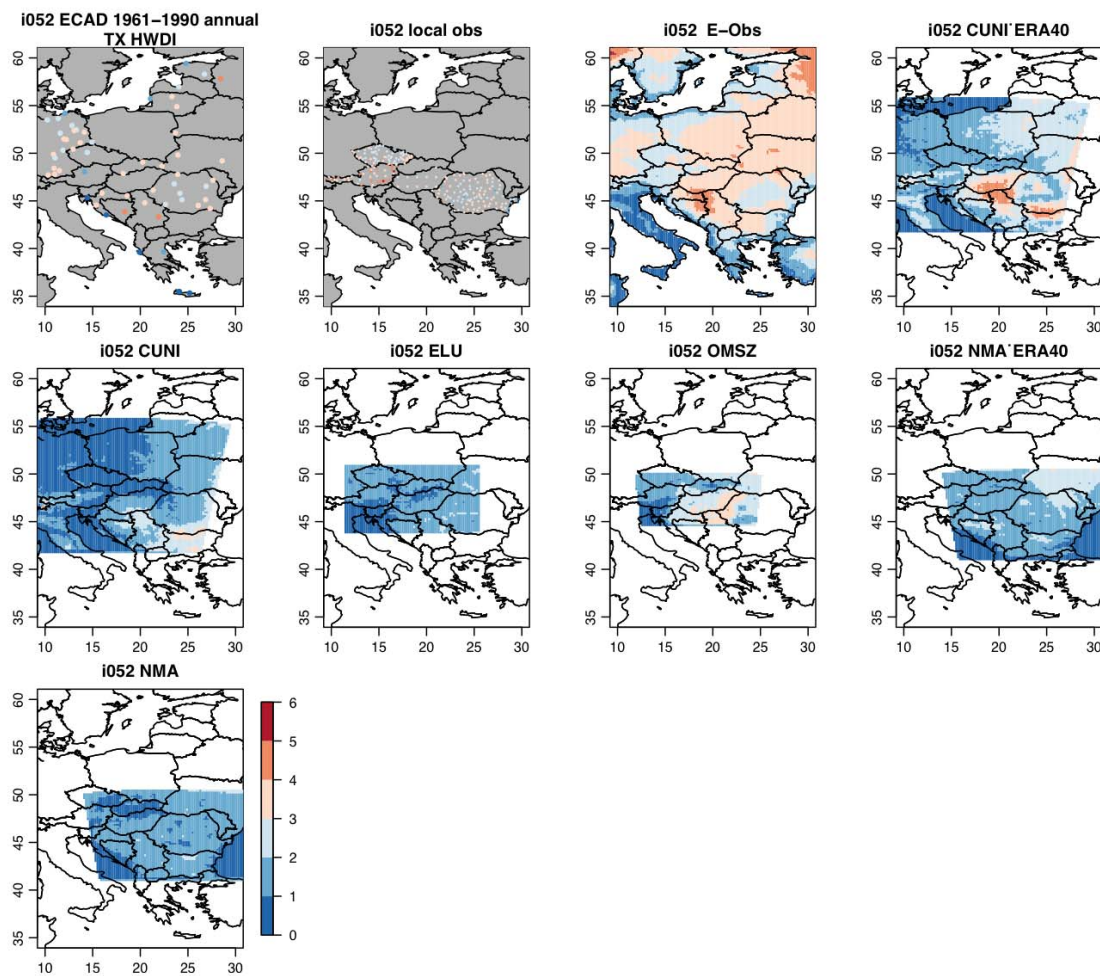
underestimation of the spatial variability in ECA&D in all cases, which is likely due to its limited spatial resolution.



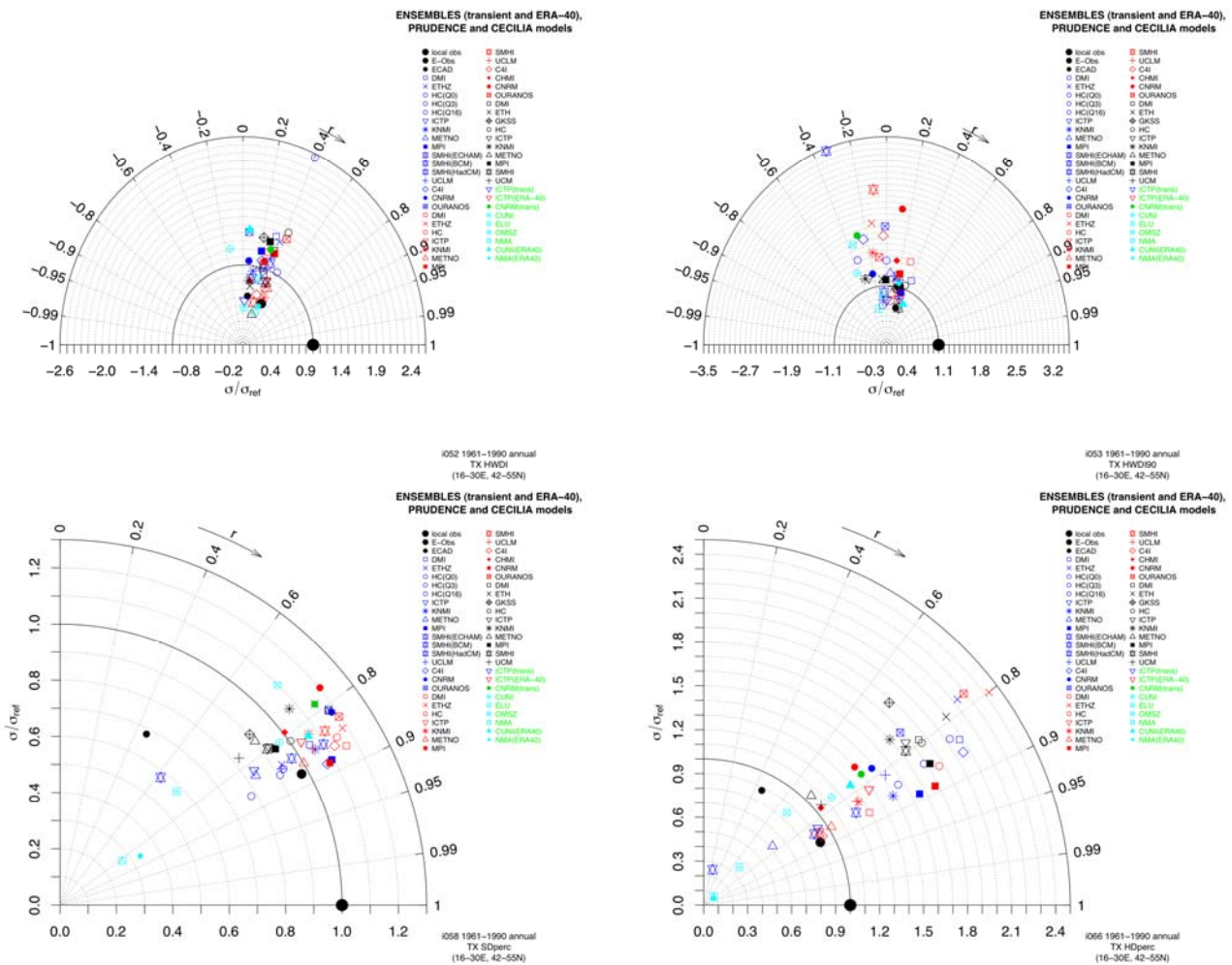
**Figure 1.** Taylor plots including the ENSEMBLES transient (blue symbols) and ERA-40 (red symbols) simulations, the PRUDENCE RCMs (black symbols), as well as the CECILIA driving and high-resolution runs (green model acronyms, cyan symbols for the high-resolution runs) compared against the local observations. For comparison, also the ECA&D and the E-Obs observations are included (also relative to the local observations). As mentioned in the text, the CECILIA driving runs from ICTP coincide with the respective ENSEMBLES runs and consequently share the same symbols and colors. (Top left) maximum temperature, (top right) minimum temperature, (bottom left) mean temperature, (bottom right) daily temperature range. Displayed are annual values for the period 1961–1990 and for the East European domain (16°E–30°E, 44°N–55°N).  $\sigma$  denotes the spatial standard deviations (normalized by the standard deviation of the observations) and  $r$  the correlation coefficients.

Figure 2 shows maps of the mean heat wave occurrence index from the ECA&D and the local station data, the E-Obs gridded observations, and the CECILIA high-resolution models. Moreover, Figure 3 shows the spatial Taylor plots for this index and additionally for the 90th percentile-based maximum heat

wave duration, the percentage of summer days and the percentage of hot days for the same data sets as in Figure 1. The spread between the models is relatively large, in particular for the percentile-based heat wave duration (Figure 3). For the mean heat wave occurrence, the spatial correlations reach 0.5 at the maximum. The results are worse for the percentile-based heat wave duration, where the correlations are mostly below 0.4. Also, in both cases there appear negative correlations for some models. The models perform better in case of the percentage of summer days and percentage of hot days indices, although the spread between the models is also relatively large for the latter.



**Figure 2.** Comparison of the mean heat wave occurrence index [%] from the ECA&D and the local station data, the E-Obs gridded observations, and the CECILIA high-resolution simulations from CUNI, ELU, OMSZ and NMA.



**Figure 3.** As Figure 1, but for two different heat wave indices, i.e., (top left) mean heat wave occurrence and (top right) 90th percentile-based maximum heat wave duration, as well as for (bottom left) percentage of summer days and (bottom right) percentage of hot days.

Figure 4 shows the temporal evolution of the basic indices mean, maximum and minimum temperature for the various observational and modeling data sets. Each observational and model time series (averaged over the East European domain) has been centered with respect to the 1961–1990 period’s average. Then the standard deviation for the same period has been used to standardize the series to account for different magnitudes of the indices. A 10-year running mean is applied to smooth the final time series. In case of the model indices, the ensemble means of the different data sets are shown, with shadings denoting the inter-model standard deviation (not shown for the two CECILIA ERA-40 driven high-resolution models).

As expected, the ERA-40 driven models more closely follow the observed curves when compared with the GCM-driven models (i.e., the PRUDENCE, ENSEMBLES transient/CECILIA driving, and the GCM-driven CECILIA high-resolution runs). In the observational data sets, the inter-decadal variability that is known as the dimming/brightening phenomena (e.g., Wild 2009) can be well observed. The ERA-40 driven models do partly capture this, however they show a less pronounced temperature increase in the 1990’s. The GCM-driven models on the other hand are not able to reproduce the observed long-term variability. In the future, the different model data sets agree well on the expected temperature increase.

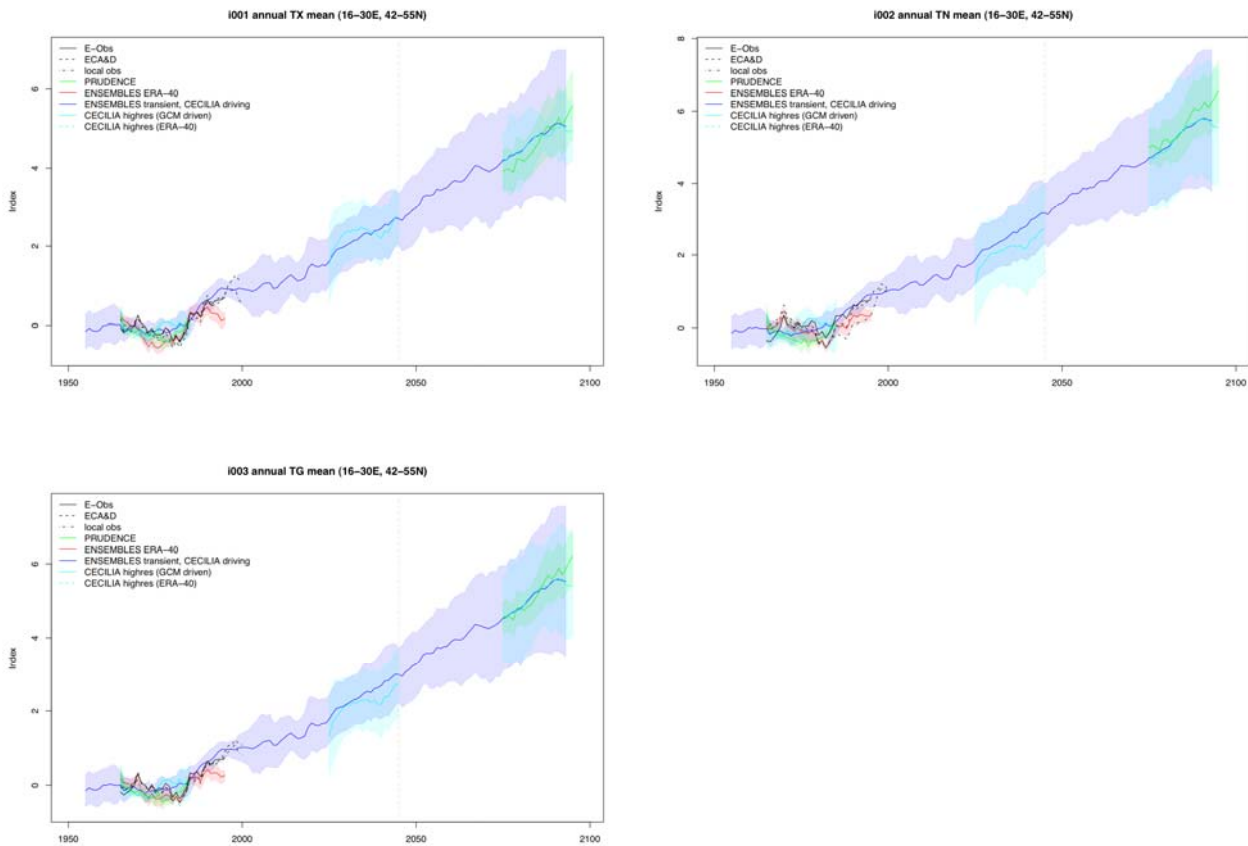


**Figure 4.** Temporal evolution of (top left) maximum temperature, (top right) minimum temperature, and (bottom left) mean temperature in the East European domain and for the various observational and modeling data sets. Y-axis units are in standard deviation, for details on the computation of the curves, see text.

Figure 5 shows the same for two heat wave indices, i.e., mean heat wave occurrence and 90th percentile-based maximum heat wave duration. The different data sets agree well in the observational period, most showing a slight decrease in the maximum heat wave duration in the early years, and a consistent increase in both heat wave indices from the 1980's on. As above, the GCM-driven simulations do not show this long-term variability. In the far future (last time slice), the CECILIA high-resolution models surprisingly show a smaller increase in these heat wave indices than the corresponding ENSEMBLES and PRUDENCE simulations.

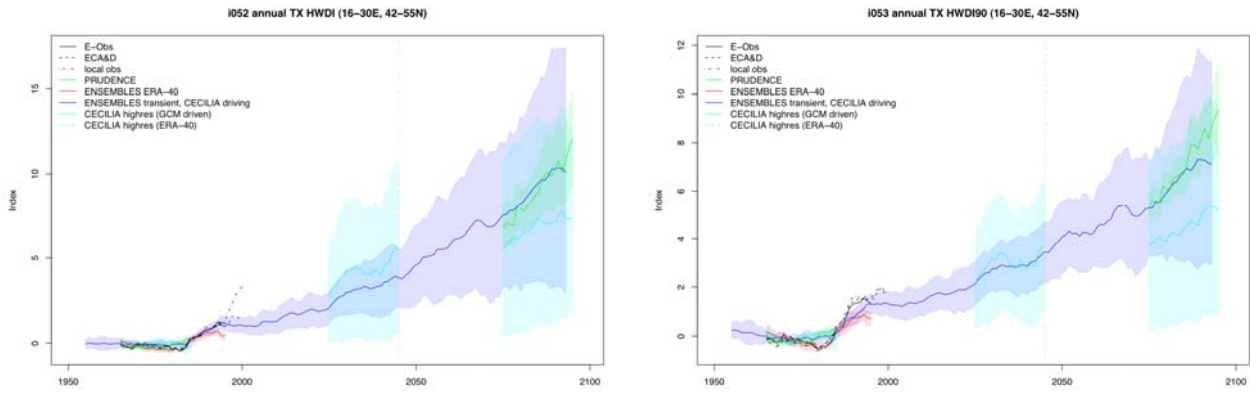


**Figure 5.** As Figure 4, but for (left) mean heat wave occurrence, (right) 90th percentile-based maximum heat wave duration.

#### D4.4.1.2 Precipitation indices

Figure 6 shows the spatial Taylor plots of mean precipitation and mean wet-day precipitation from the PRUDENCE, the ENSEMBLES and the CECILIA driving (CNRM, ICTP) and high-resolution (CUNI, ELU, NMA, OMSZ) simulations, compared against the local station observations (reference). Again, for comparison also the ECA&D and the E-Obs observations are included in the plots (also relative to the local observations). The spread between the models is relatively large (in particular for mean precipitation), and the spatial correlations with the local observations are mostly below 0.6.

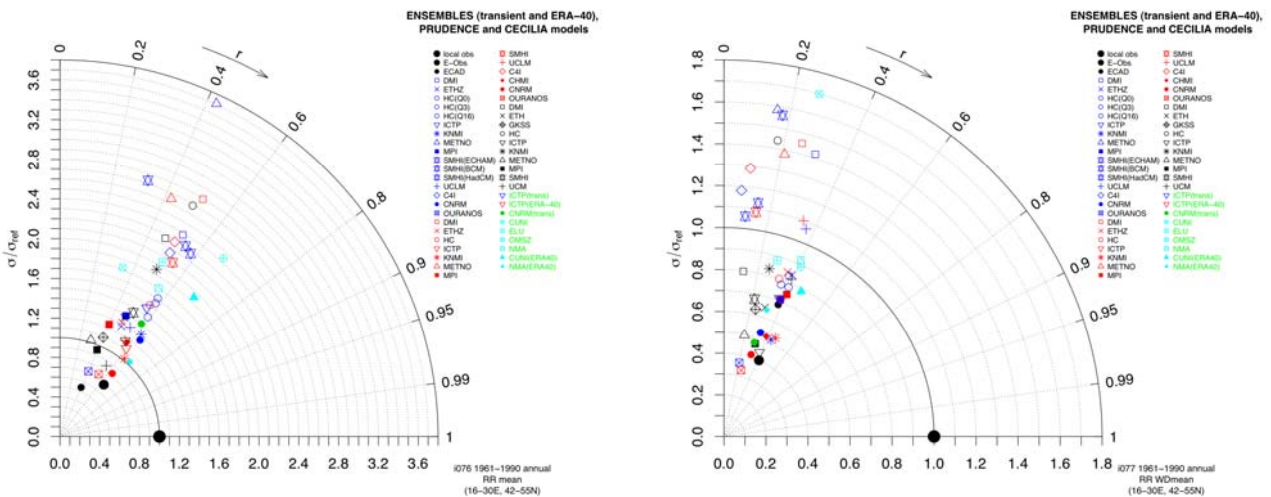


**Figure 6.** As Figure 1, but for (left) mean precipitation, and (right) mean wet-day precipitation.

Figure 7 displays as an example of a derived precipitation index maps of the max. number of consecutive wet days (for the same data sets as in Figure 2), and Figure 8 spatial Taylor plots for this and additional

precipitation indices (i.e., max. number of consecutive dry days, median dry spell length, median wet spell length, greatest 1-day and 5-day total precipitation). It is apparent on the maps that the CUNI and OMSZ models show larger spatial variability in the max. number of consecutive wet days, both compared to the other high-resolution models and to the observational data sets. This is also visible in the respective Taylor plot (Figure 8, top right). In terms of spatial correlation, the models seem to be better capable of reproducing the spatial patterns of the dry indices (i.e., higher correlations, top and middle left panels of Figure 8) when compared with the corresponding wet indices (top and middle right panels). However, as for mean precipitation and mean wet-day precipitation, the spread between the models is relatively large. This is also the case for the greatest 1-day and 5-day total precipitation indices (bottom row).

Figure 9 finally shows the temporal evolution of mean precipitation and mean wet-day precipitation (for details on the calculation of the curves, see previous section). In both cases, inter-decadal variations are apparent in all observations and in the ERA-40 driven models. These are not captured by the GCM-driven experiments. No clear future trend is observable for mean precipitation, whereas mean wet-day precipitation shows a trend towards more precipitation.

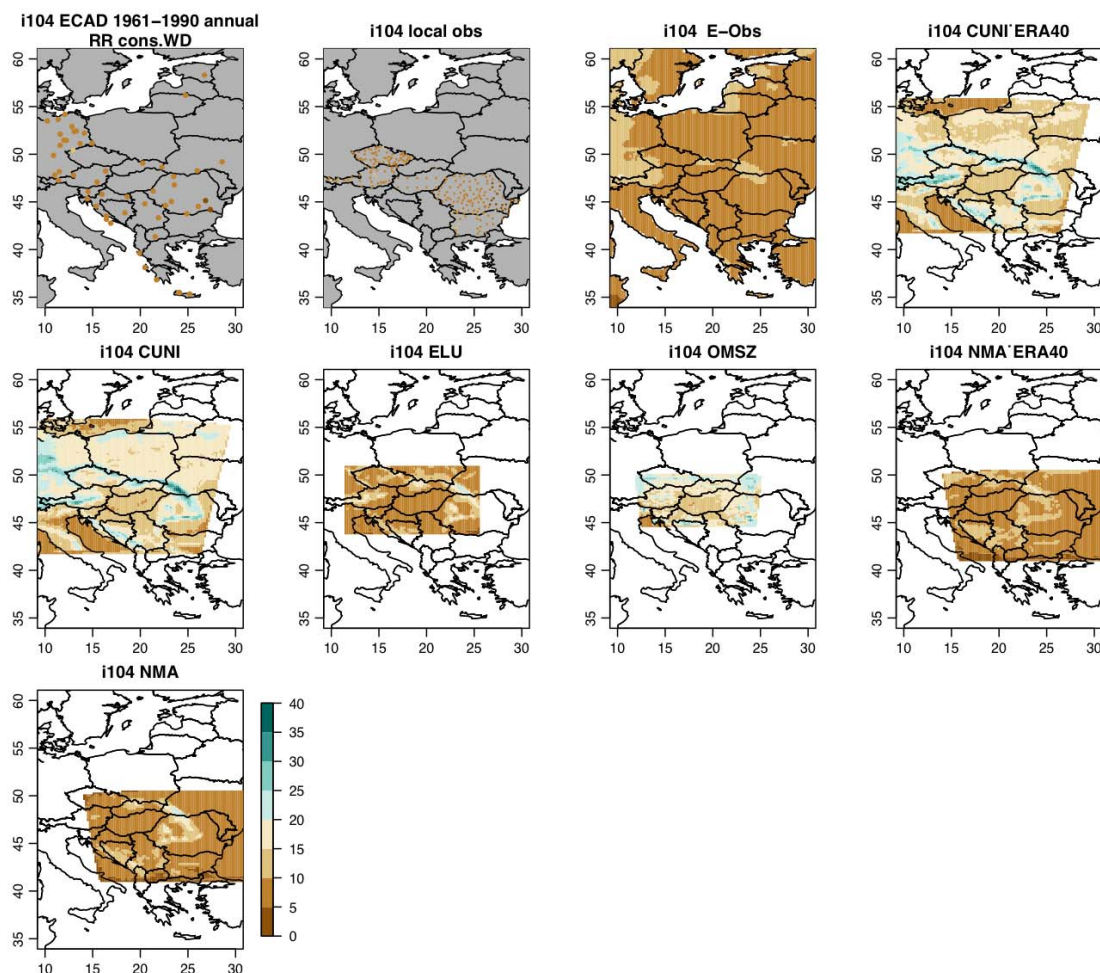


**Figure 7.** Comparison of the max. number of consecutive wet days [days] from the ECA&D and the local station data, the E-Obs gridded observations, and the CECILIA high-resolution simulations from CUNI, ELU, OMSZ and NMA.

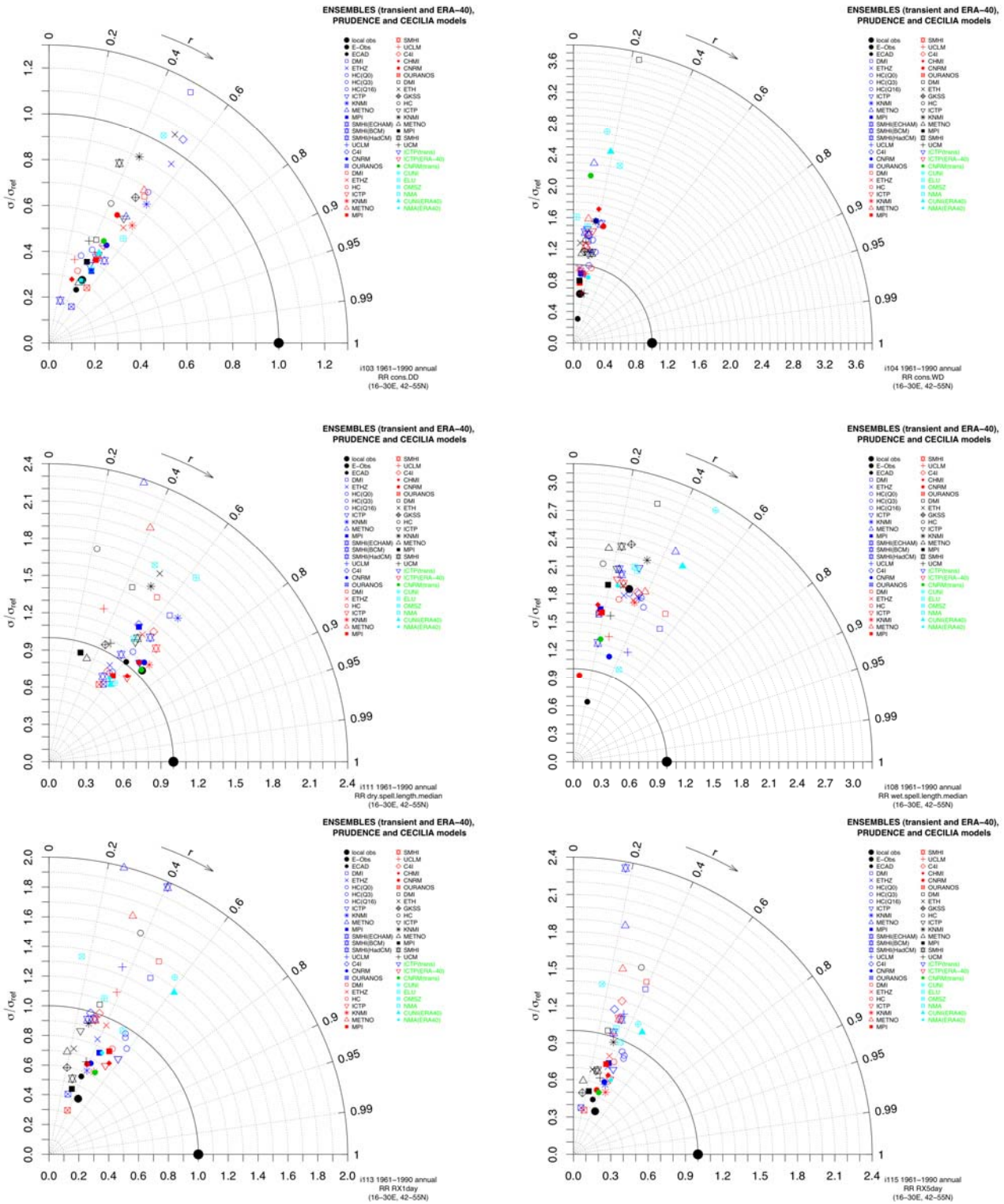


**Figure 8.** As Figure 1, but for derived precipitation indices. (Top left) Max. number of consecutive dry days, (top right) max. number of consecutive wet days, (middle left) median dry spell length, (middle right) median wet spell length, (bottom left) greatest 1-day total precipitation, (bottom right) greatest 5-day total precipitation.

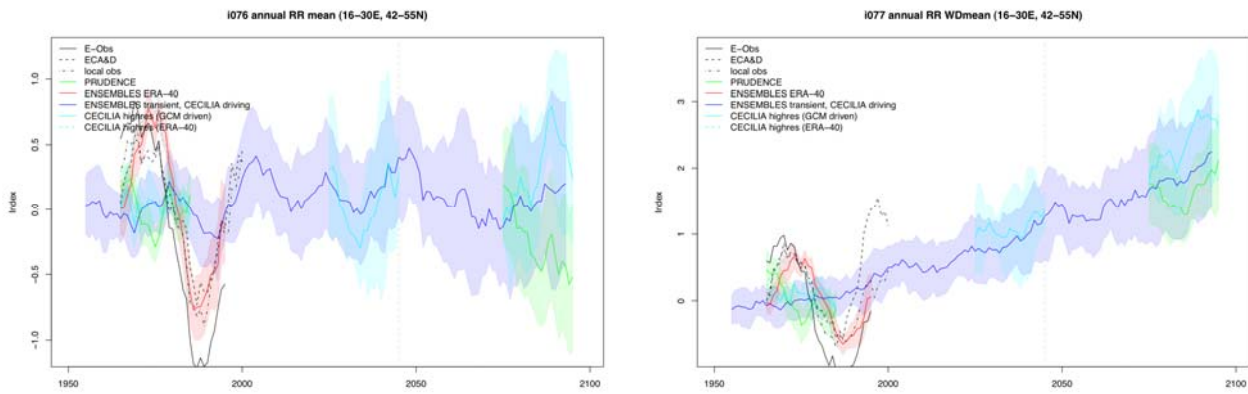


**Figure 9.** As Figure 4, but for (left) mean precipitation and (right) mean wet-day precipitation.

#### D4.3.4 References

Haylock, M. R., Hofstra, N., Klein Tank, A. M. G., Klok, E. J., Jones, P. D., and New, M. (2008). A European daily high-resolution gridded dataset of surface temperature and precipitation for 1950–2006. *Journal of Geophysical Research*, **113**(D20119):doi:10.1029/2008JD010201.

Klein Tank, A., et al. (2002). Daily dataset of 20th-century surface air temperature and precipitation series for the European Climate Assessment. *Int. Journal of Climatology*, **22**(12):1441–1453.

Taylor K. E. (2001). Summarizing multiple aspects of model performance in a single diagram. *Journal of Geophysical Research*, **106**(D7):7183–7192.

Wild, M. (2009). Global dimming and brightening: A review. *Journal of Geophysical Research*, **114**(D00D16):doi:10.1029/2008JD011470.